Impact of heterogeneity on natural and managed aquiferrecharge in weathered fractured crystalline rock aquifers

Madeleine Nicolas

UNIVERSITE ECOLOGIE
BRETAGNE GEOSCIENCES
LOIRE AGRONOMIE ALIMENTATION

UNIVERSITÉ DE RENNES 1

THÈSE DE DOCTORAT DE

L'UNIVERSITÉ DE RENNES 1
COMUE UNIVERSITÉ BRETAGNE LOIRE

ÉCOLE DOCTORALE N° 600
École doctorale Écologie, Géosciences, Agronomie et Alimentation
Spécialité : Sciences de la Terre et de l'Environnement

Par
Madeleine NICOLAS

Impact de l'hétérogénéité sur la recharge naturelle et artificielle des aquifères cristallins altérés et fracturés

Application aux sites de Maheshwaram et Choutuppal (Inde du sud)

Thèse présentée et soutenue à Rennes, le 07/05/2019
Unité de recherche : UMR 6118 – Géosciences Rennes

Rapporteurs avant soutenance :

René LEFEBVRE	Professeur des universités – INRS Québec
Valérie PLAGNES	Professeur des universités – Université Paris VI

Composition du Jury :

Président :	Laurent LONGUEVERGNE	Directeur de recherche CNRS – Université Rennes 1
Examinateurs :	Jean-Christophe MARÉCHAL	Ingénieur de recherche – BRGM Montpellier
	Sylvain MASSUEL	Ingénieur de recherche – IRD
	Richard TAYLOR	Professeur des universités – University College London
Dir. de thèse :	Olivier BOUR	Professeur des universités – Université Rennes 1

Invité(s)

Adrien SELLES	Chef d'équipe – BRGM, IFCGR, Hyderabad

Impact of heterogeneity on natural and managed aquifer recharge in weathered fractured crystalline rock aquifers

Insights from two instrumented sites at different scales (south India)

Madeleine NICOLAS

Indo French Center for Groundwater Research

CEntre Franco-Indien de Recherche sur les Eaux Souterraines

Foreword

March, 2019

This project results from collaboration between the National Geophysical Research Institute (NGRI) and the French geological survey (BRGM), and was carried out under the tutelage of the University of Rennes 1. It is the culmination of three and a half years of work consisting both of field campaigns and measurements and numerical and analytical investigations. The first half of the PhD research was conducted at the Indo-French Centre for Groundwater Research, within the NGRI campus in Hyderabad, and the second half of this work was completed at the Geosciences Rennes laboratory at the University of Rennes 1 campus, in Rennes. This work mainly benefited from CARNOT Institute BRGM funding. The Choutuppal Experimental Hydrogeological Park has also benefited from INSU support within the H+ observatory.

This thesis is made up of two parts. The first of its two parts provides the theoretical framework for comprehending the scientific, societal and theoretical challenges discussed in this thesis. The second part presents the numerical and experimental research carried out to address these challenges and further our understanding of groundwater flux dynamics in heterogeneous environments. Experienced readers should focus especially on the second part of this work, as this is where the core of the innovative scientific work is summarized.

Acknowledgements

As readers may well know, a single scientific advancement is never an individual success. It is the culmination at one point in time of the work advanced by an entire scientific community, ranging from the near-celebrity status researcher, to the unpaid intern sifting through endless databases. I wish I could thank every person participating in this particular chain of events that has led me here, but alas, that would be impossible, so this non-exhaustive list will have to do.

First and foremost, I am grateful to my supervisors Olivier Bour and Jean-Christophe Maréchal, and my non-official supervisor Adrien Selles, for trusting me to carry out this ambitious and difficult project. Their contributions and advice were essential to the optimal development of this thesis and helped me find a clear sense of direction and purpose throughout this journey.

I would also like to thank the different teams I had the privilege to work and interact with. The first half of my PhD, during which I was working at the Indo-French Centre for Groundwater Research (IFCGR, Hyderabad), would not have been possible without the indispensable help of the team there. Scientifically, administratively and professionally I owe a lot to Adrien Selles, Shakeel Ahmed, Subash Chandra, Marion Crenner, Mohammed Wajiduddin, Nilofar Begum, Adil Mizan, Tanvi Arora, Ravi Rangarajan, Atulya Mohanty, and many others. Fieldwork would have also been a lot more difficult and a lot less fun had it not been for the amazing and hard work of people who I had the good fortune to work in the field with: Adrien, Marion and Wajid, again, Joy Choudhury, Vidya Sagar, Yata Ramesh, Yata Muthyalu, Pittala Krishna, Nilgonda Kishtaiah and Pittala Anjaiah. I'd be remiss if I did not also acknowledge the work done by previous researchers and students within the framework of this collaboration, work I built on and benefited from, and that contributed to our global understanding of the hydrogeology of fractured crystalline environments. Specifically, I'd like to thank Nicolas Guihéneuf, Alexandre Boisson, Jérôme Perrin, Devaraj de Condappa, Amélie Dausse, and all the other team leaders, PhD students, post-docs, volunteers and interns that have strengthened and nurtured this research centre. On another note, my experience in Hyderabad would not have been half as enthralling, fun and crazy had I not found other kooks to share it with outside of work as well : Adrien, Marion and Coline, ma famille loin de la famille, Mélissande, Chipten, Alex, Léa, Vamshi, Guillaume, Imran, Mohit, Julia, Billie the cat, and JC the goat (R.I.P.).

The second half of my PhD, during which I was working with the Géosciences Rennes team at the University of Rennes 1 (in Rennes, France) was also a success thanks to the scientific, professional and administrative competence of the team there.

Thanks to Olivier Bour, of course, Laurent Longuevergne, Jean-Raynald de Dreuzy, Tanguy Le Borgne, Philippe Davy, Dimitri Lague, Philippe Steer, Nicolas Lavenant, and many others. From a personal standpoint, I cannot thank enough all of the friends I made in Rennes, i.e. *Les Tchoustchous*: Alex, Aurélie, Allison, Baptiste, Behzad, Camille, Charlotte, Claire, Diane, Etienne, Jean, Justine, Lucille, Luca, Marie-Françoise, Maxime, Meruyert, Quentin, Thomas (c'est dans l'ordre alphabétique pour ne pas faire de jaloux! Sauf ceux que j'ai oublié…). Vous êtes devenus ma communauté, mes compagnons de voyage, mes compagnons d'infortune dans les temps difficiles, ou mes compagnons de fête dans les temps plus gais. Vous avez préservé ma santé mentale et vous m'avez aidé à me sentir chez moi à Rennes ; les choses ne se seraient certainement pas passées de la même manière sans vous, je vous kiffe !

The Bureau de Recherches Géologiques et Minières (BRGM, Montpellier) is responsible not only for financing this project, but also was a place of fruitful interaction, a place where help was always available, and where I was encouraged to grow as a researcher. The team there was very important in helping me further my scientific reasoning and ensuring my stay in India went well: Jean-Christophe, of course, Benoit Dewandel, Vincent Bailly-Comte, Sandra Lanini, Emilie Lenoir, Carine Vedie, fellow PhD students and interns, and the rest of the team.

I am also indebted to the researchers that guided me towards this PhD subject in the first place. First of all, to Pierre Ribstein, an amazing professor who truly cares about his students, for pointing me towards Hydrology and Hydrogeology when I was a bachelor student in need of guidance. And to Ghislain de Marsily, for being an inspiration and a role model, and for helping me find this subject and introducing me to the people in charge.

Finally, thank you to all of you who supported me from a distance. To my mother, my father, my sister, and my grandparents, and to my friends in and from Mexico and those scattered in Europe: whether you helped with my English ramblings, listened to me in times of need, had faith in me, came to see me, or supported me from afar, I am grateful to all of you and I love you all dearly.

(/◕ヮ◕)/*:･ﾟ✧ now stop reading the acknowledgements and go read my thesis !

Contents

List of figures

List of tables

"Hard rock hydrogeologists, the world over, are therefore divided into two main groups: those interested in obtaining ground water for domestic, irrigational or industrial use by exploring fractured and permeable zones in a relatively less permeable matrix of hard rock, and those interested in locating impermeable or the least permeable zones for storage of hazardous nuclear waste.

Ironically, for the first group even the most permeable zones are often not good enough to yield adequate water supply, while for the second group even the least permeable zones are often not good enough for safe storage of hazardous nuclear waste over a prolonged period of a few hundred years."

- (Limaye, 2010)

Introduction

The Industrial and Technological Revolution

In a rapidly industrializing world, challenges regarding water are incessantly increasing. Explosive population growth, combined with a strong expansion of irrigated agriculture and industrial development, are adding stress on the quality and quantity of natural systems. Prior to the Industrial Revolution of the late eighteenth and nineteenth century, both population growth and living standards remained relatively static (Harris & Roach, 2018). Thereafter, rapid technological progress and the advent of the market economy set off a staggering population growth that significantly altered established patterns. This led British economist Thomas Malthus, in 1798, to propose the hypothesis that: "The power of population is indefinitely greater than the power in the earth to produce subsistence for man" (p. 9), i.e. populations were bound to outgrow their food supplies. During the period that followed, while thousands of individuals continued to be victims of drought and famine, mankind as a whole has disproved the Malthusian hypothesis. Although the world's population has skyrocketed from one to over seven billion in the last 200 years, economic output per person has in fact grown and living standards have risen, even in the face of significant and increasing inequality (Harris & Roach, 2018). However, the essential core of the Malthusian argument remains valid–growing human populations and economic systems can outrun their biophysical support systems. In fact, over the past few decades, the scope and urgency of issues related to increasing resource demands have become a central focus of global awareness and efforts to mitigate environmental degradation. During the 1992 United Nations Conference on Environment and Development (UNCED), attention was focused on the major global issues threatening mankind: the depletion of the ozone layer, destruction of forests and wetlands, major species extinction and the steady build-up of greenhouse gases causing climate change. Twenty years later, countries of the world reaffirmed their commitment to including environmental issues in their development goals at the United Nations Rio +20 Conference. However, the 2012 United Nations Environment Program (UNEP) report found that, with the exception of ozone depletion, all of the global environmental problems identified at UNCED have continued or worsened. In fact, further UNEP reports have identified increasingly destructive side-effects of indiscriminate economic growth, many of which impact our freshwater sources (e.g. eutrophication and acidification of aquatic systems, declining groundwater supplies, overexploitation of ocean and freshwater ecosystems, etc.).

Groundwater, which accounts for by far the largest volume of unfrozen freshwater on Earth, is among the most important of our natural resources. Compared with surface water, groundwater is of higher quality, better protected from pollution, less subject to seasonal and perennial fluctuations, and much more uniformly distributed across large regions. Furthermore, considering the increasing variability of water supplies, especially under climate change, groundwater constitutes a crucial buffer in coping with current and upcoming environmental challenges. These advantages, combined with the fact that groundwater is for some countries (e.g. Saudi Arabia, Malta, Denmark) the only or most important source of water, have made groundwater the most exploited resource on earth (UNESCO, 2004). Over the past decades, groundwater use in agricultural and other economic sectors has soared, contributing to massive improvements in the quality of life in many parts of the world. As such, it has served as one of the largest and most potent modes of poverty reduction in recent decades (Sharma et al., 2005).

The Silent Revolution

Irrigation is the most important water use sector, especially in arid and semiarid climates, accounting for 70% of global freshwater withdrawals and 90% of consumptive water uses (Siebert et al., 2010). The spectacular increase in groundwater use that has led to the current situation began in the twentieth century, during a phenomenon that has been called "the Silent Revolution" (Llamas & Martínez-Santos, 2005a). At the start of the century, the boom in groundwater development was limited to a few countries, with Italy, Mexico, Spain and the United States among the leaders. A second wave began later, in the 1970s, in South Asia, parts of China, the Middle East and northern Africa, and continues today (Van der Gun, 2012). Overall, since the 1950s, groundwater use, most significantly for irrigation, has significantly increased in many parts of the world (FIGURE 0.1). In Spain, it has increased from 2 km^3/year to 6.5 km^3/year, accounting for 15-20% of all water used in the country (Hernández-Mora et al., 2010). In the United States, groundwater use for irrigation increased from 23% in 1950 to 48% (i.e. 46 to 113 km^3/year) of total freshwater withdrawals in 2015 (Dieter et al., 2018). In India, groundwater use has soared from 10-20 km^3/year before 1950 to a world-record-breaking over 250 km^3/year today (Siebert et al., 2010), making India by far the largest exploiter of groundwater on earth. Yearly abstractions in India are more than double those of the second runner-up, China, whose yearly abstractions average about 110 km^3/year (Van der Gun, 2012), despite China's greater population. This is due to an interplay of factors, such as the implementation by the Chinese government of a metered tariff regime, and an overall lesser dependence on groundwater (in India 55-60% of the population depends on groundwater vs. 22-25% in China) (T. Shah et al., 2003). In subhumid to arid areas, specifically, groundwater abstraction has increased from 126 ($\pm$ 32) km^3 in 1960 to 283 ($\pm$ 40) km^3 in 2000 (Wada et al., 2010). While in the US, Spain,

Mexico and North-African countries like Tunisia or Morocco total groundwater use peaked during the 1980s or thereabouts, and has since decreased, in South Asia and parts of China the upward trend that began during the 1970s is still ongoing. Furthermore, it is predicted there will likely be a third wave of exponential growth in groundwater abstraction in many regions of Africa and some southeast Asian countries such as Vietnam and Sri Lanka (Molle et al., 2003).

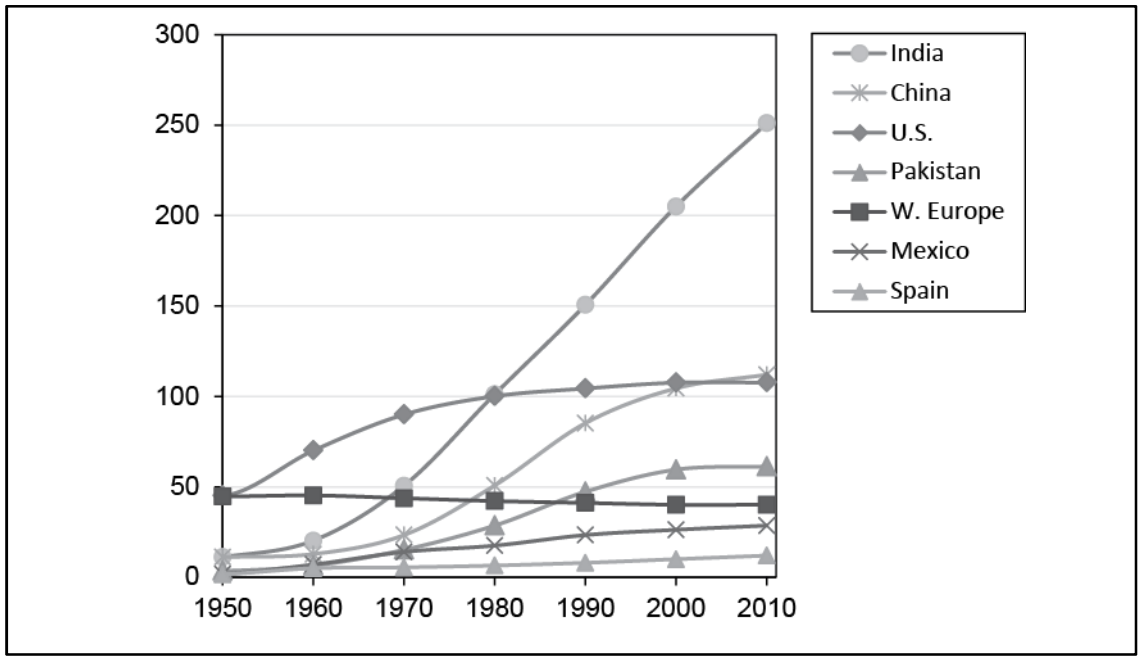

FIGURE 0.1: Approximate groundwater abstraction trends in selected countries (in km3/year modified from Shah, 2005 and Van der Gun, 2012)

This worldwide boom can be attributed largely to numerous individual decisions by millions of modest farmers pursuing the significant short-term benefits to be derived from groundwater use. Decisions were made without centralized planning or coordination; this is why it is called "the Silent Revolution". Technological and scientific advancements are at the core of this "Revolution". Improvement in well-drilling techniques, advancements in hydrogeology and the popularization of the submersible pump dramatically reduced abstraction costs. Today, the total cost of groundwater abstraction is only a small fraction of the economic value of the guaranteed crop. This has allowed farmers to progressively shift from low-value crops to cash crops, which are also more water-intensive. As an example, a hectare of cereal can be valued at around USD$500, while tomatoes or cucumber can be worth more than USD$60,000, i.e. over 100 times more valuable (Llamas & Martínez-Santos, 2005a). Although water use by these farmers has frequently been incentivized by soft loans or energy subsidies from governmental sources, most governmental agencies have overlooked the real effects and extent of groundwater development. Instead, they have focused mainly on the maintenance and control of surface water (Llamas & Martínez-Santos, 2005a). However, despite the fact that govern-

mental subsidization of surface water often makes it cheaper than groundwater, many farmers prefer groundwater. There are several reasons for this choice: first, groundwater can be obtained individually, thus bypassing often time-consuming negotiations with other farmers and government officials (Llamas & Martínez-Santos, 2005a). Second, and most important, groundwater is more resilient in dry periods and more generally available (as opposed to surface water). In practice, most farmers rely on the conjunctive use of surface water and groundwater, assuming the latter is readily available.

The combination of an exponential increase in individual borewells and the lack or ineffectiveness of regulation has led to adverse effects in places like South Asia, where the current situation has been described as "colossal anarchy" (T. Shah, 2005). Indeed, this sudden boom in groundwater exploitation has triggered a series of harmful side effects (Sharma et al., 2005): groundwater level declines leading to wells running dry, rising energy and pumping costs, and growing vulnerability to drought (Castle et al., 2014; Famiglietti, 2014; Scanlon et al., 2012; Van Loon et al., 2016), saltwater intrusion in coastal areas (Werner et al., 2013), and health hazards derived from the aquifer itself (e.g. arsenic and fluoride contaminations) (Amini, Abbaspour et al., 2008; Amini, Mueller et al., 2008; Chuah et al., 2016; Rodriguez-Lado et al., 2013) or external sources including agriculturally derived chemicals (Böhlke, 2002; Hallberg, 1989; Pimentel et al., 1992; Rattan et al., 2005; Spalding & Exner, 1993). In many parts of the world, groundwater abstractions exceed natural groundwater recharge, which has caused overexploitation and persistent groundwater depletion in these regions (FIGURE 0.2 and FIGURE 0.3). Among the current "hot-spots" of groundwater depletion worldwide, the most notable are Pakistan, India (see also Rodell et al., 2009), North-East China, central U.S. and California, Yemen and Spain (FIGURE 0.3).

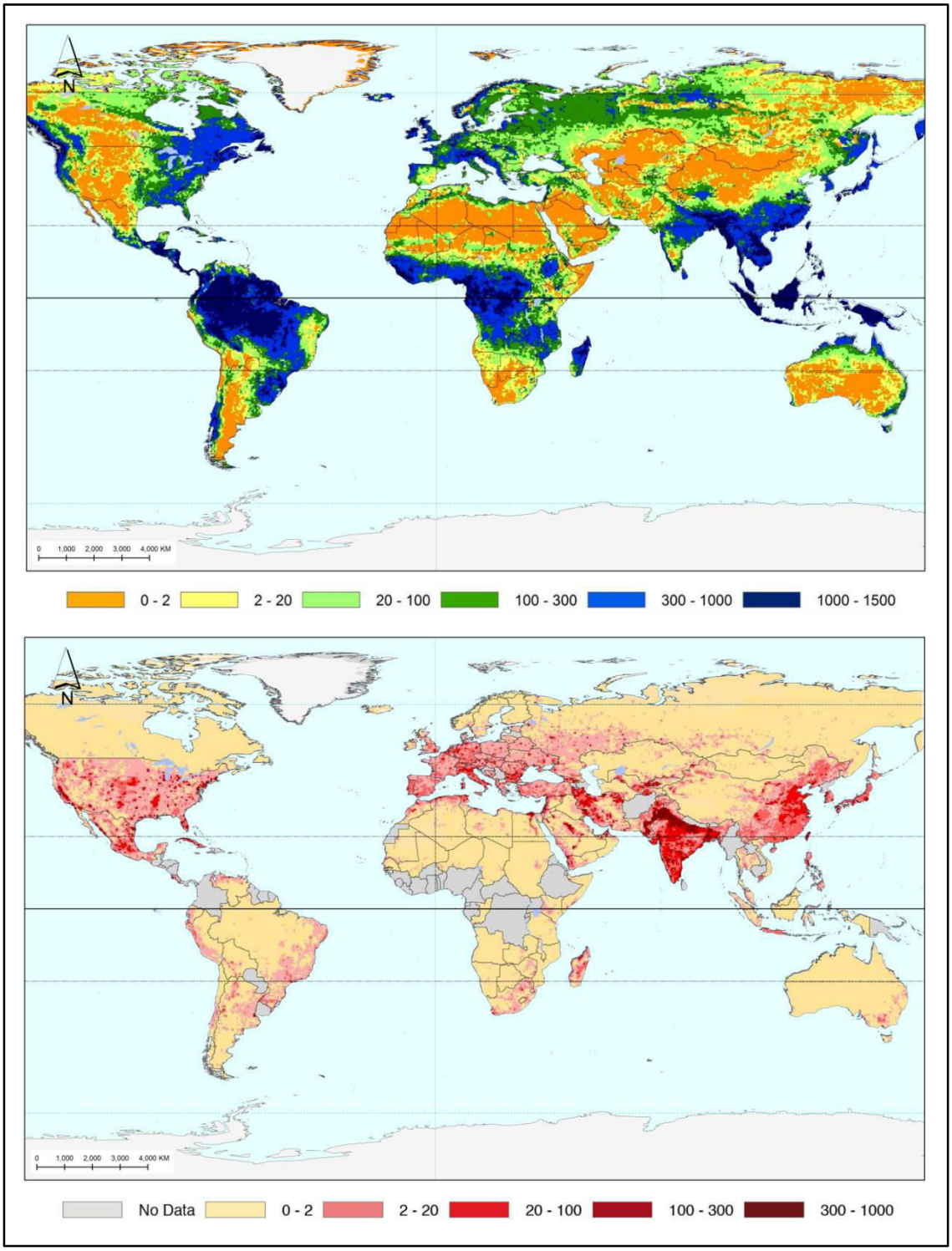

FIGURE 0.2: World map of simulated average groundwater recharge (top) and of the intensity of groundwater extraction (bottom) (in mm/year modified from Wada et al., 2010)

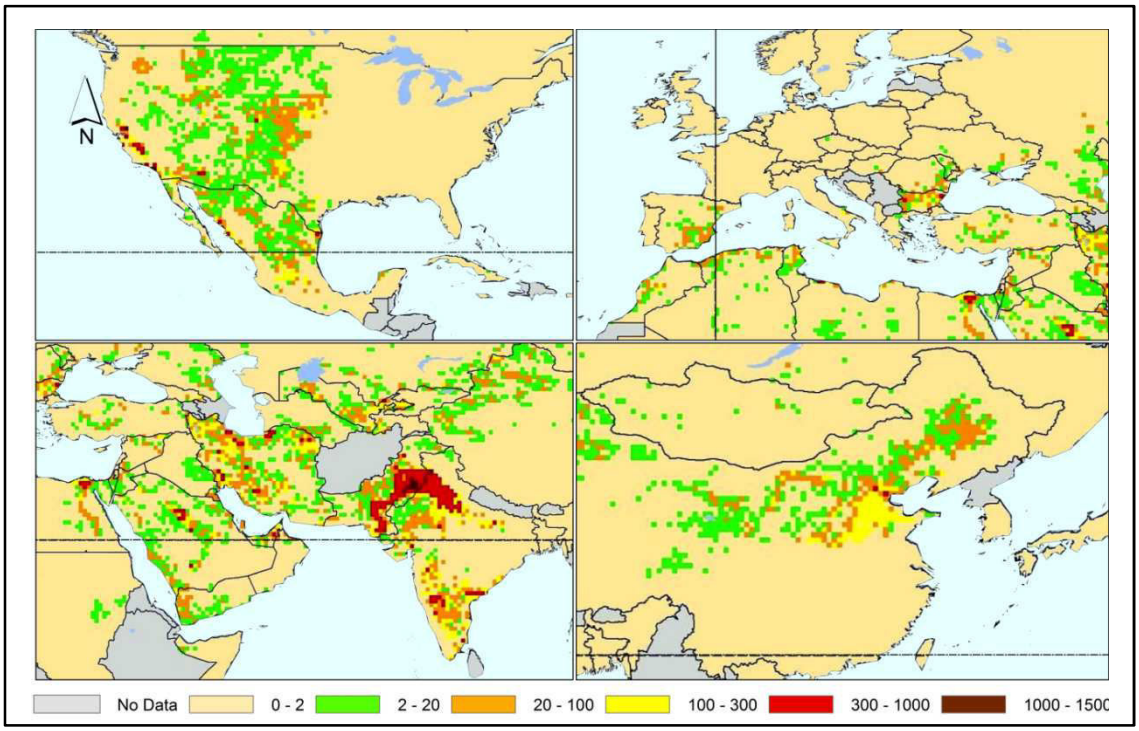

FIGURE 0.3: World map of simulated groundwater depletion in the regions of the U.S.A., Europe, China and India and the Middle East for the year 2000 (in mm/year modified from Wada et al., 2010)

On the importance of crystalline rock aquifers

Countries situated in arid and semiarid regions are the most dependent on groundwater for their water supply. However, a substantial area of the semiarid and arid regions of the world is underlain by crystalline rock in which the bulk of the available groundwater is found. Conservation management and planning of water resources is particularly challenging in these environments. This is because crystalline rock aquifers are characterized by their extremely low primary hydraulic conductivities and porosities, regardless of their origin or lithological type (UNESCO, 1999), which makes them very little receptive to the transmission and storage of water. Further, crystalline rock aquifers are complex geological formations; aquifers are often compartmentalized (Ayraud et al., 2008; Guihéneuf et al., 2014; Perrin et al., 2011; Roques et al., 2014), and their hydraulic properties vary very widely, both vertically and horizontally, due to the media's intrinsic heterogeneity (Acworth, 1987; Boisson, Guihéneuf et al., 2015; Chilton & Foster, 1995; Dewandel et al., 2012; Maréchal et al., 2004). These disadvantages are further accentuated in arid and semiarid climates. First, because storage is essential in water-scarce areas, yet as mentioned above, igneous and metamorphic rocks do not permit a sizeable subsurface storage of groundwater (UNESCO, 1999). Second, because dry conditions compounded with the high variability of rainfall events leads to non-linear recharge patterns which are heavily biased to heavy rainfall events (Taylor et al., 2012).

Also, as aridity increases, direct recharge becomes less important than localized and indirect recharge (i.e. through the beds of surface-water bodies, and depressions joints and rivulets) (de Vries & Simmers, 2002), which is more difficult to quantify and less spread-out.

The fact that crystalline rock aquifers are poor water reservoirs can dampen the agricultural development potential of the regions that rely on them and prevent them from attaining the level of socio-economic affluence enjoyed by other regions that have access to sustainable and reliable water supplies (UNESCO, 1999). Despite the existing research in this field, groundwater flow and transport in crystalline rock are still not fully understood. To give a few examples, the processes that control recharge quantities and distribution (in both time and space) in crystalline environments remain of keen interest in the scientific community (e.g. Clark & Douglas, 2000; Gleeson et al., 2009; Jiménez-Martínez et al., 2013; Neves & Morales, 2007; J Perrin et al., 2012; Rohde et al., 2015). Similarly, determining the limits of admissible groundwater withdrawal (or artificial storage potentials) is still a matter of widespread debate (e.g. Hammond, 2018; Piscopo & Summa, 2007; Sarma & Xu, 2014; Van Tonder et al., 2001); and the study of pollutant and tracer transfer dynamics in these environments still provides fertile ground for current and future research (e.g. Guihéneuf et al., 2017; Levison & Novakowski, 2012; MacQuarrie & Mayer, 2005; Shapiro, 2001; see Neuman, 2005).

India, where about two thirds of the geographical areas are underlain by hard rocks, best exemplifies the challenges and implications characteristic of fractured crystalline rock water resources. Unfortunately, this country has become infamous for having some of the world's most severe aquifer over-exploitation problems in the world (Rodell et al., 2009; T. Shah et al., 2012) with the result that 54% of the territory faces high to extremely high water stress (Shiao et al., 2015).

The Indo-French Centre for Groundwater Research

It is in this context that the *Indo-French Center for Groundwater Research* (IFCGR) was created in 1999. It is the result of cooperation between the French geological survey (or BRGM, *Bureau de Recherches Géologiques et Minières*) and the *National Geophysical Research Institute* (NGRI). The IFCGR is situated within the NGRI campus in Hyderabad, the capital of the state of Telangana. One of the main objectives of this collaboration is to better understand hydrogeological processes in fractured crystalline rock. To date, a substantial amount of data has been obtained by instrumenting and monitoring at different scales several sites in Archean granitic terrain, two of which were used for this thesis (see Maréchal et al., 2018).

The first is the Maheshwaram catchment, situated South-East of Hyderabad. It covers an area of 53 km^2, and represents a typical inhabited catchment in granitic terrain.

The many field surveys and publications carried out at this site since its establishment have allowed researchers to ascertain many of its characteristics (such as the hydraulic properties of the aquifer and its overlying soils, its geology and aquifer structure, and many others) greatly facilitating the elaboration and validation of models and hypotheses for medium to large-scale processes.

The second is the Choutuppal experimental site, a highly instrumented and continuously monitored observatory. This site is equipped with 30 borewells over a surface of about 40 hectares, and allows the detailed analysis of medium to small-scale processes. As with the Maheshwaram catchment, previous studies have provided a good estimation of the site's characteristics and hydraulic properties. In 2016 the latter was equipped with a Managed Aquifer Recharge (MAR) basin. This basin was built as part of a much broader project launched by the Indian government, which aims to alleviate groundwater overexploitation. To do so, the aim is to increase aquifer recharge from 9% of total rainfall under natural conditions to 15% by 2020 (Government of Andhra Pradesh, 2003) through the development of large-scale MAR schemes. The Central Ground Water Board has proposed the building of 11 million MAR structures nation-wide, as well as the reparation, renovation and restoration of the already existing structures, the total costs tallying up to over 12bn USD (Central Ground Water Board, 2013). The Choutuppal site thus provides an exceptional opportunity to study the efficiency of this remediation technique and the potential of crystalline aquifers as artificial reservoirs.

Objectives

This thesis focuses specifically on the problem of recharge which is among the most important components of the groundwater budget. Analyzing, quantifying and mapping recharge processes is essential to both better our understanding of fractured crystalline rock aquifers and for the improvement of groundwater management strategies. For example, the study of recharge can help in defining sustainable yields and storage potentials, in the prevention of groundwater pollution, and can assist in the location of high and low yielding areas to optimize borewell and MAR placement. The overarching goal of this research is to improve our understanding of recharge, both natural and artificial, in fractured crystalline aquifers under semi-arid conditions and weathering processes. To that end, data from present-day monitoring, and datasets and outputs from previous studies were combined to produce an up-to-date detailed analysis of the factors controlling recharge distribution and water flow propagation at medium and large scales. Numerical and analytical models were used to integrate the different sets of available data into saturated and unsaturated hydrogeological models of varying complexity, which in turn allowed us to better understand how and where recharge occurs in heterogeneous fractured media.

Part I

THEORETICAL DESCRIPTION OF NATURAL AND ARTIFICIAL RECHARGE IN FRACTURED CRYSTALLINE ROCK

Chapter 1
Groundwater resources in fractured crystalline rock

1. Geography of fractured crystalline rocks

A large portion of the earth's surface (about 34%; Blatt & Jones, 1975) features igneous and/or metamorphic rocks (i.e. crystalline rocks) which outcrop or lie close to the surface under a thin layer of alluvial or glacial deposits (FIGURE 1.1; Larsson, 1984). These outcrops are particularly present in the vast Precambrian shields which are located in every continent; they occur in the American continent (Canada, Northwest of the United States, Brazil…), Asia (South India and Sri Lanka, China, Siberia…) in northern Europe (most importantly in the Scandinavian countries), central and eastern Africa, and the Pacific region. For countries situated in temperate climates with abundant and high-quality surface water, problems linked to crystalline rock as a groundwater reservoir are of little importance. Although groundwater may still be exploited in these regions, other uses of crystalline rock such as exploitation for their mineral wealth or as a building stone, or their use for storage of hazardous nuclear and chemical waste, may garner more attention. We can, for example, cite experiments performed to assess the potential for nuclear waste repository in several such regions: in the Canadian Shield (e.g. works from the URL in Canada; see Fairhurst, 2004), in the Fennoscandian shield (e.g. the Stripa Project; see Nordstrom et al., 1989), or at the Kamaishi Mine in Japan (e.g. Nguyen et al., 2001).

Nevertheless, large parts of the crystalline geological domain are located in tropical and subtropical regions where many developing countries are situated. In these cases, crystalline rock aquifers are often the only perennial source of groundwater. This is especially the case in northeastern Brazil, India, western Africa (from Senegal to Cameroon), the Red sea region, and parts of the highlands of central and eastern Africa. In these regions, the lack of reliable water supplies has acted against economic and social development by impeding proper agricultural development and by dampening the potential of other industries (such as mining) which require large amounts of processing water (Larsson, 1984). This is because compared to other types of aquifers, borewell yields in fractured crystalline environments are quite modest (from less than 2-3 m^3/h up to 20 m^3/h; Ahmed et al., 2008; FIGURE 1.2). Some cases have been found where major tectonic structures provide pathways for significant flow to take place (e.g. Neves & Morales, 2007; Roques et al., 2016; Seebeck et al., 2014), but these remain exceptions,

especially in the vast tectonically stable Precambrian shields. Despite this, their widespread presence makes them well suited to scattered settlements and small to medium cities, and has allowed certain regions to benefit from their use by contributing to the development of irrigated agriculture where surface water is limited.

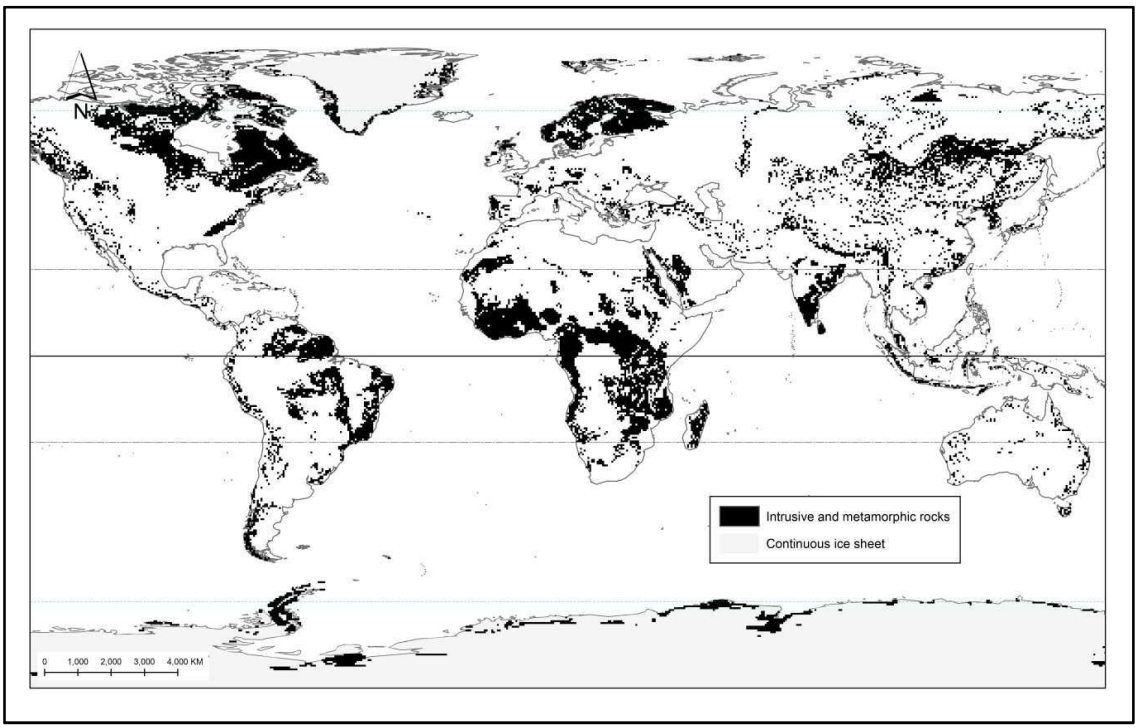

FIGURE 1.1: World map of crystalline rock distribution gridded to a 0.5° spatial resolution (data from Hartmann & Moosdorf, 2012)

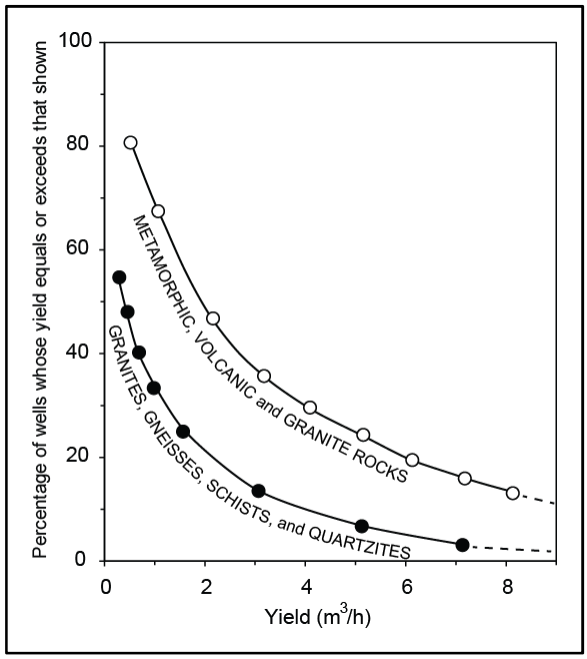

FIGURE 1.2: Relationship between well yield and lithology in Niger (modified from UNESCO, 1999)

From an environmental perspective, however, these regions are among the most fragile parts of the world (FIGURE 1.3), which puts the livelihoods of millions of people at risk. Aside from mismanagement of crystalline aquifers due to sociopolitical reasons, it is some of the hydrodynamic characteristic features of crystalline aquifers which make them most vulnerable to overexploitation and contamination. Irrespective of their origin or lithological type, crystalline rocks are defined by (see Larsson, 1984; National Research Council, 1996; Singhal & Gupta, 2010; UNESCO, 1999): (i) extremely low primary hydraulic conductivities and porosities (ii) strong heterogeneity of hydraulic parameters in time and space which leads to compartmentalization and formation of preferential flow pathways (iii) shallow occurrence of water in useful quantities which decreases in depth (FIGURE 1.4) (iv) generally poor yields (where drawdown in pumping wells is often almost equal to the saturated thickness of the aquifer). In sum, groundwater occurrence in crystalline rocks is heterogeneous, complex, and overall not very significant. The non-receptiveness of these aquifers to the ready receipt, transmission and storage of water (and thus resistance to recharge) makes them specifically vulnerable to overexploitation, while their strong heterogeneity and complexity hinders the management and implementation of responsible and sustainable water resource exploitation strategies.

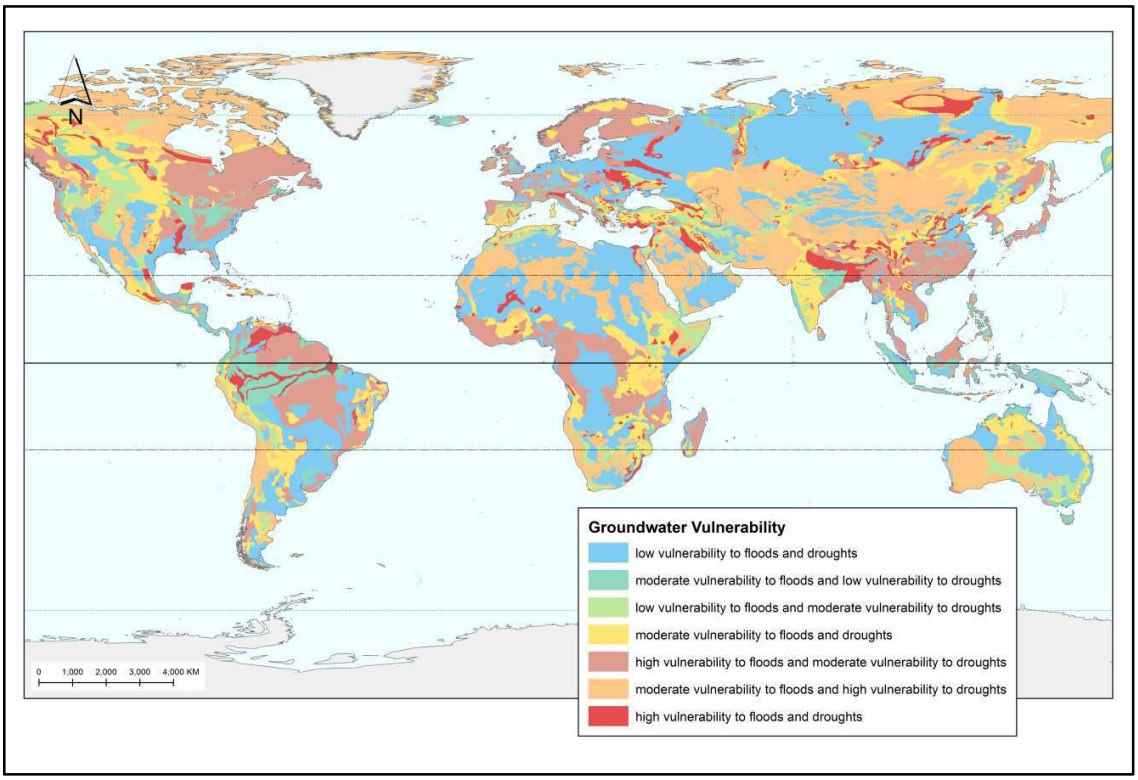

FIGURE 1.3: Global Groundwater Vulnerability to Floods and Droughts (Richts & Vrba, 2016)

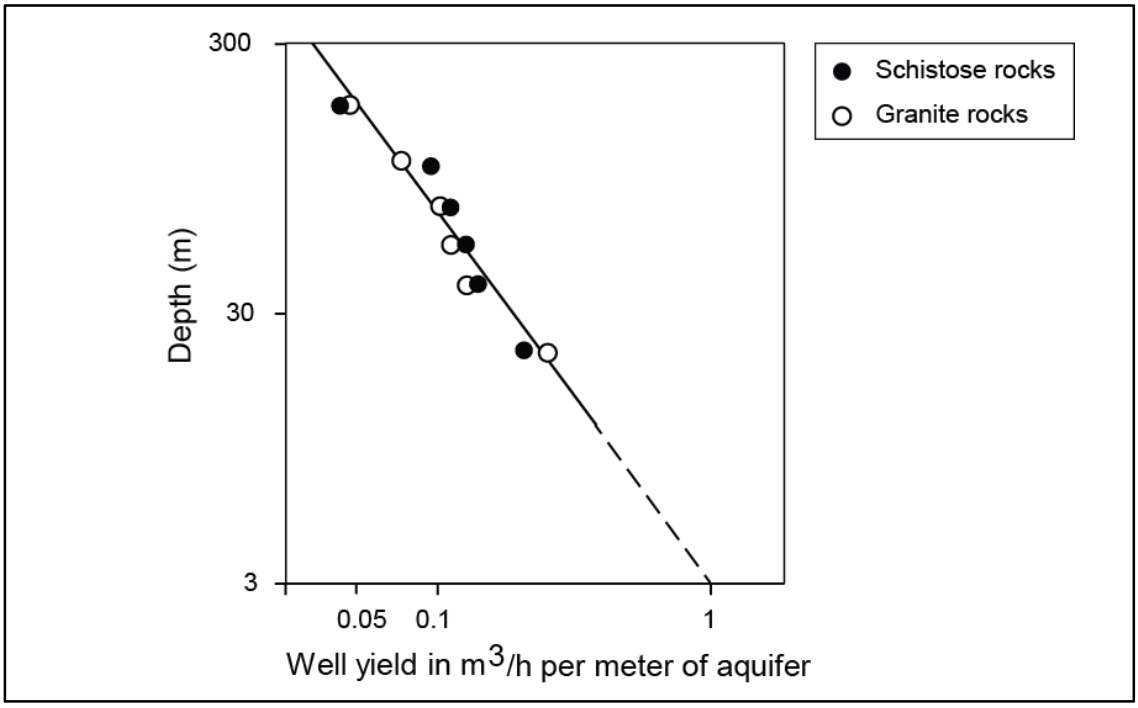

FIGURE 1.4: Relationship between well yield and depth in crystalline hard rocks of eastern United States (modified from Davis & Turk, 1964)

2. Geology of fractured crystalline rocks

2.1. Definition

Crystalline rocks are composed almost entirely of crystallized minerals without glassy matter. Intrusive igneous rocks, those that congeal at depth, and metamorphic rocks, resulting from the transformation of preexisting rocks subjected to great heat and pressure, are virtually always crystalline. This thesis will focus specifically on intrusive igneous rocks. Also termed plutonic rocks, these rocks are formed from magma that cools and solidifies within the Earth's crust, where temperatures and pressures are much higher than at its surface. This leads the hot magma to cool slowly and crystallize completely, thus prompting the growth of minerals large enough to be identified visually with a microscope (i.e. phenocrysts; FIGURE 1.5). Intrusive igneous rocks are composed of many kinds of minerals, but the dominant ones are invariably quartz, plagioclase feldspar, and potassium feldspar (Migoń, 2006). Minerals of the mica group, muscovite and biotite, often occur in significant proportions as well. These rocks are exposed at the surface after long periods of weathering and erosion or by tectonic forces that may push the crust upward (or a combination of the two).

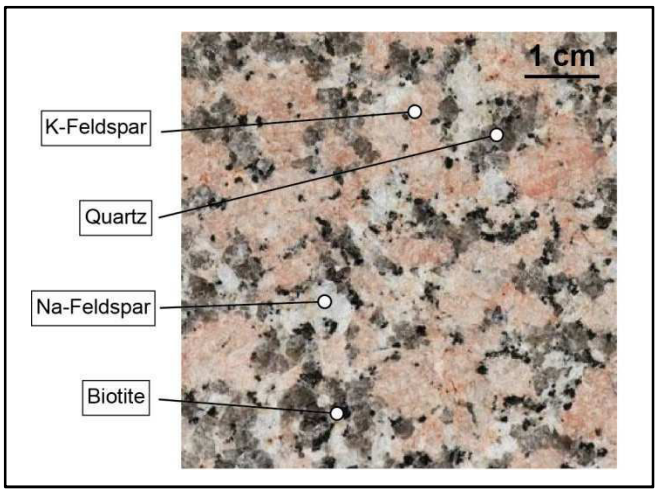

FIGURE 1.5: Typical granite mineralogy

Because of the size and contiguous disposition of crystals, plutonic rocks have negligible intergranular spacing, which is associated with almost negligible primary porosities and permeabilities: the matrix (the assemblage forming the intact rock) thus cannot contribute to groundwater resources in any meaningful way. Flow and storage in plutonic rocks is only possible if the rock undergoes chemical and physical modifications leading to the formation of fractures within these rocks (i.e. a *secondary* porosity) whose porosity is much higher than the rock's intrinsic primary porosity. The formation of a secondary porosity allows water to penetrate into the rock in sufficient amount for it to eventually be considered a reservoir.

2.2. Crystalline rock fracturing

Fractures are mechanical failures in rock that occur when local stresses exceed the breaking point of a given rock. The term "fracture" is a generic term that denotes all discontinuities within the rock, regardless of their size (which can range from under a millimeter to several hundred kilometers). There are two types of brittle fractures (FIGURE 1.6), tensile, when the displacement develops perpendicular to the surface of displacement (mode I), or shear, when the displacement develops tangentially to the surface of displacement (mode II and III).

The two main fracture-forming processes in hard rock are:

- *Weathering* is a chemical and mineralogical modification of the rock under favorable temperature and precipitation conditions, decreasing the cohesion of materials leading to fissuring of the material. By causing the dissolution and evacuation of the most soluble cations, weathering causes a change in mineralogical phases leading to the formation of clayey minerals. These minerals will then generate stress as they occupy more space than the original mineral, which will in term shatter the rock. The degree of weathering is dependent on the interplay of numerous factors, either relating to the rock itself (such as the relative surface area of the rock and its modification by mechanical weathering, the permeability of

the rock mass, its mineralogical composition…) or to the external forces driving the weathering (such as the composition, amount and distribution of percolating water, the position of the water table, the activity of the macro- and microflora and fauna in the system…) (Larsson, 1984). Weathering-related fissures form orthogonally to the weakest stress (in most cases sub-horizontally) and decrease from the top downward, generally becoming non-existent at about 50 m deep (Dewandel et al., 2006; Wyns et al., 2004).

- *Tectonic fracturing* is the formation of brittle fractures when the rock is submitted to mechanical stresses. The control of the type, distribution and degree of opening of tectonic fractures depends on their formation mechanism and their orientation with respect to the current stress field (Ashby & Hallam, 1986). The tectonic stress field consists of three principal comprehensive stresses, two of which are near the horizontal, and the third, due to the overburden load, near the vertical. The exact relationship between tectonic stress and the degree of fracture opening is however disputed, especially in the subsurface (i.e. <100 m depth), as it may be masked by other factors, such as topographic effects (St. Clair et al., 2015).

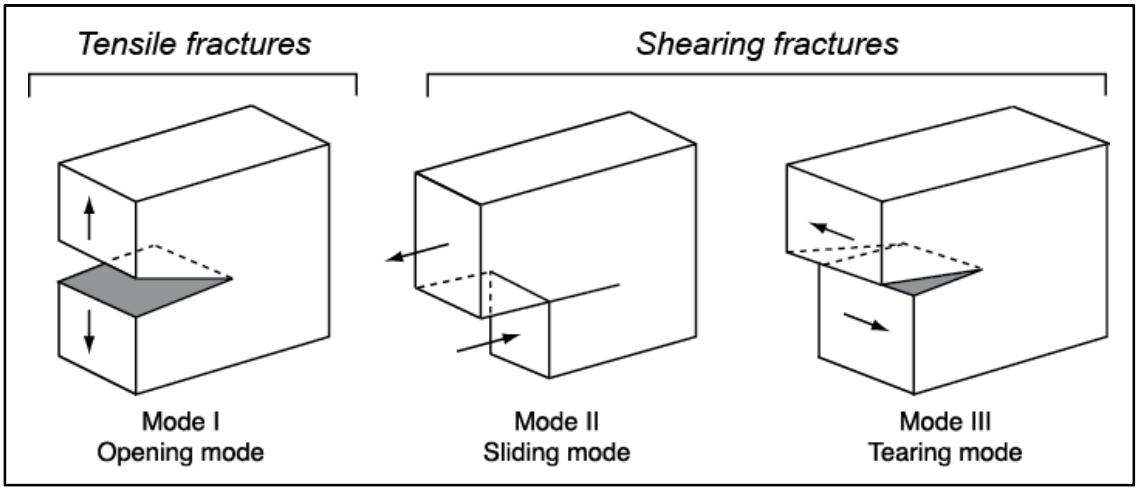

FIGURE 1.6: Relative displacements according to fracture type (modified from Martel, 2017)

In tectonically stable regions (like shield zones) the most commonly encountered fractures are mainly opening-mode (mode I) fractures which are parallel to topography. These fractures, also called exfoliation joints, break down the rock into a typical foliated structure which makes up the fissured zone of the aquifer. The foliation provides greater surface areas for subsequent chemical and physical weathering to take place, contributing to further breaking down the rock. This, in term, can lead to the *in-situ* formation of a layer of loose, heterogeneous superficial deposits called *saprolite*, which is the ulti-

mate stage of weathering. Exfoliation joints, which extend over several meters, must not be confused with a smaller-scale exfoliation phenomenon, spheroidal weathering (Ollier, 1971) (FIGURE 1.7). Mostly attributed to chemical weathering (Buss et al., 2008; Fletcher et al., 2006), spheroidal weathering leads the rock to break down in a concentric manner thus forming spherical layers of highly decayed rock (i.e. the saprolite).

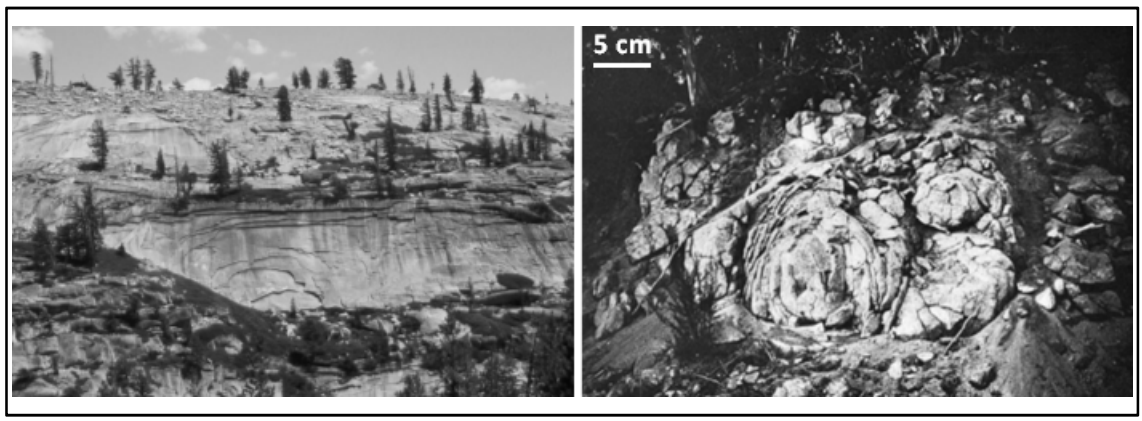

FIGURE 1.7: Photo of exfoliation joints on granite slopes (from Migoń, 2006) in Sierra Nevada, California (left) and of spheroidal exfoliation of granite in the Kosciusko area in Australia (from Ollier, 1971; right)

Several different hypotheses have been set forth to explain the formation of exfoliation joints [see Guihéneuf, 2014]: (i) gravitational unloading (discussed in Twidale, 1971), where the pressure release resulting from eroding upper layers causes the rock to fracture, (ii) weathering, causing the swelling of certain phyllosilicate minerals by hydration (most importantly of biotite) (Lachassagne et al., 2011; Wyns et al., 2004), or (iii) strong compressive stresses combined with topography (Holzhausen, 1989; Martel, 2006; St. Clair et al., 2015). Nevertheless, whatever the processes of formation of foliated structures, field observations agree on the aquifer's general characteristics. Joints are sub-horizontal or parallel to topography, generally following the surface of the body of intrusive igneous rock (the pluton). The spacing between joints increases with depth (conversely to the fracture density), ranging from a few centimeters up to about ten meters, although joints may be found up to a hundred meters deep. Fractures tend to develop until they intersect other preexisting fractures or a body of healthy bedrock.

Overall, the genesis of fractures in a geological reservoir is essential to understand its hydrological functioning. The geometrical characteristics of fractures can give clues as to the history of the lithosphere's movements and their associated stress fields. This information can in term give an estimate of the directions in which fractures develop and where the main fluid circulations take place. Depending on the determined dominating fracture-forming process, several different conceptualizations of how basement aquifers are structured may be proposed. For example, if it is assumed that the most important

water-bearing zones are tectonic open fractures (i.e. faults, mode II fractures), and that most of the subsequent fracturing of the aquifer is formed along these fault zones, then the resulting aquifer conceptualization will feature a very discontinuous aquifers (i.e. only very locally permeable) (Lachassagne, 2008), schematized in FIGURE 1.8a.

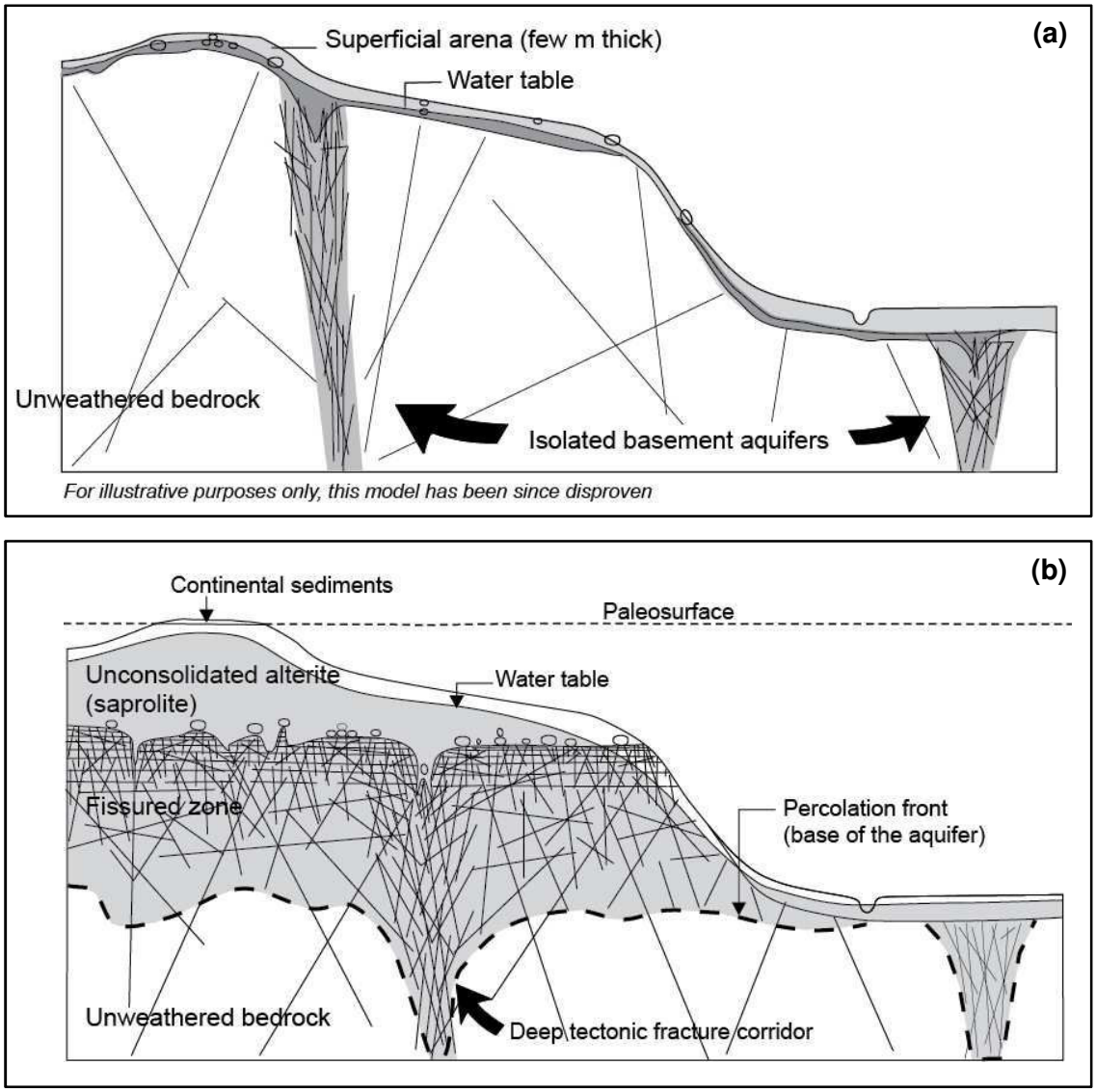

FIGURE 1.8: Conceptual model of a crystalline aquifer, **(a)** under strong tectonic constraints and **(b)** in tectonically stable, weathering-dominated areas (after Wyns et al., 2004 and Lachassagne, 2008)

Most areas where crystalline rocks outcrop, however, are generally stable areas. These zones have been exposed during very long periods, which allows for significant weathering to take place. As such, these rocks may be overlain by several meters of thick superficial weathered layer (especially in tropical areas). In certain conditions, the weathered layer can even reach thicknesses of several tens of meters, like in Nigeria and Sudan where thicknesses are reported to reach up to 50 m (Larsson, 1984). These types

of aquifer are best described by the stratiform conceptual model of weathered crystalline aquifers defined (among others) by Wyns et. al in 2004 at a plurikilometric scale (FIGURE 1.8b).

2.3. Weathering profile

The formation of a secondary porosity depends on interplay of factors that vary strongly in time and space. The process of breaking down healthy bedrock into a reservoir is strongly non-linear, and thus the resulting lithology is highly heterogeneous. Nevertheless, while there is considerable potential range in the thickness, areal extent and physical character of the weathered layer from place to place and region to region, there is a general weathering pattern in tectonically stable areas (namely the vast Precambrian shields) which leads to the typical weathering profile which will be described in full below and in FIGURE 1.9. Note that although transitions between strata may be progressive, they are generally defined as distinct entities; this is because hydraulic properties vary quite significantly along the vertical axis so this distinction is useful.

According to Chilton & Foster (1995) and Singhal & Gupta (2010) the typical lithological profile is thus composed of the following layers, from top down (FIGURE 1.9):

(1) A **residual soil** of sandy clay or clayey sand texture, no more than a few meters thick

(2) **The saprolite**, an accumulation zone for secondary minerals (i.e. clay) with subordinate silty sand and occasional rock fragments. Some stable primary minerals may be preserved in their original form. It presents a millimeter-spaced horizontal laminated structure and coarse sand-size clasts and a few preserved conductive fractures (Dewandel et al., 2006). Its thickness is quite variable, ranging from being completely absent to up to 30 meters. As we move downward the proportion of primary minerals and rock fragments increases.

(3) **The saprock**, an intermediate zone at the interface between the upper weathered layer and the underlying fractured bedrock. The rock is partially decomposed and highly horizontally fractured, weathering has taken place mainly though the main discontinuities. This layer can reach up to 20m in thickness.

(4) **The fissured bedrock**; largely unweathered, some fractures are visible towards the top, and the fracture density decreases with depth. It has very little storage potential, but permeability can be quite high within the fracture system (Maréchal et al., 2004).

The above-mentioned sequence is the result of a typical single phase weathering. However, the thickness and presence of each of these layers is dependent, on one hand,

on the intensity and interconnection of the weathering processes, but can also significantly be modified if the erosion and weathering process occurs in several phases (i.e. a multiphase process with alternation of weathering and erosion-dominated phases; Dewandel et al., 2006).

Many different descriptions of the lithology and associated hydrogeological properties of weathered crystalline rock aquifers have been published (Acworth, 1987; Boisson, Guihéneuf et al., 2015; Chilton & Foster, 1995; Dewandel et al., 2006). FIGURE 1.9 features the description made by Chilton and Foster (1995). Although there are slight differences between publications, there is a general agreement on the relative properties of each layer. The saprolite is globally characterized by a greater porosity, while its permeability is low. The bedrock, on the other hand, is defined by its extremely low hydraulic conductivity as well as porosity, except where fractures are formed. Fractures provide discontinuous areas of high permeability, but do not contribute significantly to the porosity (Maréchal et al., 2004). Finally, at the base of the saprolite, overlaying the fractured bedrock (i.e. at the interface between these two layers), is an intermediate zone ("saprock" in FIGURE 1.9) which is the most transmissive and porous zone in the aquifer. Most productive wells (for rural water supply, livestock or small-scale irrigation) tap aquifers at the saprock zone (FIGURE 1.9) of the weathered profile. If this section is dry, or the weathered layer is too thin or absent, groundwater will occur in the fracture systems of the fractured bedrock (Larsson, 1984).

The high variability of hydraulic properties results in a complex combination of diffuse recharge and preferential flows (Alazard et al., 2016; D. V. Reddy et al., 2009; Sukhija et al., 2003), where the latter have often been shown to dominate groundwater recharge processes (Cuthbert & Tindimugaya, 2010; Gleeson et al., 2009; Sukhija et al., 2003). Generally speaking, groundwater in fractured crystalline rock will move mainly within the most permeable pathways of the aquifer: these are the open fracture systems in the massive granite and the highly fractured interface (Larsson, 1984). If flow and transport of water occur mainly within these discontinuities, then the interconnection between them decides the effective porosity and permeability of a given rock mass. Interconnection between discontinuities however depends on a multitude of factors which manifest themselves across all scales, ranging from the fracture scale (e.g. fracture aperture and filling) to the landscape scale (e.g. variations in the thickness of the weathered layer). To better understand flow processes in such complex media it is necessary to understand how each scale of heterogeneity affects flow individually and as a whole.

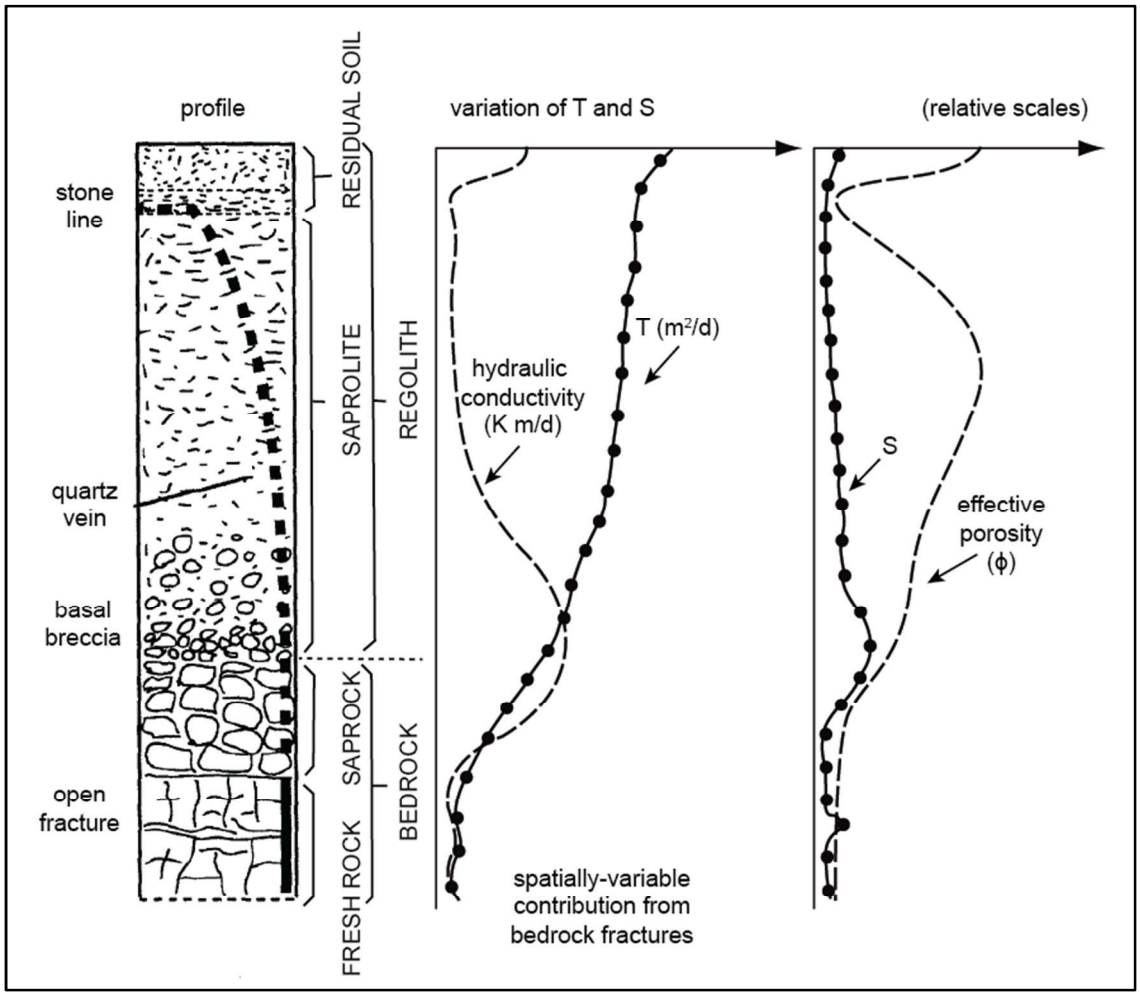

FIGURE 1.9: Conceptual hydrogeological model for the weathered crystalline-basement aquifer in Africa (modified from Chilton & Foster, 1995 and Singhal & Gupta, 2010)

3. Multi-scale heterogeneity

This part will focus on the cross-scale heterogeneity that characterizes weathered crystalline aquifers: where the heterogeneity originates, and what its impact on flow is.

3.1. Fracture heterogeneity (micro to macro)

3.1.1. Individual fractures (micro to meso)

Individual fractures have a limited spatial extent and are discontinuous in their own plane. They are characterized by their orientation (dip direction and amount), genetic nature (shear/tensile), trace lengths and fracture aperture and asperity. Flow within an individual fracture is defined by the Boussinesq equation (1868) (Witherspoon et al., 1980), also termed the Cubic Law where flow in fractures is proportional to fracture aperture and fracture length. Aperture refers to the perpendicular distance separating the adjacent rockwalls, in which the intervening space is air or water-filled (Singhal & Gupta, 2010). Aperture may increase by dissolution, particularly in the weathered zone.

To account for width variations within the fracture the term 'equivalent aperture' may also be used. Tsang (1992) introduced the term and 'hydraulic aperture', wherein he was able to estimate fracture aperture from measured transmissivities, which, based on the Cubic Law, give:

$$T_f \propto a^3 \tag{1.1}$$

where T_f is the transmissivity of the formation, a measure of how much water can be transmitted [L^2/T]. These equations are generally applicable in cases where the fracture is relatively open. Clogging (biological or mineral) and the asperity of the walls may also affect the fracture hydraulic properties and lead to local channeling effects (Sausse, 2002; Singhal & Gupta, 2010) (FIGURE 1.10). This reduces the effective porosity and makes flow velocities irregular, which may lead to an overestimation of flow by the Cubic Law (Zhang et al., 2014), and has strong implications on transport mechanisms inferred from tracer experiments (Becker & Shapiro, 2000; Guihéneuf et al., 2017).

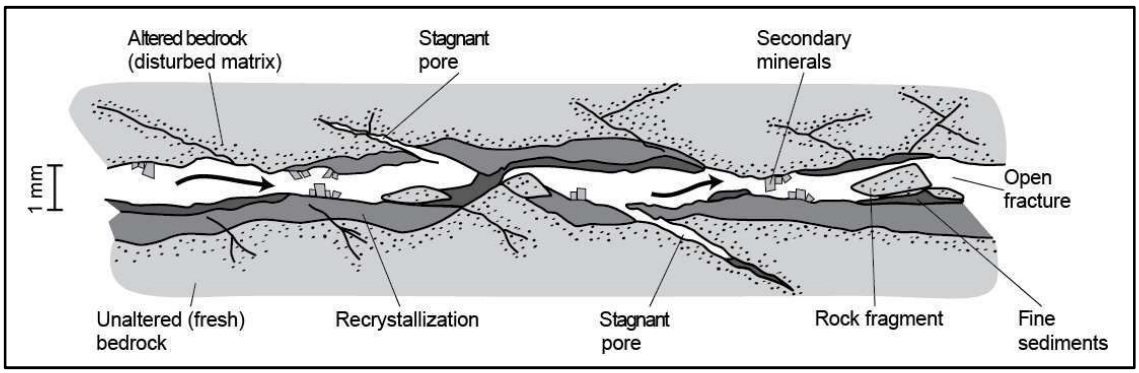

FIGURE 1.10: Fracture-scale heterogeneities, illustrated by an example in diorite in Aspö, Sweden (based on Winberg et al., 2000; modified from Guihéneuf, 2014)

3.1.2. Fracture networks (meso to macro)

By mutual intersection, various fractures form interconnected networks which allow for greater hydraulic conductivities. The way fractures are arranged (i.e. the fracture patterns and orientation) and their density will have an impact on the values and spatial distribution (heterogeneity, degree of anisotropy) of the aquifer's hydrodynamic parameters. Greater fracture densities overall lead to higher hydraulic conductivities (FIGURE 1.11). However, as was noted in 2.3 fracture density decreases with depth, which explains in part why yields decrease with depth in crystalline environments. Further, parallel fractures lead to strong anisotropies in the rock mass, whereas large numbers of more interconnected fractures tends to reduce anisotropy (Singhal & Gupta, 2010). For example, in areas where weathering processes (mostly defined by sub-horizontal fracturing) dominate over tectonic processes (where fracture directions depend on the tectonic stress

field), horizontal permeabilities have found to be 2 to 30 times stronger than vertical permeability, leading to a strong anisotropy (Maréchal et al., 2004).

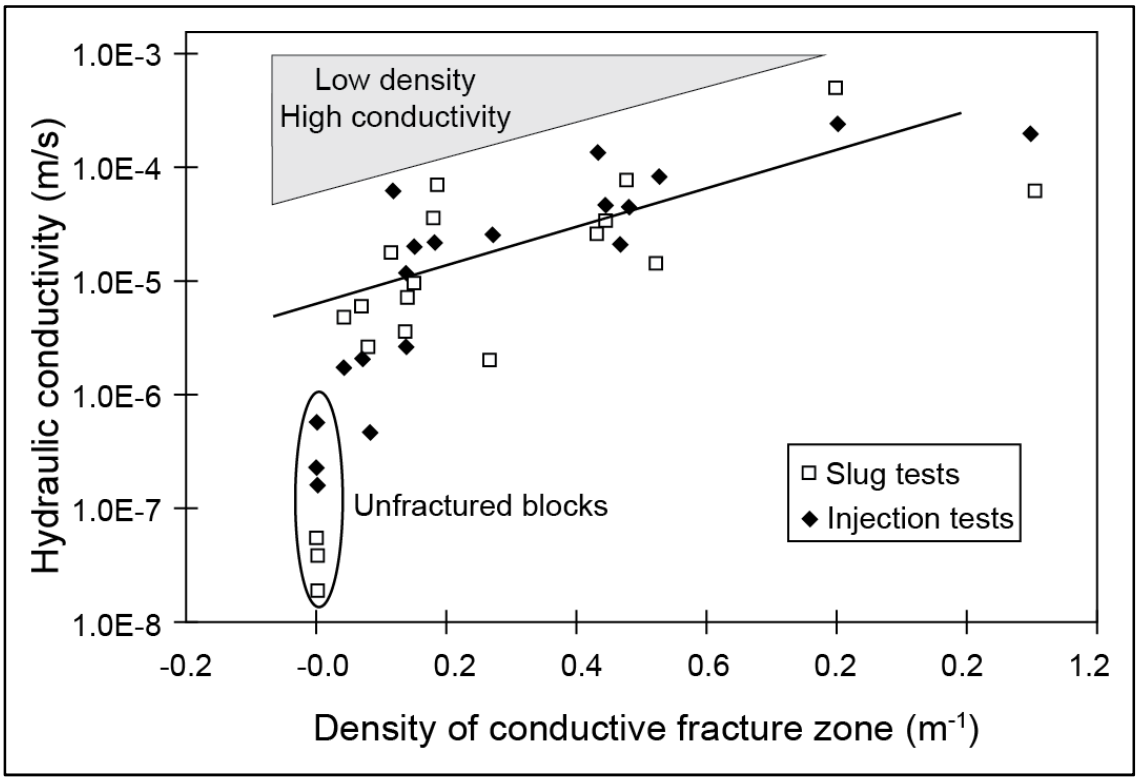

FIGURE 1.11: Relationship between fracture density and hydraulic conductivity (modified from Maréchal et al., 2004)

Another important element to consider is the scale dependence (Hsieh, 1998), which results from the presence of heterogeneity over broad ranges of spatial scales. For example, at centimeter scale, a random rock volume may appear in a number of ways: with no fractures, with one of more fractures, very highly fractured, or even as a void within an enlarged channel. As the scale of observation increases, features that are correlated over larges distances (e.g. the highly fractured saprock) tend to merge together to become a single large feature, while smaller isolated features (e.g. few interconnected fractures) lose their prominence (Hsieh, 1998). This means that using different exploration methods might lead to different conceptualizations of the hydraulic conductivity field (Hsieh, 1998) depending on the study scale. Practically speaking, different scales may be investigated using different methods: laboratory tests, for small scales, single borehole tests and cross borehole tests, for small to medium scales, and pumping tests and calibration of regional or basin scale models for medium to large scales (FIGURE 1.12).

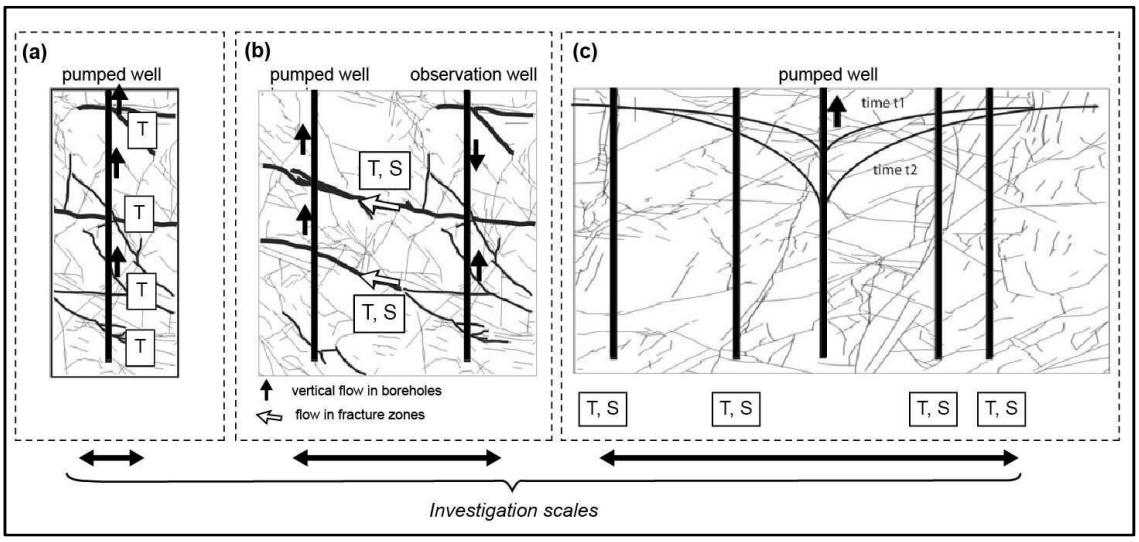

FIGURE 1.12: Illustration of some techniques used to estimate transmissivity and storage coefficient (T and S): **(a)** single borehole flowmeter test, **(b)** cross-borehole flowmeter test, and **(c)** long term pumping test with observation wells (modified from Le Borgne et al., 2006)

Many authors have undertaken this type of comprehensive study where the dependence of hydraulic conductivity to scale is evaluated by comparing the outputs of several different methods which operate at different scales (e.g. Hsieh, 1998 shown in FIGURE 1.13; Le Borgne et al., 2006; Maréchal et al., 2004; Martinez-Landa & Carrera, 2005; Rovey & Cherkauer, 1995). As an example we can cite the study by Hsieh (1998) in Mirror Lake, New Hampshire which was aimed at comparing the hydraulic conductivity at three scales (meter scale, 100 meter scale, and kilometer scale). The resulting distribution of hydraulic conductivity values spreads out over six orders of magnitude, although no significant scale effect was found. Contrariwise, Maréchal et al. (2004) showed a dependence of hydraulic conductivity to scale, where hydraulic conductivity increased with scale. They identified two scales of fracture networks, the primary fracture network (PFN), which affects the matrix at a decimeter scale by increasing the permeability and storage capacity of the blocks, and the secondary fracture network (SFN) which is responsible for the larger scale permeability of the weathered-fractured layer. The permeability of the PFN was found to be about 3 orders of magnitude weaker than that of the SFN. In sum, these studies show that scale dependence is linked to the connectivity of preferential flow paths (De Dreuzy et al., 2012), although this is still debated by some authors (e.g. Illman, 2006; Le Borgne et al., 2006; Martinez-Landa & Carrera, 2005), who have highlighted the shortcomings of applying such methodology. For example, there is no straight-forward way to estimate the true scale of influence of a given test. Further, the models often used to interpret data assume medium homogeneity, while the medium that needs to be described might be quite heterogeneous (Le Borgne et al.,

2006). To overcome the latter, one option is to build large-scale models that incorporate point values and geological information concerning connectivities (Martinez-Landa & Carrera, 2005). To do so, some authors have opted for Discrete Fracture Network (DFN) models, which account explicitly for fracture network connectivity (e.g. Davy et al., 2010; De Dreuzy et al., 2012; Long & Witherspoon, 1985). Fortunately, numerical simulations have also found that permeability is susceptible to vary with scale, and that these scale effects are more significant if there are transmissive zones that are long enough to bridge fracture intersections within a fracture plane.

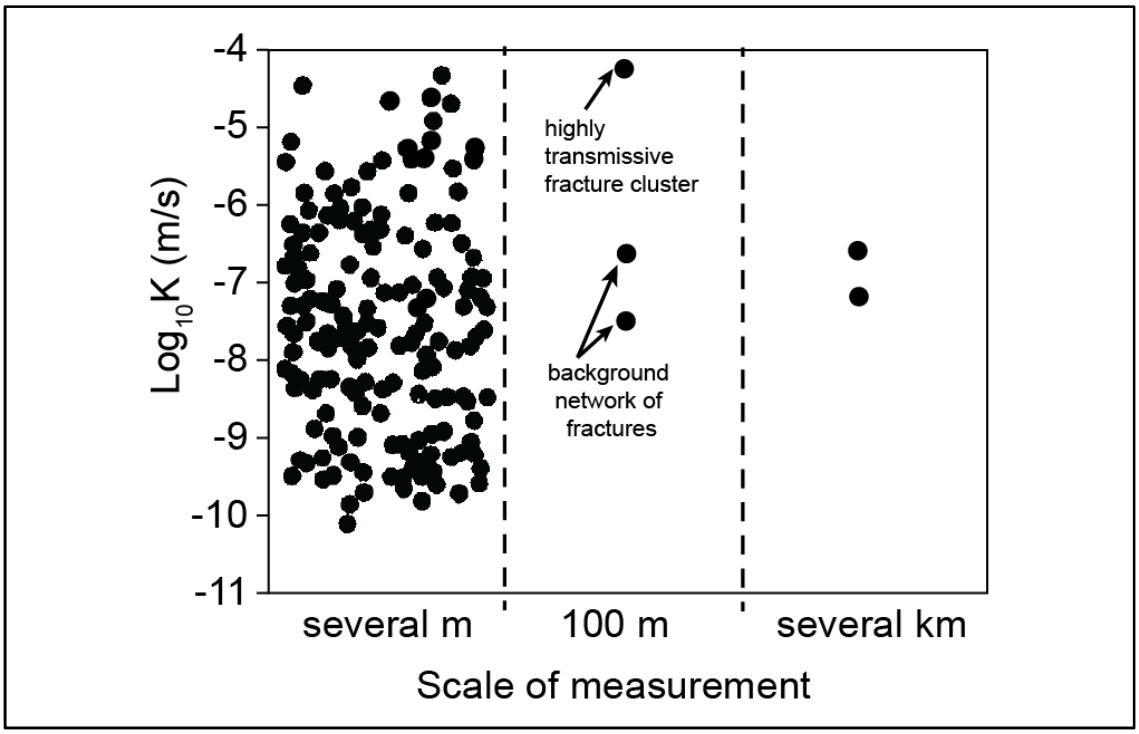

FIGURE 1.13: Relationship between scale of measurement and hydraulic conductivity (modified from Hsieh, 1998)

3.1.3. Scaling up fracture properties

It follows from the above paragraphs that fractures exist over a broad range of scales, ranging from the rock grain to the scale of tectonic plates. Interestingly, it has been found that the characteristics that determine groundwater flow in crystalline rock (e.g. fracture density, aperture, connectivity) scale as fractals (Bonnet et al., 2001), which means that fracture patterns at one scale are in many cases relatively similar to patterns at an entirely different scale. These similarities provide a rationale for extrapolating pattern data from one scale (preferably at which fractures may be easily described) to another (such as a larger scale where fracture networks are difficult to characterize). Many studies have examined how to quantitatively scale fracture data (e.g. Bour et al., 2002; Gillespie et al., 1993; National Research Council, 1996 and references therein). The existing fractal methods are however still regarded as experimental for several reasons, such

as the difficulty to test it rigorously, as cataloging all fractures at all scales is not feasible, or because a single technique can yield significantly different spatial distributions of fractures. So far, stochastic methods which blend aspects of deterministic methods and fractal scale methods (e.g. Cacas et al., 1990; Darcel et al., 2003; Molz, 2004) are the most promising (National Research Council, 1996).

3.2. Landscape scale heterogeneities (macro)

Regional and catchment-scale conceptualizations of crystalline aquifers pose a significant challenge, particularly in the assessment of the structural controls on groundwater flow related to the multi-scale heterogeneity of this type of medium (Comte et al., 2012). To do so, two aspects need to be taken into account: the geological setting that defines the geometry of the hydrogeological environment (i.e. structure, the static properties), and the spatial and time variations of available water (i.e. recharge, the dynamic properties) (Krásný, 2002). This part will focus on the former.

As we have seen, the main sources and reservoirs of groundwater in crystalline rock are the weathered layer and fractures. In view of this, the large-scale geometry of the aquifer can be dissected as, on one part, the heterogeneity and anisotropy of fracture systems at the meso- and macro-scale (see above), and, on the other, the heterogeneity of the geological structure and weathering patterns at the macro-scale (Comte et al., 2012). Weathering patterns at the macro-scale shape the landscape. They determine the landform sequences, where each landform type has a general groundwater potential, and they determine the thickness, extent and characteristics of the weathered layer. These, in turn, depend on several factors (i) climate (both past and present), where significant rainfall contributes to thicker weathered layers, (ii) topography, where weathered layers are mainly formed in erosional peneplain areas of low relief, (iii) the lithology and texture of the parent rock, and (iv) the time span involved in weathering.

3.2.1. Landforms and drainage network

The most commonly developed landforms in crystalline rock are structural hills, inselbergs, pediments, buried pediments, and valley fills. Their characteristic features are [see Singhal, 2010] (FIGURE 1.14):

Structural hills These large-scale structures outcrop after combined processes of tectonism and denudation. These rocks are hard and compact, and thus act as run-off zones and have negligible groundwater potential. Some infiltration may take place in fractures and joints, which may then either discharge as springs or as seepages along the valley portions. **Inselbergs** are small residual hills which stand above the general level of the surrounding erosional plains.

Pediments Formed due to the process of denudation, these broad, flat, or gently sloping areas develop at the base of mountain fronts or plateau escarpments.

Groundwater potential of these units is limited due to the thinness of the weathered material. **Buried pediments** form when the sloping surface of the pediment gets gradually covered with soil and colluvial material. These areas form better groundwater potential zones as they have a better retention capacity and storage volume.

Valley Fills As pedimentation progresses, channel deposits may develop. These areas are characterized by gentler slopes, and better water retention. They are the most important landforms for groundwater development.

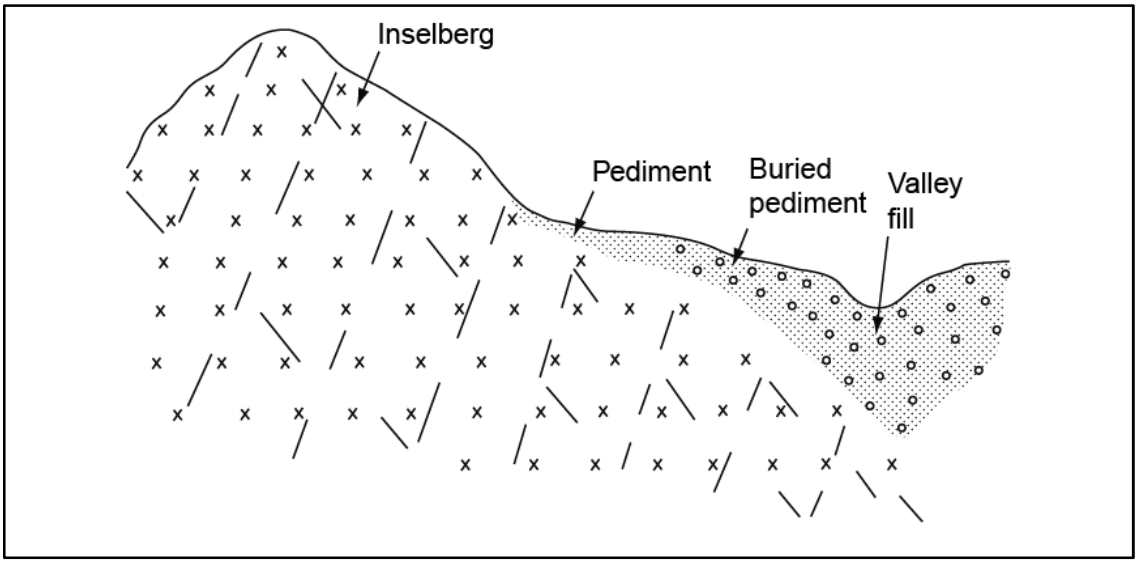

FIGURE 1.14: Schematic profiles of landforms in a crystalline rock terrain; note that weathering patterns within the depositional landforms are not illustrated here (modified from Singhal & Gupta, 2010)

The drainage characteristics of a basin, specifically the drainage pattern and density, are also useful in the assessment of groundwater resources. Drainage patterns are the spatial arrangement of streams, which can be studied and mapped on topographic maps, aerial photographs or satellite images. Dendritic drainage patterns (irregular, branching of streams, resembling a tree) are typical of massive crystalline rocks, while rectangular/angular patterns (streams have right-angled bands) are indicative of fractured rocks. Drainage density, D_d, is the ratio of total channel lengths of streams within a basin to the area of the basin. Generally speaking, low densities are characteristic of regions with highly resistant or permeable surfaces and low reliefs, while high drainage densities are found in regions of weak or impermeable rock (Strahler, 1964). Among drainage network characteristics, other factors such as basin shape, stream frequency and bifurcation ratio are of hydrological interest (Singhal & Gupta, 2010)

3.2.2. Weathered layer

To contain enough water to be considered a groundwater reservoir, the weathered layer must attain a minimal areal extent and thickness, and have sufficient permeability and porosity to store and yield water (Larsson, 1984). Extensive and thick weathered layers thus generally make up the most viable and productive aquifers. Thin weathered layers, on the other hand, may not possess significant storage possibilities, but can sustain perennial aquifers, provided they are high recharge zones (natural or artificial).

At the regional scale (i.e. several hundred km), the thickness of the weathered layer is controlled by the climate and the geodynamic conditions. The thickest weathered layers generally develop in subhumid and humid tropical regions (where annual rainfall exceeds 1000 mm). For example, in the savannah belt of West Africa (Ghana, Ivory Coast, Togo, Benin), where the average annual rainfall is of about 1100 mm, weathered layer thicknesses can reach several tens of meters. Some semiarid regions also feature thick weathered layers which are due to past climate conditions. For example, in Rajasthan (western India), weathered layers are as much as 25 to 30 m thick even though annual rainfall is only about 400 mm: this is because the development of these profiles occurred during warm pluvial cycles of the Pleistocene (Larsson, 1984). Weathered layers may also be eroded during or after their formation, so the ratio of the weathering rate must be greater than that of the erosion rate (Dewandel et al., 2006). At smaller scales (i.e. landscape), differences in weathered layer thickness may be attributed to topography and stage of geomorphic evolution. The most extensive and thickest layers are commonly found in erosional peneplains of low relief. The fraction of erosional residuals (hills and inselbergs) over the total peneplain depends on the age of the geomorphological cycle, where older ages are linked to smaller percentages of erosional residuals (Larsson, 1984).

4. Aquifer conceptualization

The challenge posed by the multi-scale variations of hydrogeological properties (from micro- to macro-scale) has made characterization of aquifers at large scales very difficult. In homogeneous mediums, Representative Elementary Volumes (REVs) are commonly employed: the hydraulic conductivity is assumed to vary with scale until it reaches a limit over which the conductivity is constant. An REV is thus the smallest sample volume which is representative of the rock mass. In fractured media, the absence of a characteristic length scale often precludes the definition of an REV that can be used to extrapolate to larger scales (Comte et al., 2012; Long et al., 1982), or the REVs are considered too large to be useful (FIGURE 1.15). However, if the scale of the study is sufficiently large (i.e. catchment or regional scale), and if there are no major faults, then REVs may be useful.

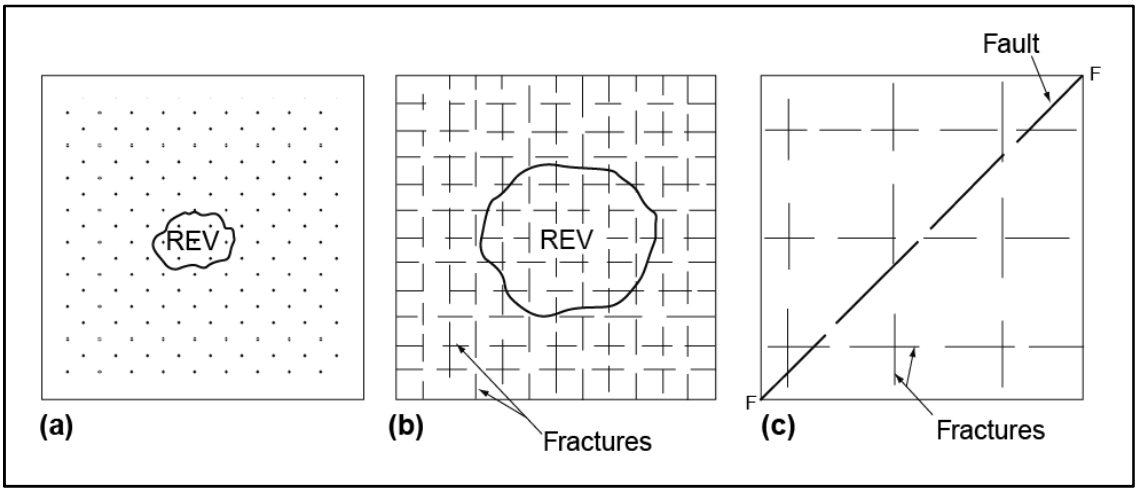

FIGURE 1.15: REV in different rock conditions: **(a)** homogeneous porous rock, **(b)** fractured rock where REV includes sufficient fracture intersections, and (c) rocks with large scale discontinuities where REV is either very large or nonexistent (from Singhal & Gupta, 2010)

Generally speaking, fractured rock aquifers are represented using one of the following model types: (a) equivalent porous medium, (b) discrete fracture network (DFN), (c) a dual porosity medium, or (d) a stochastic continuum (SC) model (Singhal & Gupta, 2010). Intermediate approaches exists as well, which consist of identifying the dominant fractures and including them in a continuum model as two dimensional features (Carrera & Martinez-Landa, 2000). Although a full description of each model type is out of the scope of this thesis [for this see Jing, 2003; National Research Council, 1996], a brief overview is given below and in FIGURE 1.16:

(a) Continuum approximations are based on considering the fractured media as an equivalent porous media, assuming Darcy's law to be valid in every point

of the flow domain (mass conservation principles can thus be applied to derive conventional flow and transport equations) (Carrera & Martinez-Landa, 2000). Individual fractures are not explicitly treated, and hydraulic properties express volume-averaged behavior of many fractures. The most appealing feature of this approach is it simplicity where high resolution fracture data is not necessary. It generally applied only for large scale calculations of flow only, transport cannot be satisfactorily modelled assuming a continuum.

(b) Discrete models consist of impervious blocks separated by fractures, so that the system is entirely controlled by the properties of the fractures. These types of models are essentially stochastic in that all fractures cannot be characterized accurately, so instead statistical properties are used (Carrera & Martinez-Landa, 2000).

(c) If the rock matrix containing the fracture network has a relatively significant amount of inter-granular permeability (such as sandstones) then the medium will exhibit two flow systems (or two overlapping continua), one pertaining to the porous rock matrix, and the other to the fracture network. To simulate this, both the fracture and block parameters must be defined, as well as exchange rates between them (Singhal & Gupta, 2010; Warren & Root, 1963). This is the double porosity approach.

(d) Stochastic continuum models are based on the notion that a formation may be described in term of physical parameters that vary in space according to spatially varying random functions. The parameter heterogeneity is treated in a statistical/probabilistic framework.

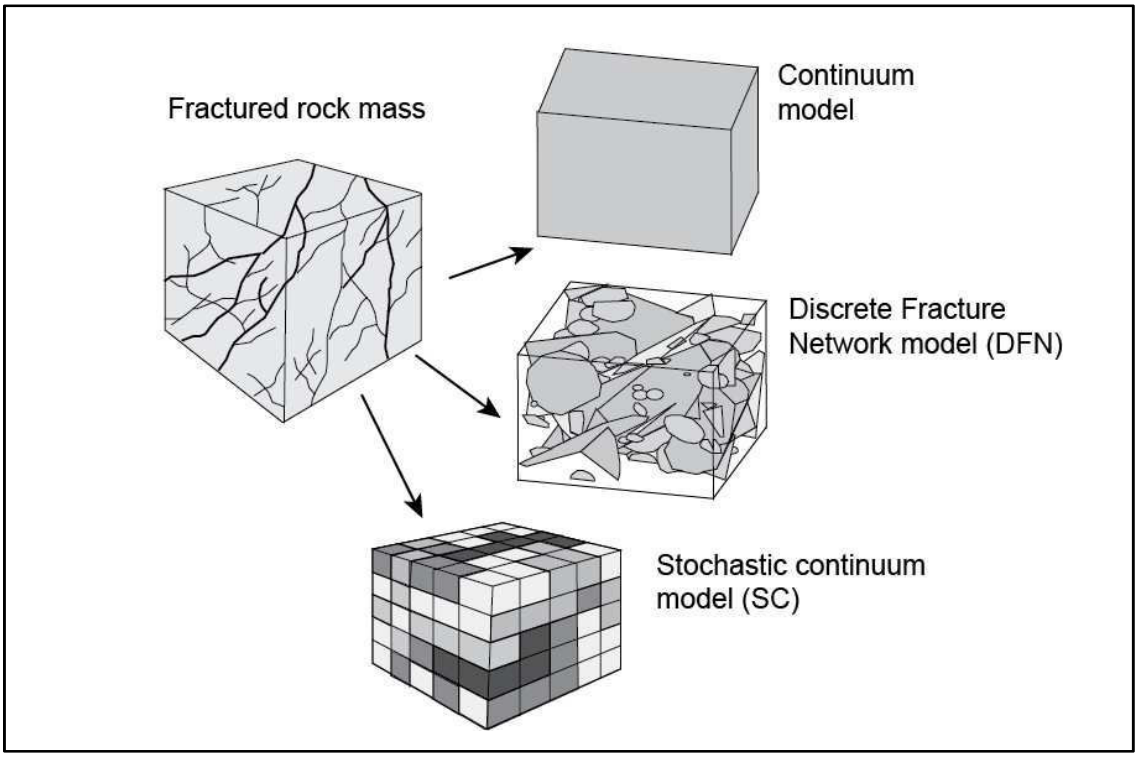

FIGURE 1.16: The three most common model concepts for numerical modelling of groundwater flow and transport through a body of rock with fractures (modified from Swedish National Council for Nuclear Waste, 2001)

Unfortunately, discrete approaches rely on high resolution characterization of structural properties and their incorporation in often computationally expensive models (Comte et al., 2012). Accurately describing cross-scale fracture networks, especially over extended areas, poses many issues (Neuman, 2005): information collected along surface outcrops may not be representative of conditions inside the rock mass, yet geophysical tools used to access information on the subsurface often do not have the precision required to register individual fractures. The most important difficulty, however, is that geology and geophysics alone provide limited quantitative information about fracture apertures of the kind required to assess fracture flow and transport parameters (Neuman, 2005).

As such, continuum approaches are more commonly adopted for macro-scale hydrogeological studies. Highly weathered aquifers, specifically, are often described as multi-layered and the hydraulic properties correlated to the nature of the unit (see 2.3). In fact, the upper weathered layer (the saprolite) and the saprolite/bedrock interface (the saprock), given their advanced level of disaggregation and relatively high permeabilities (mostly within the saprock), are often assimilated to a homogeneous porous medium when considering flow only (e.g. Cook et al., 1996; Kirkby, 1988; Li et al., 1997). Transport simulations, however, often require considering a double porosity to account

for storage effects in the matrix (e.g. Reedy et al., 1996; Van der Hoven et al., 2003). Recent studies (Guihéneuf et al., 2014) have shown that, under high water-level conditions, most of the flow takes place in the well-connected highly permeable pathways (FIGURE 1.17a). Contrariwise, under low water-level conditions, the aquifer becomes highly compartmentalized, flowing only within fracture networks and thus limited by their extent and connectivity (FIGURE 1.17b).

Nevertheless, regional and catchment-scale conceptual modelling of hard-rock aquifers remains a challenge in the hydrogeological sciences; particularly in the assessment of the structural controls on groundwater flow related to the multi-scale, heterogeneity of fractured rock (Comte et al., 2012). This includes the arrangements between the different lithological units, the heterogeneous relief of the well-connected bedrock/saprolite interface, as well as local heterogeneities such as deep weathered intervals associated with regional fracture zones.

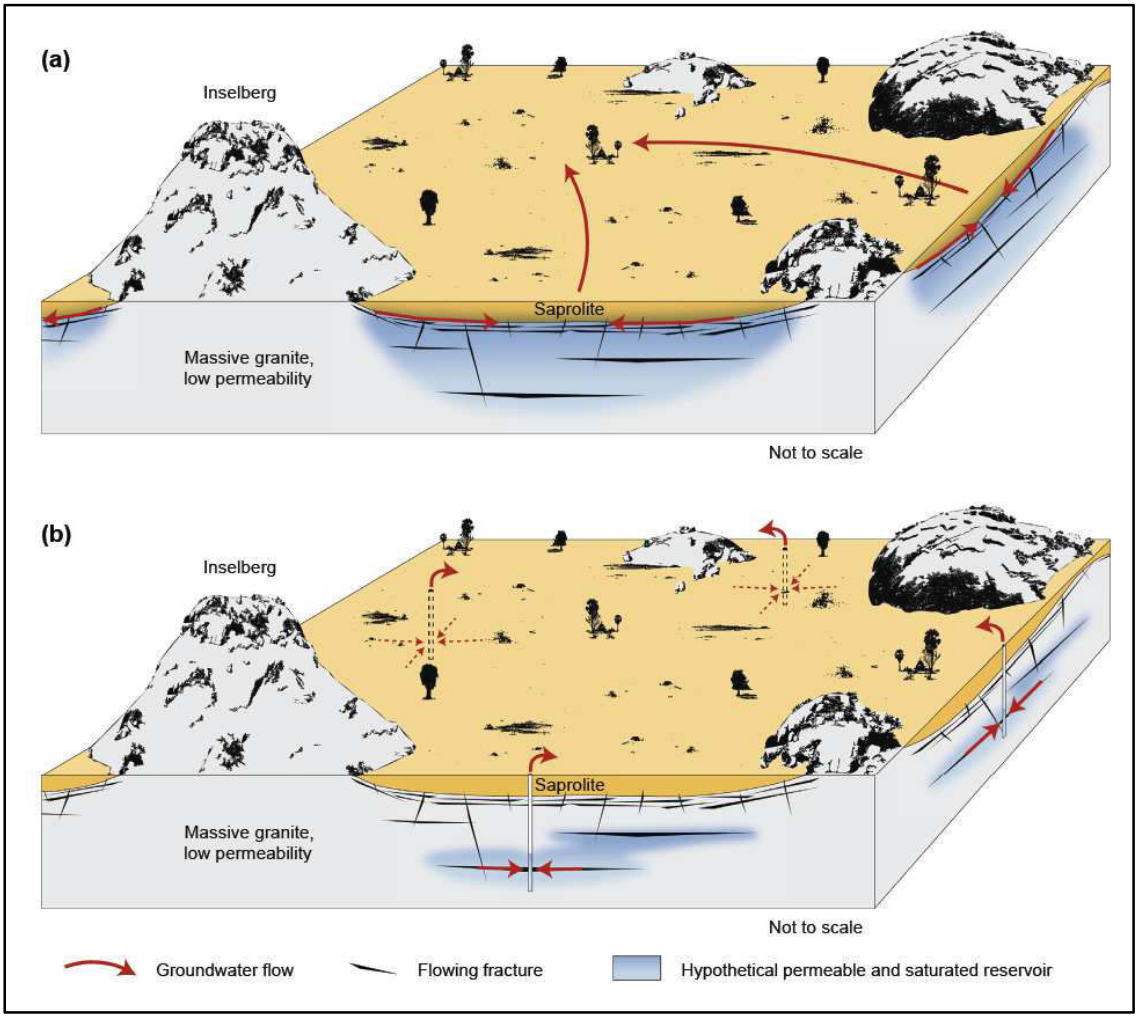

FIGURE 1.17: Conceptual groundwater flow model at the watershed-scale as a function of water level conditions: **(a)** under high water level conditions and **(b)** under low water level conditions (from Guihéneuf et al., 2014)

Chapter 2

Aquifer recharge and the water cycle

Water moves continuously on, above, and below the Earth's surface. It moves from one reservoir to another, such as from river to ocean, or from the ocean to the atmosphere. A portion of continental water drains back to oceans in the form of discharge, either on the surface (through runoff) or underground (through deep groundwater flow). Acting as a counterpart to these discharge processes is *recharge*, which represents the replenishment of aquifers that is critical to maintaining water supplies and ecosystems. This process usually occurs either naturally as part of the water cycle, or artificially when rainwater and reclaimed water are intentionally rerouted to the subsurface for management purposes (i.e. "artificial recharge"). The relative magnitudes of recharge and discharge rates give a basic indication of the health of the aquifer and related systems. Some authors, in fact, argue that recharge is the single most important factor in the analysis and management of groundwater resources, especially in arid and semi-arid regions, yet it is also usually the least well-known quantity in hydrogeology (Kinzelbach et al., 2002).

Generally speaking, the continuous use of groundwater in excess of recharge is called groundwater mining or overexploitation, and leads after some time to adverse effects such as regional water-table declines, saltwater intrusions, mechanical problems such as land subsidence, and many others. Across the globe many countries are reporting declining water levels in their major aquifers at various rates. In some countries, even, the groundwater being exploited is "fossil" water, meaning it will never again be replenished, at least not on a human timescale. All major aquifer depletions are due to groundwater use for irrigation, by far the largest groundwater consumer. As such, the problem of groundwater is also a problem of food security (Kinzelbach et al., 2002).

Accurate estimation of groundwater recharge is thus essential to proper management and protection of valuable and vulnerable groundwater resources. Furthermore, accurate recharge quantification is a key component in any model of groundwater flow, and may be useful for contaminant transport modeling. Delineating zones of low recharge is important for radioactive and hazardous waste disposal, while delineation of zones of high recharge is critical to determining zones that are vulnerable to contamination [see Scanlon et al., 2002 and references therein].

In this chapter recharge will be defined in context with the global water cycle. A brief description of the different components of the water cycle will be given, with emphasis on infiltration and runoff, their intensity and distribution being strongly correlated to recharge processes. Finally, a detailed description of the different types of recharge, their driving mechanisms and the overall global recharge distribution will be given.

1. The water cycle

1.1. Generalities

1.1.1. Global water stocks and fluxes

Of all freshwater on earth, about two thirds are ice, and one third is non-solid water. Groundwater accounts for about 30% of all freshwater resources, and for almost 99% of all non-solid freshwater resources, followed by lake water (about 0.8%), most of which is interrelated to groundwater, soil water (about 0.2%), and river water (about 0.02%) (Gleick, 1993; Oki, 2006). In temperate and humid environments, most surface discharge originates from groundwater (Seiler & Gat, 2007), while in (semi-)arid climates surface discharge most often contributes to groundwater. TABLE 2.1 shows an estimate of water distribution on the globe. This table features only an approximation of the order of magnitude of each value, as estimates vary quite largely depending on the authors.

Water source	**Water volume (10^3 km^3)**	**% of freshwater**	**% of unfrozen freshwater**
Oceans, Seas, & Bays	1,338,000	--	--
Ice caps, Glaciers, & Permanent Snow	24,064	68.71	--
Ground water	23,400	--	--
Fresh	10,530	30.07	98.8
Saline	12,870	--	--
Soil Moisture	17	0.049	0.16
Ground Ice & Permafrost	300	0.86	--
Lakes	176	--	--
Fresh	91	0.26	0.85
Saline	8	--	--
Atmosphere	13	0.037	0.122
Rivers	2	0.006	0.019
Biological water	1	0.003	0.009
Wetlands	17	--	--

TABLE 2.1: Estimate of global water distribution (percentages are rounded so will not add to 100) (from Oki, 2006)

While the quantification of water resource stocks may be useful in giving an idea of the distribution of water resources across the globe, a more adequate measure of water availability are the global *fluxes* (FIGURE 2.1). This is because, in contrast to other geological deposits of economic value, water circulates, forming closed hydrological cycles. These cycles result in the renewal of water resources in relatively short spans of time, ranging from a few days to a few years (although it can be much longer, see TABLE 2.2). To give an example, even though river water at any given moment in time accounts for only 2,000 km^3 of continental freshwater, annual discharge is actually about 44,800 km^3/year.

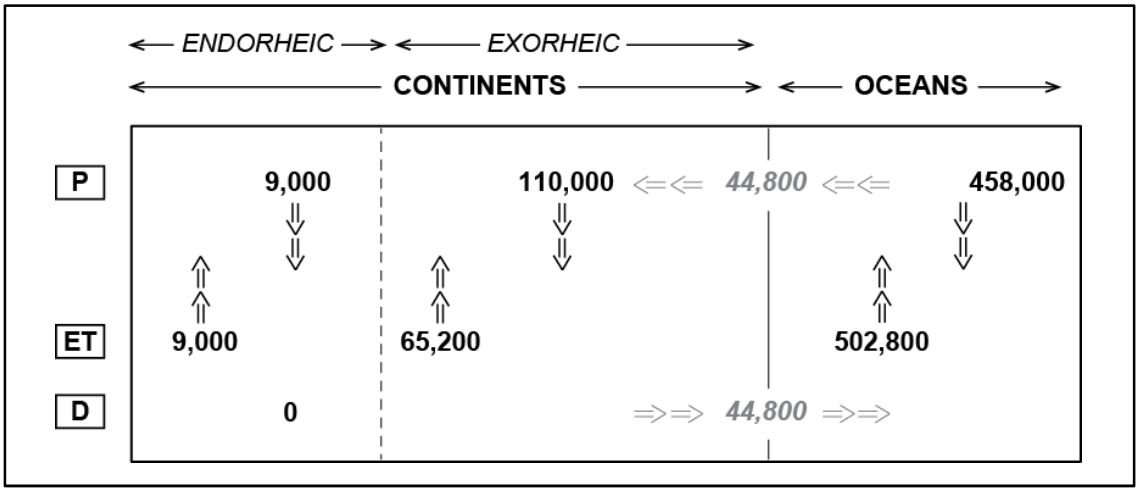

FIGURE 2.1: Schematic diagram of the hydrological cycle fluxes in km^3/year (modified from Seiler & Gat, 2007); P refers to precipitation, ET to evapotranspiration and D to discharge.

When considering water fluxes as the most relevant measure of water availability, the speed of water circulation becomes crucial. Mean residence times of water molecules—i.e. how long they stay in a given reservoir—can be estimated by dividing the volume of the reservoir by the main flux into and out of it. Rivers unaffected by human use have a mean residence time of about two and a half weeks. In contrast, groundwater aquifers may recharge at very slow rates, with mean residence times going from a few weeks up to hundreds of thousands of years, depending on the overall volume of the aquifer (TABLE 2.2). Aquifers with very long residence times are sometimes called fossil or ancient water, and are often considered to be a non-renewable resource. Accumulation of water in such reservoirs either took place over very long periods of time, or took place under past climate conditions. Fossil water must be exploited cautiously to avoid negative feedbacks. It is estimated that less than 6% of groundwater is "modern", meaning that it was recharged within the last 50 years through the present water cycle (Gleeson et al., 2016).

Water reservoir	Approximate residence times
Atmosphere	A few hours to a few days
Continental glaciers	A few hundreds to thousands of years
Surface waters	A few days to a few months
Aquifers	A few weeks to a few hundreds of thousands of years

TABLE 2.2: Approximate residence times in the main water reservoirs (from Gilli et al., 2016)

Unfortunately, despite progress in the definition and determination of sustainable pumping rates, non-adapted management and excessive demand have become evident in many parts of the world. For example, the Yellow River runs dry over increasing periods of time (Fu et al., 2004), the Aral Lake and Dead Sea are shrinking at an alarming rate (Micklin, 2007; Salameh & El-Naser, 2000), and many parts of India (Rodell et al., 2009), the Middle East and North Africa region (Lezzaik & Milewski, 2018), among many others, are facing continuous groundwater level declines.

1.1.2. The global hydrological cycle

The global hydrological cycle, which ensures renewal of freshwater sources, is simply the circulation of water between ocean, atmosphere and land (FIGURE 2.2). This cycle is driven by the latent-heat energy provided by the sun which generates kinetic energy, mixing water vapor in the atmosphere and driving the cycle against the pull of gravity. Water evaporates from the ocean surface, and goes into the atmosphere where it circulates in vapor form depending upon temperature gradients and wind velocity. Under suitable atmospheric conditions, the vapor condenses, which forms precipitation in the form of rainfall or snow, some of which will reach the land surface. Part of this precipitation is immediately intercepted by the canopy, and quickly rejoins the atmosphere by evapotranspiration. The rest of the water which reaches the land surface will either drain as surface flow or runoff, or seep into the ground by infiltration. Part of this infiltration will then reach the water table (i.e. *recharge*), thus being added to the groundwater reservoir, while the rest either returns to the atmosphere through the process of evapotranspiration, or flows laterally in the unsaturated zone under the existing hydraulic gradient to be discharged into the stream. Infiltration can be a diffuse process (piston flow[1] through the unsaturated zone), or it can be focused following water accumulation in depressions and rivulets, or in drainage networks (infiltration then takes place in the riverbed). Of the water which reaches the groundwater reservoirs, a part will also flow lat-

[1] Piston flow is when water added to the soil surface moves downward by pushing the older water beneath, in turn will pushing still older water further below, thereby ultimately adding water from the unsaturated zone to the groundwater reservoir.

erally under its hydraulic gradient to be discharged to rivers, lakes, or oceans as *baseflow*. More detail on the different components of the water cycle, namely runoff and infiltration, can be found in Section 2 of this chapter and on recharge processes in Section 2.5 of this chapter.

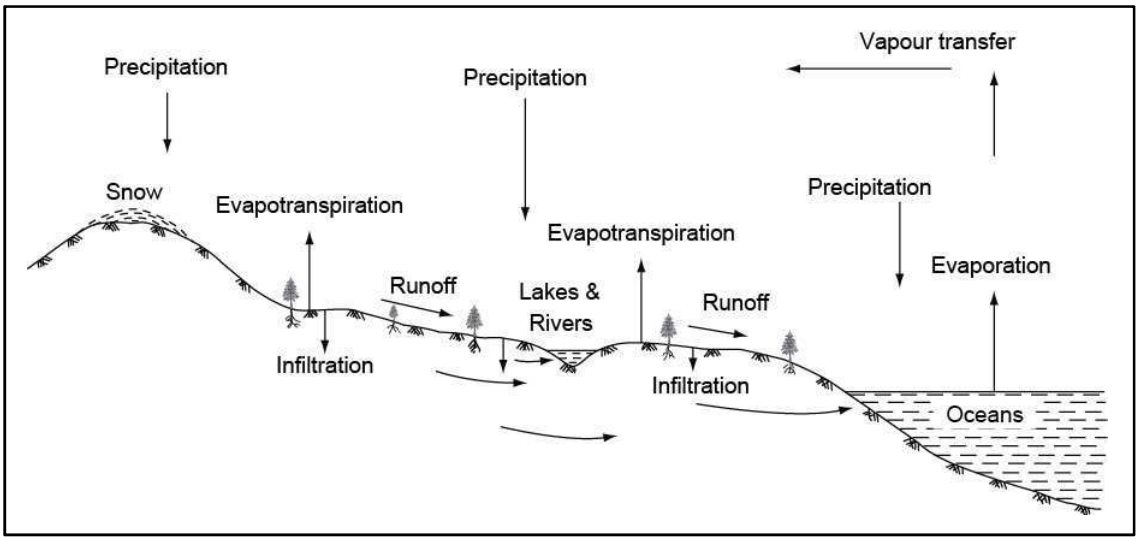

FIGURE 2.2: Schematic diagram of the hydrological cycle (from Singhal & Gupta, 2010)

The water cycle can be divided into two components, continental and oceanic, which are interconnected (FIGURE 2.1). Most of the water that evaporates over oceans falls back as precipitation in this same reservoir. Only about 9% (about 45,000 km^3) of the water vapor of from oceanic evaporation precipitates on continents; this water eventually returns as surface or subsurface run-off to the oceans (in exorheic areas, meaning externally drained). There is also an endorheic water cycle branch (meaning a closed system, with no outflow), the intra-continental cycle, which includes some of the world's biggest endorheic lakes, like the Aral Lake, the Baikal Lake and the Dead Sea (Seiler & Gat, 2007).

According to Seiler & Gat (2007) the water cycle in humid temperate and tropical climates appears mostly at steady-state[2] at the century scale (although to a lessening degree if one considers the increasing effects of climate and land-use change), while in (semi-)arid environments, or at shorter time-spans, it often appears transient. Further, groundwater management and use often contribute a man-made transient behavior to groundwater flow, which is not always immediately discernable (Seiler & Gat, 2007). By means of water quantities, the main sources and sinks in the water cycle are oceans. On

[2] A system or process is in a *steady-state* condition if the variables (called state variables) which define the behavior of the system are unchanging in time. If a system is not at stead-state, i.e. a process variable has been changed, then the system is said to be in a *transient* state.

long timescales, the naturally waxing and waning ice shields and permafrost areas also act as a significant source and sink term of the water cycle and produce ocean level fluctuations of 150 to 200 m compared to the present ocean level. On short timescales, however, these variations are not discernable compared to inter- and intra-annual climate-related variations (Seiler & Gat, 2007).

1.2. The "Water Budget Myth"

In the past, it has been widely accepted that the maximum rate of pumping (i.e. the sustainable pumping rate) should be more or less equal to the rate of "virgin" recharge. Recent studies have since challenged this common misconception, which has been dubbed "The Water Budget Myth" (Bredehoeft, 2002; Devlin & Sophocleous, 2005; Zhou, 2009). According to these authors, sustainable pumping rates have little to do with natural recharge, and instead depend on "capture" induced by pumping. "Capture" refers to the increased recharge (for example, resulting from induced recharge from surface water bodies) and decreased discharge (for example through the interception of groundwater discharging to streams) resulting from groundwater pumping. Some authors, in fact, have stated that recharge estimates are virtually unnecessary when it comes to defining sustainable extraction rates (Bredehoeft, 2002). Bredehoeft's island aquifer illustrates this concept well (Bredehoeft, 2002). In this example, a land mass is surrounded by a lake and underlain by an aquifer (FIGURE 2.4). Under natural conditions, the aquifer receives recharge from rainfall and discharges into the lake. If the aquifer is however pumped, the capture zone may go past the island boundaries, therefore reversing the role played by these boundaries. Lake water may begin to enter the system, and thus a discharge boundary then becomes a recharge boundary.

This statement has been moderated in more recent studies: despite the evidence supporting the idea that virgin recharge rates may be irrelevant to sustainable pumping, this is not always the case (Zhou, 2009), and this does not signify that recharge rates are irrelevant to *sustainability* (Devlin & Sophocleous, 2005). Sustainability here refers to a broader concept, which encompasses, for example, water quality, ecology, and socioeconomic factors. Indeed, even if a pumping rate is sustained by capture, the capture may cause depletion of stream flows, drying of springs and loss of riparian ecosystems and wetlands. Finally, these authors insist on the importance of recharge in numerical modeling of groundwater: any modern assessment of groundwater sustainability requires a recharge component to assess the behavior of the aquifer and its sustainable pumping rate (Devlin & Sophocleous, 2005; Sophocleous & Devlin, 2004).

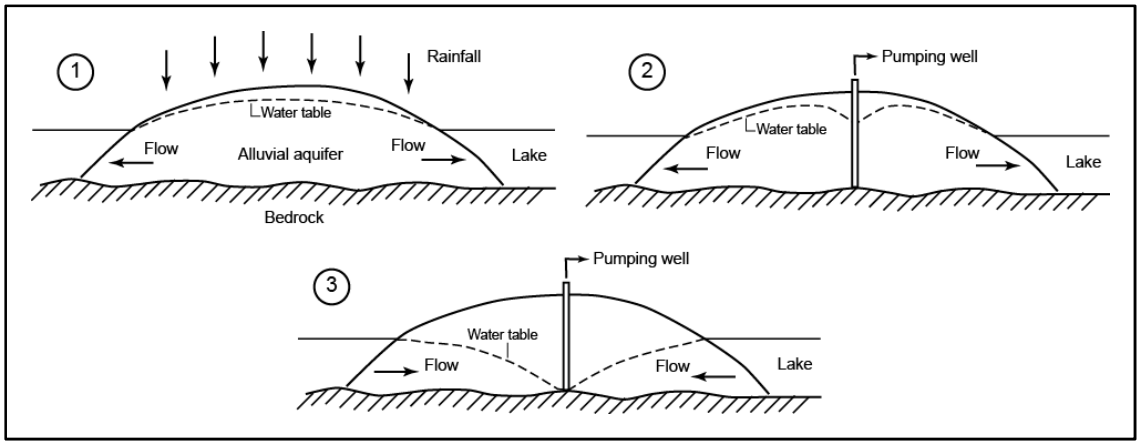

FIGURE 2.3: Schematic cross-section of an aquifer situated on a circular island in a freshwater lake being developed by pumping (modified from Bredehoeft, 2002)

2. Components of the water cycle

The various components of the hydrological cycle are described briefly below.

2.1. Precipitation

Precipitations (P) are the result of condensation of water vapor around hygroscopic nuclei (i.e. particles that capture moisture from the air) in the atmosphere. The recharge-runoff relationship depends on the intensity and frequency of precipitation events: rainfall of moderate intensity will generally be more effective for groundwater recharge, while short rainfall spells of high intensity will generate more runoff than infiltration (Singhal & Gupta, 2010). Rainfall is measured using rain gauges and is expressed in terms of water depth, generally in mm or cm. Areal distribution of precipitation and precipitation rates are influenced by topography, air temperatures, frontal activity (the interactions between air masses of different density) and wind directions in relation to moisture sources. The seasonal distribution of precipitations has important hydrologic and climatic implications; this is especially the case in monsoon climates present in much of Asia and Africa, where the seasonality of precipitations is particularly pronounced (Dingman, 2015).

2.2. Evapotranspiration

Evapotranspiration (ET) consists of two components, evaporation, which is the loss of water to the atmosphere due to vapor pressure gradients between the water surface and the air, and transpiration, which is the use of water from vegetation when the vapor pressure in the air is less than in the leaf cells (Singhal & Gupta, 2010). The amount of evaporation is controlled by several climatic factors, such as temperature, wind velocity, and humidity. Evaporation from soils decreases with depth, and also depends on the

depth of the water table relative to the ground surface (Coudrain-Ribstein et al., 1998) and type of soil (Jalota & Prihar, 1986) (FIGURE 2.4). The amount of transpiration depends on the type, density and size of plants, as well as on the factors influencing evaporation. Evaporation and transpiration are difficult to consider separately, which is why the conjunctive term *ET* is most often employed. Thornthwaite (1948) introduced the term Potential evapotranspiration (*PET*), which is the maximum water loss by evapotranspiration if the soil has sufficient water to meet the demand. It is different from Actual evapotranspiration (*AET*) which is the amount of water which *actually* evapotranspired under the existing field conditions, usually about 50-90% (although it can be much less) of the potential value (Singhal & Gupta, 2010). *AET* may be *energy-limited*, meaning *P* exceeds *PET*, or *water-limited*, where *PET* exceeds *P*. In water limited environments (i.e. subhumid to arid climates) *AET* losses can be quite significant relative to total rainfall. In fact, these zones are defined by a *P* to *PET* ratio below 0.75 (Cherlet et al., 2018; TABLE 2.3). *PET* is thus greater than *P* most of the year, so most infiltration is episodic occurring only in short and unpredictable intense rainfall events (Gee & Hillel, 1988).

	P/ET ratio	**Rainfall variability in % of the average**
Hyper-arid	<0.05	100
Arid	0.05–0.02	50–100
Semi-arid	0.02–0.5	25–50
Sub-humid	0.5–0.65	<25

TABLE 2.3: Classification of different forms of aridity (Cherlet et al., 2018)

Free water surface evaporation (from surface-water bodies) is generally measured using evaporation pans. *AET* losses in soil are often estimated by performing experiments under various soil moisture and vegetative cover conditions. Historically, *AET* measurements have mostly relied on the use of lysimeters (e.g. Liu et al., 2002; López-Urrea et al., 2006), although flux tower measurements have gained popularity in the past years (e.g. Li et al., 2011; Ramoelo et al., 2014). Empirical formulae are also developed to estimate *AET* from readily available meteorological data such as temperature, wind speed and humidity [see Dingman, 2015]. General areal *AET* patterns are correlated to mean annual temperature distributions and overall available water. At the global scale, the highest *AET*s occur in the tropical rainforests of South America, Africa and Southeast Asia while the lowest *AET*s occur in the Sahara Desert, Antarctica, arctic North America and central Asia.

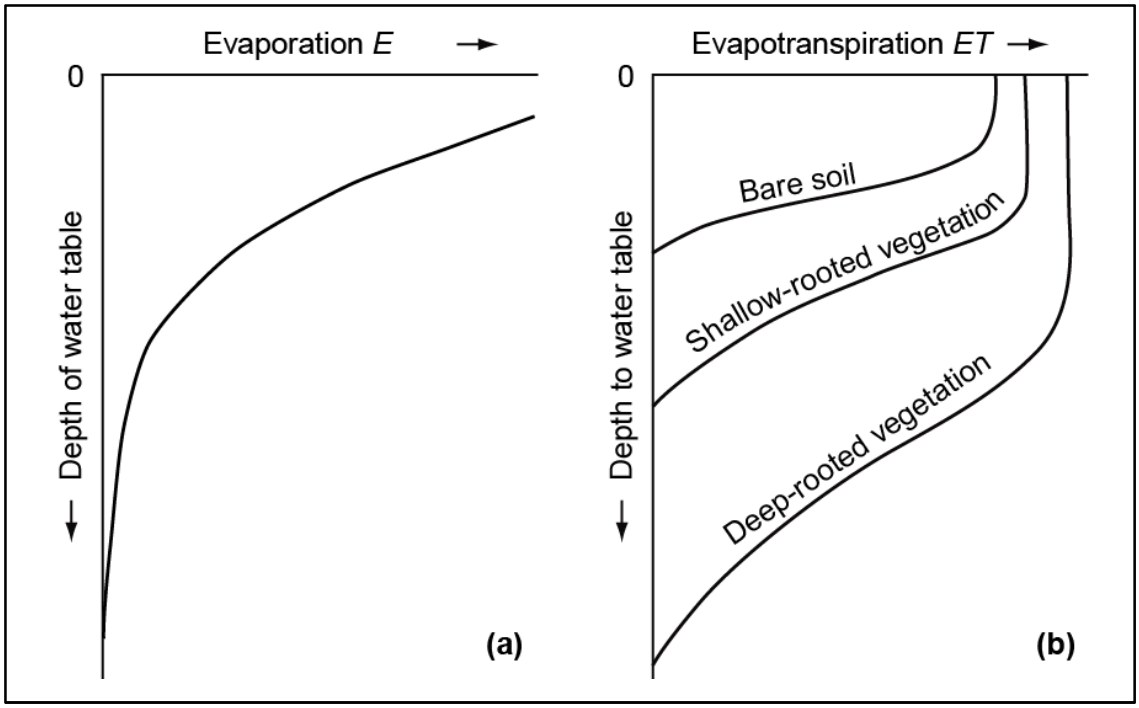

FIGURE 2.4: Relationship between (a) depth of water table and rate of evaporation (modified from Chen & Cai, 1995) and (b) depth of water table combined with terrain conditions on evapotranspiration (from Bouwer, 1978; modified by Singhal & Gupta, 2010)

A full description of the physics of evaporation and transpiration is beyond the scope of this thesis, but for more information readers are referred to any hydrology textbook which addresses this subject in full (e.g. Dingman, 2015; Fetter, 2000).

2.3. Runoff

Runoff is the part of precipitation not ultimately evaporated or transpired, most of which is returned to the oceans through streams and groundwater outflow (Dingman, 2015). In practice, runoff is divided in two parts: indirect runoff and direct runoff. Direct runoff is composed of *overland flow* (or surface runoff, the excess flowing overland when rainfall can no longer infiltrate), *interflow* (water flowing laterally in the unsaturated zone), and *channel precipitation* (rainfall falling directly onto a stream) (TABLE 2.4). The remaining runoff is indirect runoff, made up of *event flow* and *baseflow*, which is the portion of groundwater which feeds into the stream.

Generally speaking, runoff amounts and patterns are controlled by topography and climactic factors–such as rainfall patterns and intensity and temperature (which controls evaporation and snow/ice melt)–and by vegetation and land use (Castillo et al., 1997; Dunne et al., 1991; Puigdefábregas, 2005). Inter-annual variations of these factors lead to a certain degree of seasonality in runoff patterns, the degree of which depends on the general climate. In humid and temperate climates, streamflow is generally present year-

round. Contrariwise, in (semi-)arid climates seasonality is so pronounced that streamflow may be episodic, as the conditions required to accumulate water in sufficient quantities to sustain flow are only met a few months or days per year: these are referred to as "ephemeral streams". Intermediate poly-zonal streams exist as well, with a source area in wet or cold climates and a downstream sink area in dry-lands (e.g. the Nile and the Yellow River) (Seiler & Gat, 2007).

I. Channel precipitation
II. Overland flow (surface runoff)
A. Hortonian overland flow
B. Saturation (Dunne) overland flow
III. Subsurface flow
A. Flow in the saturated zone
1. Baseflow
2. Event flow
B. Flow in the unsaturated zone (interflow)
1. Matrix (Darcian) flow
2. Macropore flow

TABLE 2.4: Classification of flow mechanisms that produce event responses (from Dingman, 2015). Processes underlined with a solid line pertain to the "direct runoff" category, and those underlined with a dashed line to "indirect runoff".

2.3.1. Overland flow

Overland flow, also called surface runoff, occurs when rain or snowmelt accumulate on a sloping surface. The soil can become saturated either from above (*Hortonian overland flow*), when the rainfall rate exceeds the infiltration rate, or from below (*Dunne overland flow*) when the water table rises to the surface (Dingman, 2015).

2.3.1.1. Hortonian overland flow

Hortonian overland flow (FIGURE 2.5a) is a process of saturation named after Robert E. Horton, a civil engineer and soil scientist who described this process in a series of papers (Horton, 1933, 1945). Hortonian overland flow occurs when water inputs exceed the saturated hydraulic conductivity of the surface; this forms a wetting front which progresses downslope, and if input persists long enough, the surface soil becomes saturated and the water that accumulates on the surface becomes runoff (Dingman, 2015). Hortonian flow is typically important in (i) (semi-)arid regions where rainfall tends to be intense and surface conductivities low due to a lack of vegetation, and (ii) regions where surface conductivity is either naturally very low or has been reduced through soil frost of human and animal activity (Dingman, 2015).

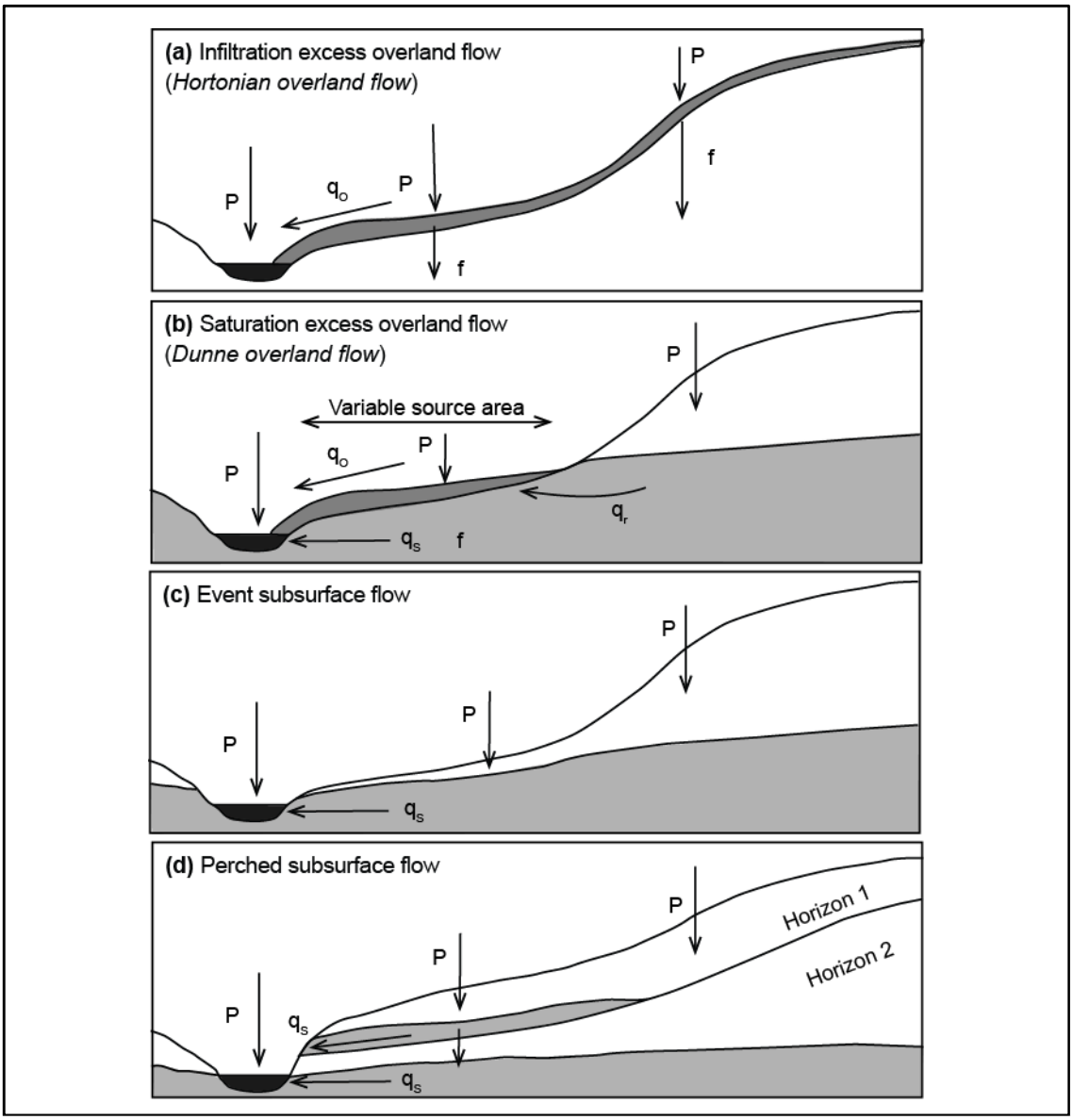

FIGURE 2.5: A classification of process mechanisms in the response of hillslopes to rainfall; (a) infiltration excess overland flow (Hortonian overland flow); (b) saturation excess overland flow (Dunne overland flow); (c) subsurface stormflow (event flow); (d) perched saturation and throughflow (modified from Beven, 2012)

2.3.1.2. Dunne overland flow

Dunne overland flow (FIGURE 2.5b), also called saturation-excess runoff, occurs when the water table rises to the surface due to saturation from below. This phenomenon was first established by Thomas Dunne during intensive field studies (Dunne, 1970, 1978; Dunne & Black, 1970). Dunne overland flow occurs under different circumstances: when the preexisting water table is shallow, when there is an underlying shallow impervious layer, or when hydraulic conductivity decreases with depth. The existence of these barriers causes the water table to rise until it reaches the surface, making further infil-

tration impossible and thus generating overland flow. This flow consists of two components: direct water inputs on a saturated area, and groundwater which breaks out from upslope when the water table intersects the surface. Dunne overland flow is most important in riparian areas and in humid climates because the water table near-stream is not far below the ground surface. The intensity of Dunne overland flow will depend on the extent of saturated areas, which vary widely in time and depend on overall watershed wetness.

2.3.2. Lateral flow in the unsaturated zone

Lateral flow in the unsaturated zone (interflow) can be divided into two categories: *lateral unsaturated* (sometimes called *"Darcian"*) *flow* through the soil matrix (lateral downslope flow), and *lateral preferential flow* in macropores and fractures which allow water to bypass the unsaturated soil matrix.

2.3.2.1. Lateral unsaturated flow

Because the unsaturated zone is under tension–i.e. less than atmospheric–pressure (FIGURE 2.8), water cannot easily move from the unsaturated zone directly into a stream. Thus, lateral unsaturated flow is not a significant source of water to streams under most circumstances. However, a downslope component of drainage can emerge *following* a water-input event [see Jackson, 1992; Lv et al., 2013]. Downslope flow effects are accentuated in anisotropic environments, where the resistance to downslope flow is reduced (Jackson, 1992). In upland watersheds this is believed to be the major source of streamflow (Dingman, 2015).

2.3.2.2. Lateral preferential flow

Lateral flow through macropores and fractures, also called lateral preferential flow or bypass flow, is usually much quicker than unsaturated or saturated Darcian flow through the soil matrix (Kirkby, 1988), allowing water to be carried at greater speeds and to greater distances though otherwise unsaturated soils. While macropores occur mostly in the upper soil layers, fractured rock featured openings at depth that can extend over tens or hundreds of meters. Preferential flow can occur regardless of the antecedent soil moisture, and sometimes only a small difference between the diameter of a pore and the grain size of the soil matrix will cause bypassing. For example, in sand of 0.5 mm a pore size of 1 mm is enough to provide a preferential pathway (Kirkby, 1988). Because the number, orientation, size and inter-connectedness of macropores are highly dependent on local factors such as geology, soils, vegetation and fauna, it is difficult to generalize about the importance of bypass flow in models. Nevertheless, macropore flow has been found to contribute significantly to event flow in many environments (e.g. Jones, 2010; Newman et al., 1998; see Beven & Germann, 1982, 2013).

2.3.3. Flow in the saturated zone

Water that enters streams promptly in response to rainfall and snowmelt events is called *event flow* (also termed storm flow, quick flow, and direct flow). This phenomenon is different from *baseflow* which is water that enters the stream in a persistent and slow manner, and that is maintained in between water-input events.

2.3.3.1. Baseflow

Baseflow is the portion of streamflow sustained by groundwater discharge between precipitation events as long as the water table remains above the stream bottom. Stream reaches characterized by high baseflow inputs tend to have low temporal flow variability. There exist many methods to identify groundwater contributions to streamflow, either by analysis of stream hydrographs (also called baseflow analysis, baseflow separation or recession analysis) or by analyzing the chemical composition of stream water. The detailed approaches can be found in Dingman (2015). However, it is important to note that (i) the concept of baseflow has no scientific basis and (ii) that the source of base flow is seldom known, and may also originate from other sources, such as the drainage of surface water or the slow drainage of soils (Hewlett & Hibbert, 1963).

2.3.3.2. Event flow

Event flow (FIGURE 2.5c) arises from mechanisms that quickly produce steep hydraulic gradients in near-stream areas, and may be a significant component of event response under some circumstances. There are two types of event flow mechanisms, those generated by near-stream groundwater mounds, or through flow from shallow saturated layers. Near-stream groundwater mounds can be formed gradually through local and upslope recharge which causes the streamward gradient to steepen. They may also be formed suddenly if water percolates to the top of the capillary fringe; this causes the menisci that maintain the tension to be obliterated, thus changing the pressure state of the water from negative to positive (Dingman, 2015). This then causes an almost instantaneous rise in the near-stream water table, forming a groundwater mound which induces streamward groundwater flow (Abdul & Gillham, 1984, 1989; Gillham, 1984). When thin permeable soils overlay relatively impermeable materials a saturated zone may form which is disconnected from the regional water table, this is called a perched water table. Downflow in these zones may thus contribute to event response; this type of situation is often referred to as a *sloping slab* (FIGURE 2.5d).

TABLE 2.5 summarizes the current understanding of the environmental factors which favor some of the different runoff mechanisms. Note that Hortonian overland-flow is prevalent in (semi-)arid areas, where vegetation is sparse and rainfall rates commonly exceed surface infiltration capacities. Conversely, subsurface flow mechanisms (supplied to a certain extent by saturation overland flow) are prevalent in humid and temperate climates where water tables occur close to the ground surface (especially during fall and winter) and thus easily saturated.

Mechanism	**Soils/Geology**	**Water table**	**Topography**	**Vegetation**	**Input rate***
Hortonian overland flow	Low surface K_S	Deep	Steep slopes	Absent to sparse	High
Saturation overland flow	Slopes: High surface K_S, gradually or abruptly at shallow depth Valley bottoms: Low to high K_S	Near surface	Concave, convergent slopes; wide valleys	Absent to abundant	Low to high
Groundwater mounding	Slopes: Deep soils with high surface K_S Valley bottoms: High K_S Silty soils enhance flow from pressurized capillary fringe	Slopes: Deep Valley bottoms: Near surface	Concave slopes, wide valleys	Absent to abundant	Low to moderate
Perched groundwater (sloping slab)	Slopes: High surface K_S, decreasing gradually or abruptly at shallow depth; macropores present	Absent to present in high K_S layer	Steep slopes; straight to convex	Absent to abundant	Low to moderate

K_S = Saturated hydraulic conductivity
* Relative to K_S

TABLE 2.5: Environmental factors favoring some hillslope response mechanisms (modified from Dingman, 2015)

2.4. Infiltration and the vadose zone

Infiltration is the process of water entering the soil after a rainfall episode or a period of snowmelt. As water infiltrates downward it may (FIGURE 2.6) (a) be added to the groundwater reservoir as *recharge* (further explained below), (b) move laterally under the existing hydraulic gradient to be discharged into the stream as *interflow* (if the hydraulic gradient is towards the stream) or (c) taken up by *evapotranspiration* (through plant uptake or exfiltration, i.e. evaporation at the soil surface) to rejoin the atmosphere as vapor. Because infiltration is one of the main sources of recharge (more so in humid climates), estimating infiltration is an important preliminary step in understanding recharge processes and distribution. The partition of water inputs from rainfall and snowmelt into the different potential outcomes of the water cycle is controlled by the unsaturated zone (the vadose zone). Indeed, conditions at the surface of and within the vadose zone will determine the hydrological response to water inputs: they determine whether

water inputs infiltrate to become subsurface runoff, recharge and plant transpiration, move downslope to streams quickly over the surface, or become evaporation.

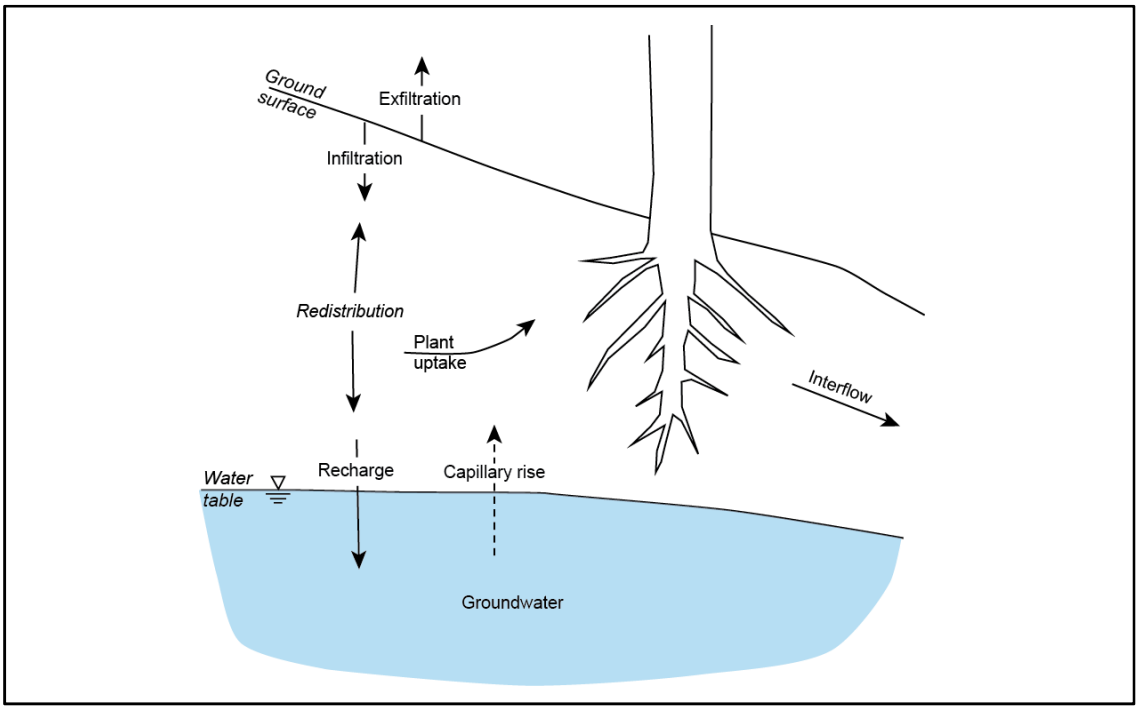

FIGURE 2.6: Water movement in the unsaturated zone (modified from Dingman, 2015)

2.4.1. The vadose zone

The vadose zone extends from the top of the ground surface to the groundwater surface, and is where the intergranular space is only *partly* filled with water, the rest being filled with air. The thickness of this zone fluctuates because its lower boundary is the depth of the water table, which moves depending on recharge and discharge.

Generally speaking (a fuller description of the physical processes of infiltration will be given in the following paragraphs) the soil properties controlling the partition and water movement throughout the vadose zone are (Dingman, 2015) (i) the propensity for water infiltration, which is a function of the size and abundance of pores, determined by the type of geologic material, the biotic activity, the soil temperature and the slope (steeper slopes tend to produce more runoff), (ii) the ability to transmit and retain infiltrated water; this is determined by pore size (large pores conduct more water but retain it less, while small pores are less conductive but more retentive) and (iii) the depth to the water table, controlling the distance over which soil pores are available to store water.

2.4.1.1. Water conditions in soils

Different thresholds describe the soil-water status of a given soil (FIGURE 2.7):

(a) *Field Capacity* (θ_{fc}) is the water content at which the gravity-drainage rate becomes negligible. In other terms, it is a measure of the water content that can be held against the force of gravity by capillary forces. If water content is below field capacity then downward movement in the soil essentially ceases, and water content can only decrease through evapotranspiration (FIGURE 2.7).

(b) *Permanent Wilting Point* (θ_{pwp}) is the water content point at which the suction (negative pressure) in the soil exceeds the plant's capacity to extract water from the soil (usually considered to be about -15 bar or -15,000 cm of water). When water content is reduced to this point, transpiration ceases and plants wilt (FIGURE 2.7).

The soil-water status, also called the *available water content* (θ_a), is considered to be the difference between the field capacity and the permanent wilting point (FIGURE 2.7):

$$\theta_a = \theta_{fc} - \theta_{pwp} \tag{2.1}$$

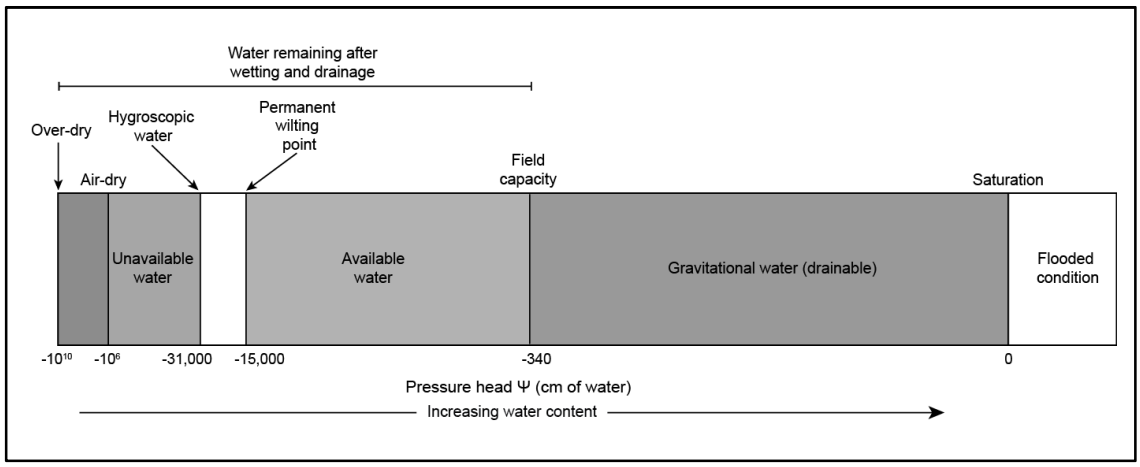

FIGURE 2.7: Soil-water status as a function of pressure. (modified from Miller & Donahue, 1990)

2.4.1.2. Hydrologic soil horizons

To describe water movement in the vadose zone, it is generally divided into soil-hydrologic horizons[3] based on the typical range of water contents and soil water pressures (FIGURE 2.8). The different horizons are, from top to bottom: the root zone (or soil water zone), the intermediate vadose zone, the capillary fringe (or tension-saturated zone) and the groundwater zone (FIGURE 2.8). The depth and thickness of these hori-

[3] The term "horizon" used here is different from the classic pedological sense of the word; here it refers to a portion or layer of the subsurface characterized by specific water content and soil water pressure.

zons vary both in time and space, and one or more may be absent in a given situation. This is because they depend on recharge and discharge fluxes which may vary periodically according to seasons, or linearly according to climate and land-use trends.

They can be described as follows (from bottom to top):

(1) **The groundwater zone** is fully saturated and the pressure is positive. In the absence of groundwater flow, the pressure is said to be *hydrostatic*, which means it increases linearly with depth. If groundwater is flowing, then the pressure at any given point is determined by the overall configuration of the flow system. The water table is at atmospheric pressure. The water table rises and falls in response to seasonal climatic variations and depends on water entering the system (through recharge from water-input events or upwelling from deeper groundwater zones) and leaving the system (through discharge into a stream, downward flow or upward flow into the intermediate vadose zone as capillary rise).

(2) **The capillary zone** (or tension-saturated zone) extends above the water table up to the height of the capillary rise which depends mainly on the size of intergranular opening. The capillary rise is strongest in media with smaller pores (like in silt where it is of about 100 cm) and weakest in media with large pores (2.5 cm for gravel for example). In this zone, voids are saturated or almost saturated with water that is held in place by capillary forces. Water in this zone is under tension (FIGURE 2.8). The pressure head at the top of this section is termed the air-entry tension (ψ_{ae}) which is equal to the height of capillary rise.

(3) **The intermediate vadose zone** is the portion of the vadose zone between the top of the capillary fringe and the base of the root zone. In the intermediate zone, water is held by capillary forces, resisting the pull by gravity. The thickness of this zone varies between 0 m (when the water table is close to the surface) to over 100 m under deep water-table conditions. Tensions in this zone are usually stronger than ψ_{ae} and depend on the soil texture and water content, which can be described using a *moisture-characteristic curve* (Miller & Donahue, 1990) [see Section 2.4.2.4].

(4) **The soil water zone** (or root zone) provides water for the growth of vegetation and is submitted to water losses from evapotranspiration, therefore showing diurnal variations. Its upper boundary is the soil surface, while its lower boundary is indefinite and irregular but generally constant in time, depending on typical root-zone depths of the vegetation types present.

Specifically, soil properties may be quantitatively linked to infiltration, storage and flow using physically based equations which will be detailed in full below.

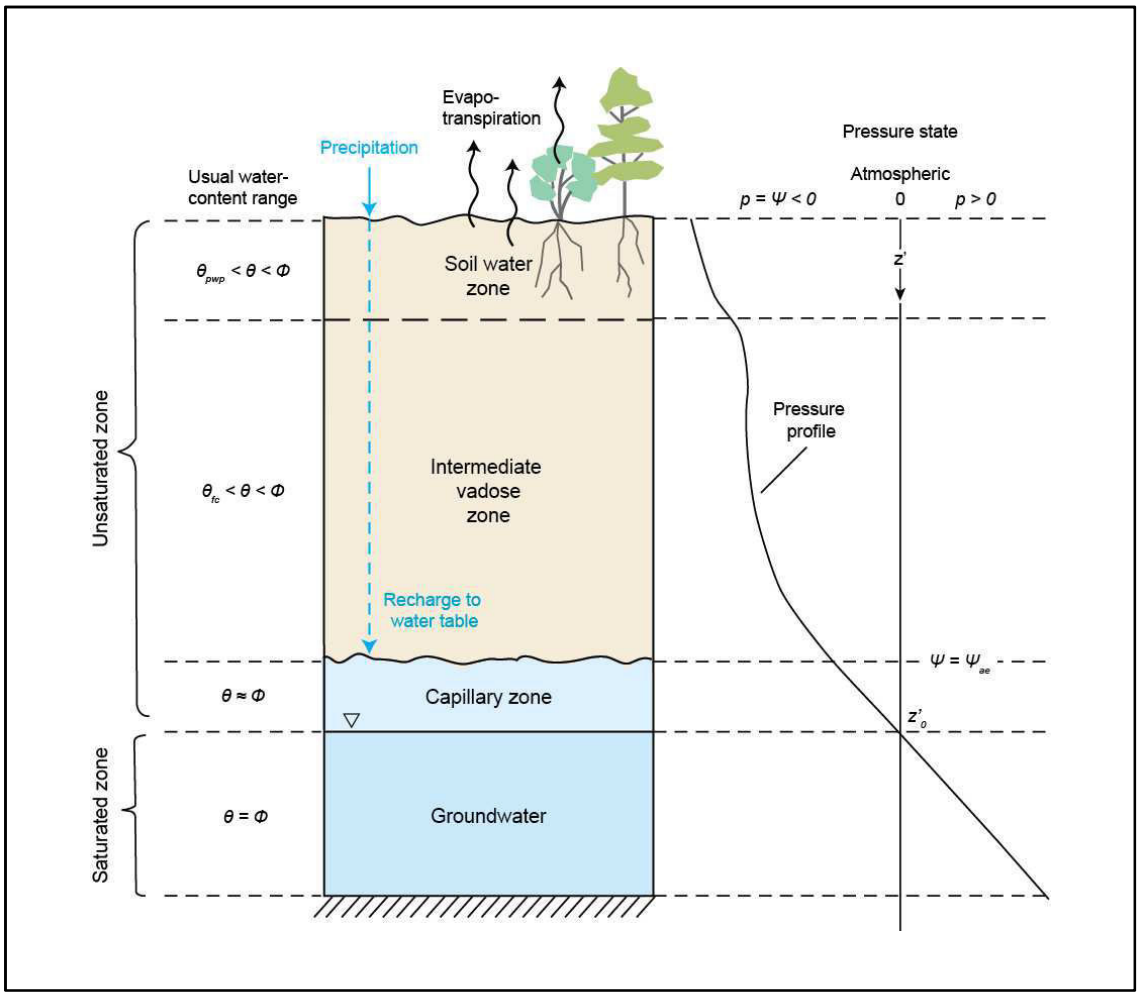

FIGURE 2.8: Classification of soil-hydrologic horizons. Note that this figure is not to scale (the vertical extent of the unsaturated zone is exaggerated) and idealized and that any or several of these "horizons" might be absent under given conditions (modified from Alley et al., 1999 and Dingman, 2015). θ_{pwp} is the *permanent wilting point*, θ_{fc} is *field capacity*.

2.4.2. The infiltration process

The rate of infiltration (*f(t)*) depends on the intensity of the input (*w(t)*, the *water-input rate*), the initial moisture conditions of the surface soil layer, and the hydraulic characteristics of the soil. The maximum amount of water that a soil can hold after excess water has drained is called *field capacity* (see section 2.4.1.1), and the maximum rate at which water penetrates into the soil is called *infiltration capacity* (*f*(t)*, also called infiltrability; note that this changes during the infiltration event). If the water-input rate exceeds the infiltration capacity, then *ponding* (*H(t)*) will occur. Note that the presence of macropores (such as those created by plant roots and soil fauna) may allow

water to bypass the primary porosity and lead to higher infiltration rates (Beven & Germann, 1982). Methods for estimating infiltration are detailed in **Chapter 3 Section 2.1**.

Three different infiltration conditions may be defined (Dingman, 2015):

(a) If no ponding occurs, infiltration rates will equal water-input rates and will be less than or equal to infiltrability. Infiltration is said to be *supply-controlled*:

$$H(t) = 0, f(t) = w(t) \leq f^*(t) \tag{2.2}$$

(b) If ponding occurs because the water-input rate exceeds the infiltration capacity, this is referred to as saturation from above and infiltration rates equal infiltration capacity:

$$H(t) > 0, f(t) = f^*(t) \leq w(t) \tag{2.3}$$

In this situation, the rate of infiltration depends on soil type and soil moisture conditions. Infiltration here is said to be *profile-controlled*.

(c) If ponding occurs because the water table has risen to or above the surface and the soil is entirely saturated, then the infiltration rate and infiltration capacity are both null:

$$H(t) > 0, f(t) = f^*(t) = 0 \tag{2.4}$$

2.4.2.1. Darcy's Law

The law that governs water flow through a porous medium was discovered in 1856 by Henry Darcy[4], and is now known as Darcy's Law:

$$Q = -K\frac{dh}{dl} \tag{2.5}$$

where Q [$L^3.T^{-1}$] is the volume rate of flow per unit area of porous medium A [L^2], K [$L.T^{-1}$] is the saturated hydraulic conductivity of the medium (the minus sign indicates flow moves from higher to lower h values), and l [L] is the length over which the pressure drop takes place. Dividing both sides of the equation by area and using more general notation leads to (in the x-direction):

[4] Henry Darcy (1803-1858), a French hydraulic engineer, was the first to clearly state a law describing the flow of groundwater in a report titled "The Public Fountains of the City of Dijon". This report detailing the engineering that was used for Dijon's water supply included results of the sand column experiments which led to the now-famous Darcy's Law.

$$q_x = -K_x \frac{dh}{dx} \tag{2.6}$$

where *dh/dx* is the hydraulic head gradient in the *x*-direction. *h* is the hydraulic head (also referred to as piezometric head), equal to the sum of the gravitational head *z* [L] and the pressure head Ψ [L], equal to the fluid pressure divided by the weight density of the fluid, so that:

$$h = z + \psi = z + \frac{p}{\rho g} \tag{2.7}$$

Hydraulic head represents the fluid potential, which is the mechanical energy per unit weight of fluid.

Although the *actual* flow of water through a porous medium is actually much more complex, Darcy's Law describes the *bulk* flow through a "small" volume representative of the whole medium (Representative Elementary Volumes, discussed in **Chapter 1 Section 4**), over which inter- and intra-pore variations are averaged. As a result, Darcy's Law does not apply to flows at scales smaller than REVs, and may not always allow an accurate representation of heterogeneous media where REVs cannot always be defined (Dingman, 2015).

2.4.2.2. Darcy's Law for unsaturated flow

Darcy's law applies to both saturated and unsaturated media. In unsaturated media, however, both the pressure head ψ and the hydraulic conductivity *K* are functions of the local water content (θ). If θ increases, then both $K_x(\theta)$ and $\psi(\theta)$ increase as well. This is reflected in Darcy's law as written for unsaturated flows:

$$q_x = -K_x(\theta) \frac{d[z + \psi(\theta)]}{dx} \tag{2.8}$$

The quantitative relationship between hydraulic conductivity and water content and between pressure and water content are key determinants of unsaturated flow and will be further examined in Section 2.4.2.4.

2.4.2.3. General unsaturated flow equation

By combining Darcy's law for unsaturated flow and the conservation-of-mass equation for three-dimensional time-varying groundwater flow we obtain the general unsaturated flow equation. The conservation-of-mass equation for three-dimensional time-varying groundwater flow is equal to:

$$\frac{\partial q_x}{\partial x} + \frac{\partial q_y}{\partial y} + \frac{\partial q_z}{\partial z} = -S_S \frac{\partial h}{\partial t} \tag{2.9}$$

where q_x, q_y and q_z are specific-discharge vectors parallel to the sides of the volume considered and S_S is the storage coefficient [L^{-1}] defined as:

$$S_S = \frac{\text{volume of water entering of leaving control volume}}{\mathrm{d}h.\,\mathrm{d}x.\,\mathrm{d}y.\,\mathrm{d}z} \tag{2.10}$$

If constant flow density is assumed, the storage coefficient (S_S, [L^{-1}]) depends on changes in water content (θ) in the control volume in response to a change in head (h):

$$S_s = \frac{\partial \theta}{\partial h} \tag{2.11}$$

Substituting Eq. (2.11) into Eq. (2.9) leads to:

$$\frac{\partial q_x}{\partial x} + \frac{\partial q_y}{\partial y} + \frac{\partial q_z}{\partial z} = -\frac{\partial \theta}{\partial h}\frac{\partial h}{\partial t} = -\frac{\partial \theta}{\partial t} \tag{2.12}$$

Specific-discharge in each coordinate direction may then be replaced using Darcy's law for unsaturated flow (Eq.(2.8)), which yields the general equation (assuming that the z direction is oriented vertically and that the $K(\theta)$ relation is isotropic):

$$\frac{\partial}{\partial x}[K(\theta)\,\frac{d\psi(\theta)}{dx}] + \frac{\partial}{\partial y}[K(\theta)\,\frac{d\psi(\theta)}{dy}] + \frac{\partial}{\partial z}[K(\theta)(\frac{d\psi(\theta)}{dz} + 1)] = \frac{\partial \theta}{\partial t} \tag{2.13}$$

Eq. (2.13) was first derived by Richards (1931) and is formally known as the **Richards equation**. The Richards equation is mostly applied for vertical downward flow to quantify infiltration, which is a starting point to then estimate its redistribution in the unsaturated zone and migration towards the saturated zone (i.e. recharge). To do so, Eq. (2.13) is generally rewritten as:

$$-\frac{\partial K_h(\theta)}{\partial z'} - \frac{\partial}{\partial z'}[K_h(\theta)(\frac{d\psi(\theta)}{dz'})] = \frac{\partial \theta}{\partial t'} \tag{2.14}$$

Where z' is the vertical downward direction ($z' = -z$) and $\partial z/\partial z' = -1$. This equation is non-linear, so there are no closed-form analytical solutions. Instead, the equation is solved by specifying appropriate boundary and initial conditions, defining the $K(\theta)$ and $\psi(\theta)$ relationships (Section 2.4.2.4), dividing the soil into thin layers, and applying the equation to each layer sequentially at small increments of time.

The first term on the left of Eq. (2.14) (i.e. $-\frac{\partial K_h(\theta)}{\partial z'}$) represents flow due to gravity and the second term on the left (i.e. $\frac{\partial}{\partial z'}[K(\theta)(\frac{d\psi(\theta)}{dz'})]$) represents flow due to the pressure gradient. In the first step of infiltration, water enters dry soil. The pressure gradient at the surface then becomes much larger than the unit gravitational gradient, and infiltration due to pressure forces is therefore large. Then, as the process continues, near-

surface water content increases, which causes the pressure-gradient forces and the infiltration rate to decline. If the water input continues long enough, then the pressure forces become small and the infiltration rates decline almost exponentially to a near-constant value that approximates the rate due to gravity alone.

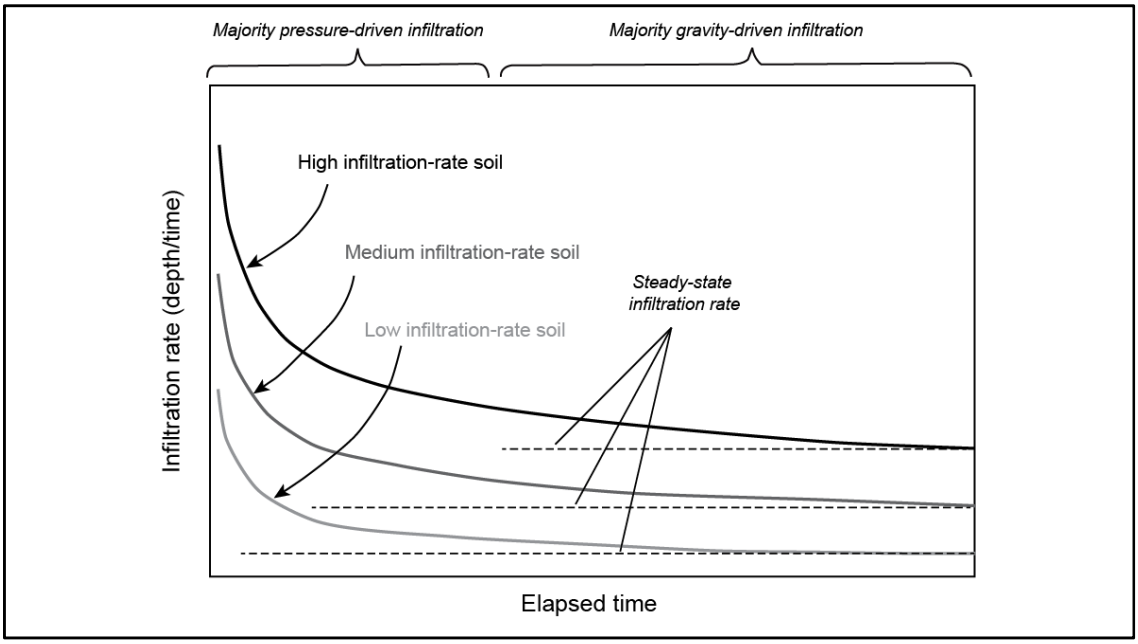

FIGURE 2.9: Typical infiltration rates over time for three soil columns (modified from Nimmo, 2005)

2.4.2.4. Hydraulic properties of unsaturated porous media

Pressure-water content relations ($\psi(\theta)$)

Pressure-water-content relations, meaning the relationship between the pressure head (ψ) and water content (θ), can also be called *moisture-characteristic curves*. As mentioned above, this relationship is highly non-linear. The typical form of this type of relationship is shown in FIGURE 2.10. Note that ψ is zero (and that pressure is atmospheric) when water content is at saturation (approximately equal to the porosity). Also, note that water content changes little as $|\psi|$ increases up to the point of inflection, a point also known as the *air-entry pressure head* (ψ_{ae}), which represents the pressure head at which significant volumes of air may begin to enter the soil pores. The air-entry pressure head is equal to the height of the capillary fringe. As $|\psi|$ continues to increase beyond the air-entry value, water content decreases rapidly, at first, and then more gradually. At very high tensions (very low water content) the curve becomes nearly vertical, which results from water being held tightly within the soil pores by surface tension and electrochemical forces. The shape of any given moisture-characteristic curve is highly dependent on soil texture. Generally speaking, $|\psi|$ is much higher in fine-grained soils (clay-rich) than in coarser-grained soils (with a higher sand and gravel content). Note that in real

soils there is not a single function of $\psi(\theta)$, but that actually the function depends on whether the soil is in a wetting or drying phase (this is due to *hysteresis*[5]). This hysteresis is however difficult to model and account for and thus generally neglected in hydrologic models.

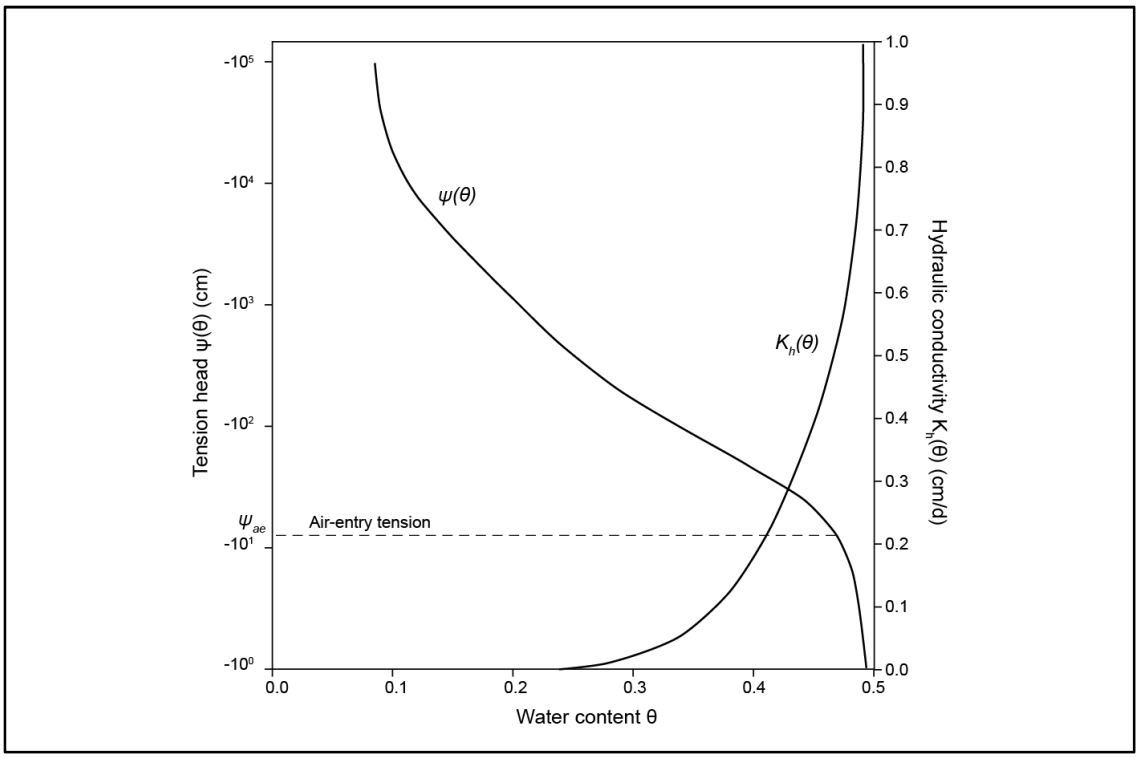

FIGURE 2.10: Typical forms of the moisture-characteristic curve ($\psi(\theta) - \theta$) and the moisture-conductivity curve ($K_h(\theta) - \theta$); in this example porosity equals 0.5 (modified from Dingman, 2015)

Hydraulic conductivity-water content relations ($K(\theta)$)

The relationship between unsaturated hydraulic conductivity and soil moisture may also be referred to as the *moisture-conductivity curve*. In the same way as the *moisture-characteristic curve*, the moisture-conductivity curve is highly non-linear (FIGURE 2.10), which indicates that hydraulic conductivity varies strongly as a function of soil moisture. If the water-content is low to moderate, then the unsaturated hydraulic conductivity will be very low, i.e. one to several orders of magnitude less than the saturated hydraulic conductivity (FIGURE 2.10). As water-content increases, so does K. When water-content reaches saturation, then K is equal to its saturated value (saturated hy-

[5] According to the Oxford dictionary hysteresis can be defined as "*the phenomenon in which the value of a physical property lags behind changes in the effect causing it*". The most commonly cited example is the phenomenon in which the magnetic flux density of a ferromagnetic material lags behind the changing external magnetic field strength.

draulic conductivity). For any given θ, the corresponding $K(\theta)$ may vary several orders of magnitude depending on the soil type (e.g. from clay loam to sandy loam). Also, for any given soil type, $K(\theta)$ may increase one to several orders of magnitude over the range of θ values. The $K(\theta)$ function is also subject to a hysteresis effect, although less apparent than for $\psi(\theta)$ and also generally neglected.

Analytical approximation of $\psi(\theta)$ and $K(\theta)$

$\psi(\theta)$ and $K(\theta)$ relations control all of the near-surface processes shown in FIGURE 2.6. These relationships vary greatly between soil types, although measuring them might be difficult and time-consuming. To get around this issue, $\psi(\theta)$ and $K(\theta)$ are generally generated analytically and related to soil texture and other properties which are more easily measurable. Many authors have proposed analytical approximations of $\psi(\theta)$ and $K(\theta)$, which allow for a continuous mathematical description of these relationships, rather than a discrete experimental determination (Brooks & Corey, 1964; Campbell, 1974; Gardner, 1958; van Genuchten, 1980).

In order to simplify the following mathematical equations, the following is used:

$$\Theta = \frac{\theta - \theta_r}{\theta_s - \theta_r} \tag{2.15}$$

where Θ is the degree of saturation, θ_r refers to the residual water content, the minimal water content possible within the considered porous media, and θ_s is the saturated moisture content, which is equal to or less than the total porosity. θ_r is generally considered to be null (de Condappa, 2005), and thus:

$$\Theta \approx \frac{\theta}{\theta_s} \tag{2.16}$$

The Brooks & Corey (1964) and van Genuchten (1980) analytical approximations are summarized in TABLE 2.6. FIGURE 2.11 shows the typical Brooks & Corey and van Genuchten moisture-characteristic curves. This figure shows how, when $-\psi$ is high, the two models are very similar. Also, it should be noted that the van Genuchten model is often preferred (i) because, in contrast with the Brooks & Corey model, it is based on a single equation rather than a two-part equation (which makes it derivable) and (ii) it is known to provide a better fit for retention data. There are several other differences between these models, which are summarized in de Condappa (2005), although the main difference lies in the applicability of each model. The van Genuchten model is based on a choice of capillary model, unlike the Brooks & Corey model. More precisely, the van Genuchten model was built using the Burdine model (1953) to estimate the moisture-conductivity curve from the moisture-characteristic curve. Unfortunately, this leads the van Genuchten model to be valid only for the soils described by the Burdine capillary

model. The use of another capillary model (e.g. Childs & Collis-George, 1950; Mualem, 1976), becomes complicated, limiting the applicability of Eq. (2.21).

Methods for estimating hydrodynamic parameters

In order to estimate pressure-water content relations and hydraulic conductivity-water content relations, it is necessary to estimate the parameters used in these equations, i.e. λ, n or η, ψ_{bc} or ψ_g, θ_s and K (TABLE 2.6). These parameters depend primarily on the soil grain-size distribution (i.e. texture), and to a certain extent on other factors such as organic content and chemistry (Wösten et al., 2001). Roughly speaking, two categories of methods exist for the determination of soil-hydraulic parameters, (i) predictive methods, which most often relate model parameters to texture, and (ii) measurement techniques (direct or indirect).

(i) **Pedotransfer functions** (**PTF**s) translate existing data (e.g. particle-size distributions, bulk density and organic matter content) into soil-hydraulic properties. These functions are generally empirical and were calibrated on existing soil hydraulic data bases. PTFs can be quite simple, for example they can be a lookup table that gives hydraulic parameters according to textural class; they may also include linear or nonlinear regression equations, or they may have a more physical foundation, for example relying on particle and pore-size distributions [see Schaap et al. (2001) and references within].

Soil-hydraulic classes are discontinuous categories determined by the proportions of clay, silt and sand (as in a soil texture triangle) in a soil. Each category is then attributed a characteristic set of soil-hydraulic parameters.

(ii) **Experimental methods** allow for in-situ estimation of soil-hydraulic properties. An extensive description may be found in Haverkamp et al. (2016). Experimental methods provide local measurements and are difficult to apply over large areas, but that are more representative than predictive methods. They generally rely on precise and time-consuming experimental procedures which can be done in laboratory or on-field.

One example of a field soil-hydraulic parameter estimation method is the *Beerkan method*. This method uses the van Genuchten water-retention function (Eq. (2.20) and (2.22)) and the Brooks & Corey hydraulic conductivity function (Eq. (2.18)) to describe the hydraulic characteristic curves. To do so, the texture-dependent shape parameters (λ and n) are estimated from a simple particle analysis, and the structure-dependent scale parameters (ψ_{bc}, θ_s and K) are estimated from field infiltration experiments at null pressure head (Haverkamp et al., 2016; Lassabatère et al., 2006).

Moisture Characteristic		Moisture Conductivity	
Brooks & Corey (1964)			
$\lvert\psi(\Theta)\rvert = \lvert\psi_{bc}\rvert\left(\frac{1}{\Theta}\right)^{\frac{1}{\lambda}}$ if $\Theta < 1$	(2.17)	$K(\theta) = \Theta^{\eta} K$ and $\eta = 2/\lambda + 2 + \tau$,	(2.18)
$\lvert\psi(\Theta)\rvert = \lvert\psi_{bc}\rvert$ if $\Theta = 1$	(2.19)	($\tau = 1$ for the Burdine capillary model)	
van Genuchten (1980)			
$\lvert\psi(\Theta)\rvert = \psi_g\left[\Theta^{\frac{n-1}{n}} - 1\right]^{\frac{1}{n}}$ if $\Theta < 1$	(2.20)	$K(\theta) = K.\Theta^{\frac{1}{2}}\left\{1 - \left[1 - \Theta^{\frac{n}{n-1}}\right]^{\frac{n-1}{n}}\right\}^2$	(2.21)
$\lvert\psi(\Theta)\rvert = 0$ if $\Theta = 1$	(2.22)	(with the Burdine capillary model)	

Symbols

$K \equiv$ Saturated hydraulic conductivity [L.T-1]
$\Theta \equiv$ Degree of saturation [-]
$\psi \equiv$ Pressure head [L]
$\lambda \equiv$ Texture dependent retention shape parameter (Brooks & Corey) [-]
$\eta \equiv$ Texture dependent conductivity shape parameter (Brooks & Corey) [-]
$\tau \equiv$ Soil tortuosity parameter (Brooks & Corey) [-]
$n \equiv$ Pore-size distribution index (van Genuchten) [-]
$\psi_{bc} \equiv$ Pressure-head parameter (air-entry pressure head) (Brooks & Corey) [L]
$\psi_a \equiv$ Pressure-head parameter (van Genuchten) [L]

TABLE 2.6: Analytic approximations of the $\psi(\theta)$ and $K(\theta)$ relations

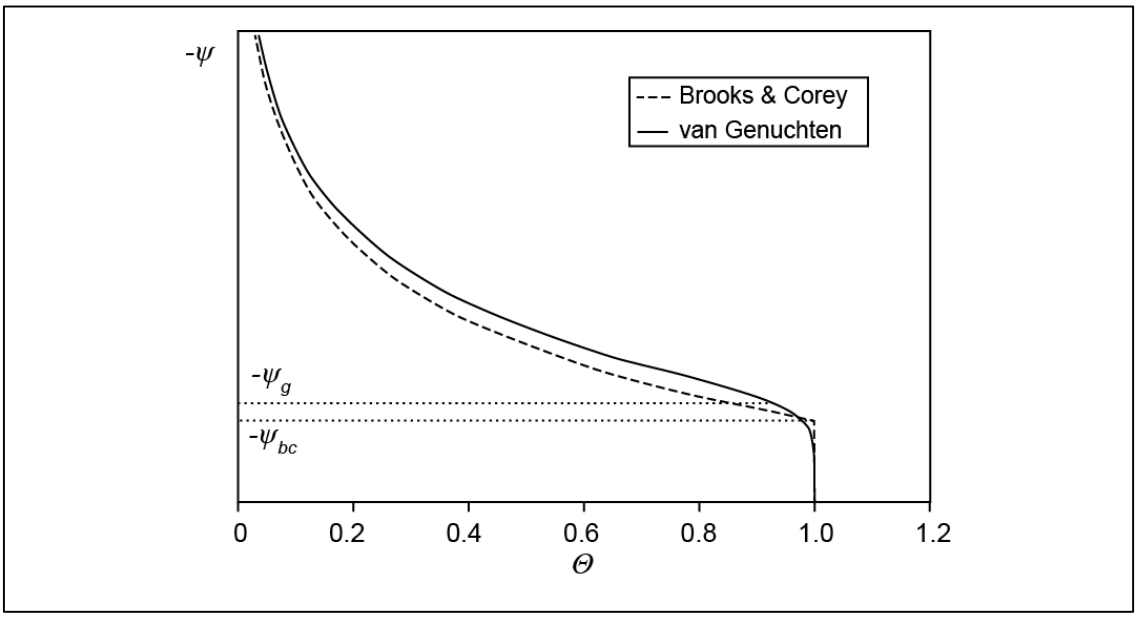

FIGURE 2.11: Typical moisture characteristic curves for the Brooks & Corey (1964) and van Genuchten (1980) models on a semi-log scale (modified from de Condappa, 2005)

2.5. The role of aquifers in the water cycle

Groundwater systems are an integral part of the hydrological cycle. Although groundwater is sometimes portrayed as a simple pool of water with transfers to and from it, groundwater systems are actually three-dimensional dynamic systems which ensure continuous movement of water in the subsurface (Alley et al., 2005). The areal extent of groundwater systems varies from a few square kilometers up to tens of thousands of square kilometers, and groundwater-flow paths from a few meters to tens, sometimes hundreds of kilometers. Groundwater flows from recharge areas to discharge areas along these flow paths, leading to the redistribution of water over large areas and to the mixing of water from different sources and of different ages (up to a certain extent). Finally, groundwater-flow systems represent a much more significant stock of water than surface water bodies, and are less subject to seasonal and perennial fluctuations. As such, they provide value not only as sources of water supply, but also as stable buffers against the uncertainty of surface water availability. In some cases, even, groundwater sustains streamflow in the absence of precipitation.

3. Aquifer recharge

3.1. Definition

According to Nimmo et al. (2005), aquifer recharge is defined as the replenishment of an aquifer as water moves from the land surface into the saturated zone, and is a fundamental component in groundwater systems. Natural replenishment occurs from precipitation falling on the land surface and from infiltration of water stored in surface water bodies, with precipitation generally being the dominant source. Artificial replenishment relies on the use of Managed Aquifer Recharge (MAR) schemes which intentionally reroute surface water into the subsurface [more on MAR in **Chapter 4**]. Recharge is commonly expressed as a volume [L^3], and recharge rates as either a flow rate [L^3T^{-1}] into a specified portion of the aquifer, or a flow rate per unit surface area [LT^{-1}].

It is important to distinguish between infiltration and recharge. Looking back at the hydrological cycle described in **Section 1.1.2**, when rain falls, a portion of it infiltrates into the soil. Nevertheless, only part of infiltration will become recharge by moving deeper into the subsurface; of the remainder, some is taken up by ET and some becomes interflow drainage to streams and rivers. In (semi-)arid environments, in fact, the portion of infiltration reaching the aquifer may be very small indeed.

Recharge processes are determined by an interaction between climate, geology, morphology, soil condition and vegetation. In humid areas, the main controls are the potential precipitation surplus (i.e. rainfall minus potential evapotranspiration, which depends

on the land cover and which varies seasonally), the infiltration capacity of the soil, and the storage and transport capacity of the sub-surface.

Because recharge represents replenishment of aquifers, which balance the total losses of water from the saturated zone (i.e. discharge processes), recharge has obvious practical importance, especially where groundwater is extracted for human use (Nimmo et al., 2005). However, recharge depends on a set of hydrological events that are vastly variable in time in space, which makes recharge estimates particularly difficult, more so in semi-arid environments. Point measurements, specifically, often do not do justice to the variability of infiltration and evapotranspiration in space caused by the variability of topography, soil type and vegetation cover (Kim & Jackson, 2012). Even precipitation, the driving force of recharge, may only vaguely be understood or monitored, particularly in large countries with limited infrastructure. Additionally, several other natural processes may also influence recharge on different scales, such as the existence of infiltration fronts[6], preferential flows in macropores, or localized enhanced seepage in topographic depressions (rivers, irrigated fields…) (Kinzelbach et al., 2002). Determining the contributions of such processes has been the object of several publications (Alcalá et al., 2011; Cuthbert & Tindimugaya, 2010; Maréchal et al., 2009) but remains a matter of widespread debate [more on this in **Chapter 3 Section 3.2**].

3.2. Types of recharge

Recharge can be divided into several categories depending on the nature of the water source feeding into the aquifer. Precipitation is usually the dominant recharge source. Water reaching the water table by percolation of precipitation in excess of AET through the unsaturated zone is called *diffuse recharge*. When recharge occurs as *diffuse recharge*, general expectations are that (i) gravity is the dominant driving force for recharge (working against matric-pressure gradients) and (ii) that unsaturated zone hydraulic conductivities are much lower than saturated zone hydraulic conductivities [see **Section 2.4.2.4** and FIGURE 2.10] (Nimmo et al., 2005). In addition to precipitation, other possible sources of recharge include perennial or ephemeral surface-water bodies such as rivers, canals, and lakes (referred to as *indirect* and *localized* recharge), and Managed Aquifer Recharge schemes such as artificial recharge basins [see **Chapter 4**]. A diagram summarizing the different mechanisms of recharge may also be found in FIGURE 2.12. In summary, recharge can belong to one of the following categories (de Vries & Simmers, 2002):

[6] According to the American Meteorological Society, an infiltration front, or wetting front, is "*the interface between soil that is unchanged from the initial state and the newly wetted zone from an infiltration or irrigation event*".

- *Direct/diffuse recharge* is the water which enters the groundwater reservoir as an excess from soil-moisture deficits and evaporation by direct vertical percolation through the vadose/unsaturated zone.
- *Indirect recharge* is the percolation to the water table through the beds of surface-water courses.
- *Localized recharge* is an intermediate form of groundwater recharge resulting from concentration of water due to runoff in the absence of well-defined channels, as well as inflow from soil heterogeneities such as cracks, macropores and fractures.

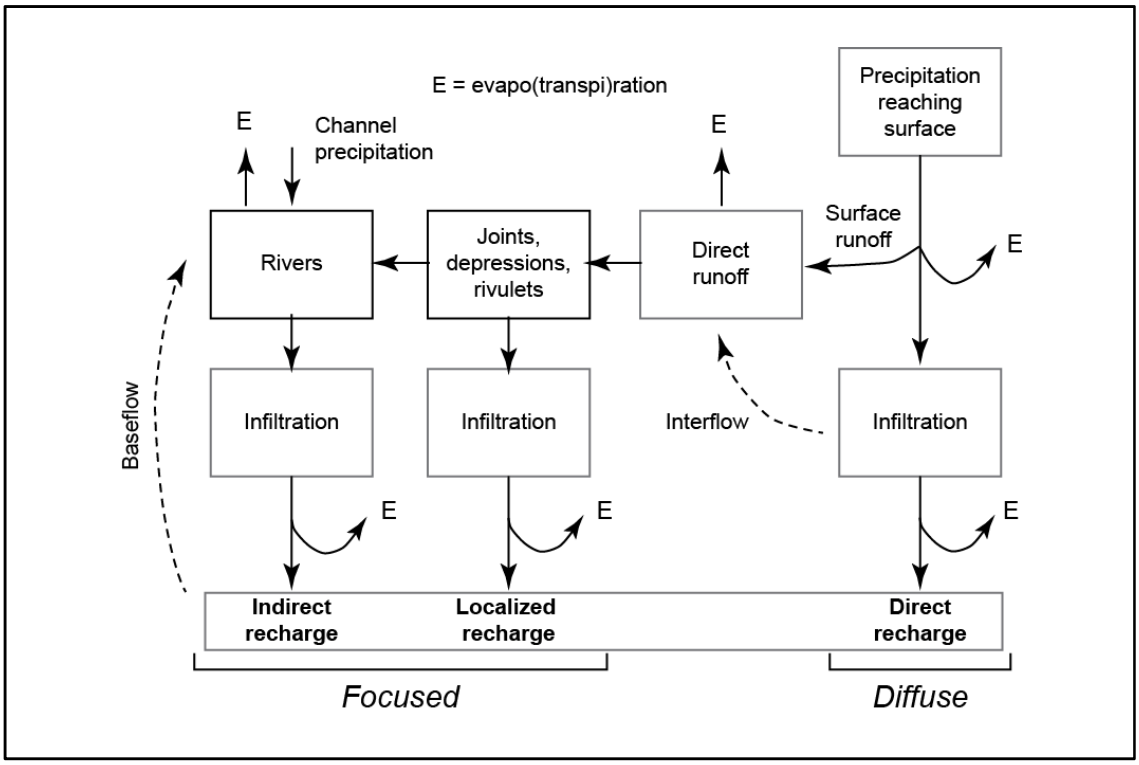

FIGURE 2.12: The various mechanisms of recharge (modified from Saether & Caritat, 1996)

Total groundwater recharge is generally a combination of several of these mechanisms, the relative contribution of each depending on climatic and geologic conditions. In (semi-)arid environments, potential evapotranspiration is much greater than rainfall (on a yearly average basis at least). As a result, recharge tends to take place mostly when short but intense rainfall episodes occur. These intense episodes generate runoff and cause water to pond on the soil surface, which allows water to escape into the subsurface as localized and indirect recharge (Kinzelbach et al., 2002). As aridity increases, diffuse recharge becomes increasingly difficult, instead giving way to localized and indirect recharge processes (FIGURE 2.13; de Vries & Simmers, 2002).

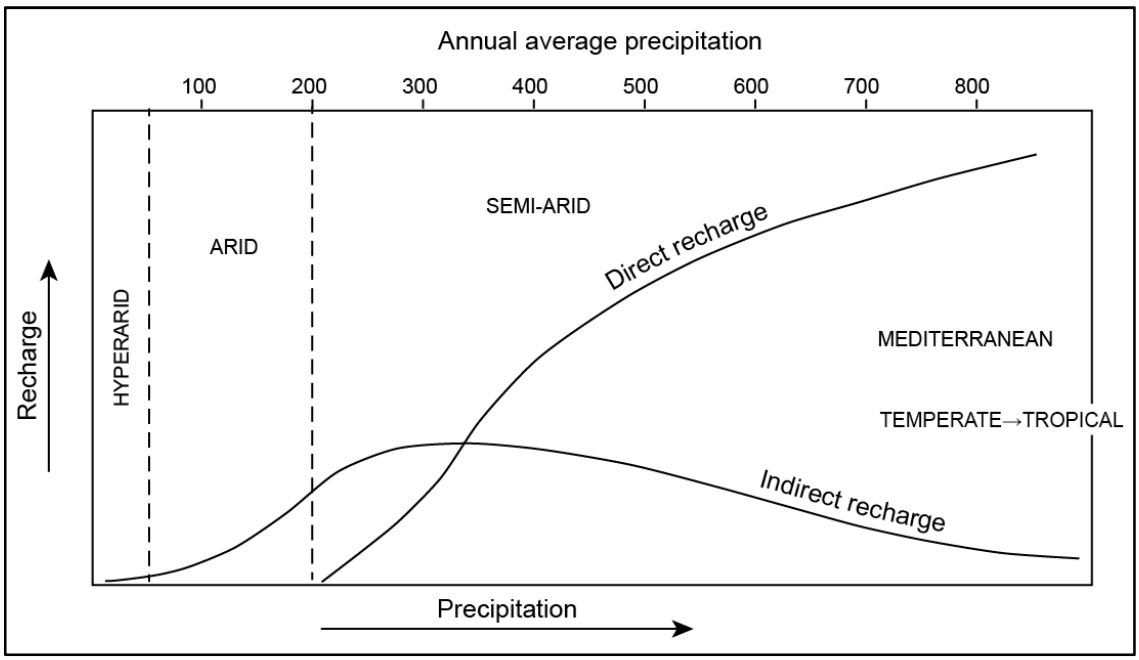

FIGURE 2.13: Recharge types in relation to general climatic conditions (modified from UNESCO, 1999)

Many studies which have looked into the relationship between recharge in rainfall under arid and tropical climates (e.g. Acworth et al., 2016; Eilers et al., 2007; Jasechko & Taylor, 2015; Mileham et al., 2009; Taylor et al., 2012) have in fact suggested a non-linear relationship between rainfall and recharge, in which recharge is biased to heavy rainfall events. For instance, the study by Taylor et al. (2012) analyzed a 55 year record of groundwater level observations in central Tanzania. In this study it was revealed that recharge occurred very episodically, and only after anomalously intense seasonal rainfall. Of the total recharge occurring over 55 years, 60% of it was due to the top 7 seasons of rainfall, the remaining recharge being confined to seasons that feature individual months of statistically extreme ($>95^{th}$ percentile) rainfall. In the study by Jasechko & Taylor (2015) 15 different sites under tropical climates across the globe were studied, and it was found that recharge in 14/15 sites was biased to intense monthly rainfall ($>70^{th}$ decile).

Note that perennial or ephemeral surface-waters are not always recharge sources. In fact, surface-water interactions with groundwater can take place in one of three basic ways (depending on the relation between groundwater head and surface-water stage) (Alley et al., 2005): by gaining water from groundwater inflow (stage<head; FIGURE 2.14**a**), by losing water to groundwater (stage>head; FIGURE 2.14**b** and **c**), or both, by gaining and losing depending on the stream section. Some regions alternate between gaining and losing streams depending on the season. Losing surface-water bodies can be connected to the groundwater system by a continuous saturated zone, or disconnected from the water table by an unsaturated zone (FIGURE 2.14**c**). Disconnected surface-water bodies occur especially in drier climates (Alley et al., 2005).

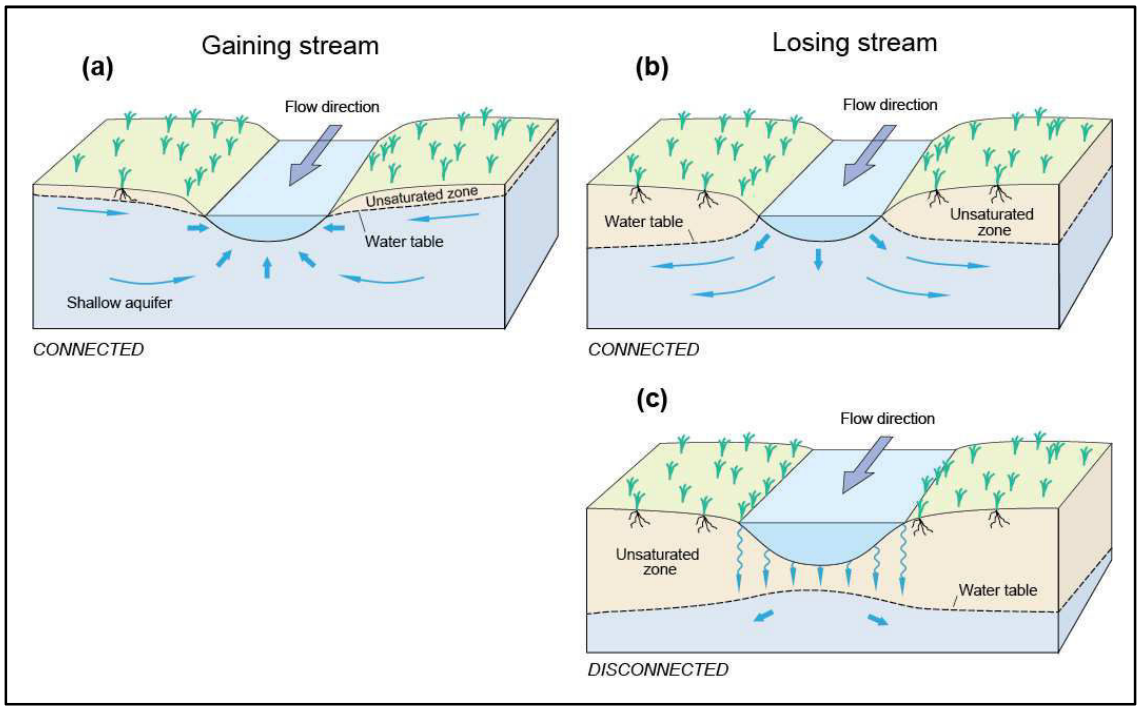

FIGURE 2.14: Different types of surface water/groundwater interactions: (a) a gaining stream receiving water from the groundwater system, (b) a losing stream discharging water to the groundwater system, (c) a disconnected losing steam (modified from Winter et al., 1998)

3.3. Recharge controls

Understanding the fundamental controls on recharge and their interactions is essential to accurately estimate, model, and map recharge. In order to classify the different types of controls, we introduce here a concept developed by Winter (2001) and summarized by Sanford (2002) which is that of the *hydrologic landscape*. Hydrologic landscapes are multiples or variations of *fundamental hydrologic landscape units* (FIGURE 2.15). A fundamental hydrologic landscape unit is defined on the basis of land-surface form, geology, and climate. The basic land-surface form of a fundamental hydrologic landscape unit is an upland separated from a lowland by an intervening steeper slope (FIGURE 2.15). Thus, any hydrologic system can be conceptualized in a uniform way, the only requirements are (Winter, 2001; FIGURE 2.15):

(i) The land-surface slope. Slopes determine the speed at which runoff is evacuated: the flatter the slope, the longer it takes for water to run off the surface. As a result, downward breaks in slope generate downward flow components (and vice-versa, upward breaks in slope generate upward flow components).

(ii) The hydraulic properties of the soils. These control the quantity and rate of runoff versus infiltration (and to a certain extent evapotranspiration rates). Permeable materials are more favorable to recharge.

(iii) The geologic framework. Geologic characteristics at large scales determine the configuration of groundwater flow paths. Water movement rates and geochemical interactions are also closely related to the geologic unit type.

(iv) The difference between precipitation and evapotranspiration. Precipitation and evapotranspiration affect the distribution, timing, and magnitude of runoff and recharge.

If the climatic and soil conditions allow for infiltration to reach the water table at a rate which exceeds the rate at which the saturated zone can transmit recharge away, then the underlying permeability of the geologic framework controls the recharge rate (we then refer to *Lithology-controlled* recharge). This situation results in a relatively shallow water table because storage of water backs up, sometimes even diverting the excess water overland (FIGURE 2.16a). On the other hand, if the saturated zone can transmit more recharge than the infiltration provided by climate and soils, then the surface factors become the limiting factors which control the recharge rate (FIGURE 2.16b) (Haitjema & Mitchell-Bruker, 2005) (this is referred to as *Climate-controlled* recharge). This results in a relatively deep water table. In this case, rainfall and topographic relief play an important role. Practically speaking, these controls will translate directly into the type of model most appropriate for representing recharge, as well as on the boundary conditions constraining the numerical models used to describe each environment. The specifics on recharge representation of in numerical models are detailed in **Chapter 3 Section 2.1.6**.

Note that this description is a very simplified overview of the factors which control recharge quantities and distribution. In reality, of course, recharge processes not at steady-state. Precipitation and *ET* naturally vary seasonally and intra-annually, and human activity in the way of land use and climate change is increasingly contributing to changing both the surface characteristics of landscapes and the rainfall and evaporation patterns. Further, there are several processes at play, and the way they interact with each other is not always immediately discernable.

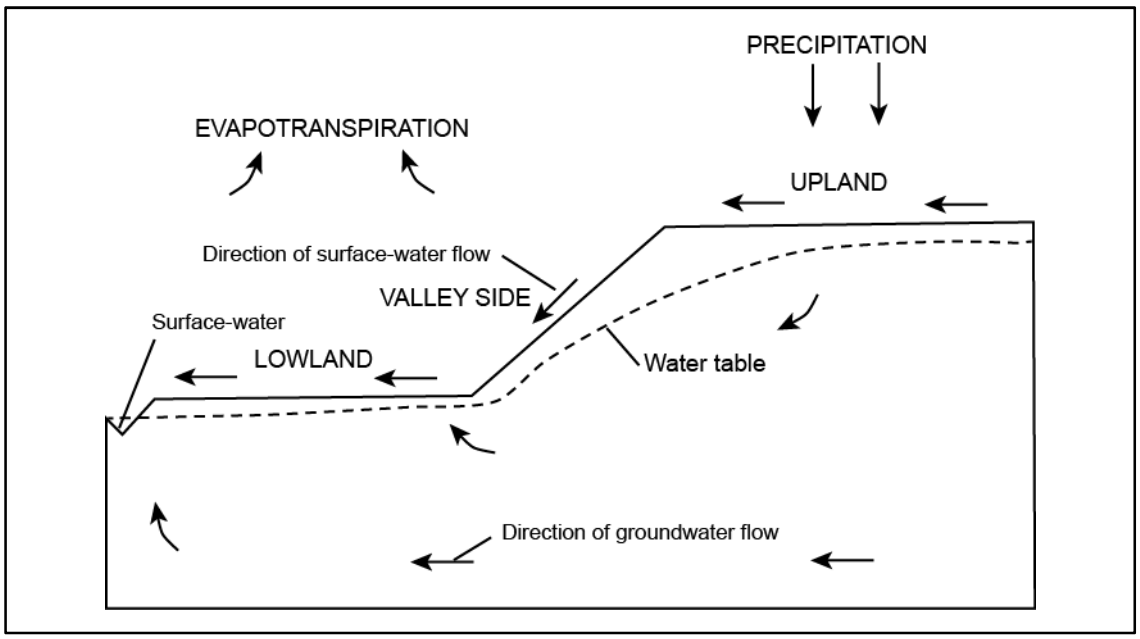

FIGURE 2.15: Fundamental hydrologic landscape unit (modified from Winter, 2001)

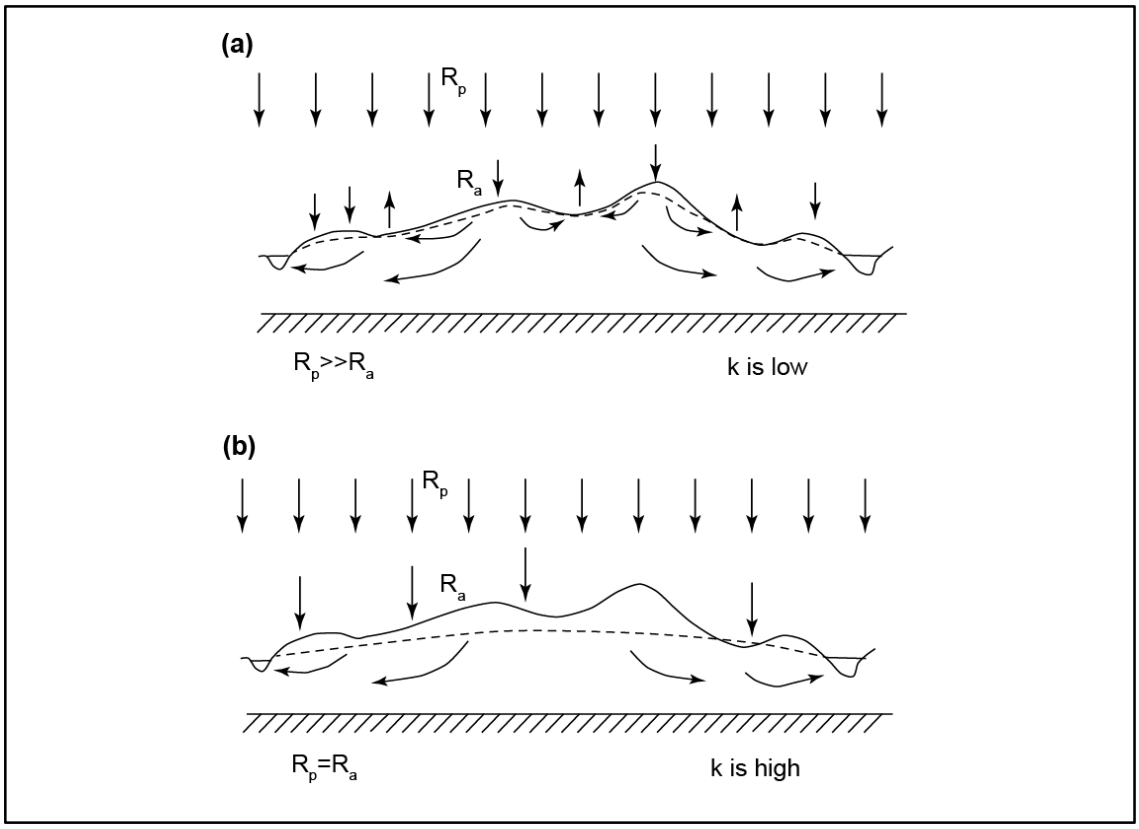

FIGURE 2.16: Low permeability aquifer with topography-controlled water-table (a) and highly permeable aquifer with recharge controlled water-table (b) (modified from Haitjema & Mitchell-Bruker, 2005)

3.4. Global recharge distribution

Groundwater recharge rates depicted on the global resource map (FIGURE 2.17) were adopted from the Groundwater Resources Map of the World (Richts et al., 2011) which is based on the results of the global hydrological model WaterGAP by the University of Frankfurt (Döll & Fiedler, 2008). Recharge estimates were calculated using data on topography, soil structure, geology and permafrost/glaciers. The study by Döll & Fiedler (2008) also features a detailed breakdown of recharge in 165 countries with an area of more than 10,000 km^2.

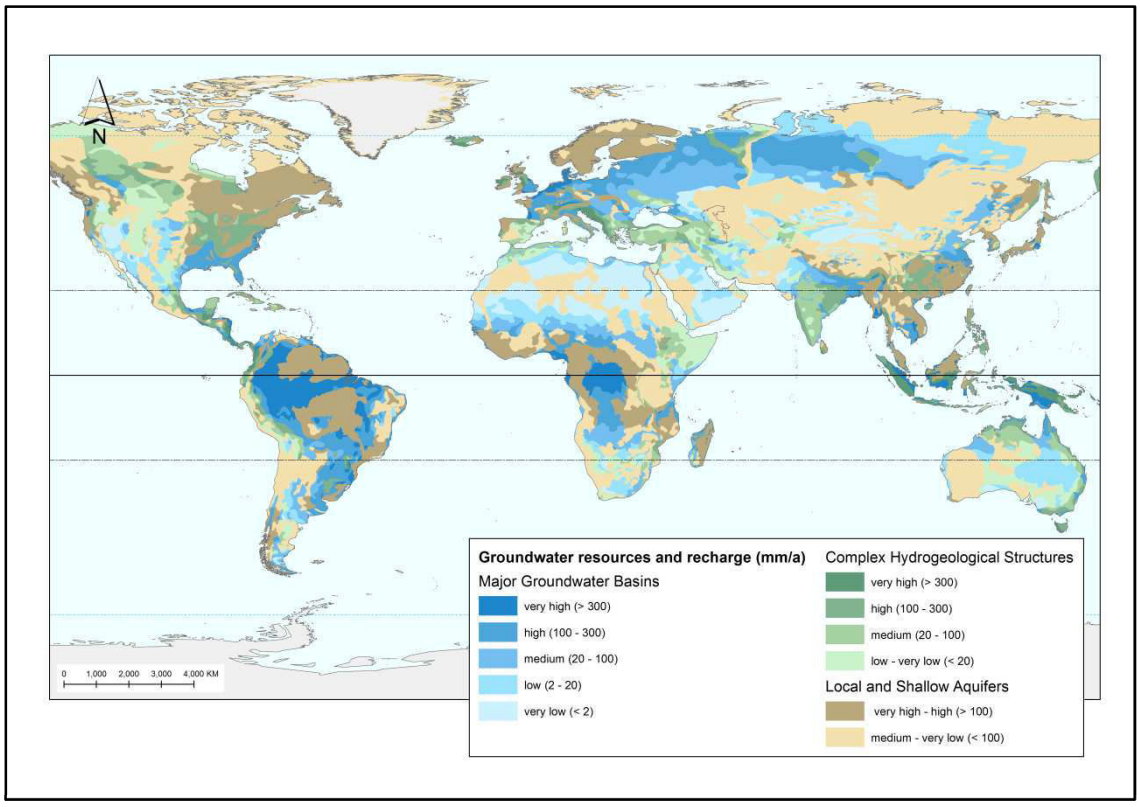

FIGURE 2.17: Groundwater resources map of the world (Richts et al., 2011)

The Groundwater Resources Map of the World (Richts et al., 2011; FIGURE 2.17) shows the various characteristics of global groundwater environments and the associated recharge estimates. Areas in blue indicate large and rather uniform groundwater basins (usually consisting of large sedimentary basins) which offer good conditions for recharge and groundwater exploitation. Areas in green correspond to more complex hydrogeological structures (for example in heterogeneous folded or faulted regions) and brown areas represent regions with limited groundwater resources in local and shallow aquifers. Each of this categories has been divided into up to five different classes depending on the potential recharge rates, which range from very high (>300 mm/yr) to very low (<2 mm/yr). Areas with low recharge estimates are generally more subject to groundwater

overexploitation, especially if they are present in (semi-)arid and highly populated environments. Recharge patterns are also an important factor for assessing groundwater vulnerability (FIGURE 1.3, **Chapter 1**): to do so, the recharge to runoff ratio is analyzed. Areas with high ratios (over 0.7), such as many European plains and the Asian part of Russia, among some other lowland areas, generally have a low vulnerability to droughts and floods. On the other hand, areas with low recharge to runoff ratios (i.e. arid and semiarid regions, mountainous regions, permafrost regions and Asian monsoon regions[7]) are particularly vulnerable. In these areas, seasonal and inter-annual precipitation variability is likely to have a significant impact. Global groundwater recharge is estimated at 12,666 km^3/yr, about 30% of total renewable water resources (Döll & Fiedler, 2008). Recharge per continent ranges from 404 km^3/yr in Australia to 4131 km^3/yr in South America. Note that the estimates shown in FIGURE 2.17 are estimates of *diffuse* recharge and do not include localized and indirect processes which are difficult to estimate at the macro-scale. This may lead recharge in (semi-)arid regions to be significantly underestimated (Döll & Fiedler, 2008).

[7] Although precipitations at a given time might be quite significant, only a small part of this heavy precipitation serves to recharge the groundwater, instead feeding into fast surface and subsurface runoff.

Chapter 3
Quantitative evaluation of recharge processes

Recharge is the single most important factor in the analysis and management of groundwater resources, especially in arid and semi-arid regions, yet it is also usually the least well-known quantity in hydrogeology (Kinzelbach et al., 2002). Quantitative recharge estimation contributes to understanding large-scale hydrologic processes [see Nimmo et al., 2005]. It is important for evaluating the sustainability of groundwater supplies; where groundwater contamination is a concern, the flux of water into the aquifer can contribute to predicting the rate of solute transport to the aquifer. Finally, the areal distribution of recharge and its intensity help us to predict aquifer vulnerability to contamination and better plan water exploitation strategies.

This section will review approaches to the quantitative evaluation of the different components of recharge. Most of these approaches are based on application of basic water-balance concepts and/or Darcy's law, in some cases employing various molecules or compounds as tracers. Ideally, a successful estimation of groundwater recharge lies in the utilization of a variety of independent methods; every method has its advantages and disadvantages, but combined they may become much more accurate [more on this in **Section 2.4.**].

1. The basic water-balance equation

Applying the basic water-balance equation to groundwater serves to identify the different groundwater balance components and how they relate to each other. As a first step in defining the water-balance of a system, a surface extent of the control volume must be defined. The most common delimitations are topographically defined watersheds or geologically defined aquifer extents. The lower boundary of the control volume is usually defined as the depth at which groundwater flow is negligible. Choosing a watershed as a control volume has an important advantage: it is usually possible to measure at least one of the balance components, i.e. surface-water outflow (streamflow), accurately. The risk of using topographically defined watersheds, however, lies in the fact that groundwater flow divides do not necessarily underlie surface divides, especially in small watersheds. This may lead to unaccounted-for groundwater inflows from deeper flow systems or other distance sources, thus distorting results from the water-balance equation. Thus, although water-balance equations are straightforward, strong uncertainty

relating to its outputs may arise as a result of [see Dingman, 2015] (a) insufficient knowledge on the system boundaries, (b) parameter estimation errors, and/or (c) failure to fully account for regional variability.

Under natural conditions (i.e. in the absence of human activity, such as pumping or artificial water storage), the *regional water balance* can be written as (FIGURE 3.1):

$$P + G_{in} = Q + ET + G_{out} \tag{3.1}$$

where P is precipitation, Q is stream outflow, ET is evapotranspiration, and G_{in} and G_{out} are water entering and leaving the control volume as groundwater. These terms can be expressed as volumes [L^3] or flow rates [$L^3.T^{-1}$] or [$L.T^{-1}$]. Note that these are long-term average values, so storage changes are assumed to be zero. Also, note that for simplicity purposes, groundwater inflow and outflow are often assumed either to be negligible or to cancel each other ($G_{in} = G_{out}$).

The long-term average *groundwater balance* can be written as:

$$R_I + R_{SW} + G_{in} = CR + Q_{GW} + G_{out} \tag{3.2}$$

where R_I is recharge from infiltration (diffuse recharge), R_{SW} is recharge from surface-water bodies (indirect recharge), CR is the movement of water from groundwater to the soil surface (i.e. capillary rise[8]) and Q_{GW} is the groundwater contribution to streamflow (also referred to as *baseflow* or Q_{BF}).

Net recharge from above, i.e. percolation minus capillary rise to supply evapotranspiration is then defined as:

$$R \equiv R_I + R_{SW} - CR \tag{3.3}$$

Combining Eqs. (3.1) and (3.3) gives:

$$P - Q - ET = R_I + R_{SW} - CR - Q_{GW} = R - Q_{GW} \tag{3.4}$$

Unfortunately, even if P, Q, and ET are well known, we can at best use Eq. (3.1) to estimate $G_{in} - G_{out}$ and Eqs. (3.2) and (3.3) to estimate $R_I + R_{SW} - CR - Q_{GW} = R - Q_{GW}$. It becomes apparent that firm knowledge of a basin's water balance requires independently evaluating at least some terms in Eq. (3.2). Approaches to obtaining quantitative estimates of some of these terms are detailed in the following sections.

[8] According to Dingman (2015), capillary rise is "*extraction of water from the unsaturated zone and capillary fringe by evapotranspiration*". It is usually considered to be negligible, and is difficult to estimate as a separate component, thus often included as a part of basin ET.

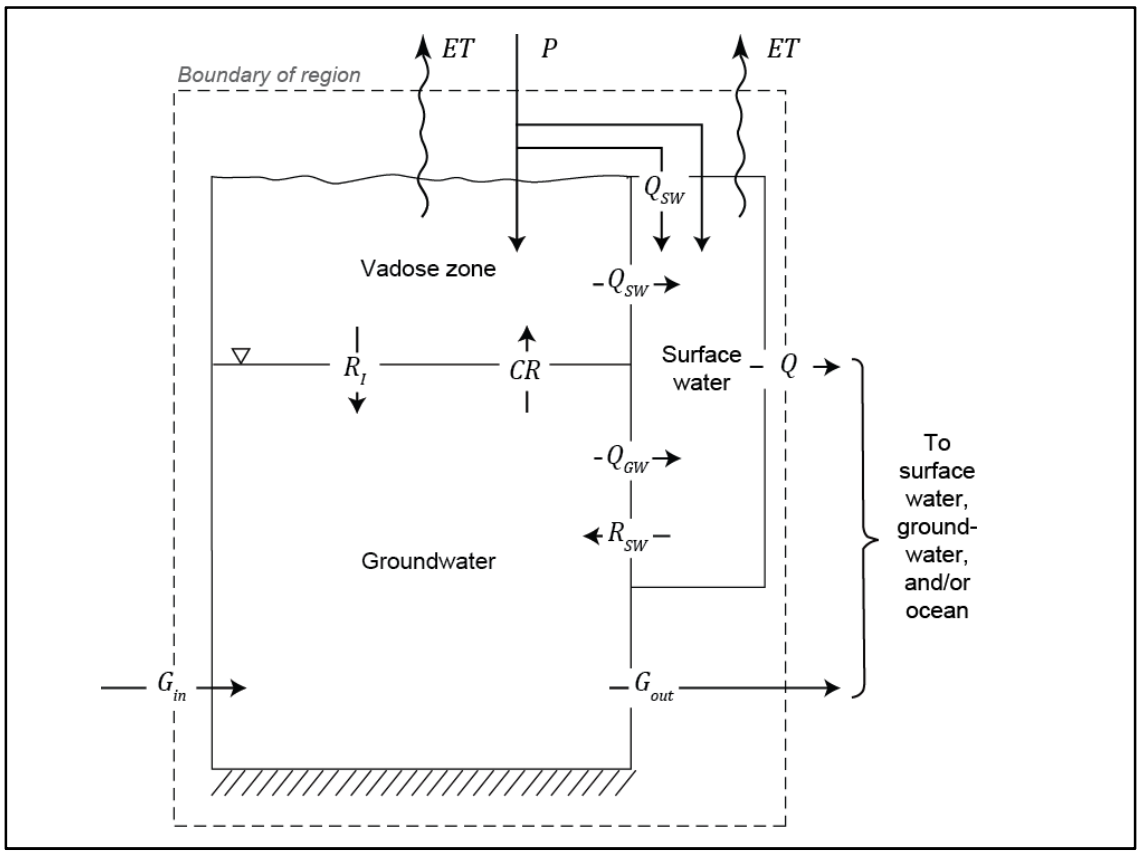

FIGURE 3.1: Schematic groundwater balance for a drainage basin (modified from Dingman, 2015)

2. Recharge estimation methods

2.1. Recharge from infiltration R_I (direct recharge)

Recharge from infiltration is the principal source of water to unconfined aquifers. Because of the difficulty in direct measurement of recharge, hydrologists have attempted to evaluate R_I by applying various combinations of water-balance concepts, applications of Darcy's law, soil physics principles, mathematical system models, and water quality measurements. The major methodological approaches are briefly described here; a full description may be found in one of the many available review papers or books on this subject, e.g. Allison et al., (1994); Gee & Hillel, (1988); Kinzelbach et al., (2002); Nimmo et al., (2005); Scanlon et al., (2002); Simmers, (1988); Healy & Scanlon, (2010). Note, however, that methods for estimating recharge from infiltration often assimilate *infiltration* to *recharge*, which assumes that all infiltration will eventually reach the water table. Actually, infiltration may more accurately be described as *potential recharge*. The difference between *potential* and *actual* recharge is due to the influence of the unsaturated zone (specifically, redistribution within this zone, FIGURE 2.6), or the aquifer may be unable to accept the potential recharge. Under some circumstances actual recharge may

be substantially less than potential recharge, for example if low conductivity layers restrict downwards flow. For simplicity purposes, however, this section will not make this distinction.

2.1.1. Direct application of Darcy's law

Darcian methods[9] allow us to estimate fluxes from head gradient and hydraulic conductivity using Darcy's law for unsaturated media (Eq.(2.8)). As stated previously, for vertical flow in the unsaturated zone, the Darcy equation takes the form:

$$R_I = q_z = -K(\theta)\frac{dh}{dz} = -K(\theta)\frac{d}{dz}(\Psi(\theta) + z) = -K(\theta)(\frac{d\Psi(\theta)}{dz} + 1) \qquad (3.5)$$

In unsaturated flows, both the pressure head Ψ and the hydraulic conductivity K are functions of the local water content θ. Thus, the main issue with this method is the difficulty to estimate the relationship between water content and hydraulic conductivity $(K(\theta) - \theta)$ and the relationship between water content and the matric potential $(\Psi(\theta) - \theta)$ both on the field and in the laboratory [see **Chapter 2 Section 2.4.2.4.**].

In theory, the advantage of directly applying Darcy's law is the use of measurable quantities. However, in reality, these measurable quantities may be difficult to estimate, and accounting for their great variability and uncertainty is not necessarily possible. Further, it is important to highlight that even when properly applied, Darcian methods do not indicate total recharge, as they only account for piston flow in the soil matrix, and do not account for flow through macropores and other preferential flow pathways.

2.1.2. Direct measurements

Direct measurements provide localized and straightforward measurements of recharge. However, these methods are often criticized due to their inherent inability to account for the spatial and temporal variability of recharge processes caused by the variability of topography, soil type and vegetation cover. Also, direct measurements often require elaborate instrumentation which is most often associated to research settings. The two main methods in this category are lysimeters measurements and soil moisture measurements, which are used to perform a soil moisture budget.

- **Lysimeters** are devices consisting of an in-situ weighable soil column. The flux by rainfall into the column, the outflow by seepage in 1-2 m depth and the weight are measured throughout the infiltration process. From them a water budget is reconstructed. The missing term—evaporation—is calculated.

[9] Darcian methods are methods which assume flow is *Darcian*, i.e. laminar flow in a uniform soil matrix.

Overall, lysimeters yield useful data, providing direct measurements of evapotranspiration, water storage changes, and drainage; annual drainage rates can be obtained with a precision sometimes below 1 mm/yr. However, recharge estimates are profoundly impacted by changes in surface conditions yet lysimeters provide only very localized measurements.

- **Soil water balances (measured)** consist of measuring changes in water storage below the root zone which are attributed to drainage. Geophysical techniques are most often used to provide indirect measurements of soil-water content. These methods measure a certain property that varies with water content, such as the electrical conductivity of the soil-water mixture. Among the most popular soil-moisture measurement methods there is the Time-domain Reflectometry (TDR) probe, which measures the dielectric permittivity of the soil and translates it into soil content, and Neutron probes which measure hydrogen density and are calibrated to determine soil-water content. Note that the absence of variation in moisture content at monitored depths may however not necessarily be an indication of no-flow, but could also be attributed to steady flow under a gravity gradient.

Generally speaking, 1-D methods can be useful to perform a calibration on more exhaustive methods, or to obtain a first estimate of diffuse recharge. For purposes requiring spatialized rather than point estimates, additional interpretation and calculations may be necessary.

2.1.3. Soil water balance method (calculated)

In the absence of detailed soil and plant information, general soil water balance approaches are generally used. One notable example of this approach is the Thornthwaite and Mather method (Healy & Scanlon, 2010; Thornthwaite & Mather, 1955), in which recharge can be obtained on a *monthly* basis by using a simple "bookkeeping" procedure (described in full in Healy & Scanlon, 2010). Although groundwater recharge is not an explicit component of these water balances, it can be estimated with a few simple assumptions. The equation solved on a monthly basis is as follows:

$$P = ET + S + Q \tag{3.6}$$

where S is the change in soil water storage, and Q is the sum of direct runoff (Q_{SW}) and base flow (Q_{GW}). PET is estimated from temperature, and actual ET, S and Q_{GW} are estimated using a bookkeeping approach: precipitation is treated as income and potential evapotranspiration as outgo, and soil moisture as a reserve that may be drawn upon as long as it lasts. S_{max} is approximated from soil texture and thickness. The user decides what percentage of the moisture surplus constitutes direct runoff, the remainder being

designated as baseflow. If ET from groundwater and changes in groundwater storage are negligible, recharge can be equated with base flow.

This method was later modified by Steenhuis & Van Der Molen (1986) to function at a daily time-step and accounting for the delay of percolation through the soil. This method has been used extensively in temperate areas. However, this method might be less accurate in semi-arid areas because R_I is generally small relative to other variables, in particular ET. In this case, small inaccuracies in values of those variables result in large uncertainties in the recharge rate (Gee & Hillel, 1988; Scanlon et al., 2002). In order to improve the accuracy of soil water balance techniques in (semi-)arid climates, Rushton et al. (2006), added a near surface soil storage to account for continuing ET on days following a heavy rainfall event, even in the presence of large soil moisture deficits.

2.1.4. Stream hydrograph methods

In watersheds with gaining streams (FIGURE 2.14), groundwater recharge can be estimated using stream hydrographs. There exist several theoretical and empirical approaches for quantifying recharge using streamflow hydrographs (Healy & Cook, 2002), the basic purpose of which rely on identifying the portion of total discharge (Q) which can be attributed to baseflow (Q_{GW}), assumed to be equal to recharge. Hydrograph analysis is usually performed in relatively humid regions, where streams are perennial and there is a well-sustained baseflow. Analytical techniques include hydrograph separation, chemical hydrograph separation, recession-curve displacement, and analysis of flow-duration curves [see Nimmo et al., 2005; Scanlon et al., 2002 and references therein]. With hydrograph separation methods, base flow is assumed to be a continuous process, and recharge is calculated by summing groundwater discharge to a stream on a daily basis over the period of interest. Recession-curve displacement methods assume that recharge is episodic, i.e. recharge and rises in stream stage occur only in response to storms. Recharge is estimated by determining the amount of streamflow that corresponds to groundwater discharge for each rise in stage and summed over all storm events.

Note, however, although the rate of groundwater discharge is strongly related to the rate of recharge, the two are not necessarily equal. This is because there may be other significant sources of discharge, such as evapotranspiration, pumping, or groundwater flow out of the basin. Many basins are thus unsuitable to hydrograph analysis method such as basins with significant groundwater withdrawals, basins with losing streams, or basins where the natural streamflow has been severely modified by the presence of dams or other barriers. Also, the accuracy of the obtained recharge rates depends on the validity of the various assumptions, such as assuming that bank storage is negligible or that

recharge is spatially uniform. These questions are however less relevant in very long-term data analysis.

2.1.5. Methods based on tracers

Many different geochemical tracers can be used for recharge estimation. These include water molecule constituents, such as tritium (^{3}H), oxygen-18 (^{18}O) and deuterium (^{2}H); naturally occurring anions such as chloride (Cl^{-}); diffuse pollution introduced by human activity; applied organic dyes (fluorescein) and dissolved gases such as chlorofluorocarbons (CFCs) or sulfur hexafluoride (SF_6). However, only a few have found widespread use at scales relevant to aquifer recharge. Recharge is estimated from chemical tracers following one of the two basic methods (Nimmo et al., 2005):

(a) **Relating tracer concentrations to mass-balance equations**. For this, a sample from either soil water of groundwater and atmospheric deposition data are required. Recharge is then deduced from the concentration in the sample and the deposition rate the tracer in question across the land surface (accounting for inputs from precipitation, dry deposition, runoff, irrigation and anthropogenic modifications).

(b) **By determining the "age" of the groundwater.** This can be done following one of two methods (or a combination of both).

- The first relies on tracers which have time-dependent input functions (originally due to varying atmospheric concentrations), such as chlorofluorocarbons (CFCs) and tritium. As the atmospheric partial pressure of the tracer changes over time, then successive water bodies coming into contact with the atmosphere will present distinct tracer concentrations (if mixing processes can be neglected), and basically reflect the time elapsed between the last gas exchange and the sampling date.
- Radioactive tracers can also indicate how long since the water was last in contact with the atmosphere. For this, the initial input concentration of the radioactive tracer should be known. If we consider a closed system, in which all isotopic changes are purely the result of radioactive decay, then the ratio of the stable daughter and radioactive mother is a direct measure for the time elapsed since the water was last in contact with the atmosphere. Other dating methods are based on the continuous increase of a particular tracer. In this case, estimation of groundwater residence times requires knowledge on accumulation rates.

Once the age of the groundwater is known, recharge can be approximated—if the mixing rate is small—through knowledge on the total volume of the reservoir (the total volume divided by mean residence times equals a mean recharge rate).

Groundwater ages can also be used to better constrain recharge through inverse applications of numerical models [Section 2.1.6.2 of this chapter].

Methods based on tracers can also be categorized depending on the type of molecule or compound used.

2.1.5.1. Chemical tracers

A chemical tracer suitable for estimating recharge must meet several criteria: (i) it must be present in measurable amounts, (ii) there should be no significant retardation or acceleration of the tracer due to interactions with the vadose zone or vegetation, and (iii) the tracer's rate of introduction should be known, being ideally either a pulse or a constant rate of input.

For a column of the vadose zone in which no horizontal flow occurs above a water table, the balance for such a tracer is:

$$C_W \times W = C_{GW} \times R_I \tag{3.7}$$

where W is the water input (generally precipitation) [$L^3.T^{-1}$], C_W is the concentration of the tracer in the water input as it infiltrates [$M.L^{-3}$ or $L^3.L^{-3}$], C_{GW} is the concentration in groundwater [$M.L^{-3}$ or $L^3.L^{-3}$], and all terms represent long tem averages.

One of the most commonly used tracers is chloride, as it presents many advantages: it is commonly present in precipitation, it is not used by plants, and not commonly involved in soil-chemical reactions (i.e. generally inert). Chloride occurs naturally at the soil surface both in rainfall and as dry fallout. In the simplest case of piston flow through the unsaturated zone, chloride concentrations should increase through the root zone up to a constant value which is then used in Eq. (3.7) (FIGURE 3.2a). Unfortunately, depth profiles of chloride in soil water often show a more complex shape than in FIGURE 3.2a. Bulge-shaped chloride profiles at some sites have been attributed to paleoclimatic variations (FIGURE 3.2c) or to diffusion to a shallow water table (FIGURE 3.2b). And, sometimes the vertical distribution of chloride can be affected by the existence of preferential flow paths (Allison et al., 1994).

Many examples may be found in literature where chloride is used to estimate recharge across the globe (e.g. Alcalá & Custodio, 2015; Bromley et al., 1997; Edmunds et al., 2002; Maréchal et al., 2011). Detailed aspects of using chloride to estimate recharge have been published by Allison et al. (1994) and Taniguchi & Sharma (1990), among others.

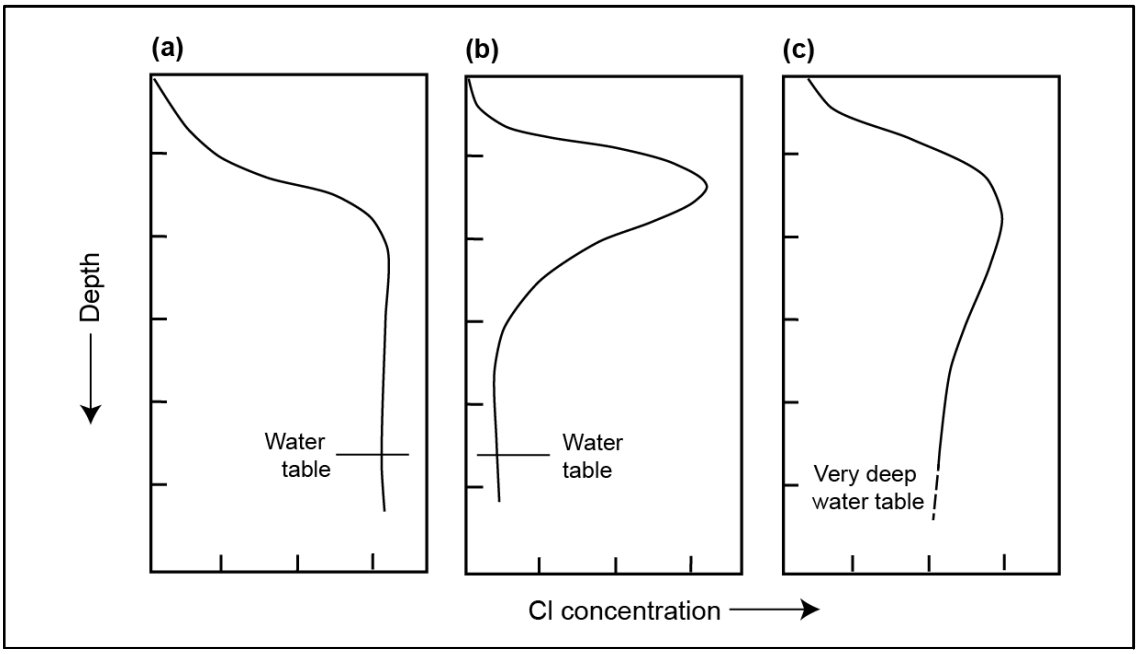

FIGURE 3.2: Schematic depth proles of the Cl concentration of soil water: (a) piston flow with extraction of water by roots; (b) same as (a) but with preferred flow below the root zone or diffusive loss to the water table and (c) a profile reflecting past recharge conditions (modified from Allison et al., 1994)

2.1.5.2. Stable isotopes

Stable isotopes of oxygen (such as ^{18}O) and hydrogen (deuterium i.e. ^{2}H or D) have also proven useful to study recharge, more particularly regarding the source and timing of recharge. Darling & Bath (1988) cite several studies in which stable isotopes of oxygen and hydrogen were used to obtain information about the seasonality and rate of recharge.

In sum, isotopes can be indicators of evaporation (but not plant transpiration). If the salinity of a groundwater sample is primarily due to the concentration of dissolved elements by evaporation, then the ^{18}O-^{2}H relationship will reflect the kinetic fractionation resulting from this mechanism—increased evaporation results in isotopic enrichment (e.g. Sami, 1992). Temperature and altitude effects may also cause differences in ^{18}O and D concentrations over a catchment area, to which mixing ratios can be applied. In regions where there is a strong topographic gradient (e.g. in mountainous areas), river water is often depleted in stable isotopes relative to local precipitation in adjacent basins. If rivers retain the depleted isotopic signature of the river source, then the difference in stable-isotope signatures of the rivers and local precipitation can be used to determine the relative contribution of these two sources of groundwater recharge using mass-balance equations, although additional information may be required (Scanlon et al., 2002).

2.1.5.3. Radioactive isotopes

The most common radioactive isotope used for recharge estimation is tritium (^{3}H). Tritium is a radioactive isotope of hydrogen with a half-life of 12.4 years; it is a non-conservative tracer which works as a time marker due to its radioactive decay. It is used to determine water ages as it moves with the water molecule. Naturally occurring tritium is rare, the majority of tritium in the atmosphere was created as a result of thermonuclear tests taking-place in the mid-1900s, before nuclear tests in the atmosphere were banned in the 1960s. Since cessation of atmospheric nuclear tests tritium concentrations have dropped, and the timing of the tritium spike, occurring in 1963, is well known. Most tritium is spread in the environment as water; it enters the hydrologic cycle as precipitation, and eventually attains groundwater. Groundwater tritium concentrations reflect the atmospheric tritium levels at the time the water was in contact with the atmosphere, and can therefore be used to estimate the age of the water, from which we deduce the rate of groundwater recharge. If ages are known along a flow line, then the recharge rate is calculated as (Nimmo et al., 2005):

$$R = \frac{\bar{\theta} L}{A_2 - A_1} \tag{3.8}$$

where $\bar{\theta}$ is the average volumetric water content, L is the length of the flow line, and A_1 and A_2 the ages at two points. For this technique to be applicable certain conditions must apply: mixing should be small, and the medium must be representable as a continuum (Nimmo, 2005).

Although tritium has proven useful in many studies to calculate recharge (e.g. Allison & Hughes, 1978; Dincer et al., 1974; Lin & Wei, 2006), it presents several disadvantages (Edmunds et al., 1988): (i) tritium can be lost by evaporation and transpiration, (ii) tritium has a relatively short half-life: since the peak in 1963 a little over 4 half-lives have elapsed, which implies tritium concentrations have been reduced by a factor of 16. With no further atmospheric nuclear weapon testing, the use of tritium of age dating is approaching an expiration date[10], (iii) sampling and processing present many challenges: samples are quite vulnerable to contamination, especially in remote areas at low moisture levels; furthermore, analysis of these samples is quite costly, (iv) quantitative measures are difficult to undertake since it is difficult to determine a tritium mass balance, and (v) the interpretation of the data may be difficult if the flow regime is not reasonably uniform.

[1010] However, even though tritium concentrations might be too low to provide a quantitative assessment of recharge, qualitatively speaking its presence may still be an indicator of the presence of "modern" water (i.e. younger than 50 years).

2.1.6. Numerical modeling

Recharge measurements in the field still contain an appreciable amount of uncertainty, and much study on the subject is still ongoing. Along with the variety of approaches used to make measurements in the field, researchers have used groundwater models to help estimate recharge. If the other model parameters are known well enough, then the model can be used to model recharge.

2.1.6.1. Representing recharge in models

In order to correctly represent recharge using a groundwater model, the *processes* that control the rate of recharge must be considered. As detailed in **Chapter 2 Section 3.3**, recharge rates are linked to the hydrologic landscape of the aquifer system, which are controlled by three main factors: climate, topography and lithology (Winter, 2001). These controls translate directly into the type of boundary condition most appropriate for representing recharge in a groundwater model. Sanford (2002) provides an extensive description of these considerations, which are summarized below.

Note that although described here, not all model dispositions are well suited to inverse methods of recharge estimation.

Lithology-controlled recharge

Lithology-controlled recharge, associated with conditions of relatively shallow water tables, can be represented by a constant-head boundary condition. The altitude of the water table is known (usually mimicking the land surface closely), and is expected to be relatively constant (FIGURE 2.16a). This boundary condition is mostly useful for steady-state models of regional systems where the position of the water table can be estimated fairly well. The advantage of this type of model is that recharge rates do not have to be estimated from uncertain hydrological measurements (i.e. ET and rainfall/runoff), but rather the rate of recharge is implicitly calculated based on the specified values of the other model parameters. The disadvantage of this type of model is that is assumes that the supply of water for recharge is infinite, which may lead to erroneously large values of recharge if the hydraulic parameters are not accurately represented. Also, this type of boundary condition is not appropriate for systems where transient drawdowns occur. In spite of these limitations, many studies exist where this type of boundary conditions was successfully implemented. One classic example is the study of the interaction of groundwater with lakes by Winter (1978), although more recent examples may also be found (W. P. Anderson & Evans, 2007; Halford, 1999; Knowling & Werner, 2016).

Climate-controlled recharge

Climate-controlled recharge is recharge which is limited to some extent by the amount of infiltration available at the land surface (FIGURE 2.16b). In this case, the groundwater system is more effectively represented by a boundary condition of specified recharge flux. Recharge is controlled by the factors at the land surface, which limit delivery of recharge. Unlike the constant-head boundary condition, the model never implicitly calculates erroneous recharge rates. Instead, recharge is specified by the modeler, who has previously estimated recharge via an independent effort (e.g. Bauer et al., 2005; Croteau et al., 2010; Jyrkama et al., 2002). This allows for better-constrained model-simulated fluxes, depending on whether recharge rates are estimated with more certainty than subsurface permeabilities. The difficulty of this method, of course, lies in the necessity to estimate recharge rates and distributions, considering the limited accuracy of estimated runoff, AET, and the soil infiltration properties. This type of boundary condition is useful in situations where significant pumping may be observed leading to the formation of transient drawdown cones, or in mountainous terrains where the high topographic relief results in high variability of the depth of the water table (e.g. Forster & Smith, 1988; Gleeson & Manning, 2008).

Variably controlled recharge

Generally speaking, it is common for both recharge controls to be present in a single location, or both types may be present throughout separate areas of a modelled domain. Sometimes the type of control will alternate in time depending on climate conditions. For these situations mixed-boundary conditions are most suitable. Many widely used groundwater models, such as MODFLOW (Harbaugh et al., 2000), offer the possibility of choosing between a variety of mixed-type boundary conditions: an external specified head is linked to the hydraulic conductivity which determines the outgoing flow. These types of boundaries are useful to describe many types of natural boundaries. A river, for example, is represented by the head in the river and the riverbed conductance. This type of model becomes further useful where surface-water/groundwater interactions are of interest. Some examples of this are the study of groundwater-lake interactions (Merritt & Konikow, 2000), groundwater-stream interaction (Workman et al., 1997), or even for studies of managed aquifer recharge (Kacimov et al., 2016). Limitations however exist concerning the accuracy of MODFLOW simulations of surface-water and groundwater, many of which are summarized in Brunner et al., (2010), such as the absence of transitional stages between fully connected or fully disconnected rivers, and possible errors arising from the use of coarse vertical discretization to avoid the drying out of cells. Although some of these mixed-boundary conditions do not represent recharge directly, there

are often used in conjunction with specified-flux recharge conditions to better represent the aquifer system.

In sum, the type of process which controls recharge (and the objectives of the study) will determine the manner in which recharge is incorporated into groundwater models. In relatively humid climates or low topographic relief, the water table is often shallow, and the geological framework controls the rate of recharge. Additionally, if the topographic relief is very low, then the water table gradient may also limit the rate at which recharge is transmitted away. In this case, recharge is most often controlled by the permeability of the geologic framework, and thus simulated using a constant-head boundary condition. In (semi-)arid regions or zones of high topographic relief, the water table is often deep and recharge will be mostly controlled by the amount of water that climate provides and the soil's ability to deliver it to the water table. This type of situation is best modelled using a specified-flux boundary condition (which implies recharge must be estimated separately).

2.1.6.2. Inverse methods for estimating recharge

The general groundwater flow equation can be incorporated into a model that accounts for an assumed regional distribution of recharge. An inverse application involves finding the values of recharge by calibration: recharge values are changed until a given *modelled* variable corresponds to the *observed* values of this variable (Carrera et al., 2005). The most commonly used variable is the distribution in groundwater heads, which is compared to on-site observations from piezometers. Groundwater ages obtained using tracers [Section 2.1.5] are also used, if an independent estimation of effective porosity is available.

Although there are several instances of these methods being applied successfully (e.g. Ebrahimi et al., 2016; Hashemi et al., 2013; Knowles et al., 2007), the risk of non-uniqueness of solutions (also termed equifinality of parameters; Beven, 2006) must be considered: this implies that here are several acceptable sets of parameters (in this case recharge distributions) that may give model outputs (head distributions or groundwater ages) that match the field observations within the uncertainty of those observations. This is because recharge and hydraulic conductivity are closely related, and hydraulic conductivity may range over several orders of magnitude. The same distribution of hydraulic heads can be produced with a range of recharge rates, as long as the ratio of recharge to hydraulic conductivity remains the same. Some studies have tackled this issue by using joint inversions that combine hydraulic heads and groundwater ages to further constrain modeling of recharge [see Sanford, 2011 and Leray et al., 2012].

2.2. Recharge from surface-water R_{SW} (indirect recharge)

The status of recharge related to surface-water bodies (i.e. indirect and localized recharge) depends on the connection between surface-water and groundwater systems (Sophocleous, 2002), and on the position of the river stage relative to the groundwater head (FIGURE 3.3). In general terms, if the groundwater head is higher than the river stage then the aquifer flows into the river; vice-versa, if the river stage is above the groundwater head then the river discharges into the aquifer. The intensity of the flow into or out of the aquifer depends on the difference between river stage and groundwater head; although in losing streams the discharge from the river into the aquifer is assumed to be relatively constant if the water-table is at a depth that exceeds two times the river width (FIGURE 3.3). Humid regions are generally characterized by gaining surface-water bodies because the water table is high enough to discharge into streams and lakes. Contrariwise, in (semi-)arid regions surface-water and groundwater are often separated by an unsaturated zone, which leads to losing surface-water bodies (FIGURE 2.14). Although there are few published studies in which R_{SW} has been estimated, the principal approaches that can be applied to the evaluation of this quantity are outlined here.

2.2.1. Groundwater balance computation

In some arid regions, average AET is nearly equal to average precipitation, so a large part of infiltrating water evaporates; recharge is essentially indirect recharge (from losing streams, FIGURE 2.14). This, for example, was found to be the case in the Amargosa River basin in Nevada in the study by Osterkamp et al. (1994) where a water-balance computation was applied in combination with streamflow measurements where it was found that only 1.6% of basin precipitation became recharge and that 90% of recharge was from streams. As a more recent example, we may cite the work by Cuthbert et al., (2016) in which implementation of a water-table fluctuation approach was combined with observations from an ephemeral stream catchment in NSW Australia. This study found that, in relative terms, groundwater recharge decreases linearly away from the mountain front to the perennial stream section, and, in absolute terms, that indirect recharge varied between 30 to 80 mm/yr.

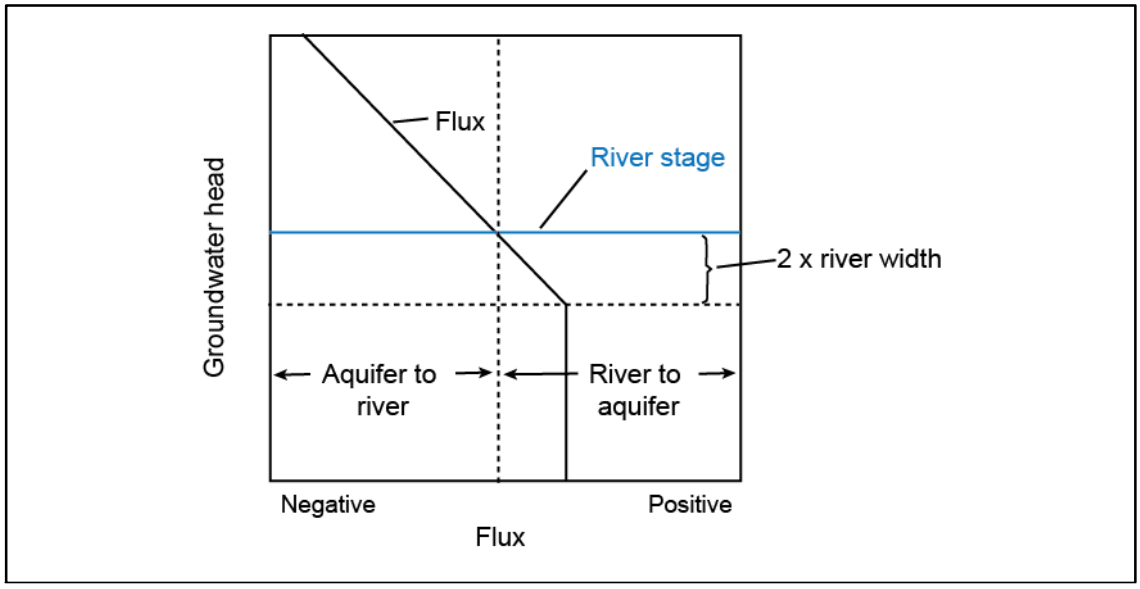

FIGURE 3.3: Water fluxes related to the degree of connection between rivers and aquifers. The aquifer discharges to the river when the groundwater head is greater than the river stage, and vice versa. Recharge values generally reach a constant rate when the water-table depth is greater than twice the river width (modified from Scanlon et al., 2002)

2.2.2. Direct measurements

2.2.2.1. Direct measurement of groundwater potential or flux

The gradient of flow entering or leaving a stream can be measured using a different set of measurements (FIGURE 3.4). One can compare the water level of the stream with the head measured in a piezometer from the subjacent bed, or the levels in two piezometers inserted to different depths below the bed. If the gradient is facing downwards, then the outgoing flux can be calculated using Darcy's law using measured or estimated hydraulic conductivities. This method does not however account for the great spatial and temporal variability which may characterize the stream, so such measures must be extrapolated with caution.

2.2.2.2. Direct measurement of streamflow increments

By calculating the difference in stream discharge at the upstream and downstream limits of a stream reach (assuming there is no overland or tributary flow), it is possible to determine groundwater inflow or outflow. The accuracy of these methods depends on the precision of streamflow measurements, and is increased by maximizing the difference between the upstream and downstream discharges. More detail on these methods can be found in Dingman (2015).

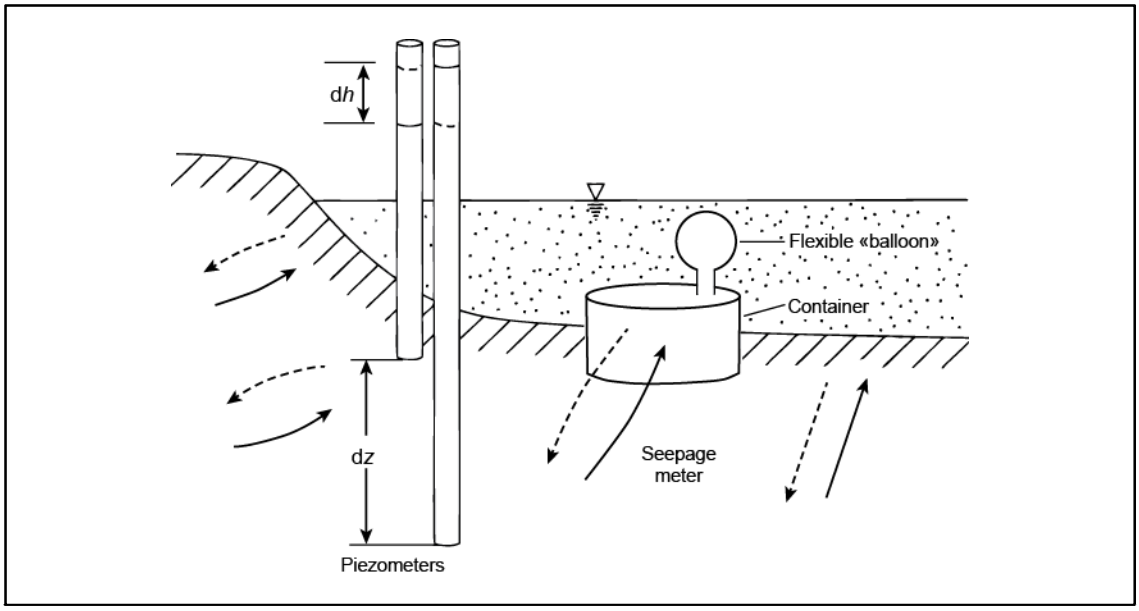

FIGURE 3.4: Schematic representation of the use of piezometers and seepage meter to measure groundwater flux into (solid line) or out of (dashed line) a stream. Arrows indicate flow direction, dh is the head difference and dz is the elevation difference between the two piezometers. Vertical flow is calculated using Darcy's law. Water flowing into or out of the container of the seepage meter is collected in the flexible 'balloon' (modified from Dingman, 2015)

2.2.2.3. Water temperature measurements

Installing stream-gauging stations may be expensive and difficult, particularly in (semi-)arid regions where streams are ephemeral. As an alternative to stream-gauging, heat can be used as a tracer to provide qualitative and quantitative information on surface-water/groundwater interactions (M. P. Anderson, 2005; Constantz et al., 1994; Healy & Ronan, 1996; McCallum et al., 2012). In the absence of infiltration, temperature distributions below the realm of seasonal temperature variations approximately follow a geothermal gradient. If water penetrates into the system it will perturb the geothermal temperature distribution, and the degree of perturbation indicates recharge rates in deep unsaturated zones. To quantify these recharge rates, measured temperature profiles are used in analytical or numerical inversions of the equations governing the coupled transport of heat and water. Stream temperatures are temporally highly variable due to daily and seasonal cycles, and their fluctuations can be approximated using sinusoidal functions. Monitoring depths vary depending on timescales, sediment types and anticipated water fluxes beneath the stream. Measurements are performed thermistors or thermocouples, although the emergence of fiber-optic distributed temperature sensing (FO-DTS) as a means to monitor hydrologic processes (Lane et al., 2008) has catalyzed the use of heat at a surface-water/groundwater tracer (Hare et al., 2015; Krause et al.,

2012; Slater et al., 2010). The accuracy of these methods generally depends on the range of surface-water temperature fluctuations (i.e. the amplitude of the input signal) at the timescale considered (Rose et al., 2013).

2.3. Total recharge ($R_I + R_{SW}$)

Methods used to estimate total recharge are generally based on the saturated-zone, in opposition to diffuse recharge measurements which tend to focus on the unsaturated zone, and as such often provide point estimates of recharge. Saturated-zone techniques generally integrate much larger areas and provide evidence of *actual* recharge rather than *potential* recharge as they are based on water which actually reached the water table.

2.3.1. Water-table fluctuation methods

Information on groundwater levels and how those levels vary in time and space can be used to estimate recharge. These techniques are the most widely applied in order to estimate recharge rates. The popularity of this method can safely be associated with the simplicity of estimating recharge rates from temporal and spatial variations of groundwater levels and in some cases the abundance of groundwater-level data. A summary of the different recharge estimation methods that depend on groundwater level measurements can be found in Healy & Cook (2002).

2.3.1.1. Groundwater budget

Water-budget methods are those that are based, in one form or another, on a water-budget equation. The most common way of estimating recharge by the water-budget method is the indirect or "residual" approach, whereby all of the variables in the water-budget equation, i.e. water entering, leaving, and being stored within the system, are measured or estimated (Scanlon et al., 2002). Recharge is set equal to the residual. Inputs correspond to the sum of recharge, irrigation return flow and groundwater inflow to the basin whereas outputs are the sum of baseflow, evaporation from groundwater, pumping and the groundwater outflow from the basin:

$$R + RF + G_{in} = E + PG + Q_{GW} + G_{out} + \Delta S \qquad (3.9)$$

in which R is total groundwater recharge, the sum of direct and indirect recharge, RF is irrigation return flow, E is evaporation from the water table, PG is abstraction of groundwater through pumping, ΔS is the change in groundwater storage, Q_{GW} is the groundwater contribution to streamflow, and G_{in} and G_{out} are water entering and leaving the control volume as groundwater. For simplicity purposes, groundwater inflow and outflow are often assumed either to be negligible or to cancel each other ($G_{in} = G_{out}$). Transpiration from the water table is also often negligible because the depth of the groundwater exceeds the maximum rooting zone. The main unknown in Eq. (3.9) is the

change in groundwater storage, which, thanks to the water-table fluctuation (WTF) method can be linked to the aquifer's specific yield S_y and water table fluctuations Δh (Healy & Cook, 2002):

$$\Delta S = S_y \Delta h \tag{3.10}$$

2.3.1.2. Water-table fluctuation method

Indeed, the WTF method links changes in groundwater storage to resulting water table fluctuations by using the storage parameter. If we equate recharge to changes in groundwater storage; the resulting equation is (Healy & Cook, 2002):

$$R = S_y \, \Delta h / \Delta t \tag{3.11}$$

To obtain a total recharge estimate, Δh is set as the difference between the peak of the groundwater rise and low point of the recession curve (obtained by extrapolating the antecedent recession curve at the time of the peak). This method presents many advantages. First, it is straightforward and simple; second, no assumptions are made concerning unsaturated zone transfers, and finally this method accounts for recharge from preferential flow paths as it is a measure of *total* recharge. This is especially important when it comes to fractured aquifers. Finally, because water level measurements in observation wells are representative of relatively large areas (tens to hundreds of meters), this method offers a more integrated approach than point measurements. Difficulties in applying this method are related mainly to the need to determine specific yield.

The importance of determining specific yield

Determination of S_y is thus crucial to the determination of recharge in water-budget methods. According to Meinzer (1923), the specific yield of a rock or soil, with respect to water, is the ratio of (i) the volume of water which, after being saturated, will yield by gravity to (ii) its own volume. The complimentary term *specific retention* refers to the volume of water having retained against the pull of gravity per unit volume of rock. The following formula is used:

$$S_y = \phi - S_r \tag{3.12}$$

in which Φ is porosity and S_r is specific retention. The term *effective porosity* has been used to mean about the same thing as specific yield, and can be defined as the ratio of (i) the volume of water a rock which will yield under any specified hydraulic conditions to (ii) the volume of the rock. Representative values of Φ, S_y, and S_r for different lithologies can be found in TABLE 3.1.

Geological formation	ϕ (%)	S_y (%)	S_r (%)
Unconsolidated deposits			
Gravel	28–34	15–30	3–12
Sand	35–50	10–30	5–15
Silt	40–50	5–20	15–40
Clay	40–60	1–5	25–45
Loess	45–50	15–20	20–30
Consolidated rock			
Sandstone	15–30	5–25	5–20
Limestone	10–25	0.5–10	5–25
Shale	0–10	0.5–5	0–5
Dense crystalline rock	0–5	0–3	-
Fractured crystalline rock	5–10	2–5	-
Weathered crystalline rock	20–40	10–20	-
Basalt	5–30	2–10	-

TABLE 3.1: Representative values of porosity (Φ), specific yield (S_y) and specific retention (S_r) (from Singhal & Gupta, 2010)

=

There are several ways to determine S_y, using either laboratory or field methods:

(a) The laboratory method consists in filling a column with undisturbed sediments and then saturating it with water; water is allowed to drain from the bottom of the column and the test continues until drainage ceases. This method presents many disadvantages and should be avoided unless it is impossible to apply field techniques. These limitations include, but are not limited to, the impact of the tube's capillarity on drainage, the non-representativeness of the volume inserted into the column (this is especially important regarding heterogeneous fractured aquifers), and having to account for evaporation taking place in the experimental chamber (Healy & Cook, 2002). Overall, the consensus is that field methods should be strongly prioritized.

(b) Aquifer tests provide in-situ measurements of S_y and other aquifer properties integrated over fairly large areas. To do so, a long term pumping experiment is put in place during which a well is pumped at a controlled rate while the drawdown in the surrounding wells is measured. Then drawdown-versus-time data from these observation wells is plotted against theoretical type curves, a variety of which exist to account for different aquifer conditions, e.g. the Theis solution (1935) for confined aquifers, the Dupuit solution for unconfined aquifers (Serrano, 1995).

(c) Development of geophysical tools, which have gained in precision and resolution, has led to the publication of works where geophysics are used to estimate S_y:

- Micro-gravity measurements of specific yield rely on the use of temporal gravity surveys which performed to measure small changes in gravity, which are then attributed to variations in aquifer storage. S_y is calculated by dividing storage changes by water-level changes (Christiansen et al., 2011; Gehman et al., 2010; Pool & Eychaner, 1995).
- Measuring changes in water storage using a soil moisture sensor can also allow estimation of S_y. There are several types of moisture sensors, such as neutron probes, Frequency Domain Reflectometry (FDR) and Time Domain Reflectometry (TDR) sensors (which use the principle of electrical capacitance) The amount of stored water is determined by calculating the difference between moisture content of the saturated material and the moisture content of the same material after it has been drained (O. R. Jones & Schneider, 1969; Said et al., 2005).
- Sometimes borehole logging is not an option, and water-table fluctuation data is unavailable. For this reason many new methods have been developed that rely on the measurement of other parameters as a proxy for S_y. This is the case, for example, of recent work relying on the use of magnetic resonance soundings to quantify S_y (Boucher et al., 2009; Vouillamoz et al., 2008, 2014).

Unfortunately, many of the above mentioned methods focus on sedimentary (porous-media) aquifers where porosities and specific yields are high (TABLE 3.1) and the medium is homogeneous. Estimation of specific yield (and other hydraulic parameters) in fractured crystalline rock, where specific yields are much lower (TABLE 3.1), is often quite difficult. On one hand, interpretation of aquifer tests in these systems leads to important problems of non-uniqueness. Further, even if S_y is somehow estimated, most methods are not sufficiently accurate to permit estimation of recharge using derived values. The most widely used technique so far for estimating S_y in fractured-rock systems is one that does not make assumptions concerning flow processes, relying on the water budget method and the water-table fluctuation method. More detail on specific yield estimation in fractured rock will be given in Section 3.4.3 of this chapter.

2.3.1.3. Double water-table fluctuation method

Maréchal et al., (2006) developed a combination of the groundwater budget and water-table fluctuation methods, which was dubbed the double water-table fluctuation method (DWTF). In regions characterized by monsoon climate, the hydrological year can be divided into two distinct seasons, each with a distinct water-level rise or decline. This allows for a split use of the WTF method, first to estimate specific yield from the water-table drop during the dry season (when recharge is null) then to estimate recharge from the water-table rise during the rainy season once all other water budget compo-

nents are known. In water limited environments and in overexploited aquifers it is common for surface water to be virtually absent: no springs, baseflow, of surface streams are observed. In these conditions, the main outflow is groundwater pumping, and groundwater discharge to surface water Q_{GW} is assumed to be null. Eq. (3.9) becomes:

$$R + RF + G_{in} = E + PG + G_{out} + \Delta S \tag{3.13}$$

The terms of this equation are the same as in Eq. (3.9). By combining Eqs. (3.10) and (3.13) we obtain:

$$R + RF + G_{in} = E + PG + G_{out} + S_y \Delta h \tag{3.14}$$

The hydrological year is divided into two parts, dry, during which $R=0$, and wet, to obtain the two following equations:

$$RF^{dry} + G_{in}^{dry} = PG^{dry} + E^{dry} + G_{out}^{dry} + S_y \Delta h^{dry} \tag{3.15}$$

$$R + RF^{wet} + G_{in}^{wet} = PG^{wet} + E^{wet} + G_{out}^{wet} + S_y \Delta h^{wet} \tag{3.16}$$

These equations are solved sequentially: first, S_y is obtained by rearranging Eq. (3.15):

$$S_y = \frac{RF^{dry} + G_{in}^{dry} - PG^{dry} - E^{dry} - G_{out}^{dry}}{\Delta h^{dry}} \tag{3.17}$$

which is then introduced into Eq. (3.16) to obtain R:

$$R = S_y \Delta h^{wet} - RF^{wet} - G_{in}^{wet} + PG^{wet} + E^{wet} + G_{out}^{wet} \tag{3.18}$$

The advantage of this method is that S_y can be estimated at large scales and that it does not require extensive in-situ instrumentation, although its accuracy increases with the number of water level measurements. Combining this technique with a geostatistical approach can allow upscaling and regionalization of estimates at watershed scales (e.g. Dewandel et al., 2012). This technique is well suited to developing countries in (semi-)arid environments where data may be scarce but where there are a high number of dugwells and borewells (e.g. in Cameroon: $S_y = 8\%$, Fouépé Takounjou et al., 2011; in India: $S_y = 1.4\%$, Maréchal et al., 2006; or in Iran: $S_y = 4.2\%$, Rezaei & Mohammadi, 2017).

2.4. Choosing the appropriate technique

There are many different techniques available to quantify recharge. The review paper by Scanlon et al. (2002) offers a good amount of insight into the differences between recharge methods and the consideration to be had when choosing a technique.

The various recharge estimation techniques vary, first of all, in the range of recharge rates that they estimate (FIGURE 3.5). They also vary in the space and timescales they represent (FIGURE 3.7 and FIGURE 3.6). The ranges shown in these figures are approximate and based on measured ranges from the literature (Scanlon et al., 2002). Ideally, each particular technique should be evaluated on a site-specific basis by conducting detailed uncertainty analyses. Nevertheless, most techniques have definite restrictions on the recharge rates that they can estimate, as well as on the timescales they are applicable at and the spatial scales they represent. For example, methods based on the use of applied and historical tracers in the unsaturated zone require a minimum recharge rate to transport the tracers through the vadose zone. Chloride, on the other hand, is one of the few techniques that can estimate very low recharge rates, and that is generally more accurate in these ranges.

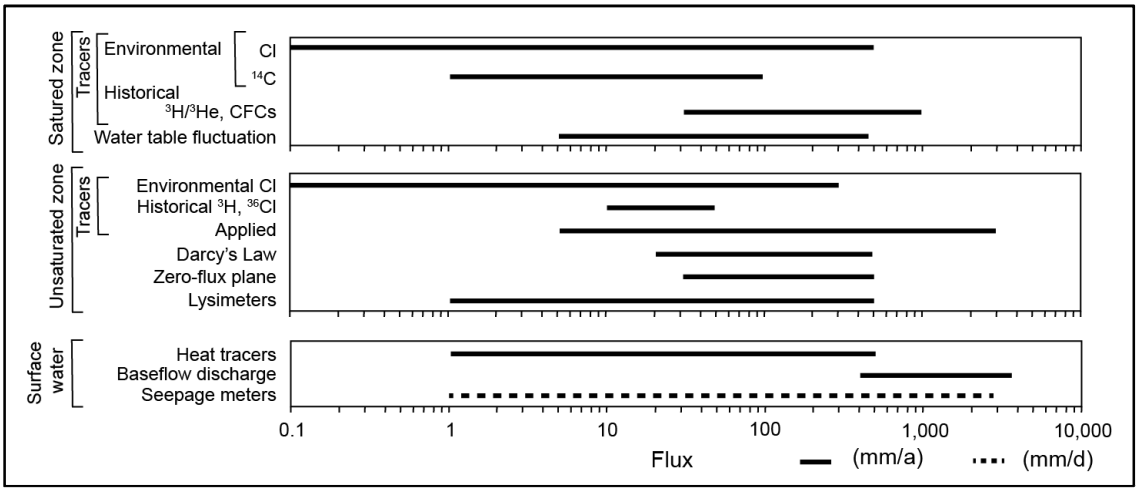

FIGURE 3.5: Range of fluxes that can be estimated using various techniques (from Scanlon et al., 2002)

The surface areas represented by a given recharge estimate will vary greatly among the different techniques (FIGURE 3.7). Generally speaking, methods based on the unsaturated zones tend to provide localized or point estimates and represent relatively small areas, while many of the surface-water and most of the groundwater approaches integrate much larger areas. Numerical modeling can be quite flexible, and allows for recharge estimation across a large range of scales.

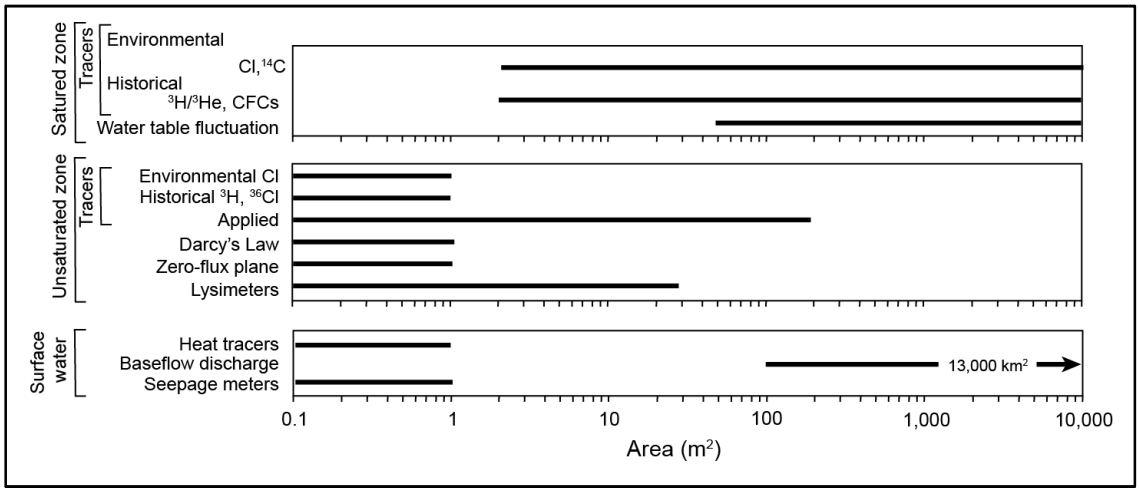

FIGURE 3.7: Spatial scales represented by various techniques for estimating recharge. Point-scale estimates are represented by the range of 0 to 1 m (from Scanlon et al., 2002)

The timescales represented by recharge estimates are quite variable (FIGURE 3.6). Methods based on surface-water are limited to shorter timescales (namely the time required for a hydrological event to take place). Many of the saturated zone techniques are also dependent on event timescales, and are thus bounded by the length of the monitoring record. Numerical modelling, again, may be used to predict recharge over any time scale, although recharge estimation based on climactic data is generally restricted to about 100 years. Tracers may be useful for providing integrated, long-term estimates of recharges. They do not, however, provide information on the temporal variation of recharge.

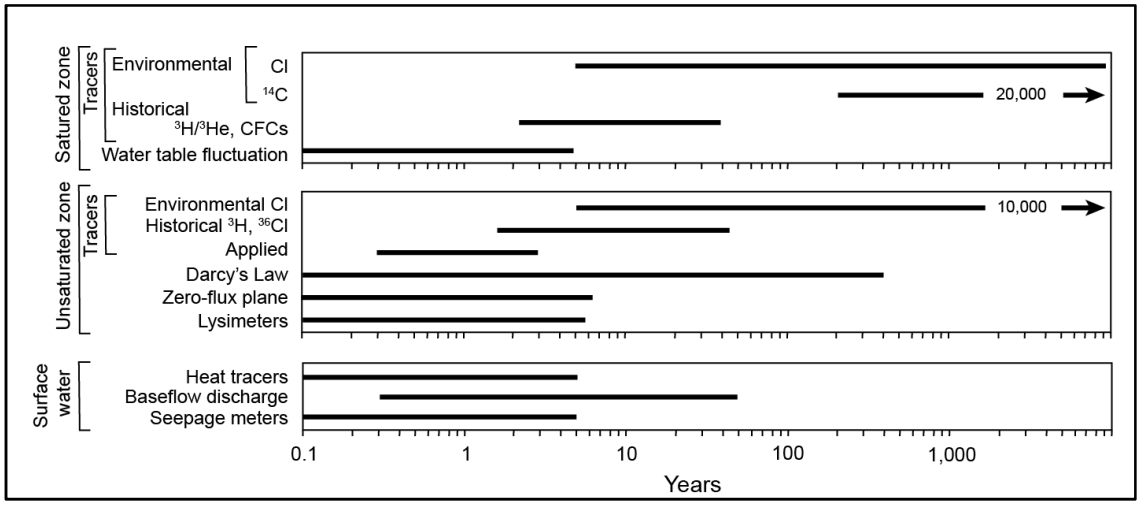

FIGURE 3.6: Time periods represented by recharge rates estimated using various techniques. Time periods for unsaturated and saturated- zone tracers may extend beyond the range shown (from Scanlon et al., 2002)

Further, depending on the climactic region (arid vs. humid), fundamental differences in recharge may call for the use of different approaches. Generally speaking, unsaturated-zone methods are more commonly used in (semi-)arid environments, while surface-water and saturated-zone techniques are more commonly used in humid environments, where the unsaturated zone might be too thin to allow the former. Watershed modeling approaches may be more accurate in humid regions, where model calibration can be performed using streamflow records.

In general, the combined use of several methods is preferred. This allows recharge estimates to be better constrained, and many methods complement each other. To cite some examples, we may refer to studies which combine soil physics (e.g. Scanlon et al., 1999) or remote sensing (e.g. Brunner et al., 2002) and environmental tracers, studies which combine methods based on surface-water (e.g. Kung et al., 2013) or soil-water (e.g. Jie et al., 2011) and groundwater, or even studies which rely on the use of several different numerical models (e.g. Meixner et al., 2016).

3. Remaining challenges in estimating recharge

Groundwater recharge has been repeatedly shown to be highly variable; also, the greater the aridity, the smaller and potentially more variable the natural flux. In addition to the difficulties associated with sparse information, particularly in (semi-)arid areas, various general problems recur. De Vries & Simmers (2002) provide an in-depth summary of some of the most recurrent challenges concerning recharge. Note that the studies cited below are meant to illustrate the challenges listed, and represent only an infinitesimal fraction of the existing published work. De Vries & Simmers (2002) summarize the main problematics concerning recharge since the beginning of the 21st century as (i) the variability of recharge in time and space and identifying the drivers of these variations and the effects of climatic and land-use changes, (ii) the assessment and regional hydrological consequences of *localized* and *indirect* recharge and (iii) the impacts of urban development on recharge. More detail is given on the two first points below, and the additional challenges identified during this thesis are also developed here.

3.1. The variability of recharge in time and space

Nowadays, many long-term records of groundwater recharge variations in time exist (Brutsaert, 2008; Deng et al., 2017; Dickinson et al., 2004), mostly highlighting the link between recharge and rainfall patterns and intensity (Barron et al., 2012; Owor et al., 2009; Taylor et al., 2012). Studies focusing on the spatial patterns of recharge are also abundant, analyzing the role played by climate, vegetation and soil patterns (Keese et al., 2005; Kim & Jackson, 2012; Zomlot et al., 2015). Finally, understanding how climate (Crosbie et al., 2015; McCallum et al., 2012; Meixner et al., 2016) and land-use changes

(Dawes et al., 2012; Pan et al., 2011; Scanlon et al., 2005) affect recharge is also a topic that has been and remains of keen interest in the scientific community.

3.2. The assessment of *localized* and *indirect* recharge

Recharge along preferential flow paths has received some attention in the past decade, with an increasing number of studies attempting to quantify their relative contribution to groundwater. The relative proportions of these phenomena fluctuate according to climatic conditions, geomorphology and geology. In arid climatic regions, specifically, localized and indirect recharge from ephemeral stream losses are thought to be the dominant recharge process (Simmers et al., 1997). Although there are few examples in the literature of studies assessing indirect and localized recharge, the existing literature suggests that overlooking the contribution of these components to total recharge may lead groundwater models to be highly misleading. Many studies rely on isotope and/or chemical tracer techniques to solve this problem (Johnston, 1987; Scanlon et al., 1999). More recent work, however, has led to the development of new methodologies to approach this issue, either by combining different sets of recharge estimation methods (Berthold et al., 2004; Cuthbert, 2010; Maréchal et al., 2009) or by developing new methods expressly for this purpose (Bansal, 2013; Cuthbert et al., 2016).

An example that illustrates the importance of assessing localized and indirect recharge is one that has been termed "*the Sahelian paradox*" (Descroix et al., 2013). In recent decades, the Sahel has been subject to a general precipitation decline. Despite this, groundwater levels have continuously increased (Leblanc et al., 2008; Leduc et al., 2001). In fact, present water levels are among the highest ever recorded. Runoff and streamflow have also increased in most Sahelian areas (Amogu et al., 2010; Gal et al., 2017). The scientific community seems to agree that the cause of this paradoxical increase is land use change. This semi-arid area has undergone intense land clearing, which in term has modified the surface-hydraulic properties of large areas, consequently increasing surface runoff. This runoff has then concentrated in temporary ponds or flowed through the drainage network, eventually infiltrating into the water-table (i.e. through **indirect** and **localized** recharge processes) (Leblanc et al., 2008). This example, although restricted to a specific area, shows how neglecting indirect and localized recharge processes can lead to a general misapprehension of hydrological processes, especially in (semi-)arid regions. Also, it should be noted that although studies in this area have been driven by the peculiarity of opposite rainfall and water-resource variations, this does not signify that these processes should be neglected in other areas. Actually, areas which feature less uncommon water-resource dynamics may also be characterized by important indirect and localized recharge contributions, though these may be masked by other processes, erroneously neglected, or falsely attributed to other mechanisms.

3.3. Humid versus arid regions

As stated previously, in (semi-)arid climates, where by common definition *PET* exceeds rainfall most of the time, there is no appreciable surplus of infiltration over *PET* when totaled over the year. However, observing temporal and spatial recharge patterns in dry regions using averages over time in space may lead to the assumption that recharge does not occur, or at least not in a discernable way. Gee & Hillel (1988) refer to this as '*the fallacy of averaging*'. Indeed, as has been largely discussed throughout this chapter, most recharge in dry regions is episodic and may be confined to restricted areas. Such ephemeral and concentrated phenomena are however difficult to ascertain using ordinary recharge quantification methods (especially if these provide point measurements). Thus, while significant progress has been made in understanding recharge phenomena in humid environments, there still exist significant areas for continued development concerning dry environments, whether it is to improve understanding of the driving forces behind recharge heterogeneity, or to develop new recharge estimation techniques pertinent in these environments. There is, in fact, a significant amount of literature aiming specifically to summarize the particularities of recharge in (semi-)arid environments and the methods available to apprehend these phenomena (Allison et al., 1994; Gee & Hillel, 1988; Kinzelbach et al., 2002; Scanlon et al., 2006; Simmers et al., 1997), as not all recharge estimation methods are applicable in water-scarce environments.

3.4. Recharge in fractured rock

The factors that govern recharge to fractured rock aquifers specifically are poorly understood. In relatively homogeneous aquifers, the rates and patterns of groundwater recharge and flow may be obtained generally easily through any of the methods cited in **Section 2** of this chapter. In these environments, parameters such as porosity and permeability can be estimated or extrapolated from point measurements with reasonable confidence. In fractured rock aquifers, however, the value of these parameters, and thus of the processes governed by them, is subject to extreme spatial variability. This is because recharge rates and patterns in fractured rock are often complicated mainly due to (i) complex and variable preferential flow/piston flow distributions and patterns, (ii) multi-scale heterogeneity, and (iii) uncertain specific yield.

3.4.1. Highly variable combination of preferential flow and diffuse recharge

Local-scale recharge in fractured rock aquifers is affected by an interplay of numerous factors: fracture aperture and connectivity, topographic features, overlying soil characteristics, soil-bedrock hydraulic conductivity contrasts, hydraulic gradients and the depth of the water table, but the relative importance of each of these factors is poorly understood

(Gleeson et al., 2009; Harte & Winter, 1993). As a result, recharge in fractured rock depends on combination of diffuse recharge (matrix or piston flow) and preferential flow (D. V. Reddy et al., 2009; Sukhija et al., 2003) that is difficult to predict. As stated previously, diffuse recharge occurs through the soil matrix as piston flow: water added to the soil surface moves downward by pushing the older water beneath, in turn will pushing still older water further below, thereby ultimately adding water from the unsaturated zone to the groundwater reservoir. Preferential flow is rapid flow occurring through fractures, flow resulting from riverbed infiltration (i.e. indirect recharge), and runoff accumulating in depressions and along alluvial fans at the base of mountains where recharge occurs more readily (i.e. localized recharge). In the former, recharge is controlled by the overlying soil characteristics; in the latter, recharge is controlled by the heterogeneous fracture networks, by topography, and the heterogeneity of surface hydraulic properties. The complex combination of these two processes results in a high variability of hydraulic responses, where preferential flow has often been found to dominate groundwater recharge processes (Alazard et al., 2016; Cuthbert & Tindimugaya, 2010; D. V. Reddy et al., 2009; Sukhija et al., 2003), although this depends on topography and degree of weathering (Cai & Ofterdinger, 2016).

In some instances, in fact, water levels in fractured rock have been noted to increase extremely rapidly, sometimes by several meters, within hours of a rainfall event (e.g. Gburek & Folmar, 1999; Gleeson et al., 2009) due to the existence of preferential flow pathways. However, while diffuse recharge is generally easy to measure and model, infiltration through preferential flow paths is much more difficult to apprehend, which is why it is often (and wrongly) unaccounted for (Sukhija et al., 2003).

3.4.2. Multi-scale heterogeneity

The main problem concerning the assessment of recharge in crystalline rocks, compared to, for example, sedimentary rock aquifers, is the existence of heterogeneity across all scales (see **Chapter 1 Section 3**). Indeed, crystalline rock aquifers are strongly heterogeneous: various degrees in fracturing and connection between fracture networks induce strong variations of properties at all scales, sometimes by several orders of magnitude (Le Borgne et al., 2006; Maréchal et al., 2004). Moreover, when exposed to weathering, these rocks develop relatively stratiform layering sub-parallel to the weathering surface (Lachassagne et al., 2011) in which hydrogeological properties are closely related to the degree of weathering (Dewandel et al., 2017, 2006; Lachassagne et al., 2011). There are many ways of dealing with spatial heterogeneity (de Marsily et al., 2005): one set of techniques relies on defining homogeneous equivalent properties, known as averaging (pumping tests, for example, typically estimate the "equivalent" homogeneous properties of an aquifer), while other techniques attempt to describe the spatial variability of the

rock properties from geologic observations and local measurements. The averaging approach has been commonly used so far in hydrogeology, but it has shown its limits. Techniques available for describing the spatial variability are either continuous geostatistical models (e.g. Dewandel et al., 2017, 2012; Jardani et al., 2012; Michael et al., 2010), discontinuous facies models (better suited to treating issues of connectivity; e.g. Allen-King et al., 1998; Fogg et al., 1998; Zappa et al., 2006), or genetic models (e.g. Bonneau et al., 2013; Giacobbo et al., 2002; Renshaw & Pollard, 1994). Transport problems, where connectivity is of great importance, require more attention be paid to heterogeneities than flow models. The scale of the problem must also be considered: small-scale problems require a detailed understanding of heterogeneous pathways, whereas for large-scale problems, flow and transport may be averaged by the crossing of several heterogeneous structures leading to the emergence of an "ensemble" average (this is referred to as *ergodic* behavior; de Marsily et al., 2005). In the latter, averaging tools may be used. Unfortunately, fractured rocks have been repeatedly shown to have non-ergodic behavior regarding both flow and transport (de Marsily et al., 2005); in these cases heterogeneity should be carefully considered. Densely fractured aquifers are the exception, where the assumption of continuity of flow and the pseudo-homogenization of hydraulic properties have so far allowed a satisfactory conceptualization of this type of media.

3.4.3. Uncertain specific yield

Specific yield (S_y) estimates are required to estimate recharge from methods relying on groundwater level variations [see **Section 2.3.1.2** and **2.3.1.3**]. S_y is generally treated as a storage term independent of time (theoretically, the release of water from storage is instantaneous). In reality, the release of water can take an exceptionally long time, especially for fine-grained and/or low permeable materials, such as the fractured-rock matrix. The amount of time allotted to the determination of S_y thus contributes (along with the natural heterogeneity of the geologic materials, and the different methods used) to S_y estimates being highly variable (Healy & Cook, 2002), and complicates its measurement. Other issues linked to S_y estimation (aside from limitations linked to laboratory methods) are (i) assumptions employed in S_y analysis are sometimes not representative of field conditions (ii) the hysteretic nature of the moisture-characteristic curve may lead to different S_y estimates depending on whether a wetting or a drainage phase are observed, (iii) aquifer test interpretations are nonunique. Estimation of S_y in fractured rock systems is particularly challenging. First of all, as mentioned above, the time required for filling or draining fractured rock materials can be extremely long. Second, the total porosity distribution of these systems is essentially bimodal, i.e. it is made up of the sum of fracture porosity (highly permeable, become saturated quickly) and the matrix porosity (again, very low). If water levels in fractures rise at greater rates than in the surrounding

matrix pores, the measured specific yield will be equal to fracture porosity. However, although fractures usually serve as the primary conduits for water movement, they account for only a small percentage of the total available storage in the aquifer. The effects of scale on storage coefficients or porosity are further poorly understood (Illman, 2005; Jiménez-Martínez et al., 2013). Finally, weathered crystalline rock aquifers can present very steep vertical contrasts in permeability as well as storage (Boisson, Guihéneuf et al., 2015). Accordingly, S_y estimation will be strongly correlated to the water levels observed relative to the aquifer lithology, and a single estimate will not capture the overall variability of S_y within the aquifer layers.

For these reasons, most methods for estimating S_y in fractured rock are not sufficiently accurate to permit estimation of recharge using derived values (Healy & Cook, 2002). The water-budget method is most widely used technique in these environments, mostly because it does not require any assumptions concerning flow processes. Overall, although considerable effort has been devoted to evaluating S_y in fractured-rock aquifers, it remains unclear whether S_y estimates in these environments are generated with sufficient accuracy to provide reliable recharge estimates (Healy & Cook, 2002).

3.4.4. Fractured rock aquifers in (semi-)arid climates

The difficulty of recharge receipt by fractured rock is compounded in (semi-)arid climates. As has been mentioned in the preceding sections, recharge processes in (semi-) arid environments are highly non-linear for several reasons. First, because potential evapotranspiration surpasses rainfall most of the year, which causes recharge to be highly episodic, and biased to heavy rainfall events. Additionally, indirect and localized recharge mechanisms become the dominant recharge processes under these conditions, yet these are more difficult to measure and apprehend. Overall, as aridity increases, recharge becomes less linear and less spread-out. In other words, heterogeneity, both spatial and temporal, increases. This heterogeneity thus adds a layer of complexity to the already-existing strong and multi-scale lithological and hydrogeological heterogeneity characteristic of fractured crystalline rock.

Research problem

We have seen in the preceding sections that estimating recharge is essential to the proper management and planning of water resources, especially in water-limited environments where groundwater may be the only source of freshwater. The non-linearity of recharge processes, often biased to heavy rainfall events, and the interaction of numerous factors which control its intensity and distribution are sources of great uncertainty. We have seen, additionally, that recharge in fractured crystalline rock aquifers is poorly understood. The existence of multi-scale heterogeneity, compartmentalization, and the bimodal character of this type of media—made up of fracture networks embedded within a variably porous matrix—make the quantification of fluxes and the hydraulic properties controlling them difficult. Finally, we have seen that recharge in (semi-)arid environments is also highly non-linear. Under these conditions indirect and localized recharge processes tend to greatly exceed diffuse recharge processes, yet these are (by definition) focused in small areas and sometimes ephemeral, making them highly difficult to estimate.

The problems that arise from these observations are the following: which factors control the intensity and distribution of total recharge in fractured rock aquifers? What is the ratio of localized and indirect recharge to diffuse recharge? And finally, how does intensive groundwater exploitation and irrigation affect recharge in these environments?

These questions will be explored in Chapter 5.

Chapter 4
Managed Aquifer Recharge

In the previous sections we discussed the generalities of aquifer recharge and the mechanisms which control recharge quantities and distribution. We have seen, additionally, that the expansion of irrigated agriculture to meet demand from a growing population, compounded with the increasing seasonal variability induced by climate change, have added a significant amount of pressure to groundwater systems, especially in regions were water was scarce to begin with. Natural recharge has often become insufficient to keep pace with over-allocation of groundwater in these areas. This has led certain regions to experience continuous water-level declines, causing wells to run dry and energy and pumping costs to rise, generally impairing irrigation potentials and increasing vulnerability to drought. Other side-effects of groundwater depletion include land subsidence and subsequent formation of sinkholes, and saltwater intrusions into freshwater aquifers (especially in coastal and insular zones).

In such contexts, integrated water resource management (IWRM) schemes are becoming increasingly implemented. IWRM is the coordinated development and management of water, land and related resources in order to maximize economic and social welfare in a way that does not compromise the sustainability of vital ecosystems. The different solutions existing to remediate groundwater depletion can be divided into one of three categories: demand management, alternative supplies and managed aquifer recharge (FIGURE 4.1a). Among these three categories, the latter is of particular interest, especially in India where it is being largely implemented.

This chapter will provide an overview of MAR as a groundwater overexploitation alleviation scheme, with a focus on infiltration basins. To do so, we will first examine some technical considerations, such as the different types of existing MAR structures and the factors determining its efficiency. Then, the possible circumstances limiting MAR potentials will be summarized, and a brief description of the approaches to predict and assess MAR efficiency will be given. Finally, the implications of setting up MAR in fractured crystalline rock will be addressed, which, as noted in the preceding sections, are highly challenging environments regarding conservation and planning of water resources. Nevertheless, MAR is increasingly employed to mitigate water scarcity issues in these settings.

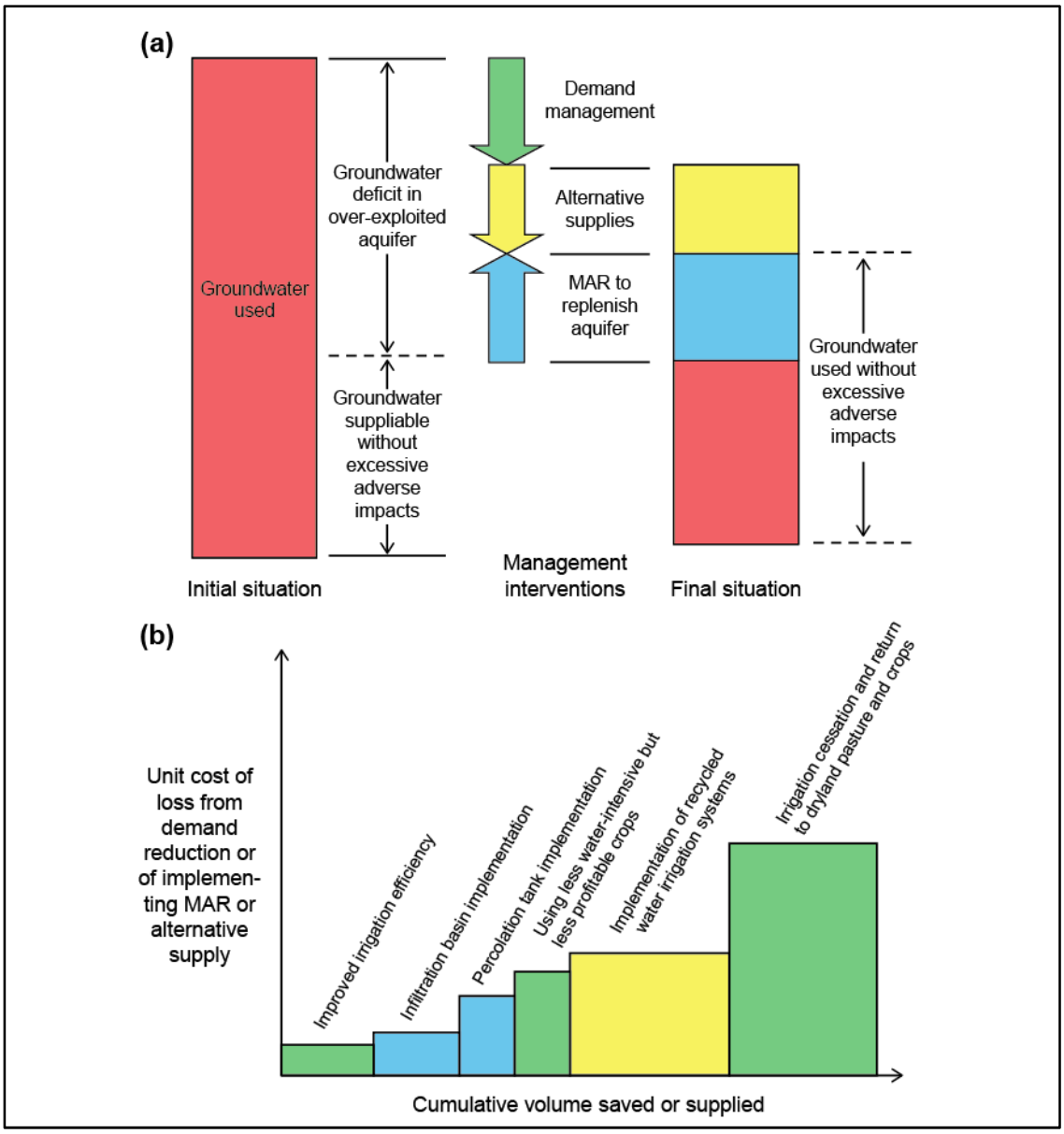

FIGURE 4.1: **(a)** Methods to bring an aquifer to hydrologic equilibrium by either reducing extraction or by increasing supply through MAR or through use of alternative supplies and **(b)** water stress reduction methods sorted by their relative costs and saved or supplied volumes (modified from Dillon et al., 2012)

1. Generalities

1.1. Definition

Managed Aquifer Recharge[11] (MAR) systems are, according to Bouwer (2002): "*engineered systems where surface water is put on or in the ground for infiltration and subsequent movement to aquifers to augment groundwater resources*".

While groundwater augmentation is the main use of MAR worldwide, MAR can be used to address a wide range of water management issues, including: reducing seawater intrusion or land subsidence, smoothing out supply and demand fluctuations, protecting groundwater-dependent ecosystems, and improving water quality through filtration and chemical and biological processes. There are many examples around the world that demonstrate the value of MAR. For instance, injection wells have been used in coastal locations in California, China and Bangladesh to protect groundwater supplies from salinization. Treated sewage effluents have been used to augment groundwater supplies in Australia, Belgium, Germany, Israel, Italy, Mexico, Namibia, South Africa, Spain, USA and elsewhere (Jakeman et al., 2016). The UAE and USA have also used MAR in conjunction with seawater desalination in order to build secure reserves of water (Jakeman et al., 2016). This chapter will however focus on MAR use to replenish depleted aquifers, especially in water-scarce environments and in contexts of groundwater over-allocation and depletion.

Note that artificial recharge is one of many techniques aimed at managing water resources and that ideally it is used in conjunction with other methods, such as demand management and use of alternative supplies (surface storage, waste-water reuse…). The complementary roles of demand management and expanding supplies either via MAR or by providing alternative supplies are graphically summarized in FIGURE 4.1a. Each option has an associated volume and unit cost, and combining the two allows identification of the cheapest option and the volume of demand reduction or supply enhancement which should be expected (FIGURE 4.1b). Improved irrigation efficiency is often the least costly option and should be implemented first. The overall decisions to be taken will depend on the relative costs of each option and the capability of stakeholders to absorb costs (Dillon et al., 2012).

[11] Managed Aquifer Recharge is also referred to as '*artificial recharge*', but adverse connotations of the term 'artificial', implying for example that the water is in some way unnatural, have led 'managed' to be the more prevalent term. As Dillon (2005) rightly points out: we don't call well pumping 'artificial discharge'.

1.2. Key issues

In order to effectively implement a MAR scheme, several issues must be taken into consideration. There needs to be a source of water, space in an aquifer to store the water, and mechanisms to recover the water for beneficial use (Gale et al., 2002). These different components need not only to be considered separately, but also analyzed in the overall context of natural recharge and discharge, including abstraction, and in terms of the projected benefits of the local population. Preliminary sociological and hydrogeological surveys in target areas may save precious money and allow for accrued benefits from well-conceived and well-implemented projects (M. Shah et al., 2017). Unfortunately, in order to save time, many water resource management schemes have so far taken a 'one size fits all' approach, based on the notion that MAR will always work and will always be beneficial. This is not to say that MAR is ineffective, but rather that the nature, scale and distribution of benefits depend on a set of location-specific factors (Gale et al., 2006), both physical and economic, that need to be accounted for from the start. We summarize here a few of these key factors (Gale et al., 2006), and some points have been expanded:

- The origin, variability, and quality of the source water
    - How much and what type of source water is available
    - How does the availability of the source water fluctuate both seasonally and long-term
- The physical effectiveness of MAR in an area
    - How much water can actually be recharged
    - Which factors influence the amount of water recharged
    - How are the MAR inputs distributed in the aquifer (shape and size of the groundwater mound)
- The needs and interests of different groups
    - What are the priorities of different groups (particularly of marginalized groups)
    - How may they stand to benefit from recharge activities
- The siting and design of recharge structures
    - What type of structures are best suited depending on the objectives
    - Which section of the watershed/aquifer
- The management of MAR structures for continued benefits

While the case-by-case approach is the most pertinent, it can be very time consuming, especially when the setting-up of numerous MAR structures (sometimes up to several thousands) is intended within a project. In these cases some entities have opted for performing pilot schemes at a number of sites deemed to be representative of the range

of different hydrogeological, meteorological and socioeconomic settings existing within the target area. We can, for example, cite the *Hinds/Hekeao Managed Aquifer Recharge Pilot Project* in New Zealand (Golder Associates, 2017), the *Kabul Managed Aquifer Recharge Project* in Afghanistan (Landell Mills Ltd., 2018), or the *Augmenting Groundwater Resources by Artificial Recharge (AGRAR)* project in India (Gale et al., 2006). While these types of studies add value to our current understanding of the role of MAR, these projects are generally too limited in time and space to assess long term impacts of MAR across the large range of environments targeted by these schemes. Also, assessing the representativeness of pilot study sites is not always a straightforward and easy task, especially in heterogeneous environments, so the existence of uncertainty related to this must be acknowledged.

2. MAR methods

MAR can be implemented in any number of ways. There are three overall categories of MAR: *infiltration methods*, *direct injections methods* and *filtration methods*. Bouwer (2002) provides a broad overview of the different existing MAR which are summarized here.

2.1. Types of methods

2.1.1. Infiltration methods

Infiltration methods, comprising spreading methods and vadose zone infiltration methods, are inexpensive and relatively easy to implement and maintain. They rely on the infiltration of water to the aquifer by means of infiltration basins (also called ponds or tanks) or trenches or wells in the vadose zone and allow improvement of the quality of recharge water using the unsaturated zone's natural attenuation capacity (Bouwer, 2002) through **indirect** recharge processes. Surface infiltration systems can be *in-channel* or *off-channel*.

In-channel systems are built by damming ephemeral or perennial streams causing the water to back up and spread out; this increases the wetted area of the streambed or floodplain so that more water can infiltrate into the soil and reach the aquifer.

Off-channel systems consist of specially built basins, lagoons, gravel pits, flood-irrigated fields, or any other facility where water is intentionally diverted to be placed in the vadose zone or spread on the ground for infiltration into the soil and movement into the underlying aquifer. Surface infiltration systems require relatively permeable surface conditions to get high infiltration rates and minimize surface requirements. The underlying aquifer should be free of clay layers or aquitards which

may restrict downward flow and must permit lateral flow away from the recharge area otherwise this might cause the groundwater mound to rise and waterlog the recharge area, which reduces infiltration rates [see **Section 4.1.2** of this chapter]. Additionally, recharge water used for in- and off-channel systems must meet certain quality standards. This, on one hand, prevents the undue clogging of the infiltrating surface [see **Section 4.1.1** of this chapter], but also to ensure that the quality of the groundwater is not being degraded through the injection of contaminated water (Bouwer, 2002).

2.1.2. Direct injection methods

Direct injection methods, the most often used MAR methods, are implemented through the use of injection wells. These methods are used when permeable soils and/or sufficient land area for surface infiltration are not available, vadose zones are unsuitable for trenches or wells and when aquifers are deep and/or confined[12] (Bouwer, 2002). The use of optimal quality water is suggested for this type of recharge method because of clogging problematics and in situations where the groundwater may be posteriorly pumped for potable uses. The design, management, and overall implication of direct injection methods are however beyond the scope of this thesis, and will only be mentioned briefly below.

2.2. Types of structures

The most predominant MAR structure types are (FIGURE 4.2, Gale et al., (2002):

- *Aquifer storage and recovery* (ASR), belonging to the category of direct injection methods, is the process of injecting water into a well for storage and recovery from the same well. Aquifer storage transfer and recovery (ASTR) is essentially the same, except water is recovered from a different well, generally in order to provide additional water treatment.
- *Riverbed and bank filtration* (RBeF and RBF), are methods which rely on natural infiltration of river water through the river bed and banks (i.e. *indirect* recharge). These methods improve the quality of the water recovered and make it more consistent in quality. In RBF, water is extracted from a well (or a gallery or line of wells) near a river or lake to induce infiltration from the surface water body. RBef is similar, although in this case a "collector"

[12] Bouwer (2002) points out that in truly confined aquifers some recharge might be possible through expansion and compression of the aquifer itself, particularly of the clay layers and aquitards that are more compressible than consolidated and unconsolidated materials in the aquifer. Nevertheless, it is also pointed out that excessive compression of aquifer materials from overpumping has been shown to be mostly irreversible.

(similar to conventional vertical wells, but horizontal) is dug directly in the riverbed and not the aquifer. The factors controlling the success of these schemes are the quality of the surface water, the permeability of the stream- or lake- bed and banks and aquifer thickness.

- *Infiltration basins*, usually built off-stream, are fed by water which is diverted through canals; the water is then allowed to infiltrate to the underlying unconfined aquifer. If the underlying aquifer is relatively permeable, then a simple dug basin is used. If the material below the basin is fine, however, rapid clogging may occur. In this case the bottom and sides of the basin can be covered with a thick layer of medium sand in order to retard the clogging process (one of the main risks of MAR implementation, see **Section 4.1.1** of this chapter). Fractured-rock aquifers are also at risk of deep penetration of suspended solids and impurities which may result in irreversible clogging (Gale et al., 2002).
- *Percolation tanks*, belonging to the category of spreading methods, are built by constructing small dams which intercept and gather intermittent flow over relatively large surfaces; this creates a pond where water infiltrates at the base. Silting over successive periods of inflow may lead to a reduction in the effectiveness of the structure, eventually compacting the sediments and further reducing their effectiveness. The hydraulic performance of these structures should be monitored to make sure the recharge structure has not become a storage structure.
- *Rainwater harvesting* is when roof runoff is either conserved for direct consumption or diverted into a well or a caisson filled with sand or gravel and allowed to percolate into the water table. This method is especially used in urban areas, and has the advantage of reducing demand on water supply systems, as well as reducing the risk of flooding.

For reasons of relevance and consistency with the field data and experimentations carried out during this thesis, the remainder of this chapter will focus primarily on infiltration basins for MAR.

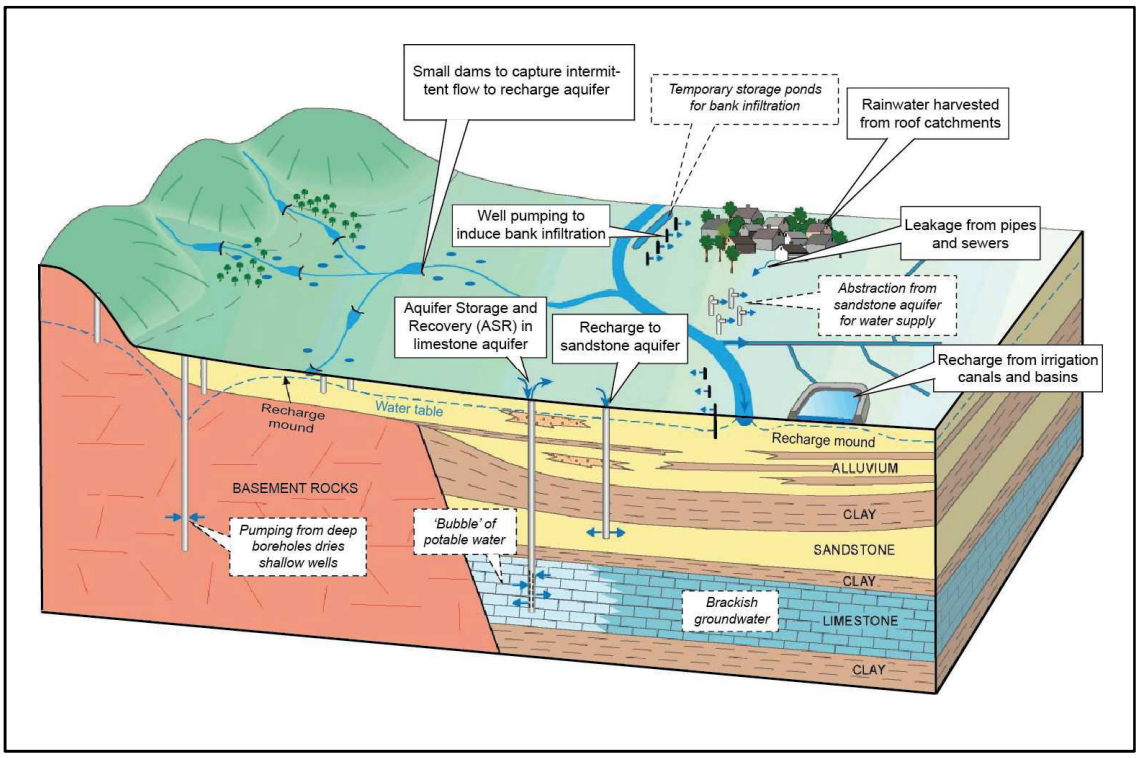

FIGURE 4.2: Diagram of different artificial recharge methods (modified from Gale et al., 2002)

3. Factors determining the effectiveness of MAR

The effectiveness of a MAR scheme is controlled by many factors. Some of these factors are operational and management considerations, which may be adjusted if necessary. Others are independent of the implementation strategies, and instead are linked to climate, lithology, and hydrogeology, such as the amount of water available to be recharged, or the aquifer's ability to permit later flow away from the recharge area (Gale et al., 2002). The following paragraphs describe the latter factors in detail. Because of the large amount of characteristics that come into play, it is difficult to generalize performance from observations on one site to another, but overall knowledge on the typology of a region in regards to the expected infiltration efficiency is a useful first step if a site-by-site approach is to be taken.

3.1. Hydrological criteria

3.1.1. Water availability

Water availability, i.e. the amount of water that can be captured from surface flows or rainfall and used for recharge, is a major factor controlling MAR efficiency and is mostly controlled by climatic and hydrological conditions. In particular, the characteristics of the water body providing the source water (volume, spatial and temporal variability), which depend on climatic and hydrological conditions, must be considered. If the

water source is permanent (such as a perennial stream) then the amount of available water is generally a straightforward calculation, made slightly more complicated by the assessment of environmental flows[13]. If it is intermittent (such as ephemeral streams) then determination of the available volume must take temporal distribution into account.

In humid and tropical environments, rainfall generally meets evaporative demands while still providing a baseflow component to streams. However, seasonal mismatch between supply and demand (i.e. the peak summer demand when water is least available vs. winter where demand is lower but availability is higher) can call for artificial recharge to alleviate water supply and storage problems (Gale et al., 2002). MAR is also used in certain cases to compensate water withdrawals, especially near large urban areas (e.g. Réfloch, 2018).

In (semi-)arid areas, as is described in **Chapter 2 Section 3.3**, average yearly *PET* exceeds rainfall. In these areas, precipitation occurs in the form of short and heavy rainstorms (especially in monsoon areas), which cause intense but short-lived surface runoff and flooding to occur. As a result streamflow is often intermittent or ephemeral, and is only perennial if surface watercourses are fed by groundwater or a distance source (e.g. glacier melt water). This greatly affects surface water availability. In fact, depending on the aridity of the area, surface water may not be available in sufficient quantities for recharge. In these cases source water is restricted to flash flood events or water from desalination plants (Gale et al., 2002), and close attention must be paid to the risk of down-stream tradeoffs [see **Section 4.3** of this chapter].

3.2. Hydrogeological criteria

The success of a MAR scheme also largely depends on the local hydrogeological conditions. The properties of the underlying aquifer determine the ability of recharge water to successfully penetrate through the unsaturated zone and determine how the water is subsequently stored in the aquifer (i.e. the shape and size of the groundwater mound). The main factors which need be considered are (i) the hydrogeological properties (i.e. hydraulic conductivity and storage coefficients) of the aquifer and the overlying formations, (ii) the physical and hydraulic aquifer boundaries, (iii) the thickness of the aquifer and the depth to the water table (Gale et al., 2002).

[13] Environmental flows are flows required to sustain freshwater and estuarine ecosystems and the human livelihoods and wellbeing that depend on these ecosystems.

3.2.1. Hydraulic properties

3.2.1.1. Surface conditions

Surface infiltration schemes require permeable soils and vadose zones for water to infiltrate efficiently into the ground and reach the aquifer. The aquifer needs to be unconfined and be sufficiently transmissive for lateral flow to flow away from the recharge area without causing excessive groundwater mounding. As such, in order to select sites for MAR, the first step is to use soil and geological maps. Knowing the soil type will give information on the surface's infiltration capacity. However, in many cases, setting up the infiltration scheme requires some digging to be done. If the soil is relatively thin, it will effectively be removed. In these cases the vertical properties of the underlying features will be of greater importance.

If vertical downward flow can occur unimpeded, infiltration will depend on the hydraulic conductivity and water-entry value of the surface layer and the depth of the wetting front, following the Green-and-Ampt equation for infiltration into a flooded soil (Bouwer, 1978):

$$q_{out} = K_v \frac{\left(H + L_f - \psi_{we}\right)}{L_f} \tag{4.1}$$

where q_{out} is the infiltration rate, K_v is the vertical hydraulic conductivity of the wetted zone, H is the water depth above the soil, L_f is the depth of the wetting front (FIGURE 4.3), and ψ_{we} is the capillary suction at the wetting front (the water-entry value). The value of ψ_{we} can be measured on-site, but is generally taken from any reference table (Bouwer et al., 1999). It can be inferred from Eq. (4.1) that when the soils are first flooded, L_f is small and therefore q_{out} is high. As the wet front moves downward and L_f increases then the ratio in Eq. (4.1) approaches a value of unity, and thus the infiltration rate becomes equal to K_v of the wetted zone (to the point of hydraulic connection, then the infiltration dynamic change, see Section 4.1.2 of this chapter) (Bouwer, 2002).

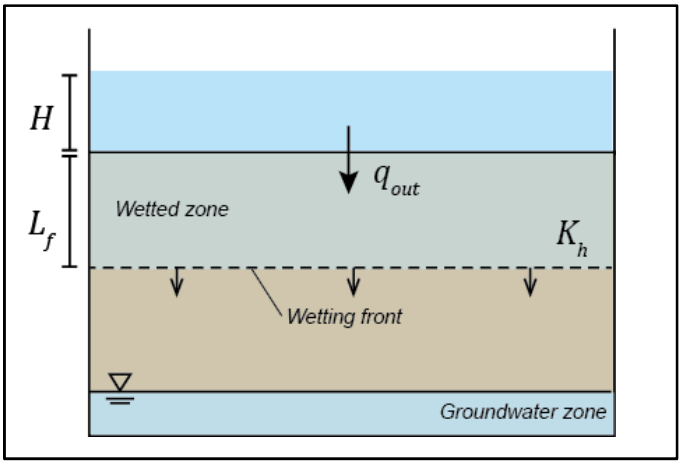

FIGURE 4.3: Geometry and symbols for Green-and-Ampt piston flow model of infiltration (based on Bouwer, 2002)

3.2.1.2. Subsurface properties

There are several properties to be observed to assess the storage availability and storage recoverability of an aquifer. First, it must be determined if the aquifer is confined or unconfined. This will determine which types of recharge enhancement methods are viable. Second, there must be a permeable formation and if there are several layers their interconnectedness should also considered (Gale et al., 2002). The receiving formation must have sufficient permeability and thickness to accept recharge at a designated rate, although too high permeabilities may result in rapid dispersal of recharge water, which complicates posterior recovery of the water. In other terms, depending on the ability the aquifer has to transmit water away from the recharge zone, the groundwater mound forming as a result of infiltration will vary in shape and size (FIGURE 4.4). The groundwater mound must remain below the bottom of the infiltration structure, as hydraulic connection results in a significant decrease in infiltration rates [see Section 4.1.2 of this chapter], but the aquifer mound must not be so spread-out that water recovery is impossible (unless the aim of the recharge scheme is to supplement groundwater on a regional scale; Gale et al., 2002). Understanding the hydraulic and physical boundaries of the aquifer is also essential: these factors will control the quantities and distribution of recharge water after it has infiltrated, and, in some cases, will also determine the infiltration rates.

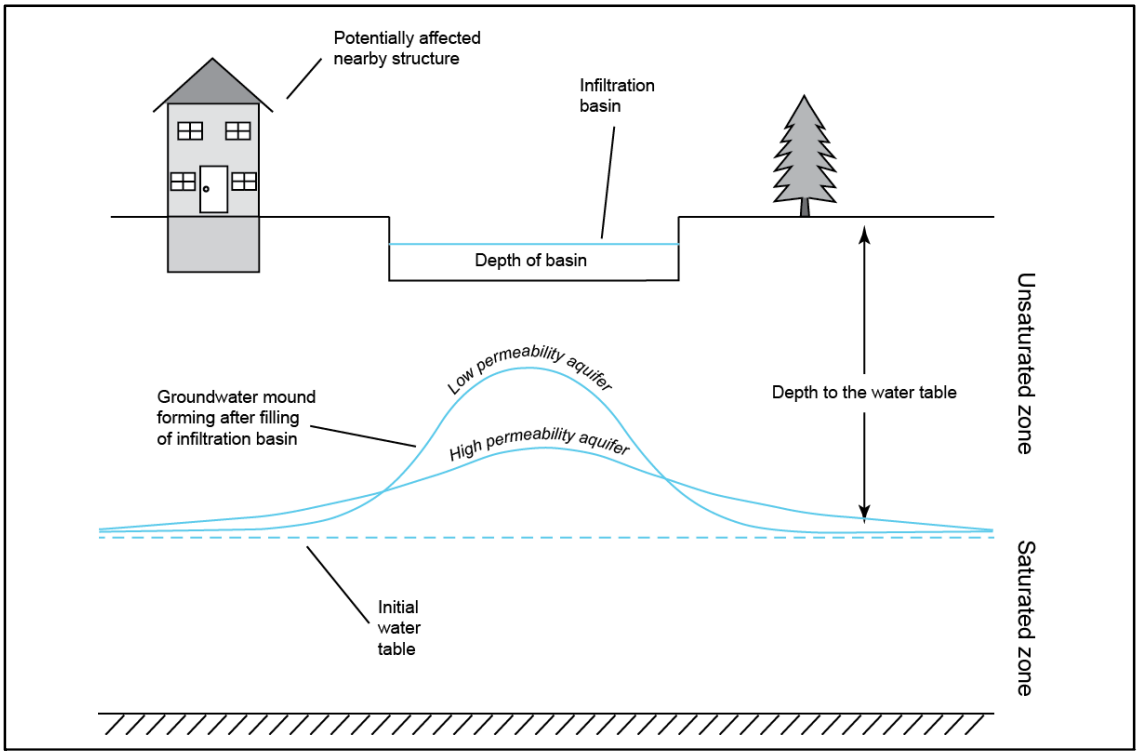

FIGURE 4.4: Schematic diagram of a groundwater mound forming beneath a hypothetical infiltration basin and the relative shape of the mound in aquifers of higher and lower permeability (modified from Carleton, 2010)

Although it is difficult to make generalizations on the capacity any given site to receive MAR inputs efficiently depending on the lithology, the general characteristics of a few hydrogeological settings are described in TABLE 4.1 (Gale et al., 2002) and the factors which may help in identifying the most suitable formations are listed in TABLE 4.2 (Dillon & Jimenez, 2008). In cases where the subsurface hydraulic properties are relatively well known or can be easily estimated, a simulation of the rise of the groundwater mound following infiltration can be done using analytical equations or numerical modeling [see Section 5.3 of this chapter]. These simulations can be used by the property developers and regulatory agencies (or any other party responsible of MAR implementation) to assess the risk posed by excessive groundwater mounding, and if a significant risk exists, either to select a new location or to determine sustainable input rates to avoid excessive mounding (either by alternating between wetting and drying phases or by limiting the depth of water in the infiltration basin).

3.2.2. Depth to the water table

The initial depth to the water table will affect recharge rates differently depending on whether there is clogging at the bottom of the infiltration basin or not.

If no clogging exists on the bottom of an infiltration basin, then the water table is susceptible to rise up to the bottom of the basin causing direct hydraulic connection. This causes flow dynamics to change. If the depth to the water table is relatively small (FIGURE 4.5a), the flow away from the basin becomes mostly lateral and flow is controlled by the slope of the water table (i.e. the hydraulic gradient) and the lateral hydraulic conductivity. On the other hand, if the depth to the water table is important (FIGURE 4.5b), then the flow remains mostly vertical and controlled by the vertical hydraulic properties of the aquifer. In the second scenario, the importance of the water level in the basin (H) will depend on how deep the water table is: if it is moderately deep, then a small increase in H will lead to a significant increase in infiltration. As Bouwer (2002) explains: if the depth to the water table in FIGURE 4.5b is 3 m, then an increase in H by 1 meter will cause infiltration to increase by 33%. If the depth to the water table is instead 30 m, then an increase of 1 m will only cause infiltration to increase by 3.3%.

If clogging does occur at the bottom of the basin, then infiltration is controlled by the clogging layer's hydraulic conductivity and the water level in the basin, and the volume below the basin will remain only partially saturated: in this case infiltration rates increase linearly with the water depth in the basin (as indicated in Eq. (4.1)).

	Alluvial aquifers	Fractured hard rock with weathered layer	Consolidated sandstone aquifers	Carbonate aquifers
General characteristics	Fluvial, marine and lacustrine deposits with thicknesses from a few tens of m to kms. Layered sequence of clays, sands and gravels. Low reliefs.	Aquifer is the fractured bedrock comprising igneous, metamorphic and volcanic rocks overlain by a regolith layer (weathered layer + soil). Storage depends on thickness of regolith. Fractured hard rock is usually in hydraulic connection with regolith.	Aquifers with a matrix of sand grains held together by a cement (e.g. calcite silica) or indurated by metamorphic processes. This results in a wide range of porosity/fracture ratios and hence hydraulic properties.	Aquifers with hydraulic properties controlled by the solubility of the rock. Solution enhanced fractures can result in karstic flow.
Phreatic or confined	Phreatic if permeable layer at surface, becoming more confined with depth. Layered aquifers with variable connectivity.	Usually phreatic in the hard-rock aquifers, depending on interconnection of fractures.	Phreatic where there is no alluvial cover or a confining clay layer.	Phreatic where there is no alluvial cover or a confining clay layer.
Porosity and drainage	Porosity high but effective storage restricted to sand and coarse layers.	Relatively high porosity and storage in the alluvium, only limited by the thickness. Low storage capacity in fractures but maintained by storage from regolith.	Proportion of storage in the matrix of these aquifers will be determined by the porosity and degree consolidation and fracturing.	Proportion of storage in the matrix of these aquifers will be determined by the porosity and degree consolidation and solution-enhancement of fractures.
Permeability and flow	Flow mainly in coarser horizons so their interconnectivity, as well as the connectivity to the recharge zones will determine the flow paths. Low hydraulic gradients will result in slow groundwater flow.	Regolith is little permeable. Fractures are highly transmissive; the greater the number the greater the yield and speed of refilling the well.	Permeability and flow will be determined by the porosity and degree consolidation and fracturing.	Permeability and flow will be determined by the porosity, the degree of consolidation and solution-enhancement of fractures.
Groundwater level fluctuations	Because of high storage capacity, fluctuations will be small; a few m. Recharge is limited by depth to water table. Pumped drawdown can create additional storage if managed carefully.	If water table is in the regolith then left box applies. If water table is in fractured hard rock then levels will rise and fall rapidly in response to recharge and pumping.	Where the porosity of the aquifer is high, the groundwater fluctuations will be relatively subdued in response to pumping and recharge	Where the fractures provide the main porosity, groundwater fluctuations will be rapid.
Infiltration capacity	High if surface layer is sandy but low if clay content is high. Coarse material needed for full zone of recharge. Aquitard layers may restrict recharge.	Relatively good. Depends on depth to water table, if hydraulic connection occurs capacity will strongly decrease.	Very high where there is no cover and the soil has developed from the sandstone.	Very high where there is no cover. Soil development is usually very thin and surface runoff minimal
Quality issues	Groundwater quality is good in active flow zones but can deteriorate where flow is slow. Weak natural groundwater movement may lead to concentration of harmful elements beyond acceptable limits. MAR can improve water quality by dilution or displacement. Vulnerability to pollution depends on the permeability of the surface layers.	Groundwater quality good in active flow zones but stagnant zones may concentrate harmful elements. Rapid flow in preferential flow paths leads to high vulnerability.	Very good quality groundwater where actively recharged but susceptible to contamination, particularly where soil cover is thin.	Very good quality groundwater where actively recharged but extremely susceptible to contamination.
Runoff generation	Surface flow will occur if infiltration rate is exceeded or soil is at capacity.	Exposed bedrock may generate intense runoff. Otherwise runoff depends on infiltration capacities of the regolith	Infiltration capacity likely to be high so natural infiltration and recharge likely to be high also. Extreme events may cause soil erosion and provide potential water for MAR.	All but the most extreme events will infiltrate. Thin soils are easily eroded.

TABLE 4.1: Factors affecting MAR effectiveness in relation to hydrogeological setting (modified from Gale et al., 2002)

Characteristic	Feature and influence on MAR	
Permeability	**Moderate to high** – High rates of recharge possible – Recharged water can be dispersed – Lower capital and energy costs per unit of water recovered	**Low to moderate** – Lower rates of recharge possible – Recharged water more localized – Greater capital and energy costs per unit of water recovered
Confinement	**Unconfined** – Surface infiltration methods viable – Unprotected from surface contamination – Storage capacity depends on depth to water table	**Confined** – Well injection methods only – Protected from surface contamination – Storage capacity depends on aquifer thickness
Thickness	**Thick** – High storage potential – More sensitive to salinity stratification if native groundwater is brackish	**Thin** – Low storage potential – May limit rate of recovery by wells
Uniformity of hydraulic properties	**Homogeneous** – Minimal mixing and higher recovery efficiencies if native groundwater is brackish	**Heterogeneous** – In karstic and fractured rock systems, limited ability to contain recharged water – Lower recovery efficiencies if native groundwater is brackish
Salinity of groundwater	**Fresh** – Recovery efficiency not limiting – Requirement to protect wider range of beneficial uses of aquifer (higher treatment costs)	**Saline** – Recovery efficiency can limit effectiveness – Less beneficial uses to protect, so treatment need be less onerous
Lateral hydraulic gradient	**Gentle** – Recharged water contained closer to point of recharge	**Moderate to steep** – Recharged water dispersed downgradient and lower recovery efficiency in saline native groundwater
Consolidation	**Consolidated** – Easier to complete wells – Easier to maintain recharge wells to prevent irrecoverable clogging	**Unconsolidated** – Screens required for injection and recovery wells – Land subsidence a consideration
Aquifer mineralogy	**Unreactive with recharge water** – Recovered water quality unaffected by geochemical reactions with aquifer matrix – Likelihood of clogging of injection wells is sometimes increased	**Reactive with recharge water** – Consider metal (e.g. arsenic) mobilization, iron and H_2S effects on recovered water and groundwater – In carbonate aquifers, less onerous treatment required to avoid clogging of injection wells

TABLE 4.2: Characteristics of aquifers and their influence on MAR effectiveness (modified from Dillon & Jimenez, 2008)

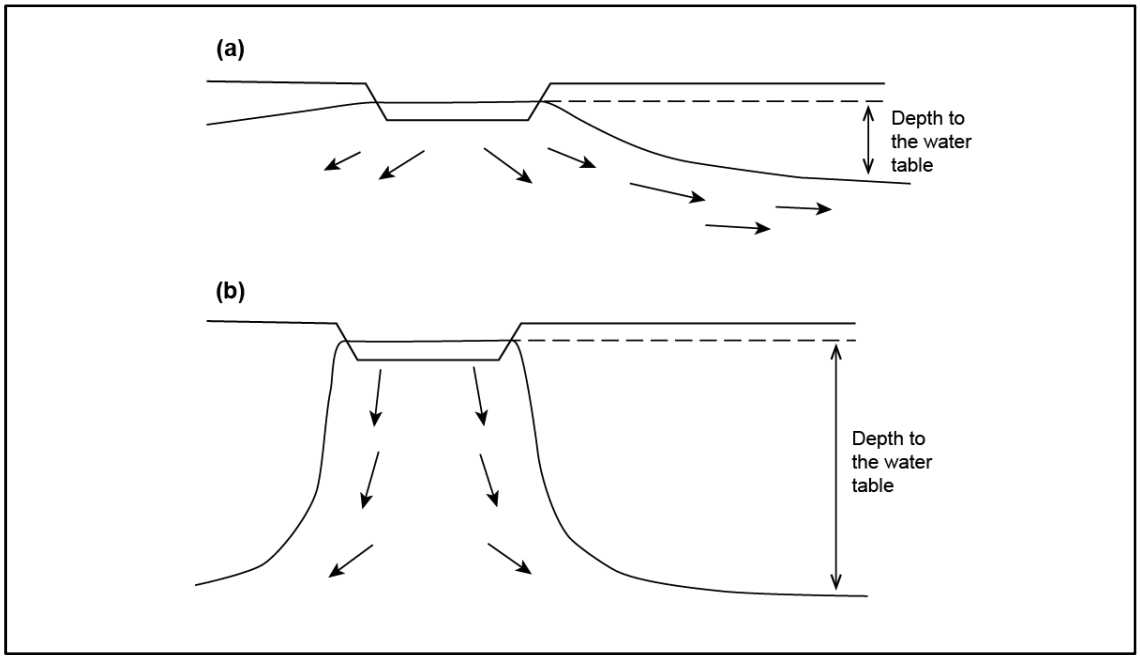

FIGURE 4.5: Diagram showing managed aquifer recharge below a basin under **(a)** shallow water table conditions and **(b)** deep water table conditions (modified from Bouwer, 2002)

4. MAR challenges and risks

Several risk factors must be considered for an optimal MAR implementation.

4.1. Decrease in infiltration potential

4.1.1. Clogging

The main problem affecting infiltration schemes is clogging of the infiltrating surface, such as the basin beds and the well-aquifer interface inside recharge wells (Bouwer, 2002). Because clogging layers are much less permeable than natural materials, they reduce infiltration rates. Clogging can be caused by many processes, physical, biological or chemical. Physical processes consist of accumulation of suspended solids in the recharge water, both organic (e.g. algae cells, microorganisms) and inorganic (e.g. clay and silt particles). Biological clogging processes include accumulation of algae and bacterial flocks on the infiltrating surface and formation of biofilms and biomass that block pores and/or reduce pore sizes. Chemical clogging is mostly linked to precipitation of certain crystals such as gypsum, calcite, generally induces by changes in pH or oxidation state.

Infiltration rates, additionally, vary inversely with water viscosity. As such, infiltration rates will be influenced by temperature. If there are large temperature differences between summer and winter, winter infiltration has been noted to be as low as about half of summer infiltration (Bouwer, 2002).

When infiltration rates become less than the saturated hydraulic conductivity of the underlying material, the zone below the basin becomes unsaturated. The resulting downward flow is then controlled entirely by gravity with a hydraulic gradient of unity. In this scenario, the infiltration rate for the basin can be calculated by applying Darcy's law through the clogging layer (Bouwer, 2002):

$$q_{out} = K_{Clog}\frac{(H - \psi_{ae})}{L_{clog}} \tag{4.2}$$

where K_{Clog} and L_{Clog} are the hydraulic conductivity and the thickness of the clogging layer, respectively, and ψ_{ae} is the air-entry tension, which is equal to the height of capillary rise. Because of the difficulty in determining the thickness and hydraulic conductivity of a clogging layer, K_C and L_C can be lumped into one parameter called hydraulic resistance (R_C) with $R_C = L_C/K_C$. Determination of R_C can be done using Eq. (4.2) using measured infiltration values across the clogging layer and using a tensiometer to determine ψ_{ae}.

In order to reduce clogging, one must address the problems causing it. For surface water, this means pre-sedimentation to settle suspended particles, and/or using coagulants to accelerate settling. Biological growth can be reduces by removing nutrients (such as nitrogen and phosphorus) and organic carbon from the water, as well as by disinfecting with chlorine or other disinfectants which may reduce biological activity. In surface infiltration schemes, periodically drying the basins allows the clogging layer to dry decompose, shrink, crack and curl up, thus generally restoring infiltration rates to satisfactory values (Bouwer, 2002). If this is not enough, clogging materials may be mechanically (e.g. using scrapers, rakes, and graders) removed at the end of the drying period.

Note that in some cases the bottoms and banks of infiltration basins are intentionally covered with a "clogging layer" that controls and reduces infiltration rates so that the underlying soil material remains unsaturated (Bouwer, 2002). This prevents the water table from rising up to the bottom of the basin and causing a hydraulic connection that will decrease infiltration rates significantly (see below). These layers are generally made up of coarse sand or fine gravel. They offer the advantage of being relatively incompressible, and if there is an accumulation of organic and inorganic deposits which may impede infiltration it may be removed and replaced with a "clean" layer.

4.1.2. Hydraulic connection

In infiltration schemes unaffected by clogging, infiltration causes the water table to rise in the form of a groundwater mound. If left unmonitored, rises in groundwater levels below infiltration systems can cause the infiltration scheme to be *hydraulically connected* with the water table, meaning the water table has intersected the recharge scheme. Infil-

tration rates are unaffected by groundwater levels up to the point where the capillary fringe reaches the bottom of the infiltration scheme. Then, they continue to decrease linearly with decreasing depth to groundwater below the water level in the basin, until they become null when the water table reaches the same elevation as the water surface in the basin.

Fortunately, in basins where infiltration rates are controlled by a clogging layer, and the water table is more than about 1 m below the bottom of the basin, infiltration rates are assumed to remain unaffected by changes in groundwater levels (Bouwer, 2002).

In cases where hydraulic connection has indeed taken place, the observations outlined in Section 3.2.2 apply: if the depth to the water table (taken at a sufficient distance from the recharge area such that groundwater levels are relatively unaffected by the recharge flow system, FIGURE 4.5) is relatively large, then the flow below the recharge system continues to be mainly downward and controlled by the vertical properties of the aquifer. If the depth to the water table is however shallow, or if groundwater levels rise causing the overall depth to the water table to decrease, then flows from the recharge basin becomes increasingly lateral until eventually they are completely controlled by the slope of the water table away from the basin.

According to Bouwer (2002), when the depth to the water table is at least twice the width of the recharge system ($D_W > 2\,W$, FIGURE 4.6) then mounding does not cause significant disturbance of the infiltration process (they are about equal to the maximum value when $D_W = \infty$). However, if $D_W < 2\,W$ then infiltration rates decrease almost linearly with decreasing D_W, reaching zero when $D_W = 0$.

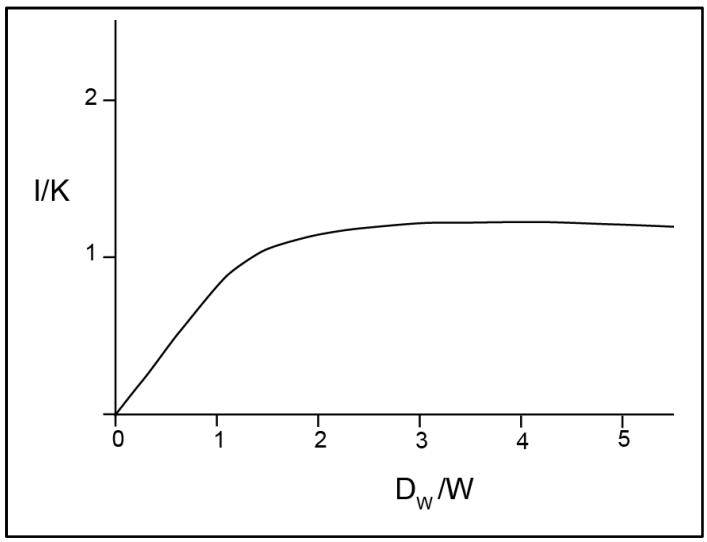

FIGURE 4.6: Dimensionless plot of seepage (expressed as I/K) and depth to groundwater (expressed as D_W/W) for a basin with no clogging layer at the bottom. I is the infiltration rate and K is the hydraulic conductivity in the wetted zone. D_W is the depth to the water table and W is the width of the recharge system (modified from Bouwer, 2002)

Note that these observations apply to uniform, isotropic underground formations of "infinite" extent. Anisotropic, heterogeneous and stratified situations need to be considered on a case-by-case basis.

4.2. Contamination of groundwater

The quality of the source water (and its variability) must imperatively be taken into account. The benefits of filtration and removal of sediment, pathogens, nutrients and other contaminants when water circulates through unsaturated sediments are not always present, or so at a degree that is satisfactory. On one hand, hydraulic connection, as well as the existence of preferential flow paths, lead to a decrease in residence times (water circulates quicker in saturated environments or when bypassing the matrix). Unfortunately, relatively long residence times, along with oxidizing conditions, are important in regards to water decontamination. Also, in cases where direct well injection is used, filtration processes will not take place at all.

Finally, in situations where the groundwater is already of poor quality and MAR is expected to decrease contamination by dilution, there is a risk of creating a 'lens' of good quality water which will not properly mix with the surrounding water. The opposite is also true, if the aim of MAR is to generate a 'lens' of potable water in a contaminated environment, then mixing with the native groundwater may degrade the quality of the injected water (Gale et al., 2002). Overall, a sound understanding of the hydraulics of this type of situation is essential to permit accurate water management.

4.3. Watershed scale impacts

An important question to consider when implementing MAR is one that is often overlooked (Gale et al., 2006): do MAR interventions merely relocate the availability of wa-

ter through aquifer storage or is a significant quantity added to the system through reduction of evaporative losses and discharges to non-potable water bodies?

At small scales (a few square meters to a few square kilometers), results have often point towards increased groundwater resources and predominantly positive impacts of artificial recharge (e.g. Massuel *et al.*, 2014; Srivastava *et al.*, 2009), which benefit mostly landholders closest to the recharge facilities. Larger-scale studies (at the watershed scale or bigger) are less common, generally because of the difficulty in obtaining relevant data at the appropriate scale, especially in complex and heterogeneous media.

In the review by Bredehoeft (2002), the main research gaps that exist concerning MAR impacts at larger scales are identified, highlighting the lack of watershed scale hydrological studies aimed at this. A summary of the documented hydrological impacts of MAR at larger scales is also made:

- **Decreased availability for downstream users and streamflow** (Calder et al., 2008; Glendenning et al., 2012), especially when in-channel systems are used. Indeed, intensification of water retention and use within watershed areas may lead to downstream water shortages. Originally, when these types of schemes are applied, the rationale is that the runoff exiting the watershed will remain unutilized. Nevertheless, although localized runoff and runoff from individual storm events may be high, annual runoff in semi-arid areas is generally only a small portion of precipitation. In fact, in some areas outflow from the watershed is observed only during the wettest years (is essence these are "closed" systems), and water retention tends to aggravate this problem. Unfortunately, "basin closure" has been shown to have significant negative social and environmental issues (such as water quality degradation and water-use conflicts). Although the subject of basin closure is beyond the scope of this study, readers are referred to Molle et al., (2010).
- **Feedback loops: more perceived water leads to more irrigated agriculture**. If MAR leads to increased groundwater availability (real or perceived), then this may cause irrigated agriculture to be further developed, or cause a shift in cropping patterns toward more water intensive crops (e.g. sugarcane and dry season paddy); if the augmentation of groundwater resources is not enough to keep pace with the increase in irrigation, or if the positive impacts were merely perceived, this will cause a negative feedback further depleting the aquifer and decreasing outflow.

5. Predicting and assessing MAR efficacy

5.1. Soil maps and hydrogeological reports

Surface infiltration systems require permeable soils and relatively thick vadose zones, as well as an unconfined and sufficiently transmissive aquifer to get lateral flow away from the recharge are without excessive groundwater mounding (Bouwer, 2002).

The first step in assessing the potential of a zone to suitably store and transmit MAR is to make use of existing information such as soil maps and hydrogeological reports to have an idea of the soil permeability and hydraulic conductivity of a given area. Soil and geological maps nevertheless provide limited information, and should only be used preliminarily to approximate the best placement for MAR within a watershed. Remote sensing methods and geographic information systems can significantly improve siting of areas suitable for MAR by refining observations on land use, geomorphology and soil types.

Nevertheless, in-depth knowledge of the site properties is essential to support assessment of the best technical option for MAR. Field investigations are thus essential for more a more accurate determination, as they allow, for example, determination of local hydraulic properties and potential infiltration rates.

5.2. Field methods

5.2.1. Surface hydraulic properties

After a large-scale assessment of potentially suitable sites for MAR placement, infiltration tests should be performed to see what kind of infiltration rates can be expected. There are many different ways to perform an infiltration test (e.g. Lassabatère et al., 2006), although Bouwer (2002) suggests the use of single cylinders with significant water depth to speed up the infiltration process. The specifics on the use and implementation of infiltrometers are available in Bouwer (2002), here only a brief summary will be made.

To estimate the surface hydraulic conductivity of an area, a metal cylinder is driven a few centimeters into the soil and subsequently filled with water. The rate at which water infiltrates into the soil, along with information on the extent of lateral wetting (measured using a shovel) and depth of wet-front penetration (measured using an auger or estimated from the total accumulated infiltration and the fillable porosity) are inputted into the Green-and-Ampt equation for unsaturated flow (Eq. (4.1)) and solved for K_v. If the resulting K_v values are sufficiently large for an infiltration system, the next step would be to put in some test basins to evaluate clogging effects and the potential for infiltration reduction (Bouwer, 2002).

Note that K_v can be used as an estimate of long-term infiltration rates in *large and shallow* inundated areas, *without clogging* of the surface and *without restricting layers* deep-down. Situations diverging from these conditions may call for more complex calculations, for example using analytical equations or numerical modeling.

5.2.2. Subsurface hydraulic properties

Understanding the potential of an aquifer to store and transmit recharge inputs appropriately first requires estimation of storativity (S) and transmissivity (T). One of the most effective ways of determining these properties is to conduct and analyze aquifer tests. There are many different ways of implementing aquifer tests, and analytical solutions used to interpret them are selected based on the assumptions made concerning the type of aquifer (confined vs unconfined) as well as other considerations (e.g. is the aquifer leaky, or is there an impervious boundary present). This topic is quite extensive and beyond the scope of this thesis, so for further information readers are referred to textbooks on quantitative hydrogeology (e.g. Cushman & Tartakovsky, 2016; de Marsily, 1986; Fetter, 2000).

5.3. Modeling the aquifer response to MAR

Once the surface and subsurface physical properties of the aquifer have been assessed, modeling can provide valuable information on the height and shape of the groundwater mound formed from infiltration and the overall lateral transmission of MAR inputs throughout the aquifer. Classically this sort of exercise is performed either using analytical equations or numerical simulations.

5.3.1. Analytical solutions

Analytical equations are partial differential equations with initial and boundary conditions that mathematically describe, in this case, groundwater flow (Carleton, 2010). These equations can be used to predict the rate of growth and shape of a recharge mound beneath a surface infiltration scheme.

In general, analytical solutions to predict the rate of growth and shape of a recharge mound solve the governing partial differential equation describing the flow of groundwater in two dimensions as given by the linearized Boussinesq equation (Warner et al., 1989):

$$K\bar{b}\left(\frac{\partial^2 h}{\partial x^2}+\frac{\partial^2 h}{\partial y^2}\right)+R=S\frac{\partial h}{\partial t} \tag{4.3}$$

where the different variables and parameters are defined in FIGURE 4.7. Many solutions to this equation have been proposed over the years (Warner et al., 1989), although the most widely cited (and used) is the solution developed by Hantush (1967). This solu-

tion simulates groundwater mound growth and decay in response to percolation, and is valid when the top of the groundwater mound is disconnected from the bottom of the recharge basin (see FIGURE 4.7):

$$Z = \frac{R\bar{b}}{2S}\int_0^t \left(\operatorname{erf}\left(\frac{\frac{L_b}{2}+x}{\sqrt{4\upsilon\tau}}\right)+\operatorname{erf}\left(\frac{\frac{L_b}{2}-x}{\sqrt{4\upsilon\tau}}\right)\right)*\left(\operatorname{erf}\left(\frac{\frac{W_b}{2}+y}{\sqrt{4\upsilon\tau}}\right)+\operatorname{erf}\left(\frac{\frac{W_b}{2}-y}{\sqrt{4\upsilon\tau}}\right)\right)d\tau \qquad (4.4)$$

where $Z = h^2 - b^2$, υ is a simplifying term with $\upsilon = K\bar{b}/S$ and $\tau = (t - t')$, the time during which percolation takes place. Initial conditions assume a horizontal water table and the boundary conditions of zero slope of the mound profile at the center of the basin and at infinity.

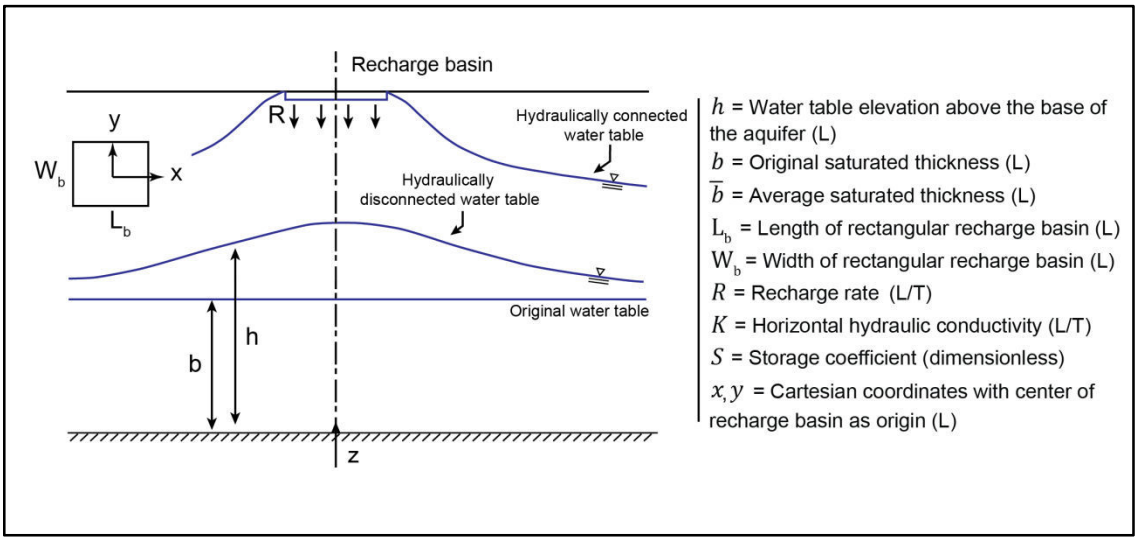

FIGURE 4.7: Schematic representation of water level variations in response to artificial recharge from an infiltration basin featuring parameters used in analytical modeling of artificial recharge (modified from Warner *et al.*, 1989)

This equation has been solved using simple tools with friendly user interfaces, e.g. using an Excel spreadsheet, or can be manually typed into any programming language and solved iteratively. The extreme simplicity of this solution is both an advantage and a disadvantage: on one hand, the only requirements are the dimensions of the infiltration basin along with the hydraulic properties of the aquifer. On the other hand, any deviation from the standard conditions assuming homogeneous media will reduce the accuracy of the output. Also, because of these assumptions, effects of aquifer geometry and boundary conditions on MAR flow cannot be analyzed.

5.3.2. Numerical models

Because of the above mentioned limitations, despite their easy and straightforward application, analytical solutions are not always suitable to simulate the aquifer response to MAR inputs. Numerical models, compared to analytical equations, offer the benefit of

representing highly complex three-dimensional conditions and including site-specific conditions such as variations in aquifer characteristics, basin shape, recharge duration (and fluctuations) and other local features (Carleton, 2010).

Ringleb et al. (2016) published a review of the assessment of MAR through modeling which takes stock of the existing case studies and the methods used for each. This study looked at the types of model used, and found that saturated flow models were the most widely used, although the use of unsaturated flow models, water balance and watershed models keep increasing. The majority of saturated flow models used to assess the aquifer response to MAR are not specifically developed for MAR applications, and are instead existing groundwater flow models, the most commonly used being MODFLOW.

There are a certain number of considerations to be had when using numerical models, which, nevertheless, also have limitations (see Brunner et al., 2010). MODFLOW, specifically, only simulates flow in the saturated zone. This means that water reaches the water table without retardation in an unsaturated zone. In reality, storage and delay of water in the vadose zone would act to lower the height of the groundwater event, and neglecting these processes leads to higher simulated groundwater mounds (this approach is nonetheless conservative, as it is better to over-estimate the height of the mound than the opposite). Also, because a greater amount of parameters come into play which may or not be estimated with great accuracy, testing the sensitivity of the results to these properties is often recommended.

5.4. Monitoring infiltration and groundwater mounding

Once a MAR scheme has been set up, monitoring infiltration rates and their variations, as well as the formation and evolution of the resulting groundwater mound, can prove very useful. Pilot studies, for example, are aimed precisely at this; monitoring of water levels in the basin and the aquifer are necessary to evaluate whether expectations were met and if the preliminary assumptions made were correct before launching a wider implementation of MAR structures in similar environments. Beyond the scope of pilot studies, assessing the effectiveness of MAR is imperative to judge whether infiltration is taking place as expected, and if not to take appropriate measures to address the limiting factors (e.g. clogging, excessive groundwater mounding).

5.4.1. The water balance approach to measure infiltration

Measuring *actual* infiltration in existing MAR schemes can give an idea of the effectiveness of the structure, which can be useful when considering future MAR schemes in similar areas, or to evaluate whether infiltration rates are as expected. The water balance approach is the most common way of doing so. For this, the different components

of the water balance must be considered: precipitation (P), evaporation (ET), inflow to the structure (q_{in}), and outflow into the aquifer (q_{out}):

$$P + q_{in} = q_{out} + ET - \Delta S \tag{4.5}$$

Ideally P and ET should be measured or estimated on-site (there are many professional-grade weather stations available on the market), although regional estimates can be used if the former are not available. q_{in} estimations will depend on the type of MAR structure implemented, and can be either measured or approximated making a few assumptions (e.g. for percolation tanks q_{in} can be estimated if rainfall and the impluvium surface intercepted are known). Finally ΔS is generally deduced from water-level variations in the basin, allowing q_{out} to be estimated at the remnant of Eq. (4.5). The water balance approach can be applied using fluxes [$L^3.T^{-1}$] or flux densities [$L.T^{-1}$].

These components should be evaluated not only on an average annual basis, but also in time and space, especially in regions with strong seasonal variations. Calculating the evaporation/infiltration ratio can further be useful to determine the magnitude of evaporative losses, and if these are too significant, measures may be taken to minimize them (e.g. declogging, scraping, alternating between wetting and drying phases). Also, note that although a single infiltration estimate is generally given per infiltration basin, infiltration has been noted to be quite heterogeneous and variable within the basin bottom as a result of heterogeneous and progressive silting (Mawer et al., 2016; Racz et al., 2012).

Nevertheless, while water budgets can provide useful guidelines for groundwater exploitation (e.g. Boisson, Villesseche et al., 2015; Perrin et al., 2009; Singh et al., 2004), many authors have pointed out their insufficiency in providing accurate estimates of sustainability and efficiency, highlighting the need to understand dynamic processes [see "The Water Budget Myth", Chapter 2 Section 1.2]. Additionally, considerations of how the recharge is transmitted throughout the aquifer, i.e. the transient aquifer response, must also be considered. For example, significant groundwater mounding may impede infiltration processes, so understanding how the recharge water is transmitted throughout the aquifer might provide useful information in regards to avoiding hydraulic connection between the MAR structure and the water table.

5.4.2. Monitoring the aquifer response to MAR

Observing how water levels vary in response to MAR requires the presence of boreholes in the vicinity of the basin. Water levels can then be measured at certain time intervals, or continuously if the boreholes are equipped with pressure sensors. Although the shape and size of the groundwater mound may be appraised through previously cited modeling techniques, groundwater level observations are essential to ensure that the as-

sumptions made when simulating the mound were appropriate. If measured water levels diverge significantly from the simulations, then the reasons for the discrepancy must be identified, along with their impact on the receipt and transfer of recharge within the aquifer, among other considerations. In some cases, observed water level variations can even be used to calibrate the simulations and obtain better estimates of the aquifer's hydraulic properties.

Unfortunately, boreholes are not always present in the recharge area, or they may be privately owned precluding measurements. In these cases some researchers have turned to geophysical methods to image the groundwater mound and its progression at a given time scale using time-lapse geophysics (e.g. Wubda et al., 2017) or microgravity measurements (see Maliva, 2015 and references therein), although if available piezometric data is still preferred.

6. MAR in fractured crystalline rock

In **Chapter 1 Section 2** we identified the defining characteristics of fractured crystalline rock aquifers. Each specific characteristic, some of which are recalled below, is susceptible to impact MAR in different ways:

(i) **Extremely low primary hydraulic conductivities and porosities**. This implies that the fractured crystalline rock matrix is not suitable for MAR. The storage capacity of these aquifers is therefore directly linked to the existence of a *secondary* porosity, and thus to the degree of weathering the rock has undergone. If we recall, a typical weathering profile is a relatively layered system (FIGURE 1.9), composed, from the top down, of a residual soil, followed by the saprolite layer (highly decayed rock resulting from intense weathering; high storage coefficients, low transmissivity), the saprock or bedrock-saprolite interface (partially decomposed, highly fractured; high storage coefficients, high transmissivity), and the fissured bedrock (mostly intact, with some fractures; low storage coefficients, high transmissivity depending on fracture connectivity). The hydraulic properties of the aquifer as a whole are highly dependent on the relative thickness of each "layer". This implies, on one hand, that the amount of water which can be stored through MAR in fractured crystalline rock will vary greatly depending on the thickness of the saprolite and saprock (where the highest storage coefficients are found). On the other hand, the ability for an aquifer to transmit water inputs away from the recharge area, which is also very important in regards to storage and management, will be directly linked to

the degree interconnection of the highly transmissive fractures, along with the thickness and disposition of the saprock.

(ii) **Strong heterogeneity of hydraulic parameters both vertically and horizontally**. The significant and multi-scale heterogeneity which characterizes fractured crystalline rock has strong implications for the predictability of the aquifer response to MAR inputs. The hydraulic properties of this type of media have been known to vary over several orders of magnitude over short distances depending on the degree of fracturing and the thickness of the weathered layers. Fractures serve as preferential flow paths, and their presence (or absence) can significantly alter the flow dynamics of an area. Overall, the complexity of this type of media precludes any straightforward assessment of the MAR potential of a given area. Even if a pilot study is performed, any extrapolation or generalization of the outcome is to be considered with caution.

(iii) **Often compartmentalized**. Fractured crystalline rock aquifers are often highly compartmentalized. Although the saprolite is relatively homogeneous and well connected, its thickness is highly variable, and is mostly linked to the topography of the unweathered bedrock (closely mimicked by the saprock)[14]. Because the underlying saprock and fracture networks are the most transmissive parts of the aquifer, the bulk of the flow occurs within them. As such, the transmissivity and connectivity of the aquifer are intrinsically linked to the saprock thickness and layout (which has been known to feature significant hilliness) the degree of fracturing and interconnection between fractures. Depending on water levels relative to these preferential flow pathways, groundwater flow dynamics may shift from a local restricted flow system, to regional-scale flows (Guihéneuf et al., 2014). In regards to MAR, the existence of compartmentalization could slow or stop the progression of infiltration fronts, leading MAR inputs to be highly focused rather than spread out. On the other hand, the existence of preferential flow pathways could enhance recharge, allowing an efficient and rapid lateral transfer of MAR inputs throughout the aquifer [more on this in Chapter 6].

[14] To better illustrate the layout of a weathered crystalline rock aquifer, we might think of them as analogous to an egg carton or an ice tray. When filled with water, each "dimple" will remain isolated, but only up to the point where the water reaches the top of the dividers. Then they become connected, and flow can happen from one side of the tray or carton to the other (see Guihéneuf et al., 2014).

In sum, fractured crystalline rock aquifers are complex, and flow dynamics within them are highly variable and difficult to predict. The potential of this type of rock to store water reliably and in sufficient quantities depends on a set of factors which cannot easily be determined. The advancement of geophysical and remote sensing methods—which are becoming increasingly accurate and accessible—is sure to reduce some of the uncertainty by providing detailed maps of the subsurface at increasing scales. Nevertheless, direct and frequent (if not continuous) monitoring of water levels in and around MAR structures remains the surest way to ensure that the storage and transmission of MAR inputs is meeting the expectations of the community the structure was intended to benefit.

There are very few published studies which focus specifically on MAR in fractured crystalline rock. Many of these studies have focused on quantifying percolation efficiencies (relative to evaporation), which were found to be quite variable. Percolation tanks have been shown to present efficiencies ranging from 30% to up to 98% (Central Ground Water Board, 2011; Massuel et al., 2014), mostly depending on the age of the structure (and thus its degree of clogging), and that are overall quite variable (Boisson et al., 2015: 67%; Massuel et al., 2014: 61%; Singh et al., 2004: 67%; Perrin et al., 2009; 56%). Most of these studies, however, are limited to estimations from water budgets.

Analysis of MAR with consideration of hydrodynamic processes in sedimentary aquifers is quite extensive, both in theoretical settings (e.g. Carleton, 2010; Warner et al., 1989; Zlotnik et al., 2017) and in applied study cases (e.g. Kacimov et al., 2016; Réfloch, 2018; Teatini et al., 2015). There are few studies which focus on hydrodynamic processes in hard rock *specifically*. For example, the study by Massuel et al. (2014) examines the impact of pumping in the vicinity of the basin on infiltration efficiencies through hydrodynamic modelling in a hard rock context.

To the best of our knowledge, however, no studies have yet looked into dynamic processes in hard rock with consideration of aquifer geometry. This is probably because it is not easy to image the aquifer's geometry or to obtain three-dimensional information about hydraulic properties in hard rock context (de Marsily *et al.*, 2005). Some studies have highlighted the existence of complex flow paths through which MAR inputs circulate (e.g. Alazard et al., 2016). Others have observed that compartmentalization due to the existence of impermeable barriers such as dykes may impede the progression of a recharge mound (Massuel et al., 2014). These are, nevertheless, qualitative observations.

7. Watershed development and MAR in India

7.1. National scale

Activities aimed at augmenting groundwater resources through MAR in India are generally part of a wider set of activities aimed at developing or rehabilitating watersheds. These activities combine a range of land development or protection, afforestation, horticultural activities as well as explicit water resource conservation and augmentation measures. Presently, microwatershed management in India absorbs over US$500 million per year, channeled mainly from central government resources (James & Robinson, 2001). Watershed development (WSD) projects have been operating in India since before independence. Essentially, WSD programs aim to restore degraded landscapes in rainfed regions to increase their capacity to capture and store rainfall, reduce soil erosion and improve soil nutrient and carbon content in order to generate greater agricultural yields (Gray & Srinidhi, 2013). They have since, however, shifted their focus from ecological objectives towards projects aimed at promoting a more bottom-up and people-centered approach, i.e. managing resources in an integrated manner that allows generation of economic resources within population inhabiting the watershed.

India, where 54% of the territory faces high to extremely high water stress (Shiao et al., 2015) is the world leader in recharge enhancement. Yearly contributions are estimated at around 3 km^3/year (Jakeman et al., 2016), most of which is to unconfined aquifers through infiltration structures in order to sustain agriculture. This volume does not keep up with groundwater depletion, especially in northern India (depletion in the states of the states of Rajasthan, Punjab, Haryana and Delhi alone is estimated at 17.7 $\pm$ 4.5 km^3/year; Rodell et al., 2009), but has contributed to prolong the resource and sustain groundwater supplies. In some part of west and south India the groundwater depletion trend has even been reversed, decadal measurements showing aquifers replenishing trends resulting from changes to groundwater management policy (Bhanja et al., 2017).

The implementation of artificial recharge schemes in India is not new. For centuries, extensive rainwater harvesting structures comprising infiltration basins and percolation tanks were built and maintained, and strongly contributed to sustaining the livelihoods of rural communities. At the time, however, water was directly taken from the basins and tanks. After independence[15] the importance of these tanks for irrigation and the surfaces depending on water from tanks declined significantly. One of the most important reasons for this decline was the disappearance of village institutions managing the struc-

[15] The Indian independence movement aimed at ending the British rule spanned a total of 90 years, ending in 1947 when the *Indian Independence Act 1947* was passed, and British India was partitioned into the two new independent dominions of India and Pakistan.

tures. Traditional systems where replaced by massive development of canal irrigation that absorbed tank-irrigated areas, further contributing to the displacement of traditional tank systems. Since 1951[16] water resource development has been carried out through 5-year plans (P. R. Reddy, 2015). Even under these 5-year plans, due attention was not given to tank maintenance (until recently), so despite irrigated surfaces increase at a rate of more than 1 million ha per year, the extent of basin irrigated areas showed a steady decline (P. R. Reddy, 2015).

In the recently published *Master Plan for Artificial Recharge to Groundwater in India* (Central Ground Water Board, 2013), it has been estimated that a total area of 941,541 km^2 (about 28% of the total land area of India) is suitable for artificial recharge, and that an annual volume of 85,565 MCM (85 km^3) of surplus monsoon runoff could be stored in the groundwater reservoir. This is equivalent to about 90 mm over the entire area, and represents about 30% of the total 250 km^3/year that are currently utilized annually. This would be achieved through the building of over 11 million recharge structures in urban and rural areas, at an estimated cost of about 79,178 crore rupees (over $US 11bn), and built over a period of 10 years. Of these structures, about 8.8 million would be structures using rainwater directly from roof tops (mostly in urban areas) for an approximate cost of about 17,986 crore rupees (about US$2.3bn) and around 2.3 million would be rain and water harvesting structures for conserving surplus runoff and recharging groundwater to aquifers at a cost of about 61,192 crore rupees (about US$8.6bn) (mostly in rural areas). The general assumption is that recharge activities will increase water availability and thus mitigate groundwater overdraft problems, in term benefiting not only the resource poor but the community as a whole. MAR, specifically, is expected to (Gale et al., 2006):

- Increase productivity of land and water leading to greater incomes.
- Protect drinking water supplies in terms of water availability, sustainability and access. Water quality is rarely intentionally managed (Jakeman et al., 2016) but concentrations in geogenic elements (providing from the aquifer itself), such as fluoride and arsenic, are expected to decrease by dilution (Brindha et al., 2016).
- Reduce vulnerability of populations depending on rainfed agriculture through creation of a buffer supply (i.e. groundwater), particularly during droughts.

[16] 1951 is the year of formation of the Planning Commission. The Planning Commission was an institution in the Government of India, which formulated India's Five-Year Plans, among other functions. In 2014 Narendra Modi dissolved the Planning Commission, replacing it by a new institution named the National Institution for Transforming India (NITI Aayog).

- Protect environmental services by maintaining stream base flows, wetlands and surface vegetation.

7.2. Telangana state-scale: Mission Kakatiya

At the end of 2014, the Government of Telangana launched an ambitious project entitled *Mission Kakatiya*, aimed at rejuvenating the 47,000 tanks and lakes spread over 9 districts by 2020. The term *Mission Kakatiya* refers to the Kakatiya dynasty in southern India that shaped the history of the state of Telangana between the 12th and 14th century. The Kakatiya rulers built thousands of small reservoirs or tanks across the region to store rainwater and make it more readily available to people and their farms in the dry season. These tanks were managed and maintained by the communities through a system of decentralized governance[17]. Over the years, land use change and encroachment of tank beds, as well as the development of alternative water sources for irrigation, led to the neglect of these structures (M. Shah et al., 2017). It was estimated in the latest Minor Irrigation Census that there are 46,531 percolation tanks in the state of Telangana (Irrigation & CAD Department, 2015). The purpose of Mission Kakatiya is to revive the tank irrigation system. To do so, this five-year program aims to restore all of the tanks identified by the Minor Irrigation Census, effectively using 7.5 km^3 of water in the Godavari and Krishna river basins, thus achieving the basins' irrigation potential of 2 M ha. The budget allocated to this project is of about 12,500 crore rupees (about US$1.7bn) for five years. Since its launch in 2015, several publications have been aimed at taking stock of the progress and limitations of the project so far (M. D. Kumar et al., 2016; M. Shah et al., 2017). These publications have similar conclusions. When implemented well, tank renovation has the potential to bring significant positive benefits to the village agrarian economy in term of expansion of irrigated areas, enhanced groundwater recharge, reduction in cost of cultivation and improved crop productivity (M. Shah et al., 2017). Unfortunately, although the structural aspects of tank building (earthwork, waste weir construction, canal lining, etc.) have been carefully considered, little attention has been focused on tank hydrology and on their physical performance, as well as watershed-scale efficiency assessments (to make sure that the tanks are not merely relocating water availability). As a result, the quality of the implementation and the responsiveness of the village community have not been uniform across the districts. M. Shah et al. (2017) propose the following points for improvement:

[17] One may, however, point out that these systems involved coerced labor, highly oppressive caste systems, the expropriation of surplus value by elites, and were overall symbols of the significant power and wealth difference enjoyed by the feudal landlords and warlords, but this is beyond the scope of this thesis. Readers are referred to (E. Shah, 2008).

(1) Attention needs to be shifted from civil works to field application, especially the desilting of the tanks, and groundwater recharge. In fact, tanks require periodical desilting, yet this is not considered in Mission Kakatiya. This could severely impact the sustainability of this project after the five-year period has elapsed. Feeder channels require more attention as well, for example to repair them and remove encroachments.

(2) Tank operations should better account for the different (and sometimes conflicting) interests of the community; for example, fishermen prefer that the tanks remain full as long as possible, while farmers would prefer the water be released for irrigation. The net positive impacts of these operations should therefore be maximized with consideration of all of the different stakeholders' interests.

(3) Finally, distinctions should be made among the total number of tanks which the government has set out to restore. In reality, almost 90% of the tanks in Telangana are small tanks with a command area of less than 1 km^2, and together they make only one-third of the total tank-irrigated area (M. D. Kumar et al., 2016). In fact, only 3,864 large tanks account for 67% of the tank irrigated area (M. D. Kumar et al., 2016). The rehabilitation and maintenance of tanks should be done with a more accurate cost-benefit analysis in order to prioritize the tanks which have the greatest potential.

Research problem

In this chapter we have seen that MAR can be useful to alleviate the problems which arise from groundwater overexploitation. Nevertheless, in order for a MAR scheme to be effective, several criteria must be examined—both before and during its implementation. Among these criteria, two are particularly important: the total water volumes infiltrated relative to the total (i.e. infiltration efficiency) and the subsequent propagation of these inputs throughout the aquifer (i.e. the formation and evolution of the groundwater mound).

Assessing infiltration potentials is a straightforward calculation, although progressive and heterogeneous silting of the basin bottom may require more detailed observations. Understanding the aquifer response to MAR is more complicated, however. In sedimentary (and thus relatively homogeneous) media, these calculations can be as simple as inputting the aquifer's hydrodynamic properties into an Excel spreadsheet. But little is known on aquifer response to infiltration in heterogeneous media. The existence of complex flow paths and compartmentalization effects have been observed, but not often have they been incorporated into hydrodynamic models.

The resulting research problem is thus: how does recharge propagate in heterogeneous settings? Do sub-horizontal preferential flow pathways facilitate this process? Or does the existence of compartmentalization hinder flow propagation? In sum, what are the specificities of MAR in fractured crystalline rock and how can they be taken into account?

These questions will be explored in Chapter 6.

Part II

EXPERIMENTAL AND NUMERICAL INVESTIGATIONS OF NATURAL AND ARTIFICIAL RECHARGE IN FRACTURED CRYSTALLINE ROCK

Preface

Water resources in India

India is made up of 29 states and 7 union territories (FIGURE 0.1a). Although India occupies only 3.29 million km^2 in geographical area (2.4% of the world's land area), it supports a significant portion of the world's population. The last census by the World Bank estimates the total Indian population at about 1.34 billion inhabitants (2017 World Bank est.), making up almost 18% of the global total (7.53 billion inhabitants, 2017 World Bank est.). Population in this country has increased rapidly and steadily (FIGURE 0.2): in the past 50 years population has tripled. The average population density in India is 450 people per km^2, reaching at most over 11,000 people per km^2 in the North Capital Territory of Delhi. In comparison, population density in China is 147 people per km^2.

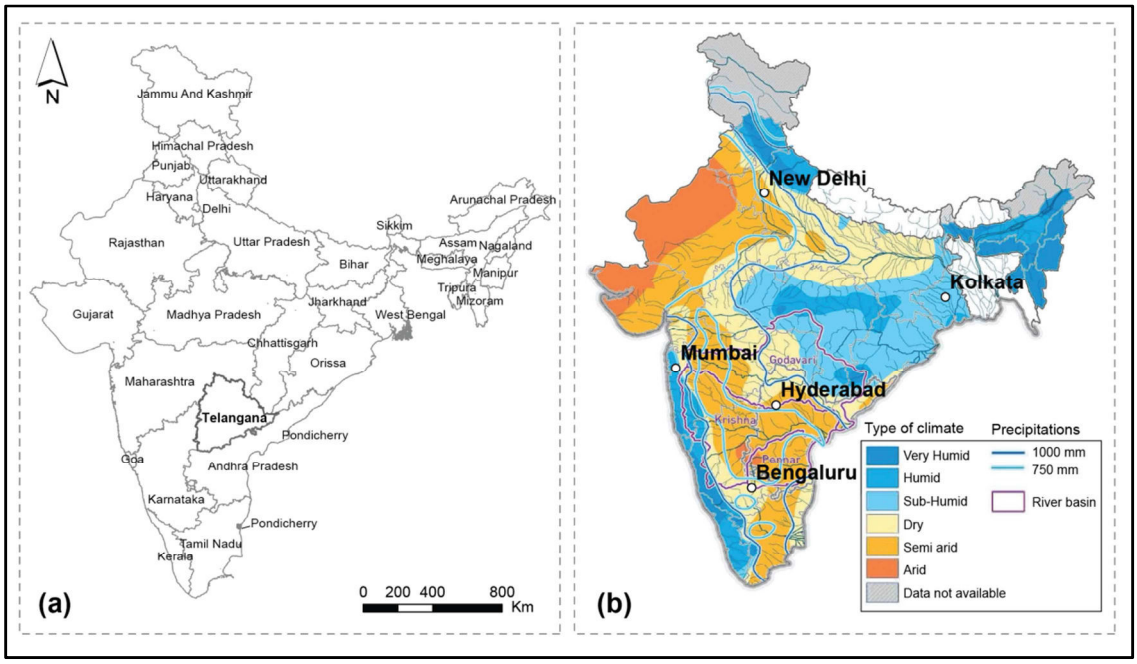

FIGURE 0.1: Map of the 29 states in India (union territories not shown) (a) and map of climatic zones in India (modified from de Golbéry & Chappuis, 2012) (b)

Climate in India is comprised of a wide range of weather conditions. There are 6 different climate zones in India, ranging from arid desert in the northwest to humid tropical regions in the southwest and northeast (FIGURE 0.1b). Mean annual rainfall is about 1160 mm, although the distribution of rainfall over time and space is highly variable (FIGURE 0.3a). Rainfall in India is highly dependent on south-west monsoons, which take place from June to September, except for the state of Tamil Nadu which is under the influence of north-east monsoons during October and November. In terms of volume,

India receives annual precipitation of about 4,000 km^3 including snowfall, of which monsoon rainfall is of about 3,000 km^3 (R. Kumar et al., 2005). Of the total, about 1,122 km^3 are utilizable, and 432 km^3 are replenishable groundwater resources (i.e. 9-10% of total rainfall) (Gupta & Deshpande, 2004).

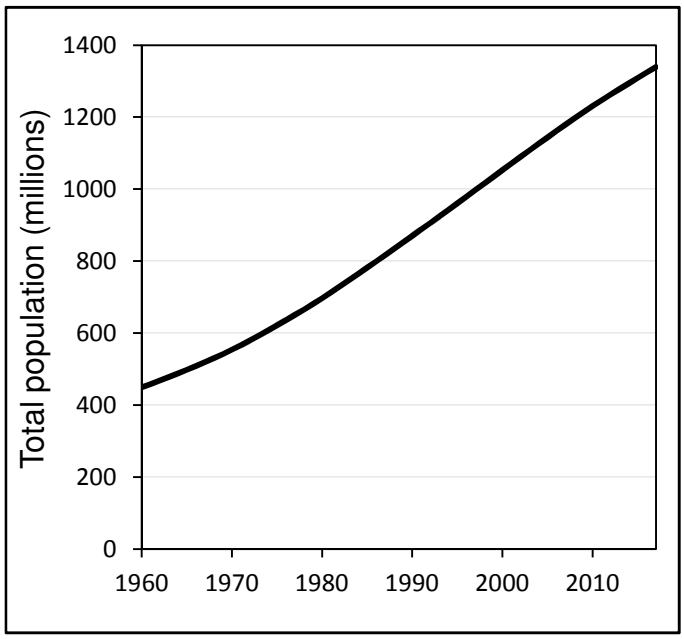

FIGURE 0.2: Total population in India according to the World Bank (*https://data.worldbank.org/*). Total population is based on the de facto definition of population, which counts all residents regardless of legal status or citizenship. The values shown are midyear estimates.

Groundwater recharge is heterogeneously distributed. In the latest nation-scale recharge estimation by Bhanja et al., (2018), shown in (FIGURE 0.3b), basin-scale recharge is noted to vary widely, between 17 mm/yr and 960 mm/yr. The extensive plains of the Indus-Ganges-Brahmaputra (northern India) present relatively higher recharge rates (>200 mm/yr), attributed to coarser sediments, higher rainfall, and intense groundwater pumping inducing recharge by increasing available groundwater storage (Bhanja et al., 2017). Lower recharge rates occur mostly in central and southern India, specifically in fractured crystalline aquifers. It was also shown that precipitation rates do not significantly influence recharge in most of the river basins analyzed, instead the human influence was found to be more significant (Bhanja et al., 2017).

There are more than 20 major rivers in India (such as the Ganges, the Indus, the Godavari, and the Krishna) with several tributaries, many of which are perennial, some of which are ephemeral. Less than 50% of water resources in India depend on water from these river systems (R. Kumar et al., 2005), the rest being assured—increasingly—by groundwater sources. According to Siebert et al., (2010), the percentage of land irrigated with groundwater in India has gone from 29% in 1951 to 62% in 2003. These figures reflect India's increasing dependency on groundwater since the mid-20th century during the

Silent Revolution[18]. In India, the number of pumps has grown from less than 100,000 in 1960 to over 27 million by 2012, with no indication of slowing down (Molle et al., 2003). Nowadays, India is the world's greatest exploiter of groundwater in the world: abstractions tally up to a staggering 250 km^3/yr, which is more than China and the United States combined (Dieter et al., 2018; Siebert et al., 2010). With yearly extractions exceeding natural groundwater recharge in many parts of India, the harmful side-effects of groundwater overexploitation are growing in scope and urgency. For example, Rodell et al. (2009) have estimated the yearly groundwater depletion rate at about 17.7 ± 4.5 km^3/yr in the northwestern part of India alone. In fact, according to the World Resources Institute, 54% of India faces high to extremely high water stress (Shiao et al., 2015) (FIGURE 0.4).

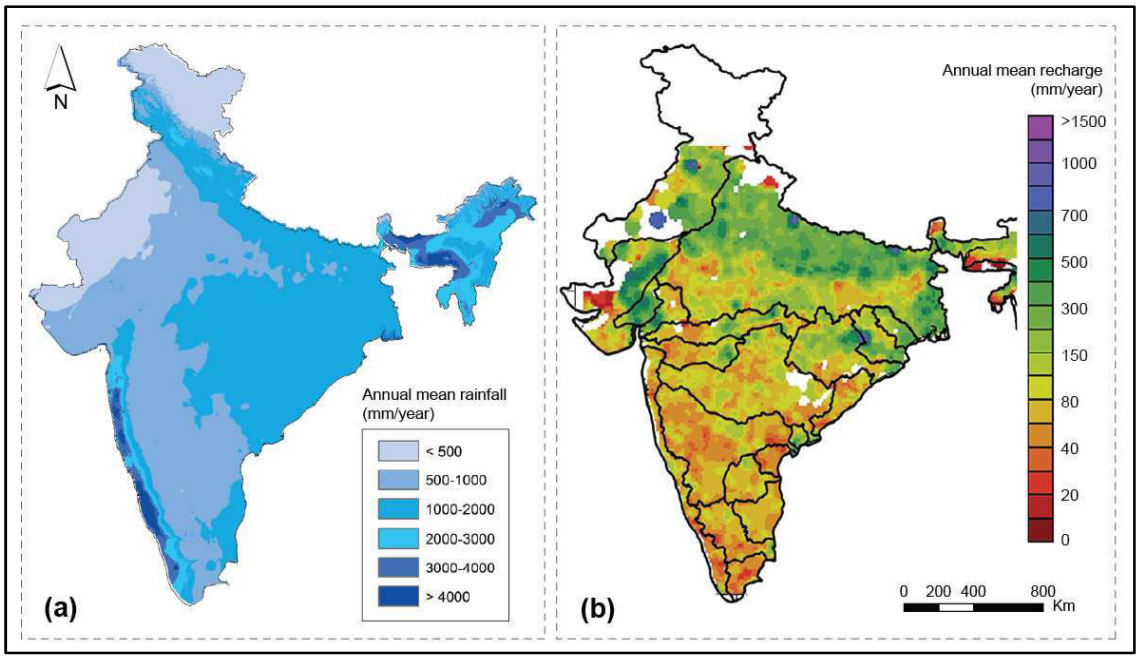

FIGURE 0.3: Annual mean rainfall (from Reddy et al., 2015) (a) and map of mean recharge for the 1996-2015 period derived from water level measurements (from Bhanja et al., 2018); white areas are areas of no data availability (black lines are the main catchment delimitations) (b) in India.

A country is categorized as *water-stressed* if the per-capita water availability is less than 1700 m^3 per year, and as *water-scarce* if it is less than 1000 m^3 per year. According to Anupam & Shinjiro (2013) water availability in India has decreased from 4,782 in 1970 to 1,949 m^3 in 2000, and is expected to further decline to 1,533 m^3 by 2050, although estimates vary quite widely among authors. Gupta & Deshpande (2004), for example, predict water availability to be 1191 m^3 in 2050.

[18] This has been discussed in length in the Introduction to this thesis, so here only a few key figures will be recalled or introduced to provide a broad overview of the water situation in India.

In summary, India supports about $1/5^{th}$ of the world population on $1/50^{th}$ of the world's land with $1/25^{th}$ of the world's water resources. India also has a livestock population of 500 million, which is about $1/5^{th}$ of the world's total livestock population (R. Kumar et al., 2005). With a continuing rapid population growth, improving living standards and decreasing water availability due to overexploitation, most of India is facing severe water scarcity problems.

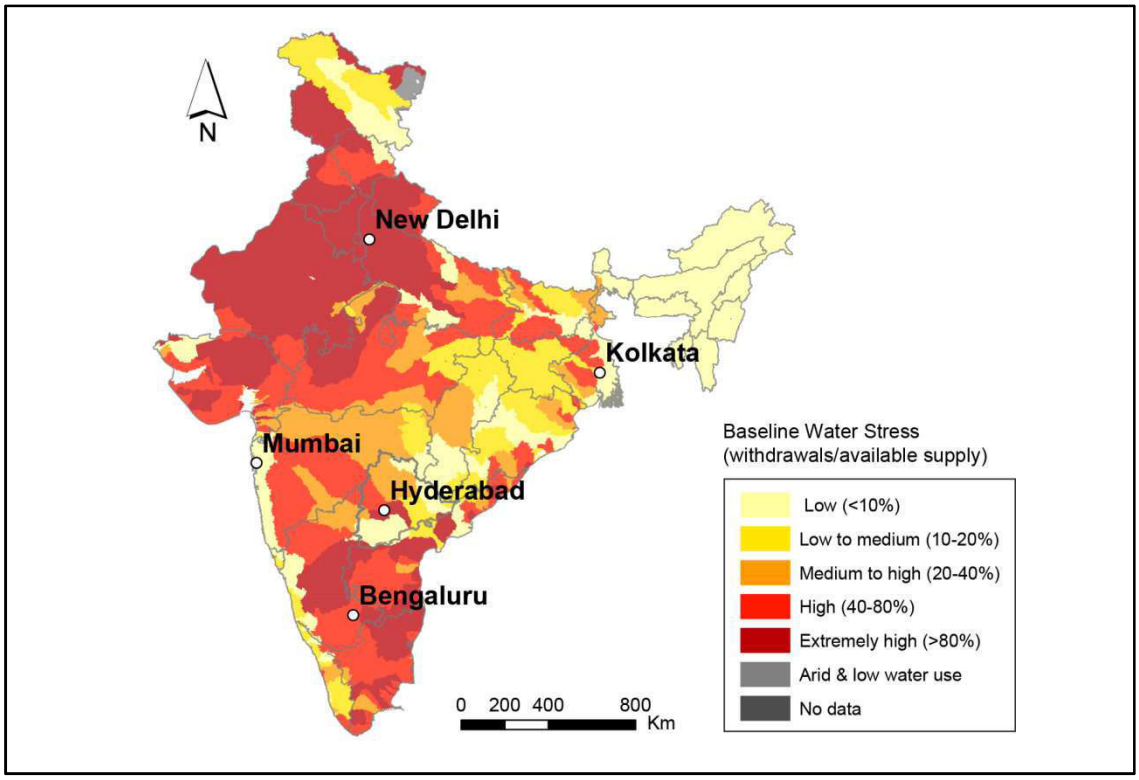

FIGURE 0.4: Baseline water stress in India according to the World Resources Institute (*https://www.indiawatertool.in/*). Water stress is calculated on the basis of the amount of annually available surface water which is used every year.

Another factor key to understanding India's water problems, which we have touched on in the preceding chapters, is that two thirds of India is underlain by crystalline rock (FIGURE 0.5). The implications of relying on crystalline rock aquifers as a perennial water supply have also been discussed in depth: their defining characteristics, such as their significant heterogeneity and overall low receptiveness to recharge, make planning and conservation of water resources in these environments particularly challenging. In this context, two sites have been set up near Hyderabad (the fourth to sixth most populous city in India, depending on the census) in the state of Telangana to observe groundwater dynamics in crystalline rock aquifers (Maréchal et al., 2018). Both sites are underlain by Archean granite and situated in a semi-arid climate, and thus exemplify quite well the flow and recharge dynamics that prevail under these conditions.

The following chapters will present the results of research carried out at these sites to improve our knowledge of crystalline rock recharge at the site and watershed scale. This work comprises two main axes of research:

- The first axis is focused on catchment-scale processes. Data from the Maheshwaram watershed was input into a physically-based model to map and quantify the contributions of natural diffuse recharge to total replenishment of the aquifer. Comparison to more inclusive recharge estimates also allowed us to infer the existence of preferential recharge and map its occurrences. Finally, as the Maheshwaram catchment is highly anthropized, it was also possible to infer the influence of human activities on recharge processes and distribution.
- The second axis focuses on artificial recharge processes at medium scales. Groundwater levels were continuously monitored following the filling-up of the artificial recharge basin on our highly instrumented site. Then, the mechanisms controlling the propagation of the infiltration front throughout the aquifer were deduced using analytical and numerical modeling that accounted for the heterogeneity of the aquifer's structure.

Descriptions of each site (geology, groundwater use and disposition, etc.) will be given at the beginning of Chapter 5, for the Maheshwaram site, and 6 for the Choutuppal site.

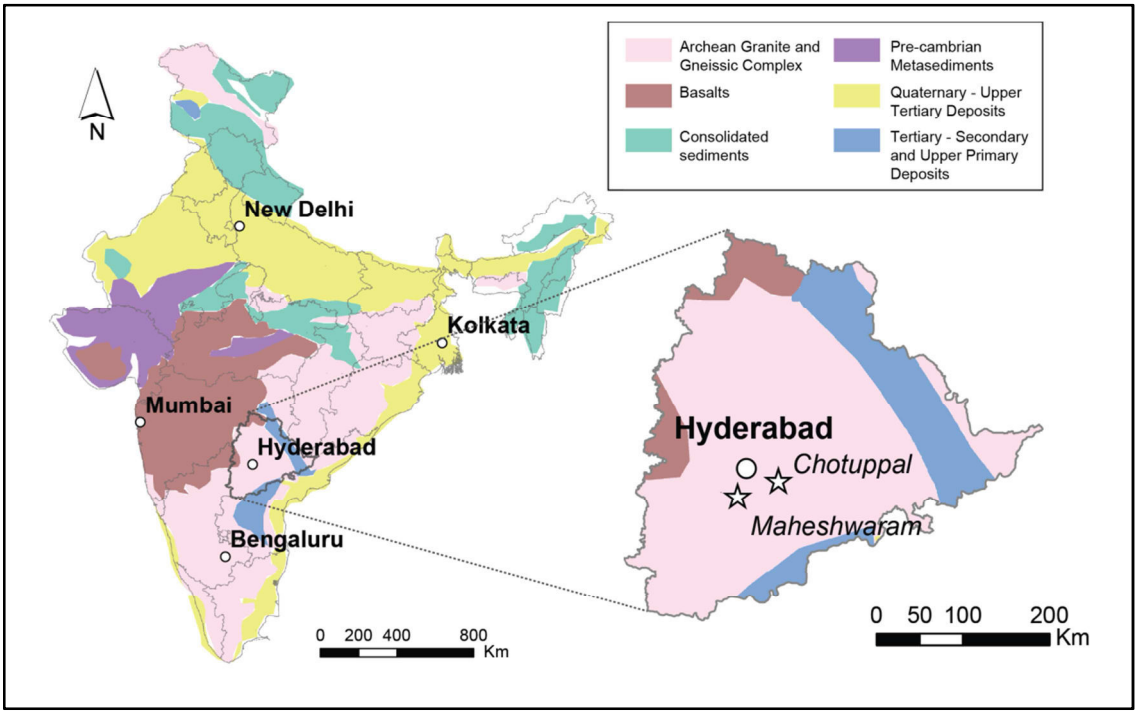

FIGURE 0.5: Simplified geological map of India and the state of Telangana and location of study sites used for this work.

Chapter 5

Natural recharge heterogeneity in weathered fractured crystalline rock

Authors's update: At the time this thesis was written, the work from this chapter had not yet been submitted for publication to a scientific journal. Pending the submission and publication of this work, readers who may find these results to be of interest are advised to contact the author by e-mail if they wish to have an update on the status of this paper or access to the latest graphs.

1. Introduction

In the previous chapters, it has been noted that the factors that govern the intensity and distribution of recharge at the landscape scale in fractured crystalline rock aquifers are poorly understood (Kinzelbach et al., 2002). It is in fact the defining characteristics of this type of media—fractured crystalline rock is highly heterogeneous—that make estimation of fluxes and the hydraulic properties controlling them difficult. Because the primary porosity of these aquifers is almost negligible, their storage capacity depends on the existence of a secondary porosity, which results from the chemical and physical breaking down of the rock matrix, a process which is highly variable both in time and space (Acworth, 1987; Lachassagne et al., 2011; Roques et al., 2016; Wyns et al., 2004). As a result, the hydraulic properties of these aquifers can vary over several orders of magnitude over short distances, both horizontally and vertically (Boisson, Guihéneuf et al., 2015; Chilton & Foster, 1995; Le Borgne et al., 2006; Maréchal et al., 2004).

Essentially, fractured rock is said to be bimodal (Healy & Cook, 2002), because it is made up of fracture networks embedded within a variably porous matrix. Recharge, thus, is a combination of diffuse flow processes—which occur diffusely through loose superficial deposits (i.e. soils and the underlying saprolite)—and preferential flow processes, which take place in fracture networks (if fractures outcrop at the surface) and macropores, when water accumulates in depressions, joints and rivulets (*localized* recharge), and in the beds of surface-water bodies (*indirect* recharge). Each of these processes is controlled by a different set of factors, leading them to present different spatial and temporal patterns. Diffuse recharge depends mostly on the difference between precipitation and evapotranspiration and on the soil hydraulic properties, while localized and indirect recharge are much more dependent on the geologic framework (e.g. slope, drainage density, and runoff generation), the land cover (vegetation type and density) and intense rainfall episodes. For simplicity purposes, the conjunctive term *focused* recharge will be used hereafter to refer to *localized* and *indirect* recharge (in opposition to *diffuse* recharge).

The relative proportions of diffuse to focused recharge are seldom quantified, probably because of the intermittent and concentrated nature that complicates the appraisal of the latter. Nonetheless, among the scarce studies which have addressed this issue, most have found focused recharge to be a significant contributor to total recharge, especially in (semi-)arid environments (de Vries & Simmers, 2002). For example, Sukhija et al. (2003) found preferential flow recharge to be 75% of total recharge in the case of fractured granites, and 33% in semi-consolidated sandstones. In the study by D. V. Reddy et al. (2009), matrix flow recharge was shown to represent only 1-5% of rainfall, while preferential flow, in the valley fills, was actually about 16% (but decreased to 5-5.5% in the plains). In Machiwal & Jha (2015) no quantitative estimate is given, but it is noted that recharge was found to be significantly higher in areas where surface-water bodies were present. Similarly, White & Burbey (2007) found recharge to be mainly controlled by a small-scale thrust fault.

Additionally, as addressed in **Chapter 2 Section 2.3.2**, after water infiltrates, it can be redistributed throughout the unsaturated zone by flowing laterally in the unsaturated zone, mostly through macropores and fracture networks (as *interflow*), and the role of this lateral flow diversion is often overlooked and generally misunderstood (Bockgard & Niemi, 2004; Harte & Winter, 1995).

The aim of this study is to characterize catchment-scale natural recharge processes in weathered crystalline rock. The factors which drive the highly heterogeneous distribution of recharge, as well as the importance of focused recharge processes, were thus investigated. First, diffuse recharge within the Maheshwaram catchment was estimated at a daily time-step and at a 100×100 m resolution using a simple hydraulic model that combines both a water balance technique and unsaturated/saturated flow theory (Dewandel et al., 2008). These simulations provided information on the distribution of diffuse recharge fluxes and their overall intensity, allowing us to infer the effect of rainfall, land use, and soil type on these mechanisms.

Then, diffuse recharge estimates were compared to estimates of *total* recharge previously obtained from water table fluctuations (Mizan, 2019). The difference between diffuse and total recharge was used to deduce the spatial distribution and relative intensity of *focused* recharge processes. This qualitative assessment provided some insight into the dynamics of this little-known process at the landscape scale.

Elaborating recharge models generally requires knowledge on the soil hydraulic properties, daily water inputs and evapotranspiration (estimated from meteorological and crop data). Fortunately, because the Maheshwaram watershed has been studied since the creation of the IFCGR in 1999, there exists a large amount of data (such as the hydraulic properties of the aquifer and its overlying soils, its geology and aquifer structure, for example) and publications on this site. The Maheshwaram catchment thus provides an

exceptional opportunity in terms of catchment-scale hydrogeology analysis, greatly facilitating the elaboration and validation of models and hypotheses for medium to large-scale processes.

2. Study site

2.1. General

The pilot watershed that was used for this study is the Maheshwaram catchment (Latitude: 17°08'41"N; Longitude: 78°26'37"E). It is 53 km^2, and is situated about 40 km south of Hyderabad, the capital of Telangana state (Southern India). The area is characterized by a relatively flat topography 590-670 m above sea level. There are about 6 villages of significant population (≥600 inhabitants), and the largest is the village of Maheshwaram, after which the catchment was named (FIGURE 5.1). The Maheshwaram catchment is representative of crystalline rock semi-arid watersheds in terms of groundwater overexploitation for irrigated agriculture (more than 700 borewells in use, Maréchal et al., 2006), its cropping pattern (predominance of rice paddies), and rural socio-economy (based mainly on traditional agriculture) (Maréchal et al., 2006). This basin is essentially endorheic most of the time (Molle et al., 2010). Along with the Choutuppal Experimental Hydrogeological Park (EHP), this site was developed and instrumented by the French Geological Survey (BRGM) in partnership with the Indian National Geophysical Research Institute (NGRI) and is part of the H+ Observatory network. Most data used in this study can be downloaded from the H+ database (http://hplus.ore.fr/en).

2.2. Geological setting

The Maheshwaram catchment is located in an Archean granitic setting, which represents over 80% of the state of Telangana. The geology of this area is relatively homogeneous, although it may be locally intruded by dolerite and quartz dykes and a few other intrusive rocks (FIGURE 5.1; Dewandel et al., 2006). The catchment is mainly underlain by biotite granite (millimeter to centimeter grain size; slightly metamorphosed and foliated), leucocratic granite (lower biotite content, better resistant to weathering, forms hills and boulders), and biotite granite with decimeter-wide pegmatite and leucogranite veins and meter-wide doleritic dykes in the vicinity of the leucogranite (FIGURE 5.1; Dewandel et al., 2006). Granite in these areas has undergone deep (~50-100 m) in-situ weathering which has led to the formation of two main "layers": the saprolite, i.e. highly decayed rock resulting from intense weathering, and the underlying fractured granite (FIGURE 5.2).

The description of typical weathered crystalline aquifers has been explored in detail in the previous chapters [namely **Chapter 1 Section 2.3**], so it will only be briefly re-

called here. Nevertheless, note that the Maheshwaram weathering profile is slightly different from the "classical" deep weathering profile. Dewandel et al. (2006) inferred this from field observations: it was noted that there was a very low sandy regolith/total saprolite ratio, a low saprolite/fractured layer ratio (meaning both the sandy regolith and saprolite here are less thick than in a classical setting) and that some preserved fractures within the saprolite could be observed. This was interpreted as evidence of a multiphase erosion process. First, an ancient weathering profile formed "classically", then, it was partly eroded down to the fractured layer, and then it was re-weathered. This multiphase erosion process is thus responsible for modifying the overall layer thicknesses and causing higher fracture densities. For more information see Dewandel et al. (2006).

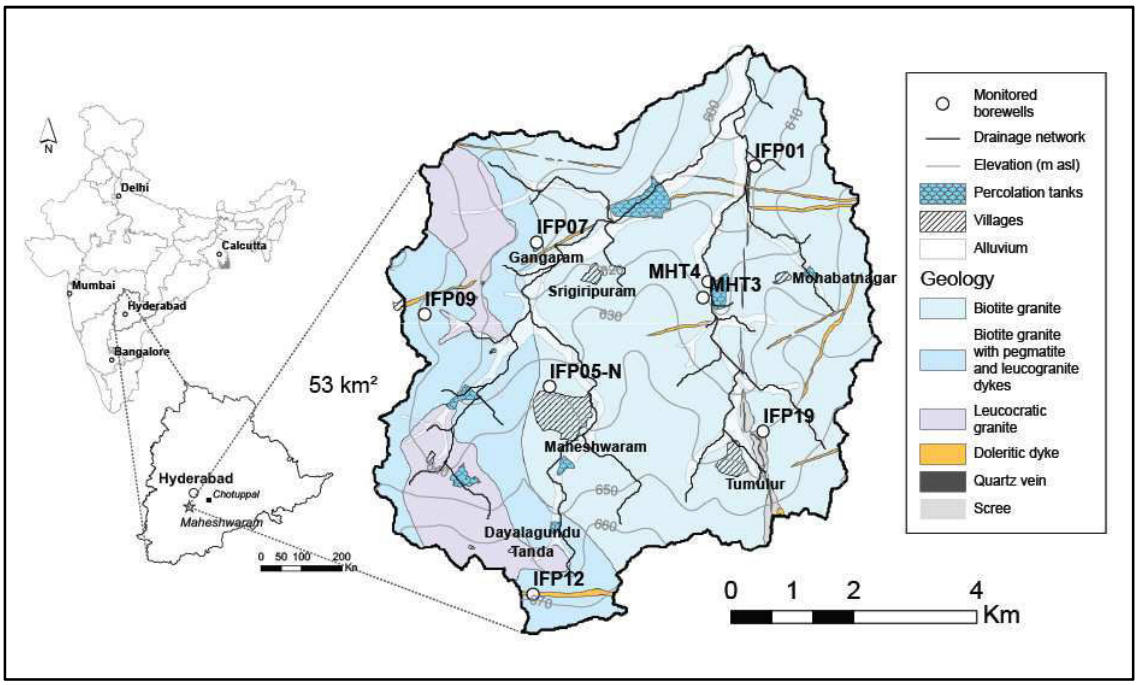

FIGURE 5.1: Relative position of the Maheshwaram catchment within the state of Telangana (India) and geological map of the Maheshwaram catchment, topography is shown as well as the main urban areas, percolation tanks and the drainage network. Flow is intermittent, ephemeral streams form only after intense rainfall episodes. The location of scientific borewells which are currently equipped with a pressure probe to continuously measure water levels is also shown.

From top to bottom, the weathering profile is thus made up of (FIGURE 5.2, Dewandel et al., 2006): a soil layer of varying thickness and composition, 1 to 3 m of saprolite with a sandy texture (sandy regolith), a thick layer (10-15 m) of laminated saprolite with some preserved fractures, 15 to 20 m fractured granite and then the "fresh" bedrock (FIGURE 5.2). The fracture density within the fractured granite decreases with depth, and is highest towards the top. Some researchers, in fact, consider the highly fractured interface between the fractured granite and the overlying saprolite to be a separate "layer", dubbed *saprock*.

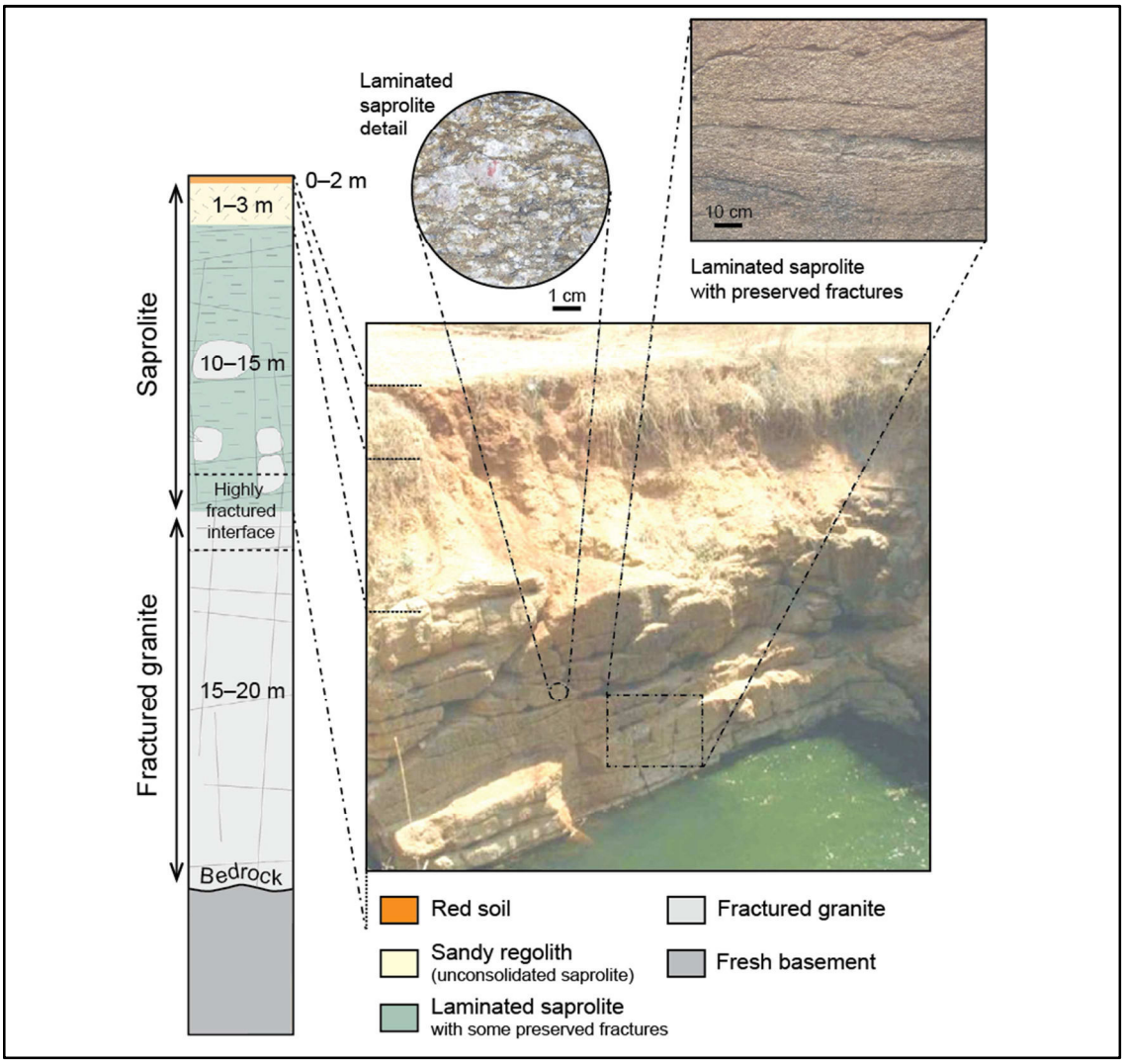

FIGURE 5.2: Weathering profile of Maheshwaram area. Photos are of a dugwell located in the biotite granite, and show the upper part of the weathering profile. (modified from Dewandel et al., 2006).

2.3. Hydrological setting

The climate of this region is semi-arid (annual PET = 1800 mm, aridity index = 0.42; Dewandel et al., 2010) and controlled by the periodicity of monsoons. Mean annual temperature is about 26°C with mean high temperatures of about 32°C which can reach up to 43°C during the dry season (November to May) (FIGURE 5.4). The year is generally divided into two seasons, a dry and a wet season. The dry season, also called *Rabi*, occurs from November to April, and the wet season, also called *Kharif*, occurs from June to October. Mean annual precipitation is about 750 mm, of which more than 90% falls during Kharif season (June to October) (FIGURE 5.3). Partitioning years into Kharif and Rabi seasons and considering them separately is often required because the hydrological conditions (such as groundwater levels, flow, cropping patterns and irrigation) vary significantly from one season to another.

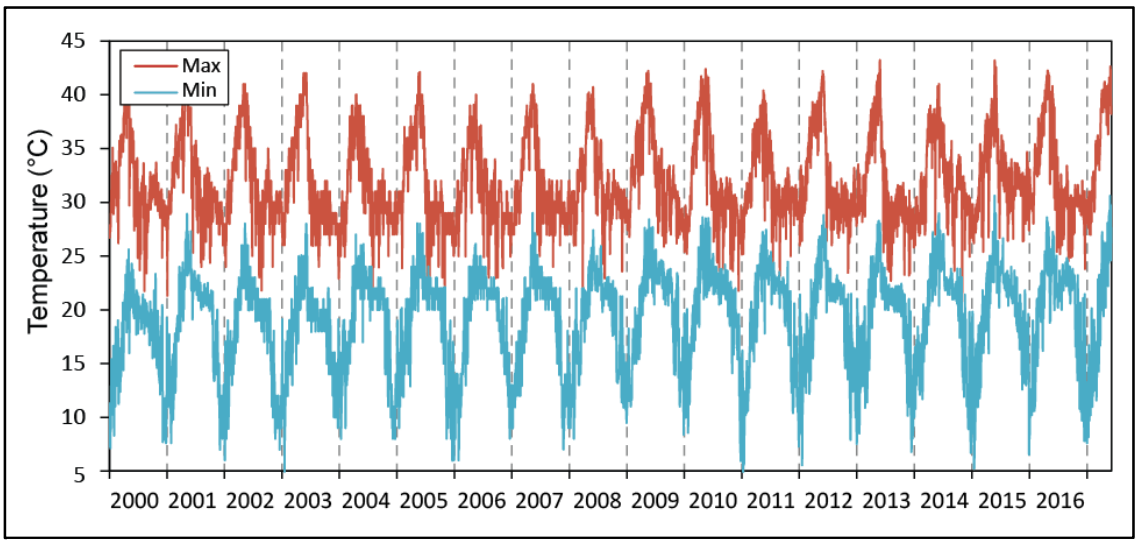

FIGURE 5.4: Maximum and minimum temperatures from 01/01/2000 to 31/05/2017 measured and provided by ICRISAT (80 km north-east of Hyderabad)

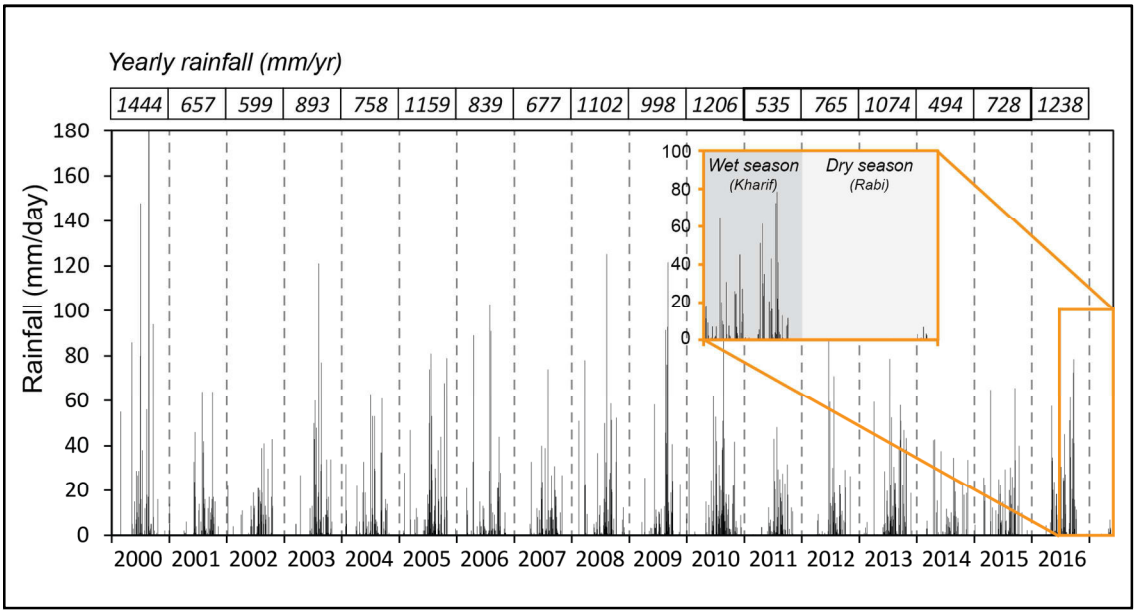

FIGURE 5.3: Daily precipitations (in mm/day) from 01/01/2000 to 31/05/2017 measured and provided by ICRISAT (80 km north-east of Hyderabad) with a zoom on the period 06/2016 - 06/2017 to show the seasonal rainfall distribution. Yearly rainfall estimates are also provided (mm/yr).

There are no perennial streams in this catchment, but after intense rainfall episodes some ephemeral streams may be observed. There are thus no streamflow measurements available on this site. Groundwater and sometimes percolation tanks are the only source of water for irrigation. This has led groundwater to be over-exploited due to the large amount of water pumped by over 650 private tube wells for irrigation of rice, vegetables, flowers, fruit trees and grapes (Maréchal et al., 2006), though rice is by far responsible for most groundwater abstractions (more on this in **Section 2.5**).

The aquifer is unconfined, and twice a year (at the end of the dry and wet season) piezometric maps are drawn from piezometric levels measured in research wells and abandoned private wells (FIGURE 5.5). The mean piezometric level is about 608 m amsl (Dewandel et al., 2010), though there are large seasonal and inter-annual variations (FIGURE 5.6). Piezometric levels approximately follow the topography (FIGURE 5.5, topography is shown in FIGURE 5.1). The highest piezometric levels are located south/south-west of the basin and the lowest levels are north/north-west of the basin; the regional hydraulic gradient is approximately 6-7$\times 10^{-3}$ in the N-S direction (FIGURE 5.5).Water levels are deeply impacted by the effects of pumping, particularly at the end of the dry season (Dewandel et al., 2012) (FIGURE 5.5a). Water levels oscillate around 30 meters below ground surface (at their lowest, almost down to the fresh bedrock) up to almost 10 m bgs (FIGURE 5.6). Most of the time the aquifer consists only of the fissured layer of granite, as piezometric levels generally reside below the saprolite/granite interface. Years of exceptional rainfall (about >1000 mm, though this depends on prior water level conditions), however, have allowed water levels to increase significantly and for this interface to be flooded for a few weeks/months at a time (FIGURE 5.6).

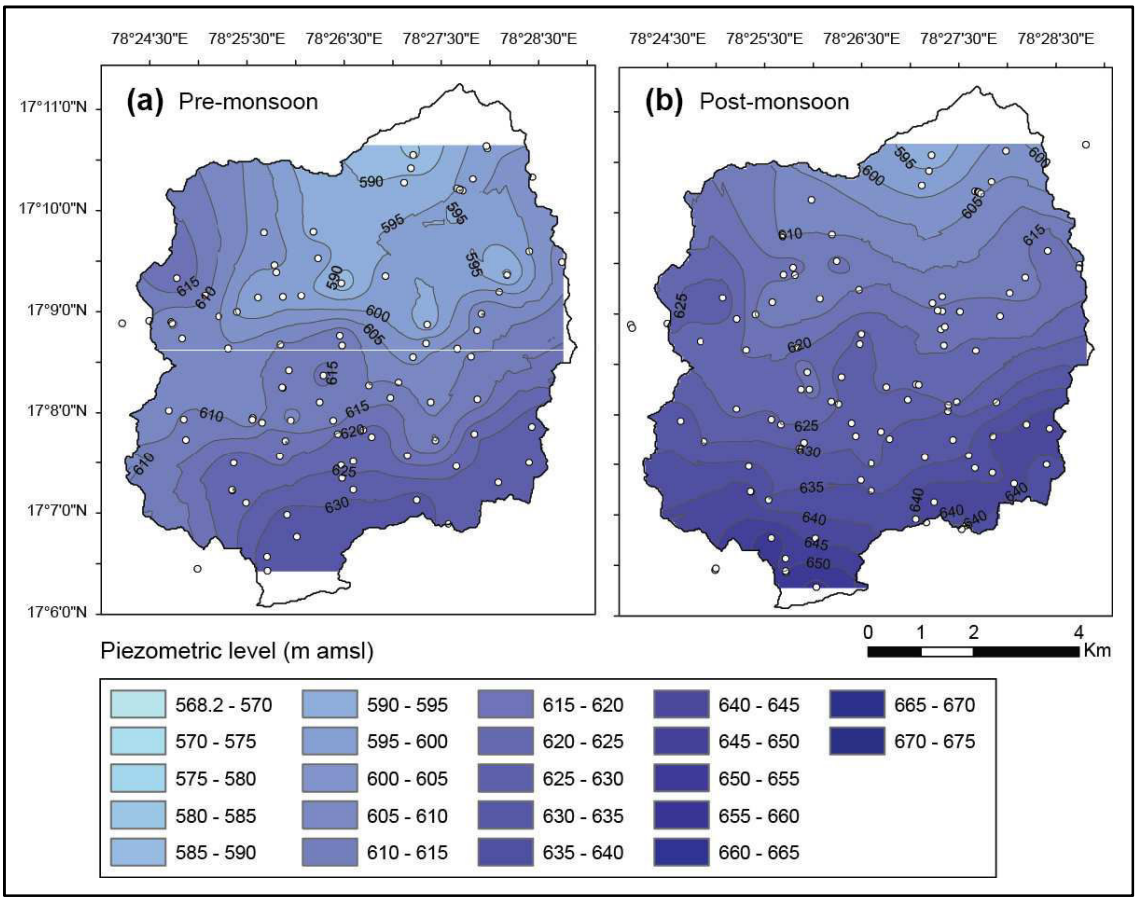

FIGURE 5.5: Seasonal piezometric maps for the year 2013 calculated from water levels in scientific, abandoned and agricultural wells (white points) interpolated using standard kriging (model: spherical; length: 900 m; sill: 42.5).

The aquifer is disconnected from surface water: there are no springs, streams or baseflow (Maréchal et al., 2006), which implies the only outflow is through groundwater pumping and evapotranspiration.

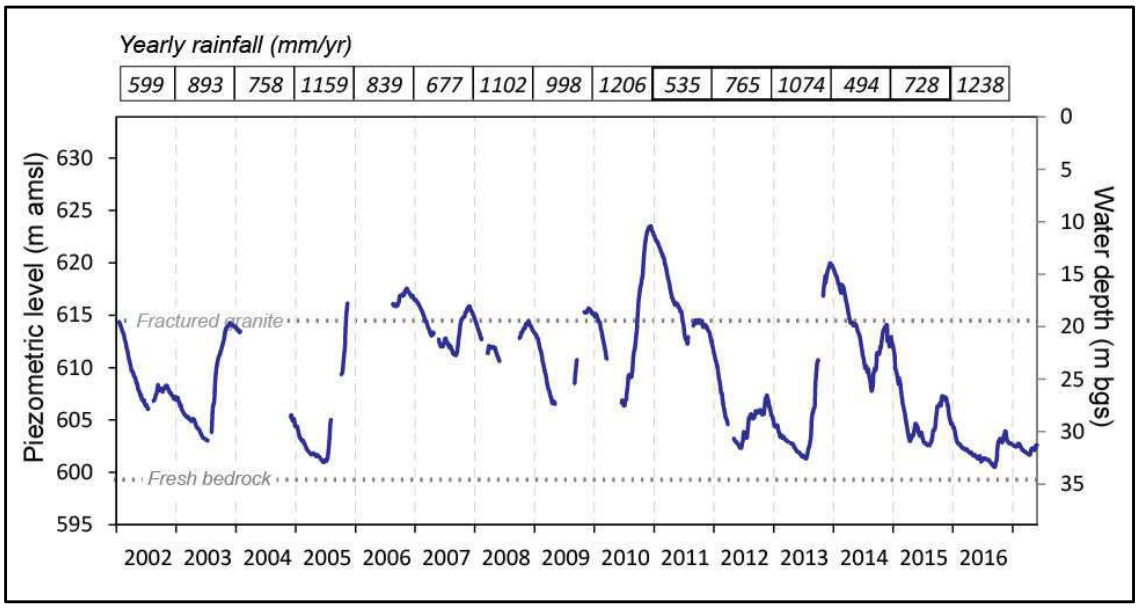

FIGURE 5.6: Piezometric level above mean sea level (left axis) or water depth below ground surface (right axis) at the IFP09 borewell at the Maheshwaram catchment from 17/01/2002 to 31/05/2017 (the full currently available time series); yearly rainfall is shown above to give an idea of the general hydrologic conditions prevailing each year.

2.4. Soil types

When calculating spatialized diffuse recharge, it is necessary to know the surface hydraulic properties, as they will determine whether rainfall infiltrates the soil, exits the system through runoff, or is taken up as evapotranspiration. Surface hydraulic properties depend on the uppermost layer's—most often the soil—characteristics: thickness, degree of saturation, total water retention capacity, permeability, etc. To obtain this data, it is first necessary to know the soil type distribution; literature values may then be used to assess their hydraulic properties. However, if possible, detailed field campaigns and experiments should provide more detailed estimates of these hydraulic properties and increase the accuracy of recharge estimates.

2.4.1. Typical soil profile

Soils typically form at the top of a weathering profile through a process known as *pedogenesis*. Pedogenesis is made up of two simultaneous processes, biological—through the accumulation and breaking down of organic matter—and physical—through release, migration and accumulation of particles and molecules (Duchaufour, 1982).

A typical soil profile is made up of the following layers (also called horizons, not to be mistaken with the soil-hydrologic horizons from **Chapter 2 Section 2.4.1.2.**), from top to bottom (FIGURE 5.7) (Duchaufour, 1982):

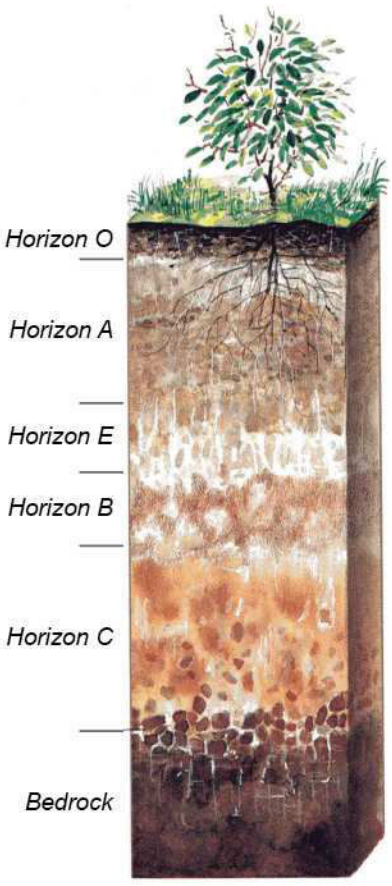

FIGURE 5.7: Typical soil horizons (modified from unknown source).

(1) **Horizon O** is an organic surface layer composed of plant residues ranging from undecomposed to strongly *humified* (i.e. converted into soil humus).

(2) **Horizon A** is the surface soil layer; it is the layer where the soil minerals have mixed with the organic matter and where soil life is most abundant. Generally the structure and chemical properties of this layer have been modified by biological processes or human activity.

(3) **Horizon E**, the eluvation horizon, is where significant leaching of clays towards the B horizon has occurred. This leads to a highly sandy texture.

(4) **Horizon B**. This is the illuviation horizon, accumulating substances that move down from the upper layers. There might also be formation of secondary minerals such as complex clays.

(5) **Horizon C**, the substratum, is a layer of non-indurated but poorly weathered rock. It is progressively harder towards the bottom, eventually merging with the bedrock. From a hydrological perspective, it is a transition zone between the soil and the rock, and is mostly unaffected by pedogenesis. In this particular case, horizon C corresponds to the saprolite (FIGURE 5.2).

Horizons O through B make up the soil profile. At the Maheshwaram catchment, specifically, the upper soil layers have significantly been eroded, and as such the soil is actually quite shallow, composed only of horizons E and B (de Condappa, 2005).

Depending on the relative thickness of each layer and their characteristics (e.g. particle soil distribution, color, pH…), soils will be classified into several taxonomic groups (i.e. *taxa*). The USDA taxonomy (USDA, 1999) is hierarchized as follows (from highest to lowest): soil orders>soil suborders>great groups>subgroups. For relevance purposes, the following description of soils at the Maheshwaram catchment will only describe the different soil orders present.

2.4.2. Soils at the Maheshwaram catchment

Information on soil type, distribution and properties at the Maheshwaram catchment comes from the doctoral thesis by de Condappa (2005). In this thesis, the aim was to determine flows in the unsaturated zone at the Maheshwaram catchment, and work carried out throughout comprises detailed and extensive field investigations on the identification of the relevant soil units and their hydraulic properties. A detailed soil map was drawn (FIGURE 5.9) by combining field campaigns and satellite imagery to complete and improve a pre-existing soil map whose source could not be determined. Then, 44 representative sites were selected throughout the catchment, and observation trenches were dug at 37 of these sites (FIGURE 5.8). Further, 42 already-present dugwells provided additional observations. 178 samples were collected overall at these sites and at different depths in order to perform particle size analysis (de Condappa, 2005).

In total, three soil orders were identified at the Maheshwaram catchment (de Condappa, 2005):

- **Alfisols**. Alfisols are characterized by the presence of E and B horizons. In terms of particle size distributions, the amount of clay present is low at the surface and quickly increases within the first centimeters. Among the Alfisols present on the site, two great groups were distinguished, *Haplustalfs* (later renamed **Alfisols 2**) and *Rhodustalfs* (later renamed **Alfisols 1**). *Rhodustalfs* have a higher oxidized iron contents, and are thus much redder. Alfisols are mostly present in the catchment's plains and are strongly linked to the underlying geology.
- **Entisols**. Entisols do not have a characterizing horizon, are very poorly developed, and have no apparent link to the underlying geology. They result from the erosion and deposition of other materials, they are alluvial soils. Greyish in color, they are often humid and poorly drained. They usually form in lowlands and areas of flow accumulation (i.e. drainage networks). Most soils observed belonged to the great group of *Ustorthents*.
- **Inceptisols**. These are poorly developed soils as well, and soil horizons are very thin, especially horizon E. There are slightly more developed than Entisols, but less than Alfisols. These soils usually form on hills and summits. Most soils identified belonged to the great group of *Ustochrept* soils.

An additional soil category was added, **Tank**, which corresponds to the soils formed under the percolation tank areas. These areas were considered to be separate units because they did not fit the description of any of the above soil categories (de Condappa, 2005).

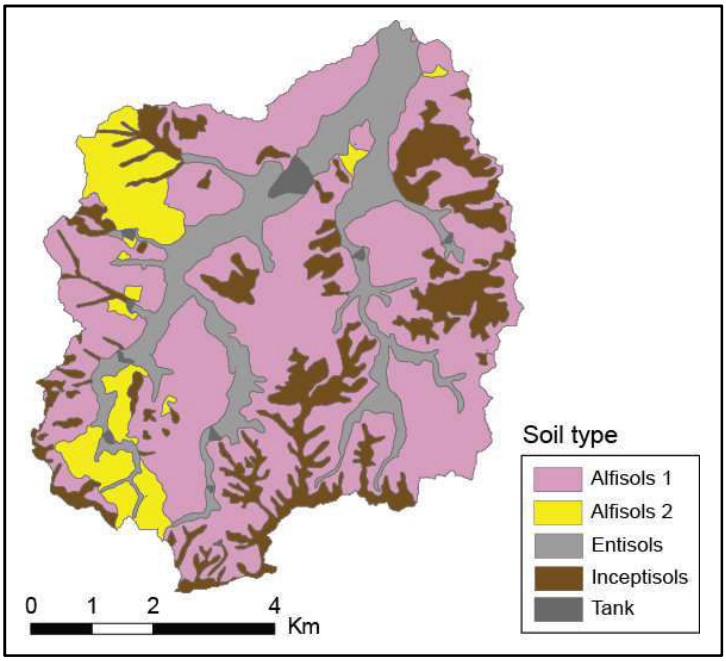

FIGURE 5.9: Map of soil type distribution at the Maheshwaram catchment (modified from de Condappa, 2005).

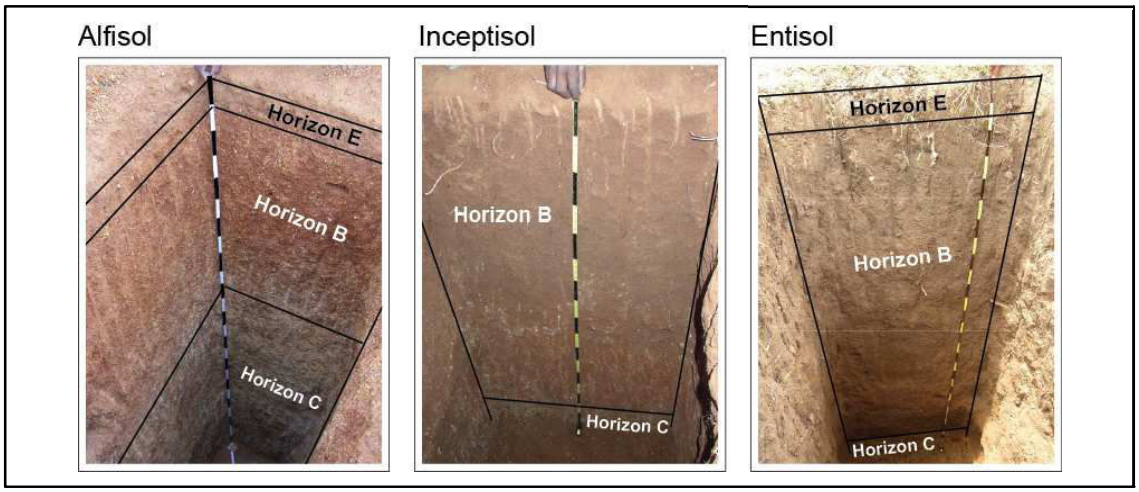

FIGURE 5.8: Photos of observation trenches dug during field campaigns to assess the soil hydraulic properties. The photos feature the different soil orders observed during the investigation carried out in de Condappa, (2005) (modified from de Condappa, 2005). Each band on the tape is 10 cm long.

2.5. Land use

When calculating spatialized diffuse recharge, knowledge on land use distribution is necessary to determine (i) irrigation inputs to the soil, if any, (ii) the amount of water evaporated depending on cropping type and stage, and (iii) irrigation return flow, if any, i.e. the quantity of water returned from the cultivated area originating from groundwater abstraction (Dewandel et al., 2008).

The Maheshwaram catchment is mostly rural with a few small settlements. Most of the land is bare or uncultivated, instead giving place to scattered scrub vegetation, such as grasses and small shrubs. A couple of wooded areas are also dispersed throughout the

catchment, mostly made up of eucalyptus trees and some scrub forest (FIGURE 5.11a). There is also a variety of crops spread out throughout the basin. The surfaces of these irrigated areas are, on average: about 210 ha of rice paddies in the dry season (about 50% more during the rainy season), about 15 ha of vegetables (tomatoes, eggplants, okras, chili, etc.), 20 ha of flowers, 47 ha of fruit trees (mangoes, bitter melon) and 55 ha of grapes (Dewandel et al., 2008, 2010) (FIGURE 5.11a).

Due to the absence of perennial surface water, these crops are irrigated using groundwater. Electricity for pumping is free in these regions[19], so groundwater is very low cost, which has severely aggravated groundwater overexploitation. Mean annual groundwater abstraction at the catchment scale has been estimated at around 10 Mm^3 (174 mm over 53 km^2) (Dewandel et al., 2010). These pumping rates are sustained by over 700 borewells spread out throughout the basin (Maréchal et al., 2006). Rice is the dominant crop both in terms of surface area and in terms of pumping: according to Dewandel et al. (2008), rice accounts for about 87% of annual groundwater abstractions in this area, whereas vegetables and flowers only use about 1–5% of groundwater abstractions. Each parcel used for rice cultivation requires 1500–2000 mm of water, and usually a few centimeters of free water in the field. Rice is cultivated twice a year in certain areas, during the rainy season (Kharif, water for irrigation is then a combination of rainfall and pumping) and during the dry season (Rabi, water for irrigation is solely groundwater) (Dewandel et al., 2008).

2.5.1. Base map

The land use map used to estimate irrigation inputs is also from de Condappa (2005). This map was based on the National Remote Sensing Agency (NRSA) map—which used remote sensing techniques to approximate land use patterns—and then improved with more detailed satellite images and on-field verification (FIGURE 5.11a). Special attention was paid to accurately evaluating paddy surface area, as they consume by far the most groundwater abstracted in the area.

Unfortunately in the monsoon season (Kharif) the region is often covered by a relatively dense cloud cover, which precludes the acquisition of satellite pictures most of the season. For this reason, only a map of dry season (Rabi) land-use was initially made. Nonetheless, it is known that paddy surfaces are increased in Kharif season: farmers size their paddy fields according to their borewell yields (Dewandel et al., 2008; Maréchal et al., 2006). In this area, specifically, it was noted that during Kharif paddy fields were

[19] Free electricity to farmers is part of a subsidized free electricity scheme provided by the government of Telangana. Up until Dec 31st 2017 free electricity was provided 9 hours a day, but since Jan 1st 2018 Telangana became the first state in the country offering free power to farmers 24 hours a day (Apparasu, 2018).

increased to 1.5 times their size in Rabi. As such, for the following, paddy surfaces were artificially incremented to 1.5 times their size in Kharif using the Buffer tool on ArcGIS.

2.5.2. On the evolution of land use patterns and the contributions of remote sensing

Land use evolves over time depending on market demand and on the availability of groundwater. For example, after a few years of consecutive drought, wells across the catchment may dry up or be affected by strong decreases in yield, leading to a decrease in the amount of irrigated area or a change in cropping patterns; the opposite is also true, years of intense rainfall may cause a significant rise in groundwater levels which may lead to an expansion of irrigated agriculture. Other feedback loops may exist; it is well known groundwater availability has an effect on land use, but the effects of land use on groundwater availability are not always well understood.

The variability of land use from one year to another can be observed in satellite images, for example those made available through the Landsat program. Paddy fields are particularly visible in these images—note the sharp contrast between the peak-season green and the bare ground surrounding it. We can, for example, compare the area occupied by paddy fields between the years 2014, when water levels were relatively high, and 2016, when water levels were relatively low (refer to the piezometric level time-series in FIGURE 5.6) (FIGURE 5.10). Paddy field areas decrease in proportion to the available water (areas circled in FIGURE 5.10), which affects the total amount of irrigated groundwater and the hydrological behavior of these areas.

Satellite imagery has in fact widely been used to establish land use maps in data-scarce areas or in general to monitor spatiotemporal land use variations. For example, we may cite recent work carried out at the Kudaliar catchment also in the state of Telangana (Ferrant et al., 2017). This study used Sentinel-1 (launched in 2014) and Sentinel-2 (launched in 2015) observations combined with a machine learning algorithm and on-field verification to produce detailed maps of flooded rice areas and surface water bodies.

Unfortunately, accurately estimating land use maps from satellite data lies beyond the scope of this thesis, first because of the paucity of clear images at the necessary periods (i.e. peak cultivation time both in the dry and wet seasons), and because of technical and time considerations. Nevertheless, the use of satellite imagery remains a point of potential improvement and development for future research in data-scarce areas such as this one and in general. For the following, it was assumed inter-annual changes in land use, specifically paddy size and approximate location, remained relatively constant.

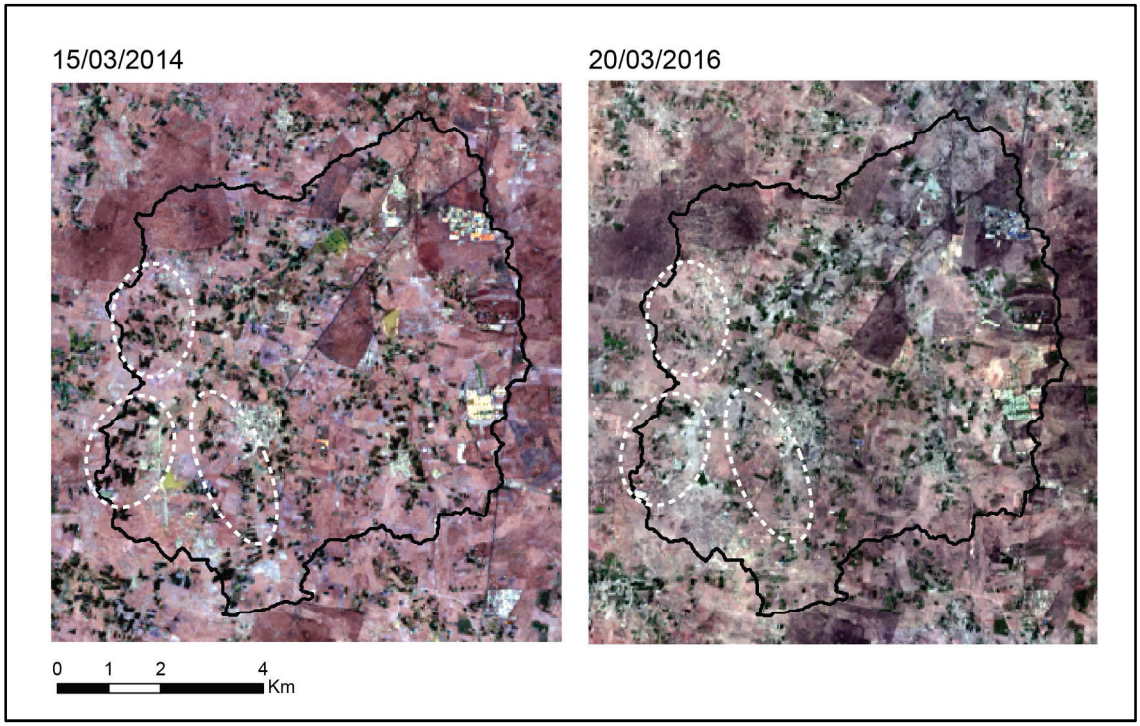

FIGURE 5.10: Satellite data acquired by the American Earth observation satellite Landsat 8 and downloaded freely via Google Earth Engine (https://earthengine.google.com/). Acquisition dates correspond to Rabi season prior to harvest, on the left during a year when water levels were high (2014) and on the right a year when they were very low (2016). Areas of significant changes in paddy field extent were circled.

2.5.3. Simplified map

To apply the hydraulic model described in the following sections, FIGURE 5.11a was simplified into 6 different land uses (FIGURE 5.11b). Categories which are assumed to be hydrologically similar (e.g. boulder zones, bare ground, fallow, land with scrub) were regrouped into single categories. Paddy fields, as stated above, are responsible for over 87% of groundwater uses, so they were kept as a separate category. This was done in view of the available data, and because the differences in daily evapotranspiration and irrigation (if any) are assumed to be negligible.

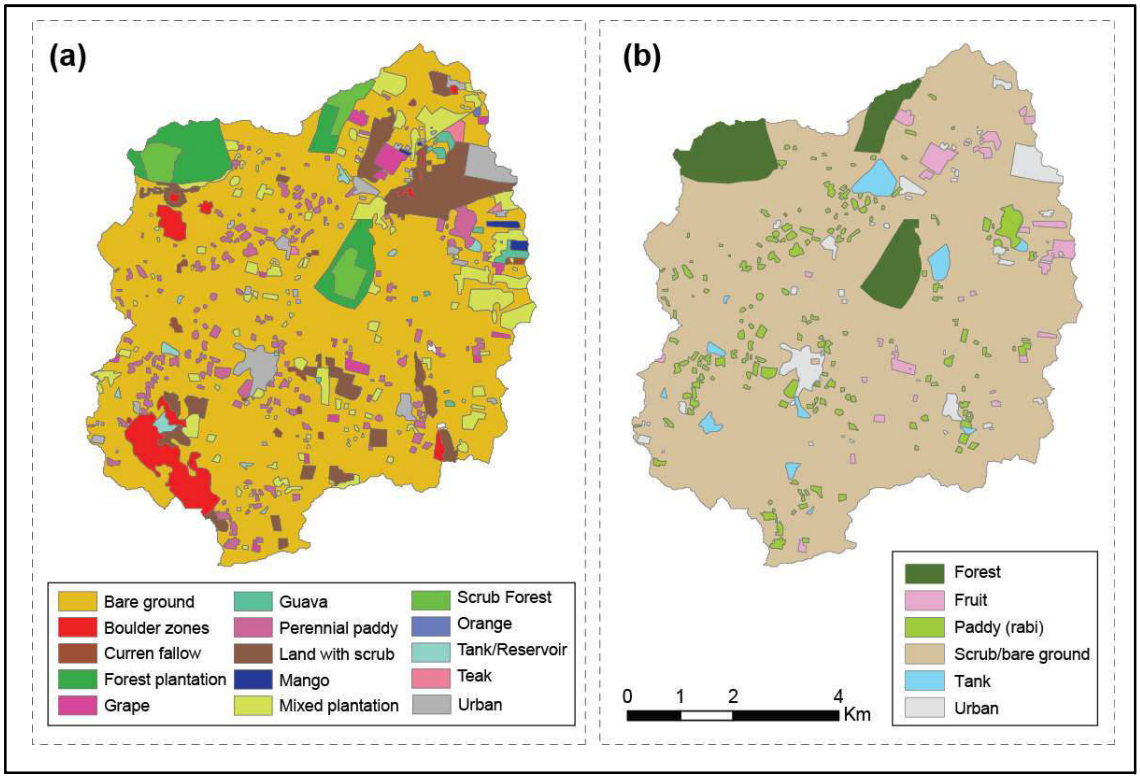

FIGURE 5.11: Land use map for the Rabi period (February 2003) initially from the National Remote Sensing Agency (NRSA) but modified by de Condappa (2005) (a) and simplified land use distribution for use in the hydraulic model used to quantify recharge (b).

2.6. Reference recharge

The distribution of *total* recharge at the Maheshwaram catchment and its inter-annual variations have been previously estimated in the work by Mizan (2019) (FIGURE 5.12). In their doctoral thesis, still in writing, the DWTF method [explained in **Chapter 3 Section 2.3.1.3**] was used to obtain 3D maps of specific yield (S_y) and spatialized recharge estimates at a 685×685 m grid scale. In view of the available data, they focused on the period from 2011 to 2015.

2.6.1. Recharge distribution

These maps (FIGURE 5.12) show the magnitude and relative distribution of regional recharge. The intensity of recharge varies significantly from year to year, mostly depending on rainfall. There is, however, a relative spatial recharge pattern which appears to recur from year to year. For instance, the eastern sector of the catchment is generally more prone to recharge. There also appears to be two parallel 'axes' of preferential recharge both oriented NE-SW. They are separated by an area of low recharge, and the outskirts of the basin are low recharge areas as well.

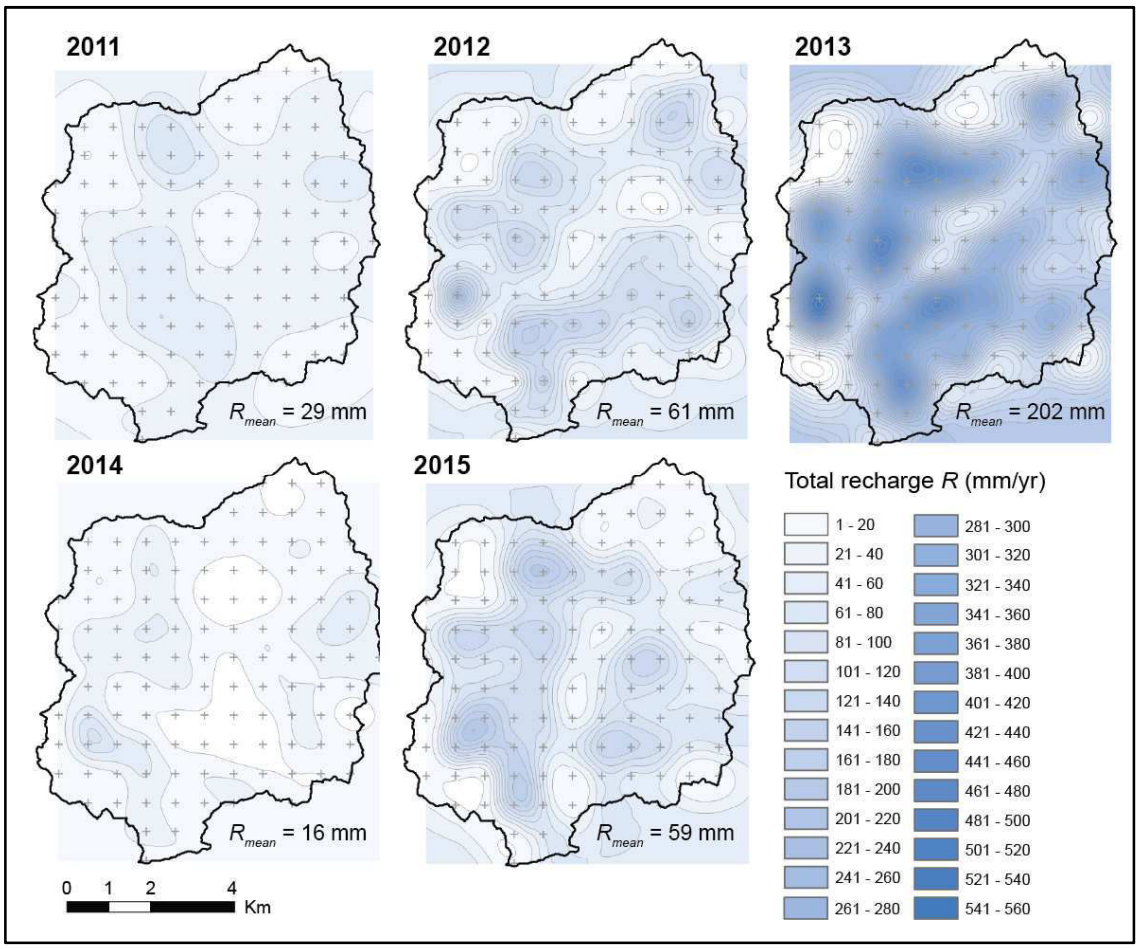

FIGURE 5.12: Reference recharge values computed for the Maheshwaram catchment using the Double Water Table Fluctuation method for 2011 to 2015. Values are calculated at a resolution of 685×685 m for each hydrological year cell values were then interpolated using standard kriging techniques (modified from Mizan, 2019).

Mizan (2019) attempted to identify the factors controlling recharge distribution, and to do so performed Pearson correlation analyses between certain variables and recharge. It was found that the items which were most strongly correlated to recharge are storativity (r = 0.54), pumping (r = 0.57) and storage[20] (r = 0.763), though this may be debated as they are variables which were used to estimate recharge, thus not independent. Note also that some of these variables are interrelated (e.g. pumping and soil type, slope and soil type). Soil typology is the second most correlated variable, although correlation coefficients are overall not very significant (<0.5). Modeling and identifying the factors which control recharge rates and distribution was nonetheless beyond the scope of their study, and will instead be explored in this chapter.

[20] Storage here is referred to as the product of specific yield (more or less equal to the storativity) and the saturated thickness of the aquifer.

2.6.2. Recharge/rainfall relationship

Total recharge, computed by Mizan (2019), was found to be well correlated ($R^2 = 0.83$) to total rainfall, and in fact fits well with past estimates of recharge computed for this catchment (Dewandel et al., 2010) (FIGURE 5.13). Points are relatively scattered, but show a clear and linear increasing trend where stronger rainfall leads to stronger recharge. According to this relationship, recharge is null for rainfall below 510 mm approximately; above this value, recharge increases at a linear rate. A simple linear regression shows this relationship follows the equation $R = 0.35 \times P - 179$ (R being total recharge and P precipitation). Overall, recharge in this area has been noted to vary between 14 mm for 758 mm of rainfall (in 2004) up to 260 mm of recharge for 1160 mm of rainfall (in 2005) (FIGURE 5.13).

The inferred relationship between rainfall and recharge featured in FIGURE 5.13 is higher than diffuse recharge estimates from other studies carried out in granitic areas of South India (Rangarajan & Athavale, 2000), which use applied tritium—not to be confused with environmental tritium—as a recharge tracer [see **Chapter 3 Section 2.1.5**] (gray trend in FIGURE 5.13). Dewandel et al. (2010) attribute this difference to the existence of focused recharge which is not measured by the tritium method. Note also that methods based on the unsaturated zone often provide estimates of *potential* recharge (as opposed to *actual* recharge), as it is possible that not all of the water moving through the unsaturated zone will recharge the aquifer (Healy & Scanlon, 2010).

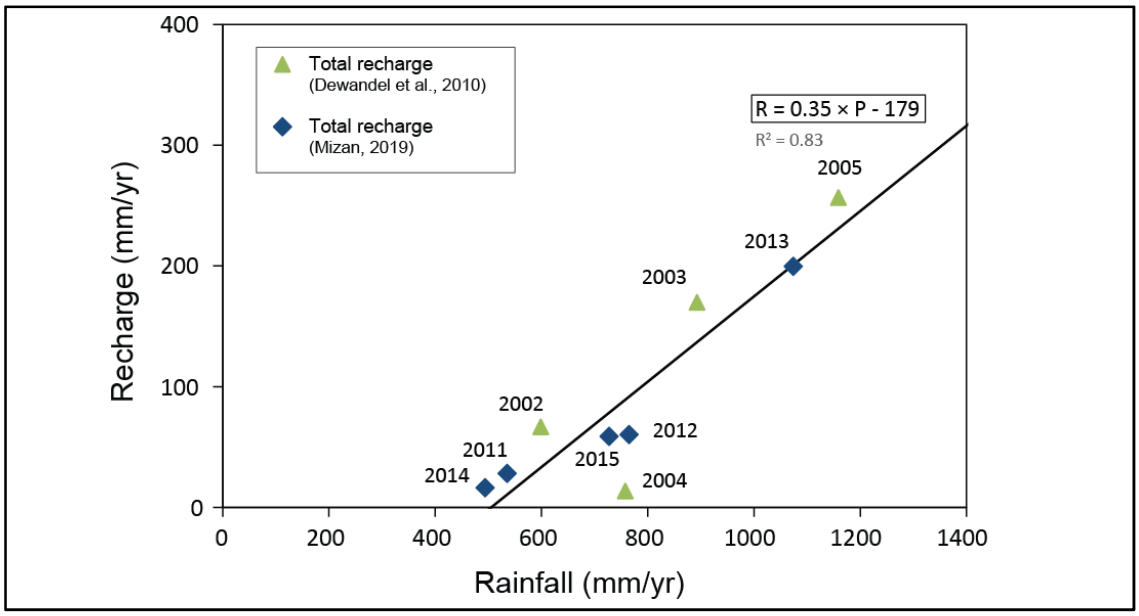

FIGURE 5.13: Annual mean catchment recharge estimated using the DWTF method and the theoretical linear rainfall-recharge relationship obtained performing a simple linear regression; the rainfall-direct recharge relationship obtained experimentally by Rangarajan & Athavale (2000) is also shown (modified from Mizan, 2019). Note that R^2 is the determination coefficient, not to be confused with R which refers to recharge.

It was unfortunately not possible to estimate total recharge for each year since the creation of this observatory in 1999: due to technical and administrative reasons, water levels were not always continuously measured at enough locations to provide the necessary amount of data to estimate total recharge from water level variations. This is why only the period from 2011 to 2015 was analyzed, and why there is a gap between the estimates by Dewandel et al. (2010) (2002-2005) and estimates by Mizan (2019) (2011-2015).

3. Methodology

In brief, the model used to estimate recharge uses meteorological data and the media's hydraulic properties to calculate infiltration and runoff (which is the precipitation surplus) by means of a simple 1D recharge model that combines a water balance technique with unsaturated/saturated flow equations (FIGURE 5.14). This model is largely based on the model by Dewandel et al. (2008) which is described in full in their publication and in the following sections.

As we have touched on in the previous sections, estimating recharge from infiltration requires (i) knowledge on overall water inputs to each grid cell and (ii) knowledge on the hydraulic properties of the soil which will determine the fate of these inputs. These quantities can be estimated if the land use, meteorological conditions and soil type properties are known. FIGURE 5.14 shows the overall structure of the model and cites the sources from which the necessary parameters and fluxes were estimated.

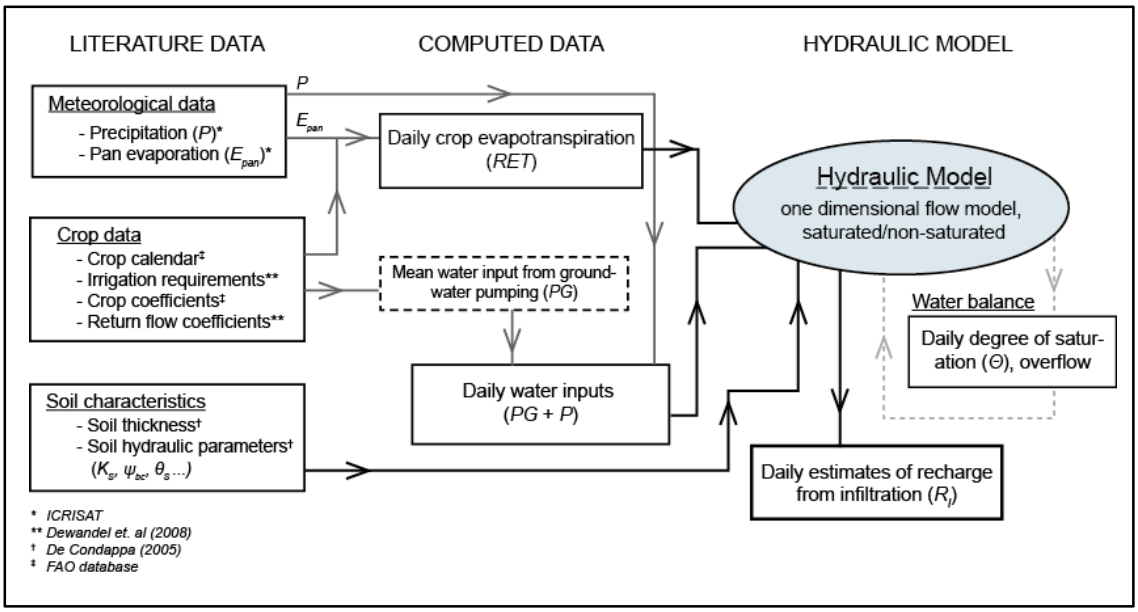

FIGURE 5.14: Method to compute recharge from infiltration (modified from Dewandel et al., 2008).

The model was run at a daily time-step and summed up over each year when necessary. The model was run using meteorological data (P and E_{pan}) from 01/01/1995 to 12/31/2015. The first 5 years were run to initialize the model, and going forward only the period 2000 to 2015 was analyzed. This allowed us to obtain estimates on diffuse recharge at a daily time-step for the period from 01/01/2000 to 12/31/2015. Comparison to the *total* recharge estimates was only possible for the period from 2011 to 2015 as this is the period for which we have *total* recharge estimates after Mizan (2019) and thus is the only period where modelled diffuse recharge could be compared to total recharge to infer possible effects of focused recharge.

3.1. Hydraulic model

3.1.1. Water balance at the field scale

The water balance at the parcel scale is calculated daily and is based on the daily variations of the water stock present in the field. The different components of the water balance are illustrated in FIGURE 5.15. This water balance can be expressed as:

$$PG + P = AET + q_{out} + D + \Delta w \quad (5.1)$$

where PG is pumping for irrigation, P is precipitation, AET is actual evapotranspiration, q_{out} is the water draining downwards toward the groundwater table, D is surface and subsurface runoff, and Δw is the variation of water stock, i.e. the changes in water depth above the parcel or the change in water storage in the soil profile. Lateral seepage is assumed to be negligible, as flow in the soil is dominated by a vertical component (Dewandel et al., 2008). All terms are in mm.day^{-1}.

In reality, a part of the water draining downwards into the aquifer is actually *irrigation return flow* (RF). RF can be defined as a portion of groundwater pumping according to the return flow coefficient (C_f) with $C_f = RF/PG$ ($0 \leq C_f \leq 1$). We then have:

$$q_{out} = RF + R_I = C_f \times PG + R_I \quad (5.2)$$

where R_I is natural diffuse recharge. By rearranging Eq. (5.2) we then obtain $R_I = q_{out} - C_f \times PG = PG \times (\frac{q_{out}}{PG} - C_f)$. If pumping is null (i.e. for scrub, forest, etc.), then $RF = 0$ and $R_I = q_{out}$. Note that RF is assumed to be an entirely diffuse process.

The aim of the study by Dewandel et al. (2008) was to obtain C_f at the parcel scale for different crop types. Their estimates allow us to expand the use of this model to estimate recharge from infiltration across the entire catchment as all other terms of Eq. (5.1) are known or can easily be estimated. C_f for paddy fields was found to vary between 0.48 in Rabi season to 0.51 in Kharif season. For all other land uses considered here, C_f is considered to be equal to 0, either because the land is not irrigated, or it is

done using drip-irrigation which is efficient and creates no irrigation return flow (Dewandel et al., 2008).

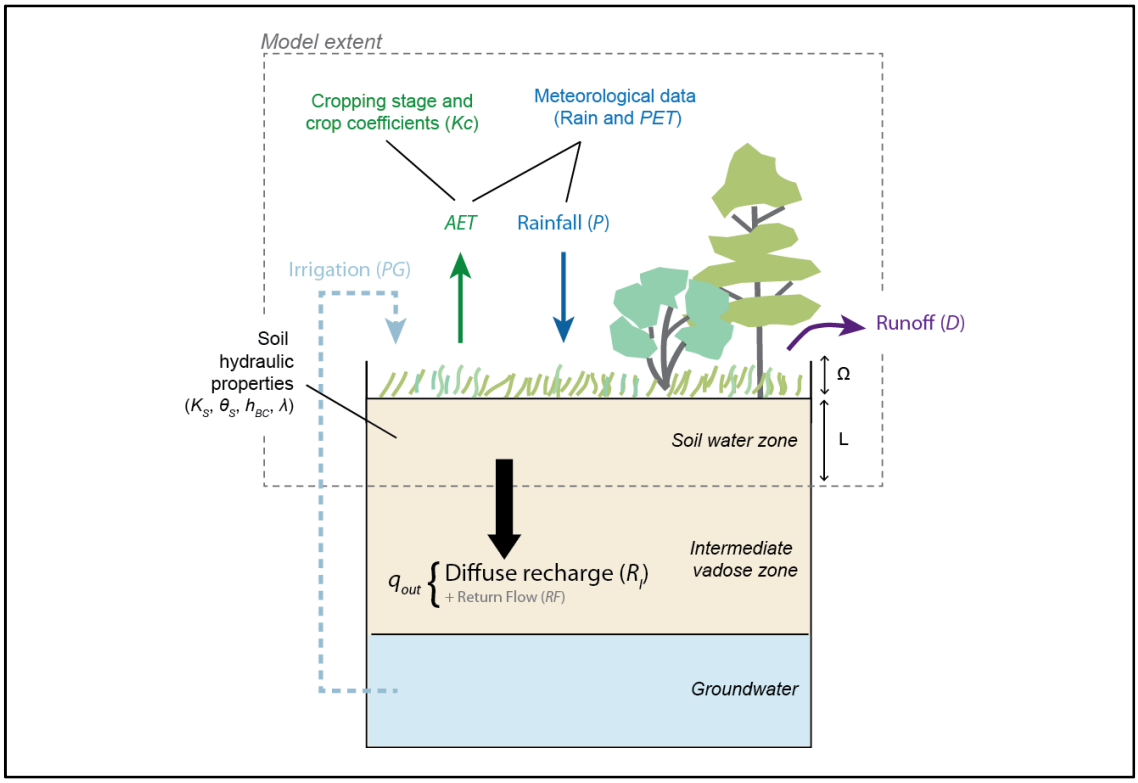

FIGURE 5.15: Schematic water balance at the parcel scale (concept from Dewandel et al., 2008, format from Alley et al., 1999). Ω is the critical water depth above which runoff is generated and L is the soil thickness.

3.1.2. Components of the water balance

3.1.2.1. Meteorological data (P and PET)

Rainfall and pan evaporation (E_{pan}) data were provided by ICRISAT, situated 80 km NE of Hyderabad. Evaporation was measured using a pan evaporimeter at a daily time-step. Rainfall estimates are inputted as-is into the model, E_{pan} data was used to calculate PET with respect to the FAO method (Allen et al., 1998; FIGURE 5.14), where:

$$PET = K_C \times (K_P \times E_{pan}) \tag{5.3}$$

where K_C (dimensionless) is the crop coefficient and K_P (also dimensionless) is a regional coefficient, equal to 0.9 in the studied area (Dewandel et al., 2008). K_C depends on the cropping stage and type (FIGURE 5.16). Unmanaged or tree crops (i.e. fruit) are assumed to have a constant K_C, while rice and vegetables fluctuate in time depending on the cropping stage (land preparation, planting, growing, harvesting). The highest K_C values are for peak cultivation rice paddies and eucalyptus forests ($K_C = 1.2$) and the lowest for scrub vegetation ($K_C = 0.7$) (FIGURE 5.16). AET is the final amount of water which *actually* evaporated in regards to the available water ($0 \leq AET \leq PET$).

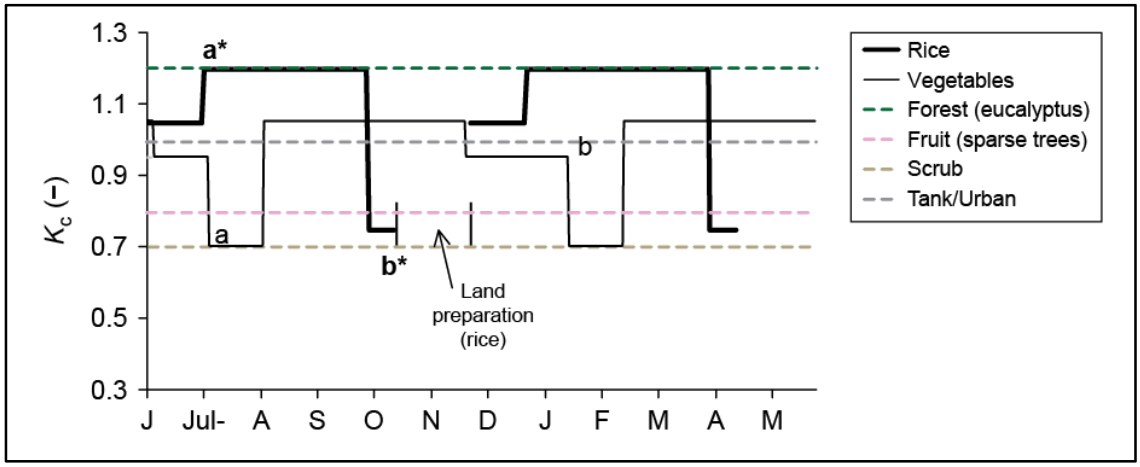

FIGURE 5.16: Crop coefficients (K_C) for a few different land uses, some of which depend on their agricultural calendar; 'a' is crop seeding, 'b' is crop harvesting (modified from Dewandel et al., 2008 with data from de Condappa 2005).

3.1.2.2. Runoff (D)

Runoff occurs when the amount of water stored in the surface (precipitation surplus) exceeds a critical water depth (Ω) in the field. This depth can be a tangible length, such as the mean height of the field edge (Ω = 0.12 m for paddy fields, Ω = 0.02 m for vegetables; Dewandel et al., 2008), or a more conceptual figure, i.e. the amount of excess rainfall which triggers runoff (Carpenter et al., 1999). Because the model used here is 1D and assumes there is no exchange between cells, estimated runoff is simply counted as water which exits the parcel, though hypotheses on its becoming are postulated later in the discussion.

Threshold runoff values depend on many factors, such as soil texture, plant cover, and rainfall intensity (Martínez-Mena et al., 1998). There is no direct way of measuring this threshold; instead, rainfall is generally inputted into soil moisture models and calibrated by comparing simulated runoff and measured streamflow data.

At the Maheshwaram catchment, because there is no perennial surface flow, simulated runoff was compared to total volume variations at a percolation tank which accumulates intermittent surface runoff, the Tumulur percolation tank (FIGURE 5.17). This percolation tank neighbors boreholes MHT4 and MHT3, and its location within the Maheshwaram catchment is shown in FIGURE 5.17c. The reconstructed 13 year (01/01/2000 to 04/12/2012) volume variation time series in the Tumulur tank (FIGURE 5.17a) were obtained through private communication from work that is yet to be published, but for which the main methodology is detailed in Boisson et al. (2014). In brief, volumes in the tank are estimated from meteorological data using a surface balance approach, and validated against measured volumes obtained from DGPS (Differential Global Positioning System) and satellite information on tank bathymetry and flooded surface area.

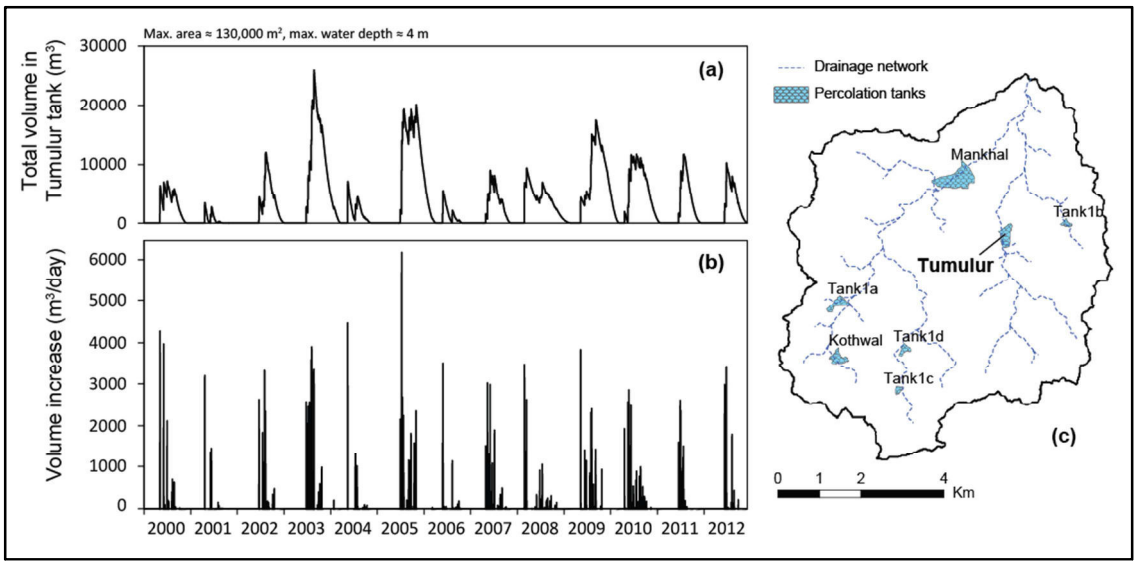

FIGURE 5.17: Variations in water volume for the period from 01/01/2000 to 04/12/2002 for a total of 4722 days (a), daily water volume increase (b) in the Tumulur tank and Tumulur tank placement within the Maheshwaram catchment and in regards to the drainage network.

To select an appropriate threshold, the number of days where the volume in the tank increased was compared to the number of days in which a runoff event was generated by the model depending on the selected threshold value. However, not all volume increases in the tank were considered relevant: there are many very small increases which are most likely linked to rainfall in the close vicinity of the basin (see FIGURE 5.17b), and not necessarily correlated with basin-wide runoff episodes.

In order to filter out these rapid and small increases, the frequency of water volume increases was plotted against volume ranges and the time series split into two, the very frequent low intensity episodes (i.e. "noise") and the less frequent high intensity episodes (i.e. significant events) (FIGURE 5.18).The minimum volume for an event to be considered significant was found to be 750 m^3, which corresponds to the slope break separating the low frequency high intensity events and the high frequency low intensity events (FIGURE 5.18). In total, there was a significant water volume increase in the tank (>750 m^3) **100 days** out of the total period of 4722 days for which we have volume estimates (01/01/2000 to 04/12/2012).

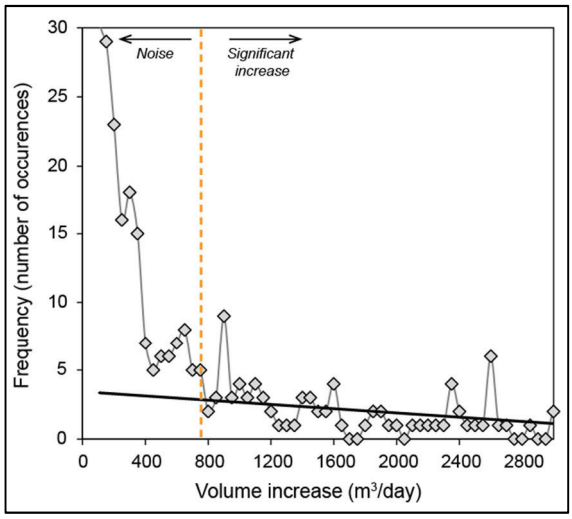

FIGURE 5.18: Filtering process for choosing significant volume increases to calibrate the runoff threshold. Volume increases below 750 m³/day are thus considered negligible.

3.1.2.3. Daily pumping flow (*PG*)

Mean daily water inputs in irrigated fields were obtained from Dewandel et al., (2008) and Dewandel et al. (2010) (FIGURE 5.14). These studies provided either average values of daily pumping flow or annual groundwater abstractions over the whole catchment area—daily water inputs are then obtained based on land use surfaces. These estimates were assessed through a survey of irrigated fields randomly distributed within the watershed during both seasons (Rabi and Kharif) and knowledge on the daily duration of pumping. The total irrigated field area was measured as well as the instantaneous pumping flow rates of the borewells supplying the field. In total, 11 paddy fields, 27 vegetable fields and 6 flower fields were surveyed (Dewandel et al., 2008, 2010). TABLE 5.1 summarizes the different mean daily water inputs (in mm/day) used in this study.

Water inputs (mm.day^{-1})	*Rabi*	*Kharif*
Rice	15.2 ± 0.8	10.1 ± 0.5
Fruits & grapes	1.9 ± n.a.	1.9 ± n.a.

TABLE 5.1: Mean water input values and field area from field investigations (from Dewandel et al., 2008, 2010).

3.1.2.4. Outflow (q_{out})

Downward vertical fluxes (q_{out}) are computed using the Darcy's Law one-dimensional flow [see **Chapter 3 Section 2.1.1**]. For an unsaturated profile (Ψ<0), we have:

$$q_{out} = -K(\theta)\left(\frac{d\Psi(\theta)}{dz} - 1\right) \quad (5.4)$$

where $K(\theta)$ is the unsaturated hydraulic conductivity [L.T^{-1}], $\Psi(\theta)$ is the pressure head [L], and z is the depth of the soil (with z positive downwards) [L]. For a saturated profile (Ψ>0), we apply Darcy's equation to a soil after it has been flooded, which yields the Green-and-Ampt equation (Bouwer, 1978) [also used for MAR, see **Chapter 4 Section 3.2.1.1** and FIGURE 4.3]:

$$q_{out} = -K\frac{(H + L - \Psi_{we})}{L} \tag{5.5}$$

where K is the saturated hydraulic conductivity [L.T^{-1}], H is the water depth above the soil (if there is ponding, otherwise $H = 0$), Ψ_{we} is the capillary suction at the wetting front [L], and L is the soil thickness [L]. Ψ_{we} is here assumed to be negligible ($\Psi_{we} \ll H + L$).

In order to apply the unsaturated Darcy equation to estimate flow through the soil zone, as stated in **Chapter 2 Section 2.4.2.4: Hydraulic properties of unsaturated porous media**, it is necessary to estimate the pressure-water content relations [$\psi(\theta)$] and the hydraulic conductivity-water content relations [$K_h\,(\theta)$]. To do so, there are a few available analytical approximations which relate ψ and K_h to θ . These solutions depend on a given set of parameters which can be obtained experimentally.

Here the pressure-water content and hydraulic conductivity water content curves are estimated using the model by Brooks & Corey (1964) [more detail in **Chapter 2 Section 2.4.2.4**, here only a brief summary will be made]. In this model, pressure head is related to water content as follows:

$$\frac{\theta}{\theta_S} = \Theta = \left(\frac{\psi_{bc}}{\psi(\theta)}\right)^{\lambda} \tag{5.6}$$

where Θ [-] is the degree of saturation, θ [L^3.L^{-3}] is the volumetric moisture content, θ_S [L^3.L^{-3}] is the saturated volumetric moisture content, ψ_{bc} [L] is the Brooks-Corey pressure scale parameter (air entry suction) and λ [-] is the Brooks-Corey texture dependent retention shape parameter. The unsaturated hydraulic conductivity is also a function of the degree of saturation:

$$\frac{K(\theta)}{K} = \Theta^{\eta} \tag{5.7}$$

where η [-] is the Brooks-Corey texture dependent conductivity shape parameter, the value of which depends on the chosen capillary model.

Calculation of θ is carried out at daily intervals and based on the continuity equation:

$$\frac{\Delta\theta}{\Delta t} = \frac{\Delta q}{\Delta z} \tag{5.8}$$

For saturated profiles, the left-hand side of the equation is zero. In this case, Eqs. (5.1) and (5.5) apply. For unsaturated layers, changes in θ are calculated from (5.8). At each time-step, θ is updated by substracting the outflow from the inflow during that time-step, dividing the difference by the layer thickness and adding the change to the

previous θ value (θ at the beginning of the time-step). In this scenario Eqs. (5.1), (5.4) and (5.6) through (5.8) apply (Dewandel et al., 2008). For the next time-step, and taking into account the new degree of saturation, the pressure head corresponding to the new moisture content $\psi(\theta)$ is computed again, and the whole procedure is repeated.

The parameters which allow us to use the previous equations (λ, η, ψ_{bc} θ_s and K_h) were obtained previously by de Condappa (2005) using the *Beerkan* method. In short, this method uses the van Genuchten moisture characteristic function ($\psi(\theta)$) and the Brooks & Corey moisture conductivity function ($K_h(\theta)$) to describe the hydraulic characteristic curves. To do so, the texture-dependent shape parameters (λ and n) are estimated from a simple particle analysis, and the structure-dependent scale parameters (ψ_{bc}, θ_s and K_h) are estimated from field infiltration experiments at null pressure head (Haverkamp et al., 2016; Lassabatère et al., 2006). A detailed description on the methodology applied, i.e. the Beerkan Estimation of Soil Transfer parameters through infiltration experiments (BEST), is beyond the scope of this thesis; readers may refer to Lassabatère et al. (2006).

The full tables containing the hydraulic properties for each soil type and horizon can be found as an Annex in de Condappa (2005), TABLE 5.2 is a summary of the mean values. For hydraulic conductivity a geometric mean was performed among the sites, while an arithmetic mean was used for the rest of the parameters.

		K_S (m.s^{-1})	θ_S (m^3.m^3)	λ -	Ψ_{bc} (m)	η -
HORIZON E						
Paddy		2.50×10^{-7}	0.36	0.099	-0.05	23.2
Default	Alf1.	1.85×10^{-5}	0.32	0.175	-0.089	14.8
	Alf2.	2.48×10^{-5}	0.36	0.193	-0.111	13.3
	Incep.	1.21×10^{-5}	0.35	0.129	-0.060	19.3
	Ent.	2.96×10^{-6}	0.36	0.117	-0.037	20.2
	Tank	2.50×10^{-7}	0.60	0.033	-0.312	63.7
Forest	Alf1.	2.61×10^{-5}	0.25	0.177	-0.117	14.8
	Alf2.	3.15×10^{-5}	0.32	0.193	-0.132	13.3
	Incep.	2.08×10^{-5}	0.27	0.129	-0.098	19.3
	Ent.	1.32×10^{-5}	0.36	0.117	-0.066	20.2
HORIZON B						
Default	Alf1.	5.19×10^{-6}	0.37	0.077	-0.041	29.5
	Alf2.	6.06×10^{-6}	0.37	0.100	-0.053	23.0
	Incep.	1.08×10^{-5}	0.35	0.096	-0.123	24.1
	Ent.	3.10×10^{-6}	0.35	0.080	-0.036	28.2
	Tank	7.50×10^{-7}	0.55	0.052	-0.055	41.7
Forest	Alf1.	1.07×10^{-5}	0.26	0.076	-0.122	29.7
	Alf2.	1.14×10^{-5}	0.37	0.100	-0.132	23.0
	Incep.	1.62×10^{-5}	0.27	0.096	-0.201	24.1
	Ent.	6.67×10^{-6}	0.35	0.080	-0.089	28.2

	hE (m)	hB (m)	Total
Alf1.	0.2	1.2	1.4
Alf2.	0.2	1.4	1.6
Incep.	0.1	1.1	1.2
Ent.	0.2	2.2	2.4
Tank	0.5	2.2	2.7

$K_h \equiv$ Saturated hydraulic conductivity
$\theta_S \equiv$ Saturated moisture content
$\lambda, \eta \equiv$ Pore-size distribution indexes
$\psi_{bc} \equiv$ Pressure-head parameter
$h \equiv$ Soil thickness

TABLE 5.2: Mean soil hydraulic parameters for each soil type and a few specific land uses from de Condappa (2005). Alf1. and Alf2. are Alfisols 1 and Alfisols 2, respectively, Incep. are Inceptisols, Ent. are Entisols and Tank refers to soils below the tank.

3.2. Basin discretization

The catchment was subdivided into 100×100 m grid-cells using ArcGIS so that the 1D model could be applied to each grid cell and then aggregated to provide a pseudo-2D estimate of recharge from infiltration (FIGURE 5.19). This discretization was necessary to provide spatialized information on R_I rather than a single point estimate. The grid-cell size was chosen in regards to the average paddy field size (7,500 m^2 in Rabi, 20,600 m^2 in Kharif, though there are often several plots grouped together; Dewandel et al., 2008), the

total simulation time, and the overall accuracy of discretized surfaces relative to the original land use map. The land use or soil type at each grid cell was automatically determined by ArcGIS as the dominating land use or soil type in terms of surface area for each cell. To ensure that the discretization procedure did not significantly modify land use surfaces (and thus their contributions to the water balance) the ratio of discretized surface to original surface was calculated, and found to vary from 0.98 to 1.07 (TABLE 5.3). The discretization process thus slightly modified the total land use surfaces. The smaller the grid, the better is the accuracy of the model, but greater is the total time required to run a simulation. With the current 100×100 m grid size one run over the basin lasts about 9 minutes, which was deemed to be an acceptable duration given the spatial resolution and the relatively low error in the total surface determination (TABLE 5.3).

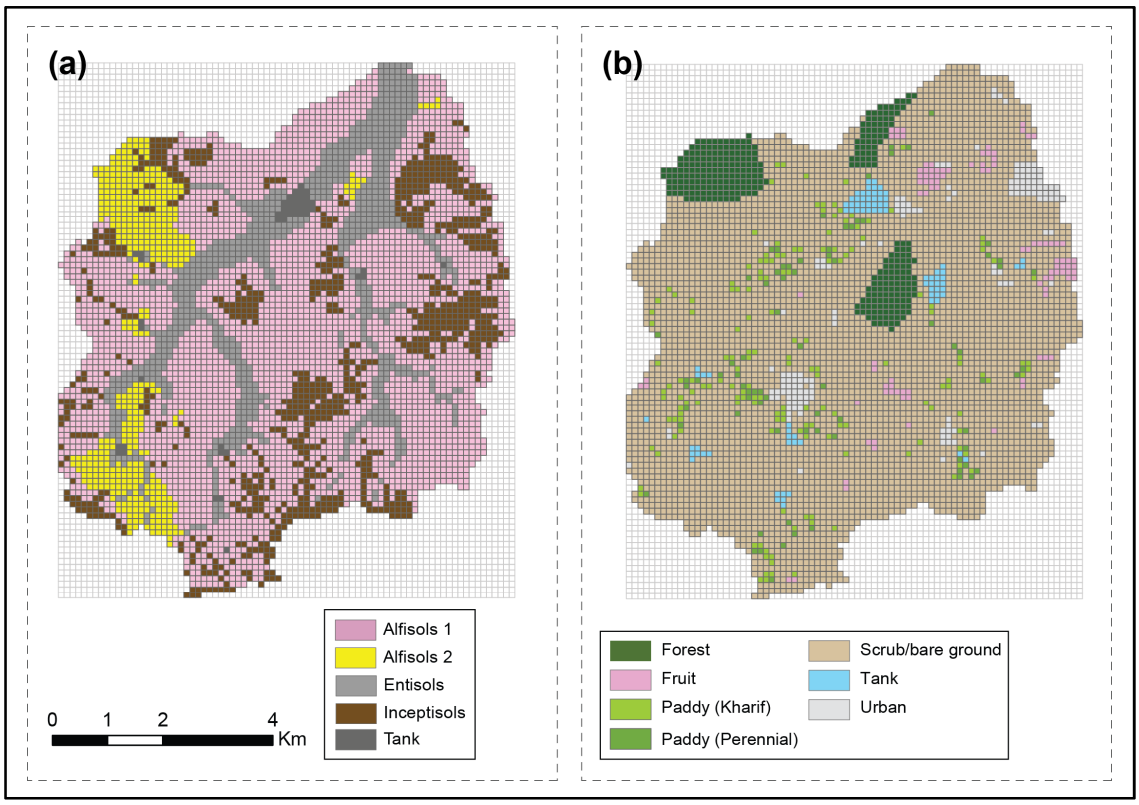

FIGURE 5.19: Discretized soil map (a) and land use map (b).

	Paddy fields					
Land Uses	*Rabi*	*Kharif*	**Scrub**	**Forest**	**Fruit**	**Urban**
Area (km²)	2.01	2.92	44.26	3.31	0.99	1.43
Ratio (Orig./ Discr.)	1.07	1.05	1.00	1.02	0.99	0.99

Soil types	**Alf. 1**	**Alf. 2**	**Incep.**	**Enti.**
Area (km²)	30.14	4.60	8.66	8.94
Ratio (Orig./ Discr.)	1.00	1.00	0.98	1.03

TABLE 5.3: Surfaces of each soil type and land use category and ratio between surfaces before and after discretization.

3.3. Sensitivity analysis

Modelled recharge depends in total on 7 parameters: λ, η, ψ_{bc} θ_s, K_h, L and Ω, though λ and η are related so only η was considered. Each of these parameters exerts a different influence on the outputs, and some exert more influence than others. Unfortunately, information on the uncertainty associated to each of these measured parameters was not always available, and Ω was obtained through model calibration. A full quantification of the ensemble model uncertainty was thus not possible. Instead, a *sensitivity analysis*—wherein the effect of each parameter on the dynamics of the system is assessed—was performed.

Sensitivity is defined as the rate of change in model output with respect to change in a model parameter (Kabala, 2001; Maréchal et al., 2008). Sensitivity was thus assessed by varying each parameter by a certain ratio relative to a reference value (while one parameter is varied the others remain at the reference value) and calculating the percentage of variation in the outputted recharge. The reference parameter set was chosen arbitrarily as the properties of an Inceptisol and input meteorological data was the same as for the recharge model.

4. Results and discussion

4.1. Threshold runoff

In order to run the model successfully it was necessary to determine a runoff threshold. This threshold determines the partition between recharge and runoff, so it was important to calibrate it against observed data. As mentioned in the previous sections, no perennial surface streamflow exists on this site. Thus, volume data from the Tumulur tank in the Maheshwaram catchment was used to calibrate this figure. Modelled runoff time-series were compared to tank volume variations, and adjusted so that the number of runoff events matched the number of significant volume increases in the tank.

The model was run with runoff thresholds ranging from 2 to 6 cm with a 0.5 cm interval. Results are shown in TABLE 5.4. The number of days generating runoff events was compared to the number of water volume increases in the tank; the final threshold was selected based on the correlation between these events.

As mentioned above, according to water volumes in the Tumulur tank, there are 100 days from 01/01/2000 to 04/12/2012 during which there are significant volume increase episodes. Looking at TABLE 5.4, we can see that the runoff threshold which best matches the number of runoff days is 3 cm, which generates 109 days of runoff over the same period. Smaller thresholds (<3 cm) produce runoff time series which are too "flashy", while larger runoff thresholds (>3 cm) cause too much water to be retained and runoff time series are too sparse.

Threshold (cm)	**Number of days of runoff**
2	176
2.5	134
3	**109**
3.5	85
4	74
4.5	61
5	50
5.5	38
6	36

TABLE 5.4: Number of days during which runoff was generated by the recharge model depending on the runoff threshold selected from 01/01/2000 to 04/12/2012.

FIGURE 5.20 shows simulated runoff using the "best fit" threshold. The number of runoff episodes should roughly match the volume increases in the tank. Note that this calibration is mainly based on qualitative criteria (an approximate match of the hydrological response to rainfall of both time series). The relative intensity of each event is not matched for several reasons. First, the runoff series shown here is a catchment-wide average (in mm), and does not account for the redistribution of water throughout the catchment. It does not account for local and regional topographic effects, nor does it consider lag times between where runoff occurred and the Tumulur tank.

In the study by Boisson, Villesseche et al. (2015) which focuses specifically on the filling dynamics of the Tumulur tank, it was found that $\Omega = 1.8$ cm. Nonetheless, soils in the area have low permeabilities due to their high clay contents, which are generally associated with higher runoff. The ensemble of soils at the basin scale is generally more permeable, so we expect the basin-wide value to be slightly higher than this. Other studies which have attempted to quantify this figure have found results to be in the same order of magnitude. For example, in Carpenter et al. (1999), state-wide runoff thresholds in the US were computed, and found to vary between 3.4 cm in the state of Oklahoma and 0.95 cm in the state of California.

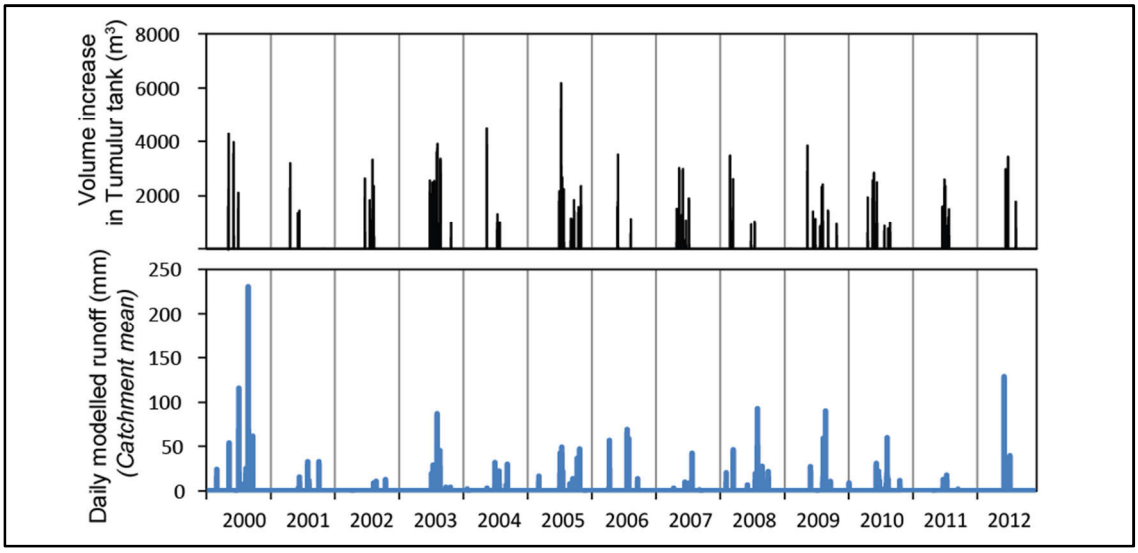

FIGURE 5.20: Simulated mean modelled runoff with $\Omega = 3$ cm (bottom) and significant volume increases in the Tumulur tank (top).

4.2. Diffuse recharge distribution

4.2.1. Recharge distribution in space

FIGURE 5.21 illustrates the simulated distribution of R_I per year. First and foremost, we observe that diffuse recharge is not very significant. Yearly diffuse recharge varies between 11 mm (for 494 mm of rainfall, i.e. 2%) up to 92 mm (for 1074 mm of rainfall, i.e. 9%). Most years (2011, 2012, 2014 and 2015) are dominated by very low recharge (<20 mm/yr) throughout the catchment (note their pale blue color). The year 2013, for which rainfall was the most significant ($P = 1074$ mm) is the exception: recharge patterns become more apparent and overall diffuse recharge is much more significant.

4.2.1.1. Effect of land use

Recharge is not homogeneously spread-out. Irrigated areas, especially rice paddies, appear to act as areas of enhanced recharge ($1000 \geq R_I \geq 250$ mm/yr approx.) which stand out relative to the surrounding uncultivated areas (i.e. the bright blue cells). This is consistent with the mechanics of unsaturated flow: both the hydraulic conductivity and pressure head increase with soil moisture. This means that an irrigated parcel will have a higher capacity to transmit water downwards. This phenomenon has been previously observed (Kurtzman & Scanlon, 2011; Ognianik & Paramonova, 2001), though some have noted recharge to actually flow out of the irrigated area laterally or vertically through preferential flow paths as *localized* recharge rather than diffuse recharge through the soil matrix (Kurtzman & Scanlon, 2011).

Nevertheless, although irrigation has a significant impact on recharge at the parcel scale, when averaged over large surfaces their contributions become much lower. This is

because irrigated surfaces make up only a small percentage of the total area, the rest being mainly scrub and bare ground. In areas where irrigated surfaces represent a significant percentage of the total land use area, however, the effects of irrigation on recharge should in theory have a much stronger influence on total recharge.

Additionally, these observations should be considered with caution: even though recharge in an irrigated parcel is increased relative to a bare surface, this does not necessarily compensate—or even slightly approach—the groundwater abstractions needed for said irrigation. Current mean groundwater abstractions at the Maheshwaram catchment, in fact, are estimated at 10 Mm^3 (Dewandel et al., 2010). If we consider that the total irrigated area in the Maheshwaram catchment is between 3 km^2 and 3.9 km^2 on any given year (TABLE 5.3), that means that irrigation requirements each year at the parcel scale vary approximately between 2464 and 3333 mm/yr. The highest mean annual recharge rate simulated by our model, however, was only of 701 mm/yr for Inceptisols used for paddy cultivation (**Annex A**). Therefore, even though irrigation increases the recharge capacity of a parcel, it does not do so at a rate which compensates for the groundwater abstracted in the first place.

4.2.1.2. Effect of soil type

Soil types also influence recharge distribution, although to a lesser extent. Differences in recharge are actually only visible in the year with the highest recharge (2013). Inceptisols, located in the hills and summits surrounding the basin, appear as the most receptive to recharge. Entisols, located in the drainage network, appear to resist recharge. This is consistent with their high clay contents and low permeabilities. Because Entisols are alluvial soils, they are found in depressions zones, and their distribution is generally guided by runoff patterns. As such, the drainage network may be defined as an area which is antagonistic to diffuse recharge, except under irrigated parcels. Alfisols, present in the catchment plains, appear to present an intermediate behavior, and Alfisols 1 seem to recharge more than Alfisols 2. The full table showing annual recharge per soil type and land use may be found in **Annex A**.

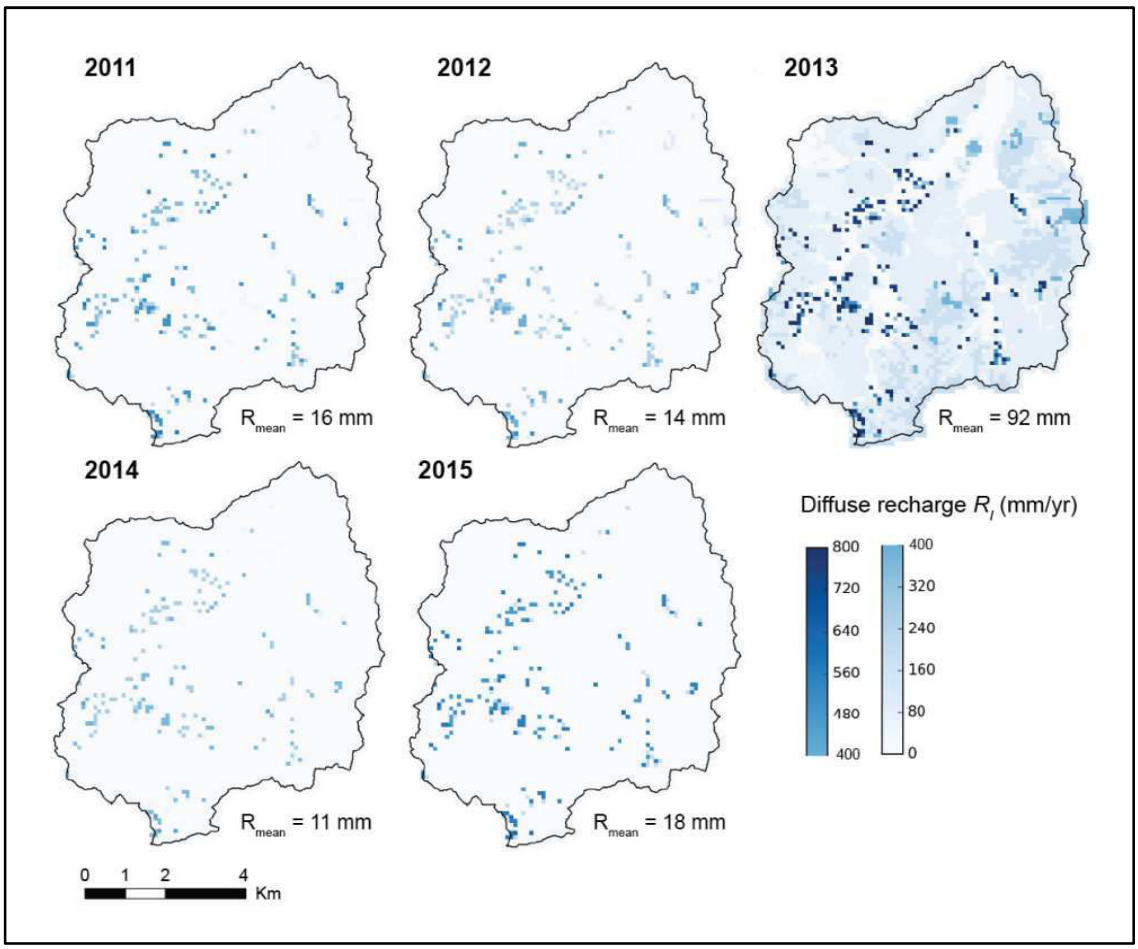

FIGURE 5.21: Yearly diffuse recharge (R_I) values computed for the Maheshwaram catchment. Values are calculated at a resolution of 100×100 m.

4.2.2. Recharge distribution in time

FIGURE 5.22 illustrates diffuse recharge variations in time for (a) two contrasting soil types and (b) two contrasting land uses. For the former, recharge from an Inceptisol with scrub vegetation is compared to recharge from an Alfisol 2 with scrub vegetation. For the latter, an Entisol with scrub vegetation is compared to an Entisol with a perennial paddy crop. Both soil types and land use have a quantifiable impact on diffuse recharge, though the effect of land use is much more significant.

Focusing on FIGURE 5.22a, we see that Inceptisols are more prone to diffuse recharge than Alfisols 2 (which we also saw in FIGURE 5.21). For the former, recharge is about 40 mm/yr for the illustrated period (2000-2015), while for the latter recharge is on average 13 mm/yr (for all values see **Annex A**). FIGURE 5.22a also shows how, in uncultivated soils, recharge is highly dependent on rainfall. Of the 15 years simulated, only 6 years—those with most significant rainfall—generate recharge for Inceptisols. The number is even less for Alfisols 2, wherein recharge is only generated 2 times over the entire simulated period.

Recharge dynamics are significantly different for irrigated soils (FIGURE 5.22b). Without irrigation, Entisols do not allow any rainfall to become recharge (R_I = 0 mm/yr)—at least not under the conditions which have prevailed over the last 15 years. When the soils are irrigated, however, recharge occurs regularly and in large quantities. The yearly recharge average for Entisols used for perennial rice cultivation (2 rotations a year) in fact is of 461 mm/yr (see **Annex A**).

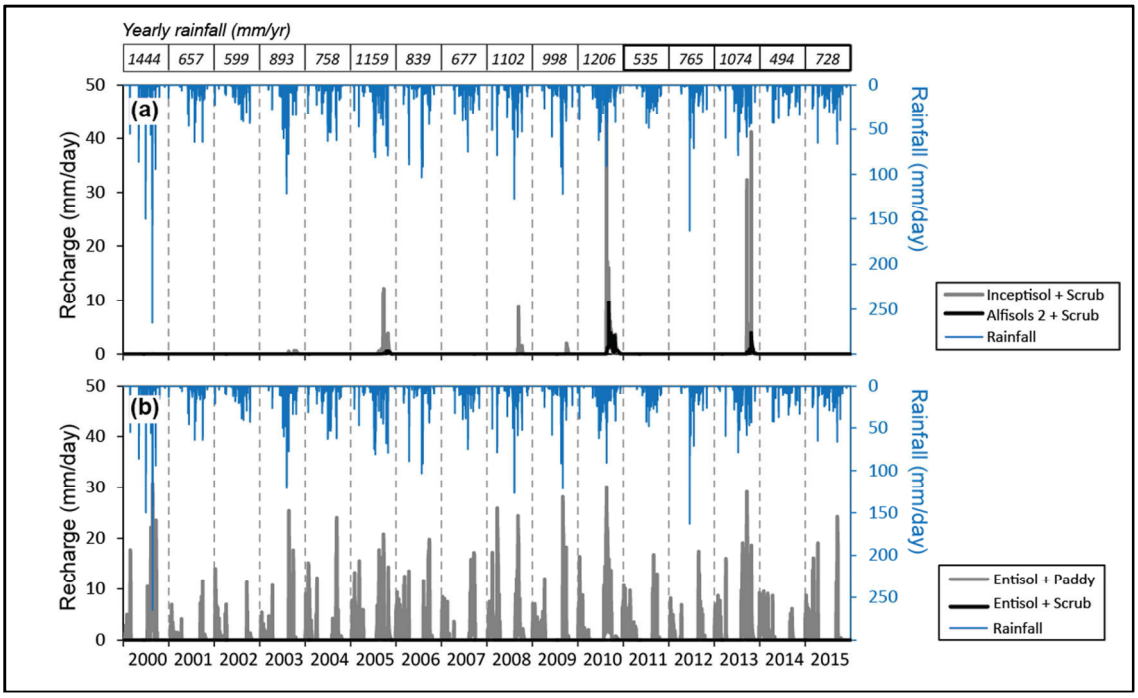

FIGURE 5.22: Rainfall and diffuse recharge variations computed for two different combinations of soil type and land use: an Inceptisol with scrub vegetation against an Alfisol 2 with scrub vegetation (a) and an Entisol with a perennial paddy against an Entisol with scrub vegetation (b). Recharge from the Entisol with scrub vegetation may appear absent from the graph but is actually zero during the illustrated period.

4.3. Diffuse recharge/rainfall relationship

FIGURE 5.21 and FIGURE 5.22 illustrate to a certain extent how diffuse recharge and rainfall are not linearly linked; we saw that for years where recharge is not very high, diffuse recharge is close to zero, with irrigated parcels being the exception. When plotting annual diffuse recharge against rainfall, the non-linearity of this relationship becomes highly apparent (see FIGURE 5.23). The ratio of diffuse to total recharge was also calculated. According to FIGURE 5.23, diffuse recharge relative to rainfall may be split into two categories:

- For rainfall below 1000 mm approximately (low to moderate), diffuse recharge increases very little with rainfall, and is overall very low. To explain this phenomenon, we may recall that diffuse recharge is highly dependent on

soil moisture, and years of low rainfall are not sufficient to compensate the soil moisture deficit present most of the year. In this precipitation range (low to moderate), the ratio of diffuse to total recharge decreases as rainfall increases. This is because, even though *total* recharge increases linearly with rainfall (Dewandel et al., 2010; Maréchal et al., 2006; Mizan, 2019; FIGURE 5.13), diffuse recharge remains relatively constant.

– For rainfall above 1000 mm, diffuse recharge becomes a significant contributor to total recharge, and increases linearly with rainfall at a significant rate. This is because, when rainfall is high, soil moisture deficits are met, and infiltration can much easily reach the aquifer, rather than be taken up by evapotranspiration. The ratio of diffuse to total recharge increases in this precipitation range. This does not imply that other recharge processes have decreased, but instead that their *relative* contribution is lower because diffuse recharge provides a significant portion of total recharge.

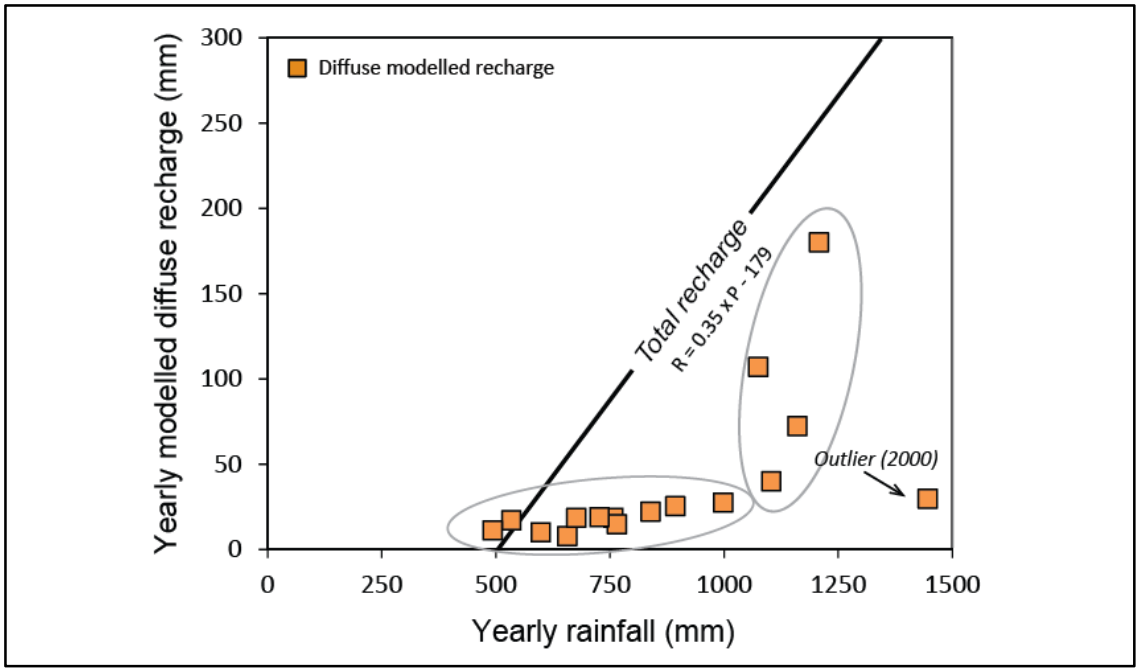

FIGURE 5.23: Modelled catchment-scale yearly diffuse recharge values averaged over the Maheshwaram catchment relative to rainfall and comparison with the total recharge trend relative to rainfall obtained from Mizan (2019). Each point corresponds to a given year; the simulation was run from 1995 to 2015 though only the years from 2000 to 2015 are shown.

There is an outlier in FIGURE 5.23: in 2000, rainfall was very high (1444 mm), but estimated diffuse recharge was very low (R_I = 29 mm). To understand why this point is an outlier, it is useful to look at rainfall the year preceding 2000. Rainfall in 1999 was 550 mm, which is extremely low: it is actually the 4th weakest rainfall year on record out of the 43 years for which ICRISAT has rainfall estimates (records go back as far as 1974). This observation seems to imply that recharge is not only linked to rainfall on a

given year, but also that recharge can be impacted by rainfall the prior years. Following this assumption, if a considerable drought occurs, then soils will not be able to transmit percolation down to the aquifer the following year, no matter how significant rainfall is the next year. Instead, water will be partly taken up by evapotranspiration, but most importantly it will drain as runoff, potentially causing harmful flooding (see also yearly modelled runoff, FIGURE 5.24). Running the model with additional data in this precipitation range (very high, >1250 mm) should further confirm that this point is an outlier and that this is due to the lack of rainfall the prior year.

4.4. Annual groundwater budget

Each component of the water budget was averaged over the entire catchment in order to estimate its overall contribution and shown in TABLE 5.5. We notice that the greatest water output by far is evapotranspiration (716 mm), followed by runoff (200 mm), and the least significant output is diffuse recharge (38 mm) when looking at means for the entire simulated period (2000 to 2015). *AET*, on average, is of the same order of magnitude as P (716 mm vs. 871 mm). This explains why, on an average year, diffuse recharge will be very weak, especially if no irrigation is present: the vast majority of precipitation will be taken up by evapotranspiration. If diffuse recharge is to take place, precipitation must exceed evapotranspiration by an appreciable amount. According to FIGURE 5.23, precipitation should be about 280 mm greater than mean *AET*, i.e. about 1000 mm – 716 mm. This surplus allows water in the soils to meet evaporative demands while remaining relatively wet, thus allowing percolation to flow downwards into the aquifer.

In order to compare diffuse recharge to total recharge, mean values were also calculated for the period from 2011 to 2015 (for which we have *total* recharge estimates). During this period, R_I accounts for only 4.6% (33 mm) of rainfall (719 mm). Mizan (2019) estimated the ratio of *total* recharge to rainfall to be about 10.1% (73 mm), which is consistent with the national average of 9% (Government of Andhra Pradesh, 2003). Total recharge is thus much higher than diffuse recharge, most likely due to contributions from focused recharge. Following this assumption, focused recharge would account for the remaining 40 mm of recharge (73 – 33 mm): this is an average of **55% of total recharge**.

Mean yearly runoff between 2011 and 2015 is estimated at 111 mm. A part of this runoff is expected to infiltrate as the above mentioned focused recharge, which leaves 71 mm (111 – 40 mm) of runoff which are "unaccounted for". On one hand, this model does not account for evaporation from surface water bodies which would fill up with runoff water (from puddles to tanks), nor for evaporation occurring below the soil zone, either

from deep rooted vegetation or though evaporation from the water table[21]. *AET* is thus certainly underestimated. Also, this basin was noted to be essentially endorheic, which implies there is no perennial drainage outwards of the basin. This does not however rule out the possibility that there might be intermittent outflow during particularly intense rainfall episodes. Finally, it is possible that diffuse recharge may have been underestimated resulting from uncertain parameter determination in the model used. This will be further looked into in **Section 4.6: Sensitivity analysis.**

	Outputs (mm/yr)				**Inputs (mm/yr)**			
	D	***R_I***	***AET***	***RF***	***P***	***PG***	***Total w***	***Δw***
2000	779	29	718	38	1444	121	17	1
2001	101	7	631	35	657	121	21	4
2002	32	9	651	30	599	121	19	-2
2003	219	25	636	36	893	121	123	103
2004	123	18	798	38	758	121	19	-103
2005	273	72	697	43	1159	121	222	202
2006	214	21	859	40	839	121	40	-181
2007	71	18	690	36	677	121	22	-19
2008	316	40	708	38	1102	121	150	128
2009	316	27	747	37	998	121	141	-9
2010	194	179	763	44	1206	121	284	143
2011	32	16	834	36	535	121	21	-264
2012	196	14	616	40	765	121	41	20
2013	206	107	635	43	1074	121	250	209
2014	39	11	755	33	494	121	20	-230
2015	81	18	717	32	728	121	19	-1
Sum	3192	612	11454	597	13929	1931	-	3
Mean 2000-2015	200	38	716	37	871	121	88	0
Mean 2011-2015	111	33	712	37	719	121	-	-

TABLE 5.5: Yearly components of the water budget averaged over the entire catchment area. *D* represents runoff, R_I is recharge from infiltration (diffuse recharge), *AET* is actual evapotranspiration, *RF* is irrigation return flow, *P* is precipitation, *PG* is groundwater irrigation, *Total w* is the stock of water in the soil at the end of each year and Δw is the change in soil moisture from the end of the prior year to the end of the year in question. All components are in mm.yr^{-1}.

[21] The latter however has been noted to account for only a couple of mm annually (e.g. in Maréchal et al., 2006 it is only 1-2 mm/yr).

4.5. Focused recharge

According to previous calculations, total recharge was shown to be demonstrably higher than modelled diffuse recharge. In this study, we postulate that this difference is representative of focused recharge processes, which would make up about 55% of total recharge. Subtracting annual diffuse recharge from annual total recharge allows us to appreciate the evolution of focused recharge in time, and most importantly, as a function of precipitation (FIGURE 5.24a). The estimated relationship between focused recharge and rainfall was surprisingly found to be extremely linear ($R^2 = 0.99$). Contrarily to diffuse recharge, it would appear focused recharge does not depend on the hydrologic conditions of the catchment's soils. Instead, focused recharge appears simply as a constant portion of rainfall which "escapes" the soil zone and reaches the aquifer quicker than diffuse recharge would (thus not subject to evapotranspiration). There is nonetheless a minimal amount of rainfall, 500 mm, below which no focused recharge takes place. Focused recharge, especially *indirect* recharge and recharge from surface water bodies (*localized* recharge) require water to flow or accumulate at the surface; in other terms, focused recharge can occur only if runoff is generated which may lead to ephemeral streams, perennial streams or ponding of water at the surface. FIGURE 5.24b shows modelled runoff plotted against rainfall. This figure supports the above statement. According to our runoff estimates, at least 500 mm of rainfall are required for runoff to be generated in an appreciable amount.

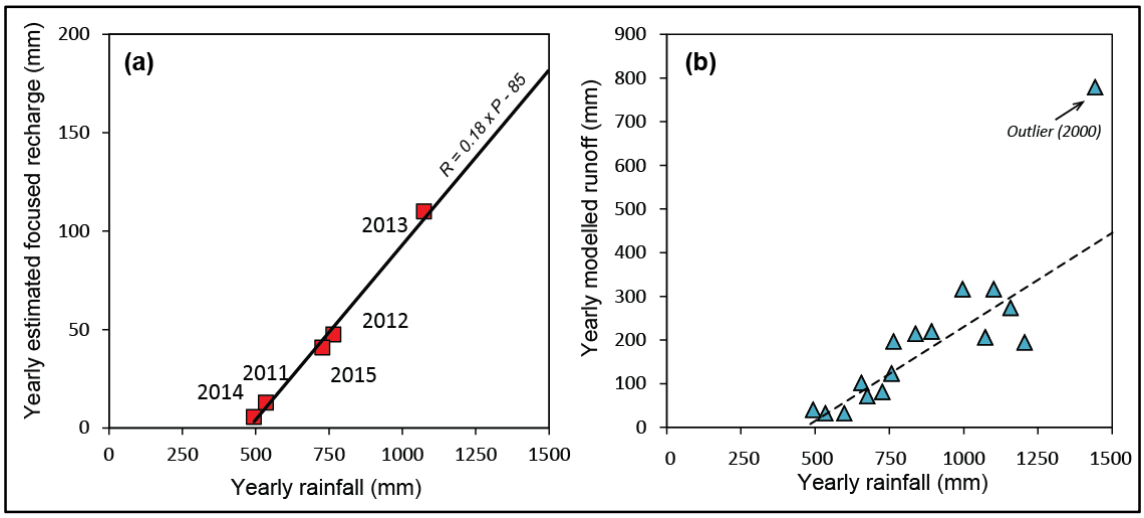

FIGURE 5.24: Estimated yearly focused recharge plotted against rainfall for the 2011-2015 period (a) and modelled yearly runoff plotted against rainfall as well for the 2000-2015 period (b); both are in mm.yr^{-1}.

Because focused recharge does not appear to depend on soil moisture, this implies that its contributions to total recharge are essential during low to moderate rainfall years, where diffuse recharge is very low. Additionally, in a context in which climate

change is becoming an undeniable reality, temperature increases are leading to higher evapotranspiration rates and more significant soil moisture deficits. Contributions from focused recharge, which would remain unaffected by these increases, would contribute to the resilience of groundwater resources under these conditions.

The exact mechanisms through which rainfall would 'escape' the soil zone to become focused recharge are however not clear when simply compared to rainfall. For this, the first step is to map out its distribution throughout the catchment, and see if the zones of enhanced recharge align with any particular structures (e.g. faults, geological boundaries, topographic depressions…).

4.5.1. Spatialized contributions

Understanding the relative importance of focused recharge compared to total recharge and rainfall is an important first step. Nevertheless, as mentioned above, annual catchment-scale averages do not accurately describe *focused* recharge processes, which, as their name rightly points out are *focused* into specific areas.

In order to get an approximate understanding of where focused recharge takes place, the upscaled spatialized *diffuse* recharge was subtracted from the *total* recharge map, and the resulting values were interpolated using standard kriging. Upscaling the diffuse recharge map was done using ArcGIS, by averaging the small-scale (100×100 m) diffuse estimates within each larger-scale (685×685 m) cell. The difference between the two spatialized estimates was assumed to map out the contributions focused recharge (FIGURE 5.25a).

Replicating the conditions responsible for the distribution and intensity of focused recharge in a numerical model is however a difficult task. This is because focused recharge, contrary to diffuse recharge, is controlled by a great number of interplaying factors which are not necessarily easily identifiable, or for which it is very difficult to obtain quantitative estimations of their contributions. These factors include, but are not limited to: the existence of preferential flow paths (e.g. outcropping fractures, large faults, contact zones, macropores), ponding of runoff at the surface (controlled by topography, the intensity of rainfall episodes, and land cover) and stream losses from the streambed (also controlled by many factors, such as the permeability of the streambed, the slope and density of the drainage network…). For this reason, observations made below are merely qualitative, and the resulting assumptions remain open to interpretation.

The resulting focused recharge map highlights areas which are more prone to these processes as well as areas which are more resistant to them. First, as noted with FIGURE 5.21, Entisols, which form preferentially in drainage networks, are areas which resist diffuse recharge. Nevertheless, comparison with FIGURE 5.12 (total recharge estimates) shows the opposite trend: these same areas actually have high total recharge.

This points towards contributions of focused recharge. During intense rainfall episodes, the infiltration capacity of soils may be exceeded, causing water to run off and create ephemeral streams. These episodes create favorable conditions for *indirect* recharge to occur. This is also visible in FIGURE 5.25b; the drainage network and topography contour lines overlap areas of higher focused recharge. Other studies in semi-arid terrain have also noted low-lying alluvial-filled valleys to act as indirect recharge terrains both in hard rock areas (e.g. van Wyk et al., 2012) and sedimentary aquifers (e.g. Acworth et al., 2016; Mahlknecht et al., 2004).

It is also possible, even if there are no significant flows at the surface, that lateral preferential flow displaces infiltration towards the lower parts of the catchment. As stated in **Chapter 2 Section 2.3.2: Lateral flow in the unsaturated zone**, however, lateral flow through the unsaturated matrix displaces a negligible amount of water because water is retained by capillarity. Instead, the greater part of lateral flows occurs through sub-horizontal structural discontinuities such as fractures, macropores, or lithological transitions. Several studies, for instance, have found the soil-rock interfaces to act as preferential flow paths and divert infiltration laterally (Bockgard & Niemi, 2004; Sohrt et al., 2014), which may lead to lower recharge rates in input areas and higher recharge rates in output areas. In this geological context, specifically, the most permeable interface is the interface between the saprolite and the fractured bedrock, i.e. *the saprock* (FIGURE 5.2). Boisson, Guihéneuf et al. (2015), in fact, found the transmissivity of this interface to be quite high ($T = 1.0\times10^{-3}$ to 7.0×10^{-4} $m^2.s^{-1}$); these values were measured at the nearby Experimental Hydrogeological Park (EHP, the Choutuppal site).

Additionally, it appears there is a N-S axis of focused recharge in the east segment of the catchment. This may in part be due to the position of the drainage network, but it also appears to align with the contact zone between the biotite granite and the slightly harder biotite granite with pegmatitic and leucogranitic dykes (FIGURE 5.1). This is consistent with literature: contact zones can be highly transmissive, and have been noted to act as areas of enhanced recharge. Geological discontinuities may also be associated with fault zones (though this is not the case here) which are highly fractured and thus constitute important drains for aquifer recharge (e.g. Leray et al., 2013; Ruelleu et al., 2010) ; other structural discontinuities, such as dolerite dykes, have been noted to act similarly (e.g. Johnston, 1987), though these may also act as barriers (Bredehoeft et al., 1992).

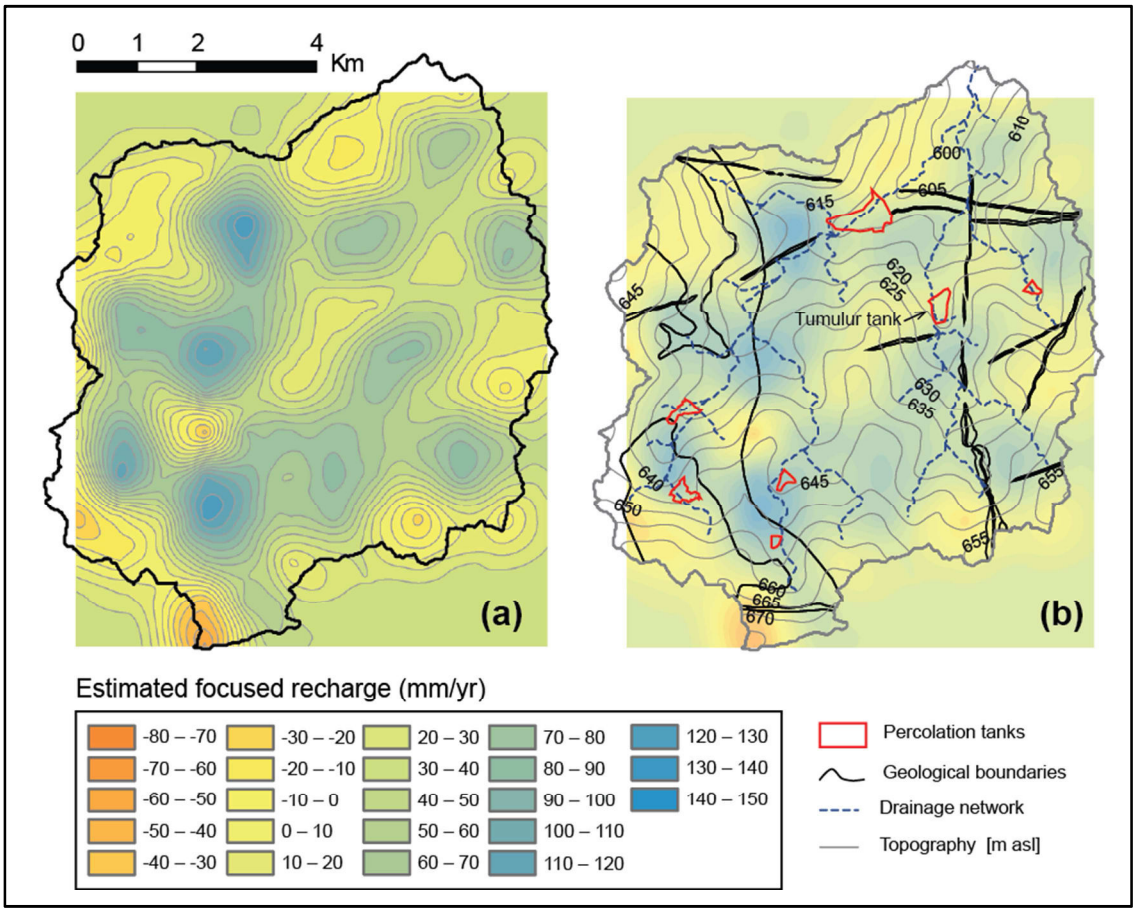

FIGURE 5.25: Raw difference between mean total recharge and mean diffuse recharge, assumed to be equal to focused recharge (a) and the same map with superimposed topography, drainage network, percolation tanks and geological boundaries in order to identify the possible contributors to focused recharge (b)

Localized recharge from percolation tanks does not appear to have a significant effect (FIGURE 5.25b). Even though the drainage network enhances recharge through indirect processes, surface water bodies such as tanks do not stand out as zones of enhanced recharge. As we have seen in **Chapter 4 Section 4**, there are many different reasons for which a basin or tank does not recharge efficiently. First and foremost, even though the approximate tank contours are drawn in FIGURE 5.25b, this does not imply that there is actually water in them for prolonged periods of time. Without on-field monitoring of tank water levels, little can be concluded on their overall efficacy and catchment-scale contributions. The only tank for which this data is available is the Tumulur tank, which does not appear to contribute to recharge either.

4.6. Sensitivity analysis of the diffuse recharge model

Possible sources of error and overall parameter significance were assessed by performing a sensitivity analysis (shown in FIGURE 5.26). Each input parameter was varied in the range between -75% to +100% of the reference value (unirrigated Inceptisol parame-

ters) and the output recharge calculated with the modified parameter was compared to the reference output recharge. Model inputs, namely P and ET, were the same as in the preceding sections. Note then that P and ET correspond to semi-arid conditions; the results of this analysis do not necessarily apply to other climate conditions, such as temperate and humid climates.

The parameter with the greatest influence was found to be Ω, followed by θ_s and L which have almost the same effect (together they determine the storage capacity of the soil) and η. K_h and ψ_{bc}, perhaps surprisingly, have very little effect on recharge outputs (FIGURE 5.26). This nonetheless aligns with observations from **Chapter 2 Section 3.3: Recharge controls**, wherein it is stated that in semi-arid environments recharge is often *Climate-controlled*. In (semi-)arid environments, recharge is often limited by the amount of infiltration available at the land surface: the importance of the runoff threshold—which determines how much water remains at the surface and how much exists through runoff—is coherent with this observation. Also, soils are completely saturated only a few days a year (if any) which means that unsaturated soil conditions prevail most of the time, and that the conductivity and pressure head are much more dependent on soil moisture than on their saturated values. Finally, η is part of an exponential function ($y = a^{\eta}$) and a is equal to the degree of saturation Θ that is <1; this means y is greatest for low η values and decreases at an exponential rate. Output sensitivity thus increases as η decreases, and reaches a plateau when total recharge is equal to rainfall (FIGURE 5.26).

This sensitivity analysis should provide a first estimate of the possible uncertainty associated with our model outputs. Nevertheless, a more complete analysis should consider the model sensitivity under different meteorological conditions, and better analyze the interdependence of parameters, using for example a different set of reference values. Unfortunately, this was not possible due to time constraints, but remains a point of possible improvement in this study.

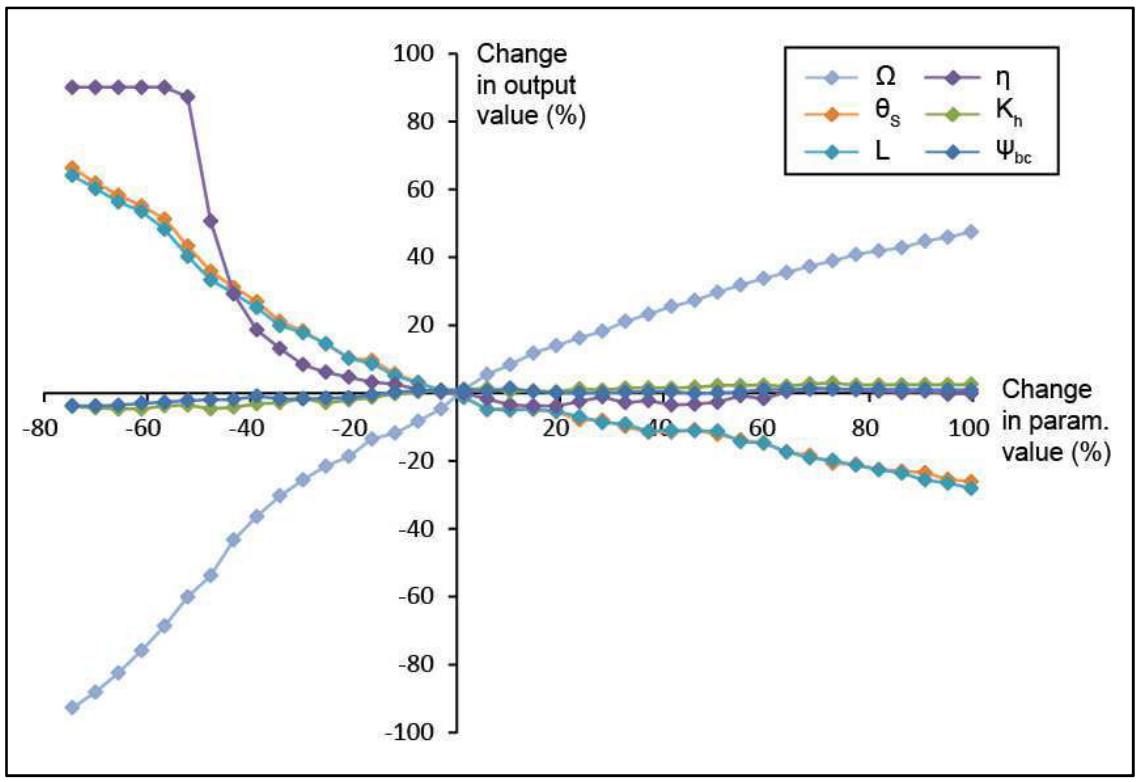

FIGURE 5.26: Sensitivity analysis of model parameters used to estimate diffuse recharge. This analysis was performed by varying each parameter individually and comparing the outputs to a reference model run, chosen arbitrarily. η is the texture dependent conductivity shape parameter [-], ψ_{bc} is the Brooks and Corey air entry pressure-head [L], θ_s is the saturated soil moisture content [-], K_h is the saturated hydraulic conductivity [L.T^{-1}], L is the soil thickness [L] and Ω is the runoff threshold [L]. Legend is sorted in order of importance.

4.7. Conclusion

This chapter attempts to elucidate the question of recharge in fractured crystalline aquifers and in (semi-)arid environments through the study of a highly monitored well instrumented pilot catchment. Our computations suggest that diffuse recharge is highly dependent on rainfall, and that the diffuse recharge-rainfall relationship is highly non-linear. For low recharge years (<1000 mm) in fact, diffuse recharge contributions appeared to be consistently very low. Beyond this threshold, which is approximately equal to the sum of (i) the average water storage capacity of the catchment soils and (ii) mean evapotranspiration, diffuse recharge appeared to increase significantly; this results from soil moisture deficits being met, which allow water to finally reach the water table. Irrigated areas were also shown to possibly significantly increase contributions from diffuse recharge at the parcel scale, though their total surface is not significant enough to impact recharge at the catchment scale, and this recharge increase does not compensate total groundwater withdrawals.

A sensitivity analysis performed on the diffuse recharge model parameters highlighted the importance of accurately estimating certain parameters above others. Namely, this analysis showed that under (semi-) arid conditions, model outputs are most sensitive to three parameters: the runoff threshold, which determines the fraction of rainfall that becomes runoff, and the parameters controlling the soil moisture retention capacity of the soil, i.e. the soil thickness and saturated soil moisture content.

Our estimates of focused recharge varied linearly with rainfall regardless of soil moisture or evapotranspiration. Focused recharge would then play an essential role in years where rainfall is too low to allow diffuse recharge. This is consistent with observations made in (semi-)arid environments in general: the greater the aridity, the higher the contributions from localized and indirect recharge processes. The spatial distribution of focused recharge was also mapped, and though no definitive conclusions were drawn, some correlations were made. Indeed, high focused recharge zones did not appear to be randomly distributed, but instead seemed related (i) to the drainage network density and disposition and (ii) to the contact zone between two types of granite.

FIGURE 5.27 was plotted to regroup the different types of recharge and their relationship to rainfall, and provides a summary of some of the different observations which were made along this section.

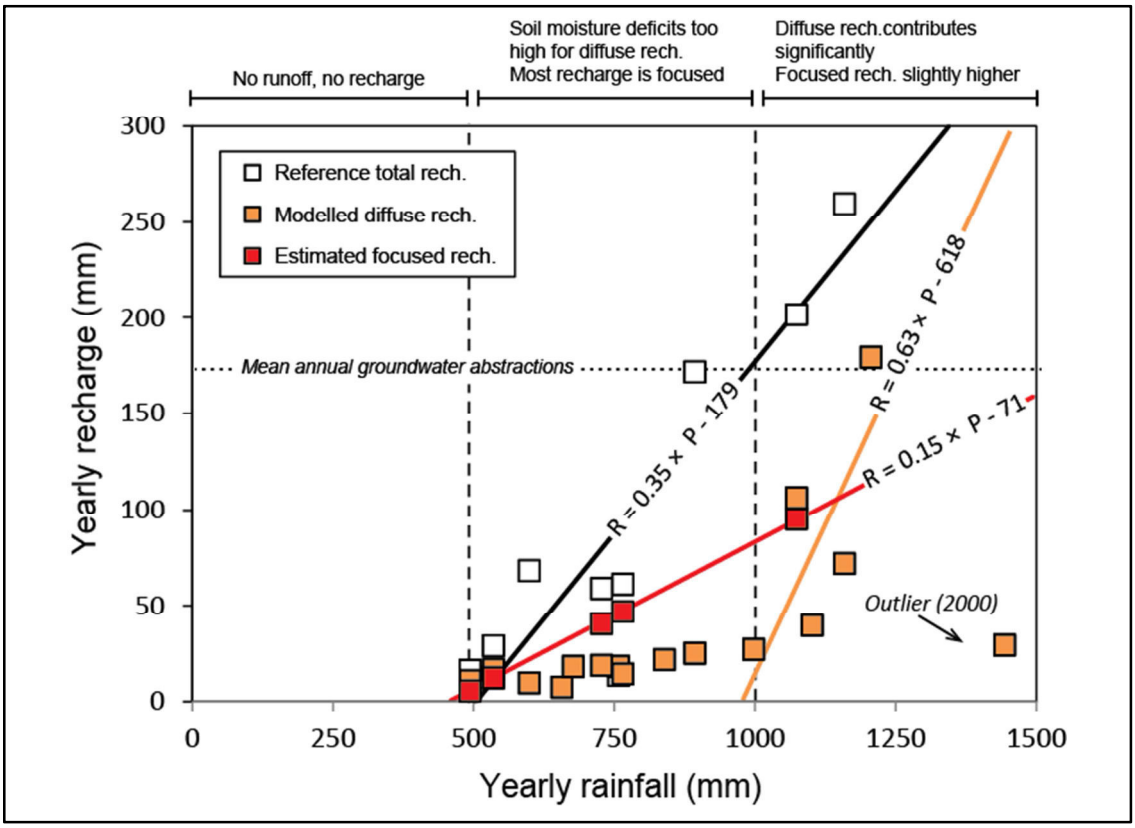

FIGURE 5.27: Summary diagram featuring the relationship between rainfall and recharge for diffuse recharge, focused recharge (this study) and total recharge (from Mizan, 2019). Mean annual groundwater abstractions shown (174 mm/yr) are from Dewandel et al. (2010).

Chapter 6

Managed Aquifer Recharge in fractured crystalline rock aquifers

Article: Managed Aquifer Recharge in fractured crystalline rock aquifers: impact of horizontal preferential flow on recharge dynamics (Nicolas et al., Journal of Hydrology)

Managed Aquifer Recharge in fractured crystalline rock aquifers: impact of horizontal preferential flow on recharge dynamics

Madeleine Nicolas [a,b], Olivier Bour [b], Adrien Selles [a], Benoit Dewandel [c], Vincent Bailly-Comte [c], Subash Chandra [d], Shakeel Ahmed [d], Jean-Christophe Maréchal [c]

[a] BRGM, Univ Montpellier, Indo-French Center for Groundwater Research, Uppal Road, 500007 Hyderabad, India

[b] Univ Rennes, CNRS, Géosciences Rennes - UMR 6118, F-35000 Rennes, France

[c] BRGM, Univ Montpellier, 34000 Montpellier, France

[d] CSIR-National Geophysical Research Institute, Indo-French Center for Groundwater Research, Uppal Road, 500007 Hyderabad, India

Article published in Journal of Hydrology

Received 30 August 2018, Revised 26 March 2019, Accepted 1 April 2019.

doi: 10.1016/j.jhydrol.2019.04.003

Abstract

To overcome water scarcity issues, Managed Aquifer Recharge (MAR) structures are currently developed in many parts of the world, including poorly permeable terrain like weathered crystalline rocks. In such geological context, characterized by relatively limited groundwater storage mainly associated with fractures located at the interface between the upper weathered layer (saprolite) and the fractured bedrock, the efficiency of MAR is poorly known. To address this question and better understand the factors that control recharge dynamics, an artificial recharge basin was implemented at the Experimental Hydrogeological Park in Telangana (South India), a well-equipped and continuously monitored site situated in Archean granitic terrain. The thickness of the saprolite and hydraulic properties are relatively well known all over the site from previous geophysical surveys and hydraulic tests.

To characterize recharge dynamics, recharge has been monitored in different boreholes surrounding the infiltration basin. Infiltration rates and water level data are interpreted by both a volume balance approach and different analytical solutions. In addition, a simple numerical model was used to show how the depth of the permeable interface between saprolite and granite controls recharge dynamics and observed water levels variations. Results show that the permeability of the saprolite/bedrock interface is sufficiently large to allow an efficient recharge that propagates laterally throughout the aquifer through this well connected interface. However, the variable depth of this permeable pathway controls the water level response, acting as a semi-impervious boundary, leading to remarkable water level variations. Thus, our findings show how the characteristics of the most permeable pathways control recharge dynamics in weathered crystalline rocks. In addition, we show how the depth variations of the permeable interface between saprolite and granite may be inferred from the monitoring of water level during recharge events.

Keywords: Managed Aquifer Recharge, Crystalline rock aquifers, Compartmentalization, Bedrock topography, Weathering interface, Numerical modeling

1. Introduction

Despite their low yields and complexity (Roques *et al.*, 2016), many regions in the world depend on fractured crystalline aquifers as the only source of freshwater (UNESCO, 1999), particularly in arid and semi-arid regions like India. Crystalline rocks cover about 70% of India's geographical area (Saha *et al.*, 2013). Furthermore, India has seen an unprecedented development of groundwater exploitation within the last 50 to 60 years. Irrigation potential increased from 6.5 M ha to 45.7 M ha (Sharma et al., 2005), out of which it is estimated crystalline rock aquifer groundwater represents more than 50%, especially in South India (Planning Commission, 2011). The advent of this "Green Revolution", aimed towards increasing agricultural output and achieving food security, has also brought on a number of water scarcity and groundwater quality degradation issues (Pingali, 2012; Pinstrup-Andersen & Hazell, 1985; R. Singh, 2000). Natural replenishment of groundwater reservoirs has become insufficient to keep pace with the excessive continued exploitation of groundwater resources in many regions, leading to a long-term drop of groundwater levels (Central Ground Water Board, 2013).

In this context, the government has set out to remediate water table depletion by increasing aquifer recharge from 9% of total rainfall under natural conditions to 15% by 2020 (Government of Andhra Pradesh, 2003) through the development of large-scale managed aquifer recharge (MAR) schemes. The Central Ground Water Board has proposed the building of 11 million MAR structures nation-wide, as well as the reparation, renovation and restoration of the already existing structures, the total costs tallying up to over 12bn USD (Central Ground Water Board, 2013). In the state of Telangana, it was estimated in the latest census of Minor Irrigation Sources that there are 46,531 percolation tanks, all of which the Department of Irrigation has set out to restore by 2020 (Irrigation & CAD Department, 2015).

Overall, common belief is that MAR initiatives are a viable and suitable solution to water scarcity issues. However, there is little consensus within published studies about their efficiency and impact, especially in hard rock context. At small scales (a few square meters to a few square kilometers), results often point towards increased groundwater resources and predominantly positive impacts of artificial recharge (Massuel *et al.*, 2014; Srivastava *et al.*, 2009), which benefit only landholders closest to the recharge facilities (Boisson, Villesseche et al., 2015; Dillon et al., 2009). Larger-scale studies (at the watershed scale or bigger) are less common (e.g. Glendenning *et al.*, 2012), on one hand, because of the difficulty in obtaining relevant data (de Marsily *et al.*, 2005), and on the other on the complexity associated with groundwater reservoirs in crystalline rock. Further, many of these studies are limited to water budget analysis and do not focus on hydrodynamic processes (e.g. Boisson, Villesseche et al., 2015; Scanlon et al., 2012).

While water budgets can provide useful guidelines for groundwater exploitation, many authors have pointed out their insufficiency in providing accurate estimates of safe yield and sustainability, highlighting the need to understand dynamic processes (Bredehoeft, 2002; Zhou, 2009). Information on dynamic processes is further necessary to make out the spatial distribution of artificial recharge.

Weathered crystalline rock aquifers are characterized by highly variable hydraulic properties (Acworth, 1987; Chilton & Foster, 1995; Dewandel *et al.*, 2012; Maréchal *et al.*, 2004) which result in a complex combination of diffuse recharge and preferential flows (Alazard et al., 2016; D. V. Reddy et al., 2009; Sukhija et al., 2003), where the latter have often been shown to dominate groundwater recharge processes (Cuthbert & Tindimugaya, 2010; Gleeson *et al.*, 2009; Sukhija *et al.*, 2003). In the aquifer, horizontal preferential flows take place in the most transmissive zones of the aquifer, which consist of the main open fractures and most importantly the bedrock weathering interface at the limit between the upper weathered layer (saprolite) and the fractured granite; this has been recognized by many authors (e.g. Acworth, 1987; Boisson, Guihéneuf et al., 2015; Chilton & Foster, 1995; Dewandel et al., 2006). The presence of these zones leads to a vertical anisotropy of permeability (Maréchal *et al.*, 2004, 2003). Since the bedrock weathering interface is in general hilly, its relief may control groundwater flows, leading to aquifer compartmentalization, where exchanges between compartments depend on water levels relative to interface topography (Guihéneuf *et al.*, 2014). The exact nature of the relationship between the bedrock weathering interface relief and recharge is not yet clearly understood. While this study focuses on fractured crystalline rock, it should be noted that the existence of sub-horizontal preferential flow pathways originating from sharp vertical contrasts in transmissivity exists in other type of media as well, such as stratified aquifers (Nimmo et al., 2017), and that the observations outlined in this paper may be applicable in these environments as well.

Artificial recharge may be affected by preferential flow paths in contrasting ways. Their existence could enhance recharge, allowing an efficient and rapid lateral transfer of percolation throughout the aquifer. On the other hand, the compartmentalization associated with these environments highlighted by previous studies, could possibly slow or stop the progression of infiltration fronts leading to focused recharge in specific areas. Monitoring of MAR infiltration front progression is therefore necessary to better understand the role of preferential flow paths on the efficiency of recharge processes in crystalline rock aquifers, not only from a quantitative standpoint but also in regards to water quality and pollution propagation issues.

The aim of this study is to characterize artificial recharge processes in weathered crystalline rock and analyze the complex flow dynamics of recharge inputs through the

main flow paths, namely the relief of the saprolite/bedrock interface. To do so, we monitored an artificial recharge basin that has been set up in an experimental site equipped with a network of observation borewells. A water balance and simple infiltration equations were used to quantify the inputs of the recharge basin and their temporal evolution, as well as the vertical hydraulic properties. Then, the lateral progression of the infiltration front in the underlying hard rock reservoir was analyzed. Analytical solutions were used to infer the lateral hydrodynamic properties of the media, while numerical modeling allowed us to quantify the effects of basement relief on recharge in order to explain the particularities of the observed recharge process.

2. Study site

The infiltration basin is situated within the Experimental Hydrogeological Park (EHP), which is a hydrological observatory located near the Choutuppal village in the Nalgonda district (Telangana state since 2014), 60 km to the south-east of Hyderabad (Latitude: 17°17'47"N; Longitude: 78°55'12"E), in South India (FIGURE 6.1). The site has been developed by the French Geological Survey (BRGM) in partnership with the Indian National Geophysical Research Institute (NGRI) and is part of the H+ Observatory network. Most data used in this study can be downloaded from the H+ database (http://hplus.ore.fr/en).

2.1. Geological setting

The site is located in an Archean granite setting, which represents over 80% of the total surface of the Telangana state. This granitic formation is intruded locally by geological discontinuities such as dikes or quartz reefs, but none are present on the EHP (Guihéneuf *et al.*, 2014). The fracturing of the granite is mainly characterized by subhorizontal fractures, which can display a lateral extension of tens of meters (Guihéneuf *et al.*, 2014). The typical geological profile in the EHP was obtained through analysis of drilling cuttings, and generally follows the description provided in Dewandel *et al.* (2006), namely:

- A thin red soil layer (a few centimeters).
- A sandy regolith layer 0-2 m thick, made up of a sandy-clay composition with quartz grains (Dewandel *et al.*, 2006).
- A laminated saprolite layer of variable thickness (ranging from 0 to 20m), derived from in-situ weathering of granite. It presents a millimeter-spaced horizontal laminated structure and coarse sand-size clasts and a few preserved conductive fractures (Dewandel *et al.*, 2006). Due to its composition, the saprolite layer can reach a quite high porosity (bulk porosities are mainly between 5% and 30%),

depending on the lithology of the parent rock and the degree of weathering (Dewandel *et al.*, 2006).

– Granite mainly consisting of quartz, potassium feldspars and biotite (Dewandel *et al.*, 2006). The few first meters of the granite, in contact with the laminated saprolite (i.e. the saprolite/granite interface), are highly weathered and fractured. The fracture density rapidly decreases with depth, although local transmissive fractures may be encountered up to 60 meters deep (Guihéneuf *et al.*, 2014) . The effective porosity of this layer is relatively low, of about 1%, and in mainly ensured by the fissure zones (Dewandel *et al.*, 2006).

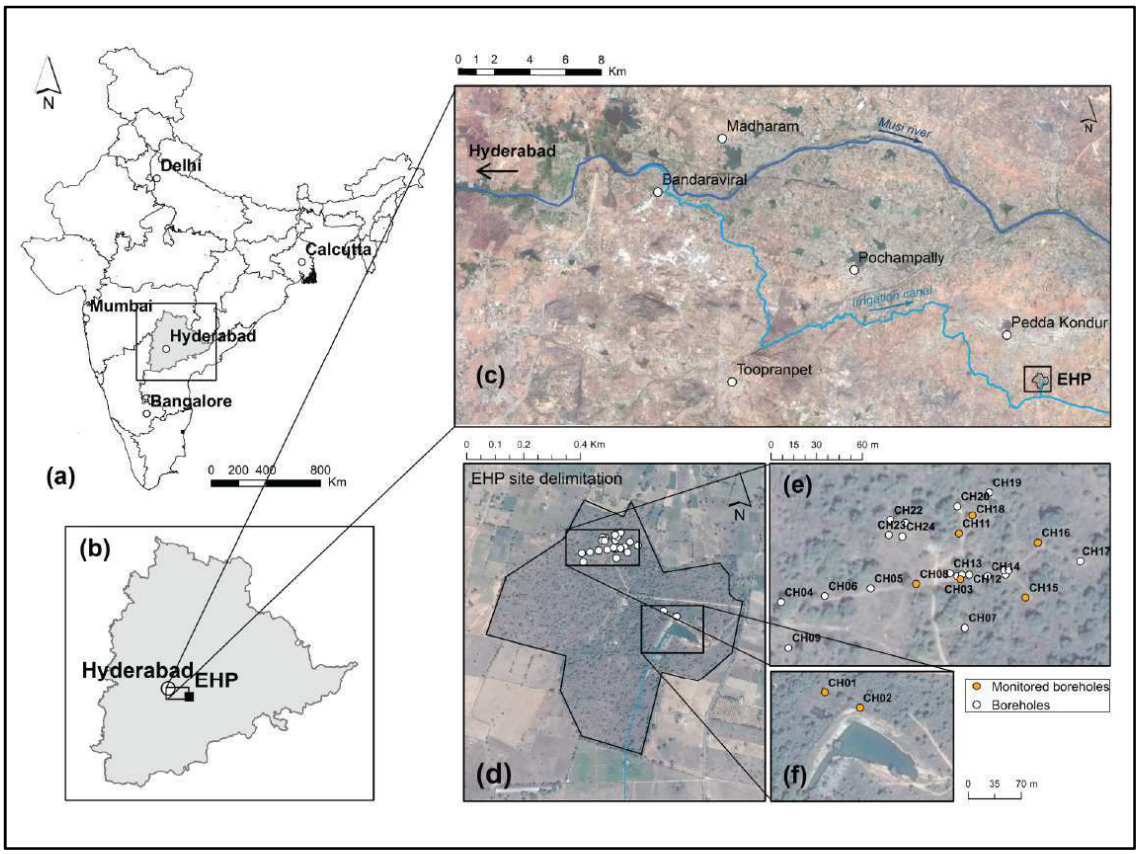

FIGURE 6.1: Study site location and position relative to Hyderabad (a, b), the Musi River and the supply channel (c); borewell position within EHP site (d, e, f), orange points are those equipped with pressure sensors.

2.2. Hydrological setting

The climate of this region is semi-arid and controlled by the periodicity of monsoons. Mean annual temperature is 28°C with high temperatures of about 45°C during the dry season. The rainy season occurs from June to November for a yearly average of about 800 mm. Ephemeral streams may be present during the monsoon but are most of the time absent. Intra-seasonal water level variations depend on groundwater recharge but

are generally comprised between 10 and 20 m below ground surface (m bgs) (FIGURE 6.2). There is no apparent straightforward relation between rainfall episodes and water

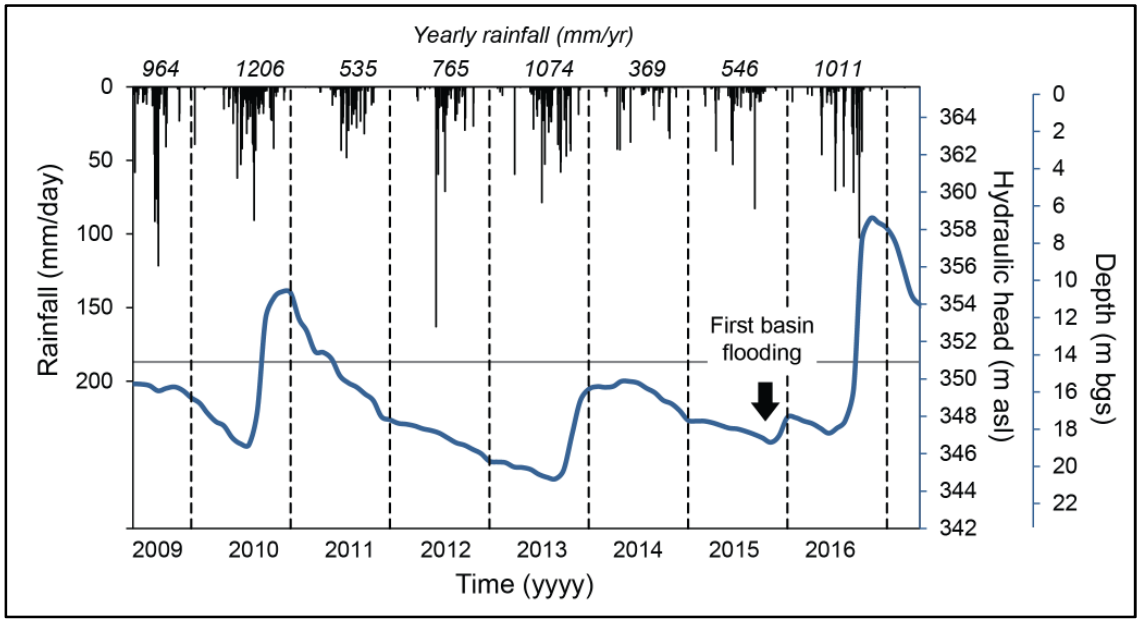

FIGURE 6.2: Hydraulic head variations in the CH03 borewell (longest on-site observed time series) and rainfall. Recharge basin was first filled by the end of 2015 (black arrow). The horizontal gray line illustrates the limit between the saprolite and the granite determined from borehole cuttings. For information relating to technical specificities of the well, refer to Guihéneuf (2014)

level variations, and some intense rainfall episodes do not elicit a groundwater response (like in 2012, 765 mm of rain, FIGURE 6.2).

Within the framework of the previously cited state-wise MAR project, an infiltration basin was dug on the EHP during 2015 to meet the demands of farmers in the area facing water scarcity. Land use in the vicinity of the observatory consists mostly of cotton fields, some rice paddies and a few orchards, although it is assumed pumping for irrigation does not impact water levels on the site as most pumped borewells are downstream from the site. The basin was dug using an excavator; its approximate dimensions are 120 m by 40 m, with a depth of about 2 m, effectively removing the regolith layer and extending into the saprolite. Debris was piled around the basin to create a bund and avoid spillovers. The basin is mainly supplied by a canal which deviates water from the Musi River, downstream the state capital, Hyderabad (FIGURE 6.1). The distance traveled by the canal between the Musi River and our study site is of about 40 km. Over this distance, the canal branches out into several smaller canals, which supply a network of infiltration basins throughout the region. The basin was initially filled by the end of 2015 (black arrow, FIGURE 6.2), but this period was not yet monitored. The continuous

monitoring of the basin began during the following filling episode which took place in July 2016. Groundwater levels significantly increased following the filling of the basin, reaching the highest levels ever monitored on-site (FIGURE 6.2). Note that in many countries, regulations state the need for an infiltration basin and the underlying aquifer to remain hydraulically disconnected (Bouwer, 2002; Carleton, 2010; Réfloch, 2018). This allows preservation of an unsaturated zone below the basin, which is necessary to allow aerobic processes to take place to partly prevent the propagation of contaminants. This criterion was not met during this study because the water supply relied on the sporadic opening of an upstream floodgate managed by a third party entity.

Previous works (e.g. Boisson, Guihéneuf et al., 2015; Maréchal et al., 2004), during which a series of hydraulic tests were performed on-site, have allowed the estimation of the media's hydrodynamic properties (FIGURE 6.3), namely the transmissivity (T, $m^2.s^{-1}$) and storativity (S). The upper fractured granite and the fractures within the granite were shown to be the most conductive with a good storativity (FIGURE 6.3) (Boisson, Guihéneuf et al., 2015). On the other hand, the saprolite layer was characterized as poorly transmissive. It must be noted, however, that several authors have suggested the potential of preserved fractures within the weathered saprolite to contribute to preferential flow (Dewandel et al., 2006; Perrin et al., 2011), and that overall knowledge on saprolite properties is currently limited.

In sum, the most transmissive zones of the aquifer are the upper fractured zone also known as the weathering interface, laterally well connected, and some permeable fractures encountered at greater depths, which conversely have a limited extension and continuity. Because the weathering interface has a variable depth (Dewandel *et al.*, 2006; St. Clair *et al.*, 2015), groundwater flow dynamics shift depending on water table elevation (Guihéneuf *et al.*, 2014). In the 2014 paper by Guihéneuf *et al.*, hydraulic tests performed under different water level conditions (high water levels and low water levels), in combination with observations on piezometric variations, revealed how aquifer compartmentalization causes this contrasting behavior. Under high-level conditions, the well-connected permeable upper granite/saprolite zone allows regional flows to take place, more specifically towards the northeast of the site (Guihéneuf *et al.*, 2014). Contrariwise, because fracture density and therefore connectivity decreases with depth, low water levels lead to a lateral compartmentalization of the aquifer. The system then shifts to an independent local flow system (Guihéneuf *et al.*, 2014).

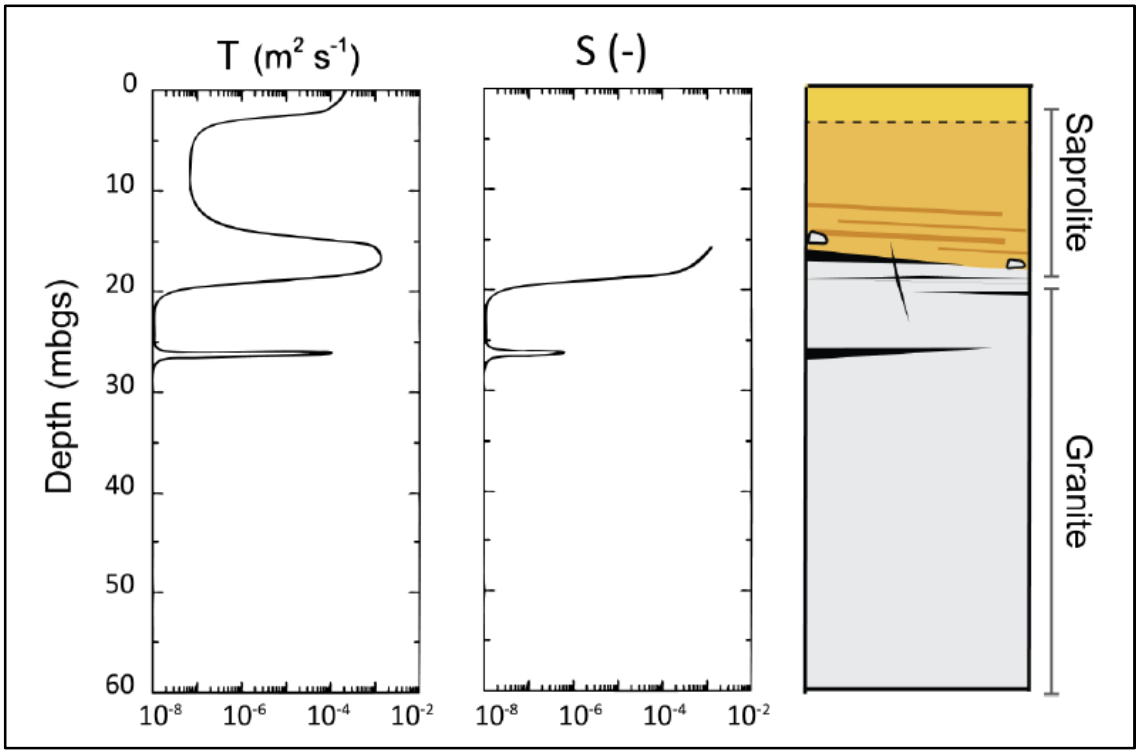

FIGURE 6.3: Conceptual model of transmissivity (T) and storativity (S) profiles by depth extrapolated from several hydraulic tests performed on-site by from Boisson, Guihéneuf et al. (2015) and schematic representation of geological log (modified from Boisson, Guihéneuf et al., 2015)(Boisson, Guihéneuf et al., 2015). Storativity measurements end at the top of the fissured bedrock because they could not be measured within the saprolite at the time of the study as the boreholes are fully cased down to the contact between saprolite and fissured bedrock

The site is equipped with 30 borewells of different depths (FIGURE 6.1), all of which are equipped with a casing extending into the saprolite, screened or open at the contact zone between the saprolite and the fractured granite. TABLE 2.1 features the technical characteristics of the site boreholes which were used for this study, and the hydraulic properties at each of these wells may be found in Guihéneuf et al. (2014). Note that the saprolite thickness, which ranges from 14 m to 24 m, is very variable (TABLE 2.1). 8 boreholes were continuously equipped with pressure and temperature sensors measuring piezometric levels and temperature during the time of this study. An additional probe was installed in the infiltration basin to monitor water levels in the basin. At the time-scales considered, the fracture system within the fractured granite and the overlying saprolite are assumed to be at equilibrium, meaning there is no significant pressure difference between the unconsolidated saprolite and the fractures in the underlying granite. This was later confirmed when superficial wells (<15 m) were dug only in the saprolite near the CH01 and CH02 boreholes (FIGURE 6.1f) which featured virtually the same hydraulic head variations as the deeper wells. This is consistent with the unconfined

response (high storativity, FIGURE 6.3) of the interface to pumping tests under packers which confirms the role of vertical fractures in connecting overlying saprolite with underlying fractures.

	X (m)	Y (m)	Elevation (m asl)	Borehole depth (m)	Casing depth (m bgs)	Estimated saprolite thickness (m)
CH01	279075.05	1913316.12	365.69	73.20	23.90	24.00
CH02	279120.68	1913296.32	366.31	73.20	18.75	19.00
CH03	278906.31	1913534.27	365.63	50.30	14.20	14.70
CH08	278876.59	1913531.05	366.11	61.00	17.30	18.00
CH11	278904.75	1913564.44	365.70	56.40	21.00	19.50
CH15	278949.36	1913522.31	364.60	56.40	18.30	17.90
CH16	278956.63	1913558.42	364.61	56.40	17.30	15.20
CH18	278914.12	1913576.32	365.57	50.30	19.80	21.35

TABLE 6.1: Boreholes characteristics of the Experimental Hydrogeological Park in Choutuppal (Andhra Pradesh, Southern India) from Guihéneuf et al. (2014). Boreholes location is provided in the UTM projected coordinate system. Borehole depth and casing depth are given in meters below ground surface.

2.3. Water level variations in response to recharge

The filling of the artificial recharge basin caused water levels to rise significantly (FIGURE 6.4). The basin remained flooded for most of the observation period, although levels in the basin varied widely from a few cm up to almost 3 m depending on the sporadic canal inputs. Each filling episode was followed by a recession period ranging from a few days to a few months, becoming longer towards the end of the observation period.

Borewells can be divided into two groups relative to their groundwater level variations. The first, composed of CH01 and CH02, is the cluster closest to the basin. The second comprises the boreholes in the cluster farthest from the basin (CH03 to CH24), out of which only 3 are shown along the AB profile (FIGURE 6.4) for clarity purposes. The two groups are characterized by different patterns of water level variations but have similarities between them. There are three identifiable phases for both clusters depending on the time, t, of observation, starting from t=0, which is the beginning of the monitoring period (July 5th 2016):

- **P1** $\mathbf{0 < t < 60}$ days (approx.). The overall range of variations is weak. The water levels for neighboring boreholes (CH01 and CH02) remain deep (about 15 m below surface) close to water levels observed before basin infilling. This suggests the water table remains disconnected from the infiltration basin during this period of time.

- **P2** $60 < t < 80$ days (approx.). An abrupt increase in water levels, of about 15 m, is observed for neighboring boreholes (CH01 and CH02), while the basin water levels vary between 1 and 2 meters. During this period, hydraulic head reaches near-surface levels (CH02 is at 366.3 m asl and CH01 at 365.7 m asl). Such variations suggest that the basin and the aquifer are becoming hydraulically connected. The increase in remote water levels (CH03 to CH24) is much weaker but shows a clear response. This phase ends at around 80 days, where an important inflection point can be observed (FIGURE 6.4) marking a change in dynamics.
- **P3** $t > 80$ days. For this period of time, water levels in the closest boreholes (CH01 and CH02) are very high, close to ground surface levels suggesting that the basin remains connected to the water table. Remote boreholes appear to increase strongly during the first 40 days where water levels reach a depth of only a few meters below ground. Interestingly, remote borehole levels appear to evolve in sync with very similar hydraulic heads measured in all boreholes.

These observations suggest that P2 is a transition phase between the disconnected phase P1 and the fully connected phase P3 during which the basin fills the whole aquifer. Accordingly, the hydraulic response for remote boreholes is delayed in relation to neighboring boreholes. When levels in the near vicinity reach a pseudo-steady-state, remote water levels begin increasing simultaneously. This indicates a sort of tipping point mechanism: the attenuation of water level increase in the near vicinity of the basin is related to the progression of the pressure front laterally.

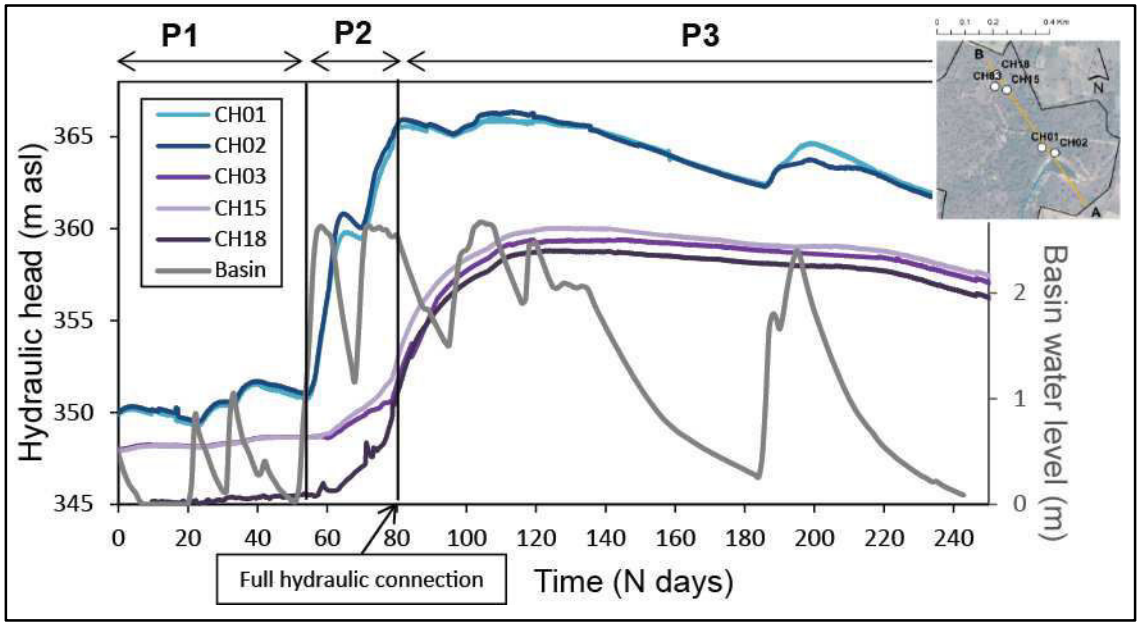

FIGURE 6.4: Basin water level variations (gray curve) and associated hydraulic head variations in site boreholes shown in FIGURE 6.1. Only 3 boreholes are shown for clarity purposes, as variations between neighboring boreholes was very similar.

3. Methods

The methodology applied aims to characterize the hydraulic properties controlling infiltration and its lateral transmission throughout the aquifer, as well as the effects of bedrock topography on the transient aquifer response. This was done through a combination of analytical and numerical modeling using water levels in the basin, meteorological data (rainfall and potential evapotranspiration) and the observed water level response in the observation boreholes. Daily rainfall was measured on-site using an automatic weather station, and daily open pan evaporation was measured and made available by ICRISAT (International Crops Research Institute for the Semi-Arid Tropics, about 80 km away from our site).

3.1. Estimating infiltration rates and vertical hydraulic conductivity

Infiltration (Inf) from the basin into the aquifer was quantified to characterize recharge, and to be used as inputs to the analytical and numerical aquifer response models posteriorly described. To do so, a volume balance approach (VBA) was applied in parallel to infiltration equations that will be described hereafter.

The VBA approach requires knowledge of all of the water balance components: canal inflow Q_{in}, rainfall P, evaporation E, and basin stock variations dH, all of which are in mm/day:

$$Inf = Q_{in} + P - E - dH \tag{6.1}$$

It was assumed that the runoff component, considering the small impluvium surface (<1ha), was negligible. Because it was not possible to measure canal inflow directly for technical reasons, the VBA approach was only applied to recession periods, where Q_{in} is assumed to be null. dH was deduced from the water levels measured continuously in the basin (H) where $dH = H_t - H_{t-1}$. E was assumed to be equal to open pan potential evaporation measurements. The equation was applied at a daily time step. The VBA approach is the most complete as it accounts for all inputs and outputs to the system although it is not applicable during basin filling periods.

In the absence of rainfall and neglecting evaporation, one also expects infiltration rates to be simply related to water levels in the basin, with greater water levels leading to greater infiltration. To examine such relationships, infiltration rates from basin water level variations during recession periods were compared to the corresponding water levels in the basin. Thus, the relationship $Inf = \alpha \times H$ (with α as the coefficient of proportionality) was evaluated empirically. If a satisfactory relationship is obtained during recession periods, such relationship may be extrapolated to all times, including infilling peri-

ods. Comparison to VBA infiltration ensured that neglecting P and E is not too strong of an assumption. Finally, with infiltration roughly deduced from basin water levels, the canal inflow Q_{in} can be calculated during infilling periods as the remnant of Eq. (6.1).

Note that these relationships can generally be described by Darcy-type equations, directly linking infiltration to water levels based on knowledge of saturated thickness and hydraulic conductivity (Bouwer, 2002). It was not possible to estimate hydraulic conductivity during the initial phases (P1 and P2) because the depth of the wetting front and the apparent hydraulic conductivity are poorly constrained in partially saturated environments.

When there is a full hydraulic connection between the basin and the aquifer (P3), one may assume that the system may be equated to a falling head permeameter during the recession periods. Flows are assumed to be mainly vertical within the saprolite before reaching the weathering interface, which is assumed to be an a priori much more conductive zone. It therefore is assumed that flows are mainly controlled by the saprolite's properties, which offer the greater resistance to flow, and the head gradient over the saprolite's thickness. The hydraulic head at the bottom of the saprolite may be given by the hydraulic head in the closest boreholes, which are very close to ground level. Thus, the head gradient may be roughly estimated equal to H/L, i.e. the difference in hydraulic head between the top of the saprolite $(H + L)$ and the bottom of the saprolite (L), with L the thickness of the saprolite. The vertical flow can be thus described using the Darcy equation:

$$Inf = K_V \frac{H}{L} \tag{6.2}$$

where K_V is the vertical hydraulic conductivity (L.T^{-1}). Knowing that $Inf \approx -\frac{dH}{dt}$ during recession periods, this equation can be rearranged to yield $-\frac{dH}{H} = \frac{K_V}{L} dt$, where the boundary conditions of this problem are $H = H_0$ at $t = 0$. If we integrate dH/H on the left hand side from H_0 to H and the right hand side from 0 to t, then $ln\left(\frac{H_0}{H}\right) = \frac{K_V}{L} t$. This yields:

$$\frac{H}{H_0} = e^{\frac{-K_V}{L} t} \tag{6.3}$$

To check the consistency of the above equation, observed water levels were plotted for each recession posterior to hydraulic connection (P3 phase). When verified, a linear regression allows estimating of $-\frac{K_V}{L}$, and with known L hydraulic conductivity can be deduced. Finally, having estimated K_V during recession period allows estimating infiltration also for the infilling periods using Eq. (6.2).

3.2. Modeling the aquifer response to infiltration

In a second step, we calibrated an analytical solution modeling groundwater level variations against observations to provide an estimate of the hydrodynamic parameters controlling lateral flow. The effects of the transmissive interface's relief on flow, however, were ascertained using simple numerical modeling since no analytical solution was available for this purpose. To do so, different scenarios were tested where bedrock relief and hydrodynamic properties were varied to assess the changes in groundwater response, and the overall likeness to the dynamics observed on the experimental site.

3.2.1. Analytical solutions

Calibration of simple analytical solutions against observed groundwater levels can allow a first-order estimation of the horizontal hydraulic conductivity and storativity controlling groundwater flow.

Groundwater mechanisms are described by different mathematical models depending whether there is a hydraulic connection between the basin and the water table or not (FIGURE 6.5). The most common analytical solutions for groundwater mounding are valid only in situations where the water table is assumed to be hydraulically disconnected from the bottom of the groundwater infiltration basin. Conversely, analytical modeling of mounds that are fully connected to any recharge structure is relatively rare and most often concerns streams or canals (e.g. Dillon & Liggett, 1983; Spanoudaki *et al.*, 2010); modeling of connected recharge basins or lagoons (e.g. Kacimov *et al.*, 2016) is much rarer. Further, if the mechanisms in place deviate from standard conditions assuming homogeneous media, then fully realistic descriptions of these processes are said to be beyond any simple analytical solutions (Alderwish, 2010). In this context, it was decided to use analytical modeling only in the initial phase of wetting and mounding (P1), when the recharge basin is clearly disconnected from the aquifer and thus flow conditions remain relatively simple and respect the initial conditions required. Because remote boreholes (CH03 to CH24) show little to no response during this phase, analytical modeling was only calibrated against observations in neighboring boreholes (CH01 and CH02), which show a clear response to basin infilling even during the initial phase of wetting and mounding (P1). We used Hantush's solution for rectangular basins (Hantush, 1967).

3.2.1.1. Hantush's solution for rectangular basins

In general, analytical solutions to predict the rate of growth and shape of a recharge mound solve the governing partial differential equation describing the flow of groundwater as given by the linearized Boussinesq equation (Warner *et al.*, 1989):

$$K\bar{b}\left(\frac{\partial^2 h}{\partial x^2}+\frac{\partial^2 h}{\partial y^2}\right)+R=S\frac{\partial h}{\partial t} \tag{6.4}$$

where the different variables and parameters are defined in FIGURE 6.5. The solution developed by Hantush (Hantush, 1967) simulates groundwater mound growth and decay in response to percolation, and is valid when the top of the groundwater mound is disconnected from the bottom of the recharge basin:

$$Z = \frac{R\bar{b}}{2S}\int_0^t \left(\operatorname{erf}\left(\frac{\frac{L_b}{2}+x}{\sqrt{4\upsilon\tau}}\right)+\operatorname{erf}\left(\frac{\frac{L_b}{2}-x}{\sqrt{4\upsilon\tau}}\right)\right)*\left(\operatorname{erf}\left(\frac{\frac{W_b}{2}+y}{\sqrt{4\upsilon\tau}}\right)+\operatorname{erf}\left(\frac{\frac{W_b}{2}-y}{\sqrt{4\upsilon\tau}}\right)\right)d\tau \qquad (6.5)$$

where $Z = h^2 - b^2$, υ is a simplifying term with $\upsilon = K\bar{b}/S$ and $\tau = (t - t')$, the time during which percolation takes place. Initial conditions assume a horizontal water table and the boundary conditions of zero slope of the mound profile at the center of the basin and at infinity.

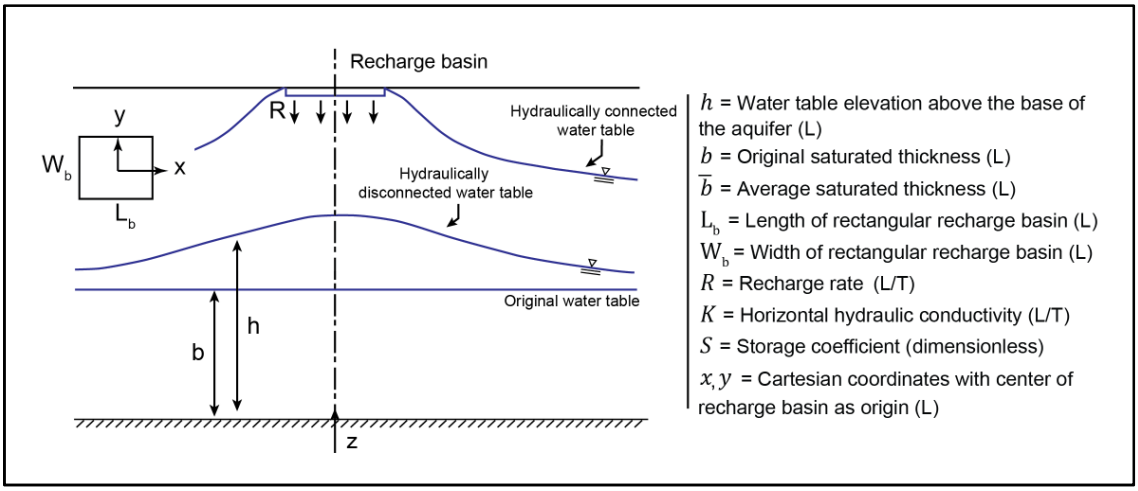

FIGURE 6.5: Schematic representation of water level variations in response to artificial recharge from an infiltration basin featuring parameters used in analytical modeling of artificial recharge (adapted from Warner *et al.*, 1989)

In Eq. (6.5), recharge from infiltration is assumed to be constant. However, infiltration was found to vary significantly in time. To get around this issue the approach was modified: rather than directly integrating Eq. (6.5) by Gauss quadrature, a convolution of the impulse response of the aquifer to $R = 1$ and the daily infiltration time-series was made, so that at a given time t:

$$Z(t) = \sum_{k=1}^{t} Z_{k-1} + ZU(k) * R(t-k) \qquad (6.6)$$

where ZU is the impulse response and R is the recharge rate assumed equal to daily infiltration. This solution was applied and calibrated at each borehole for which hydraulic head measurements are available, where x, y, b, and $\bar{b}$ were set to match the borehole's position and initial water table conditions.

Hydraulic conductivity (K) and storativity (S) were obtained by optimizing the analytical models' performance, i.e. minimizing the root mean square error (RMSE) between h_{sim} (simulated water table elevation) and h_{obs} (observed water table elevation). The 2D parameter space was thus explored in order to reach a parameter set for which the error was minimal and which fit realistic standards. The resulting 2D RMSE matrix was then analyzed to assess whether the model converged towards a unique solution, as opposed to a situation where there is equifinality of parameters, which implies there are several acceptable sets of parameters that cannot easily be dismissed and should be considered in the evaluation of uncertainty (Beven, 2006).

Because this solution simulates how recharge inputs move laterally throughout the aquifer, and considering the important vertical anisotropy of hydraulic conductivity in fractured crystalline aquifers (Maréchal *et al.*, 2004, 2003), K is assimilated to horizontal hydraulic conductivity.

3.2.2. Numerical modeling for connected basin

While analytical solutions are easily and straightforwardly applied, they do not account for the geometry of the aquifer and specific boundary conditions. Under these circumstances, we tested the effect of bedrock relief on drawup, i.e. the increase of water level due to basin infiltration, using MODFLOW and its BCF2 package (which allows wetting of previously dry cells) (Harbaugh, 2005). MODFLOW is a US Geological Survey block-centered finite-difference modular flow model, and the source code is free public domain software. The model was run using FloPy (Bakker *et al.*, 2016), a Python package for creating, running and post-processing MODFLOW-based models.

The numerical simulations were based on very simple conceptual models. First, a synthetic scenario with constant recharge was tested in order to analyze the causal relationship between the boundary conditions imposed by the bedrock relief and the groundwater response to recharge. Synthetic results were roughly compared to field results. At this stage however the objective was not to attempt to perfectly match the observed groundwater response to infiltration. Then, in a second step aimed at better reproducing the recharge dynamics, actual estimated infiltration rates were used as inputs to the model.

The conceptual models tested all consist of a rectangular, unconfined aquifer overlain by a thick unsaturated zone with an infiltration basin in its central part (FIGURE 6.6). The infiltration basin covers 6400 m^2 and recharges the aquifer at a rate R of 1 $\times 10^{-6}$ $m.s^{-1}$ (about 85 $mm.day^{-1}$) for the synthetic tests, or at a transient rate determined by previously calculated infiltration for the final applied scenario. Recharge is applied to the highest active cell (which is automatically determined), meaning there is no retardation

or storage of water in the unsaturated zone. This is equivalent to simulating a partially or fully hydraulically connected environment, i.e. P2 and P3. The initial phase P1 was not simulated due to poorly constrained boundary conditions during this unsaturated phase, and because the MODLFOW model does not accurately accommodate transient unsaturated flow. Hydraulic parameters S and K were varied over one and an half and two orders of magnitude respectively ($1 \times 10^{-3} < S < 5 \times 10^{-2}$ and $1 \times 10^{-5} < K < 1 \times 10^{-3}$ m.s^{-1}) to test the sensitivity of the model to these parameters while remaining in a realistic range and were later fixed respectively at 1×10^{-2} and 1×10^{-4} m.s^{-1} to match the first-order estimation of parameters from the analytical model for the synthetic tests, or more precise values for the applied scenario. The ratio of vertical to horizontal conductivity was fixed at 1/10 according to Maréchal *et al.* (2004) results.

We only simulate one quadrant of the aquifer (FIGURE 6.6a) because all four quadrants are symmetrical (therefore there is no flow between quadrants). The hydrological system was simulated using a grid of 100 rows and columns with a 20 m spacing (for a total model size of 2000×2000 m, size at which it was estimated the outer boundary conditions did not affect the results for the simulated duration) and six 5 m thick layers (necessary to model stability) (FIGURE 6.6b). To ensure that the grid size and disposition were stable tests were performed where the size of the model and of the grid cells were varied to ensure water levels near the boundary remained stable. Initially, layers 1-5 are dry, head is 5 m and only the deepest layer is saturated. The evolution of the groundwater mound over time was modeled using a transient simulation, which was run for one stress period of 300 days with a one day time step using the PCG2 solver.

Two scenarios were tested using two model configurations: a reference scenario, in which there is no compartmentalization, and a compartmentalized scenario where an impervious boundary was added (FIGURE 6.6c). The reference scenario was used to simulate water table mounding resulting from local recharge in homogeneous conditions with a sub-horizontal bedrock. The other scenario accounted for the more complex boundary conditions imposed by the basement relief, by featuring a cuboid depression at the center. The depression was aimed at representing a topographic depression at the granite/saprolite interface, as it was determined from previous Electrical Resistivity Tomography (ERT) soundings that the recharge basin is located above a bedrock depression. This was done by adding an impermeable (K and $S = 1 \times 10^{-20}$) layer covering the bottom of the aquifer except at the center where the compartment is located (FIGURE 6.6). We tested different compartment widths (ranging from 100 m to 1000 m with a 100 m interval) and heights (from 5 m to 25 m with a 5 m interval) to test their causal relationship to groundwater drawup dynamics.

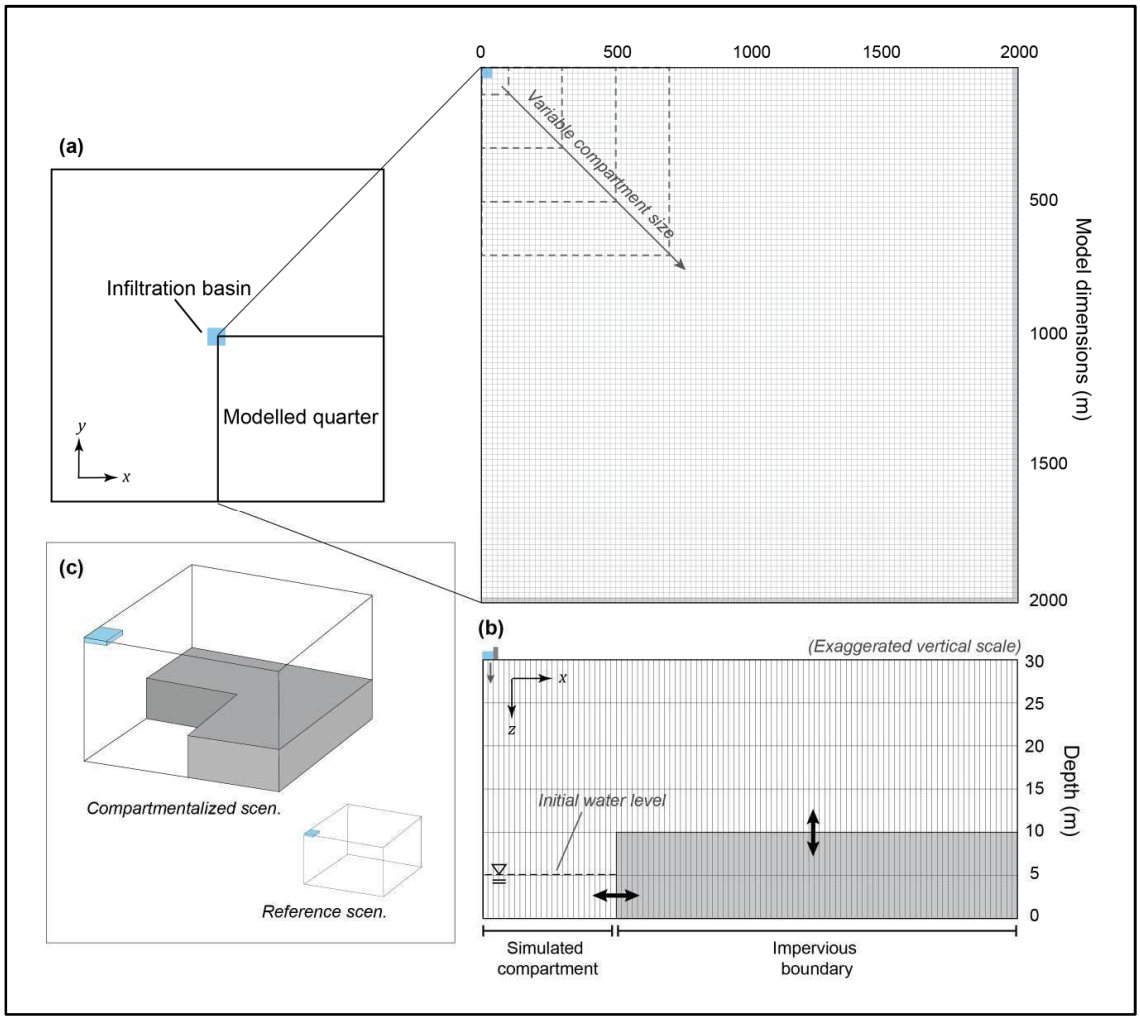

FIGURE 6.6: Model grid (a) and layer (b) configuration used for numerical modeling (modified from Chiang & Kinzelbach, 1992) with a conceptual 3D representation of the model's two scenarios (c)

Finally, a simulation was run using the site's actual infiltration estimations from 3.1 as inputs to account for the observed variability of inputs over time and fit the model to observations. Hydraulic parameters were set equal to those obtained with the analytical solution, only the compartment size was adjusted to fit the simulation to the observed data. This allowed us to test the model's ability to simulate the observed groundwater variations by assuming a heterogeneous basement elevation.

4. Results

4.1. Infiltration estimation and relative contributions

Estimating infiltration from the VBA (Eq. (5.2)) or from water levels in the basin (Eq. (6.2)) was almost equivalent. Rainfall and evaporation do not have a strong effect on stock variations, relative to canal inflow and infiltration. In total, it was estimated canal inflow accounted for 97% of inputs to the basin, and infiltration for 95% of outputs (TABLE 6.2): they are the main drivers of stock variations. Note that infiltration from recession periods was obtained using a volume balance approach, and then linked to water levels in the basin to obtain relationships that could be extrapolated to filling periods. These relationships were indeed found to be linear and are shown in full below. As explained in the previous section, canal inputs were estimated as the remnants of Eq. (5.2) with known infiltration.

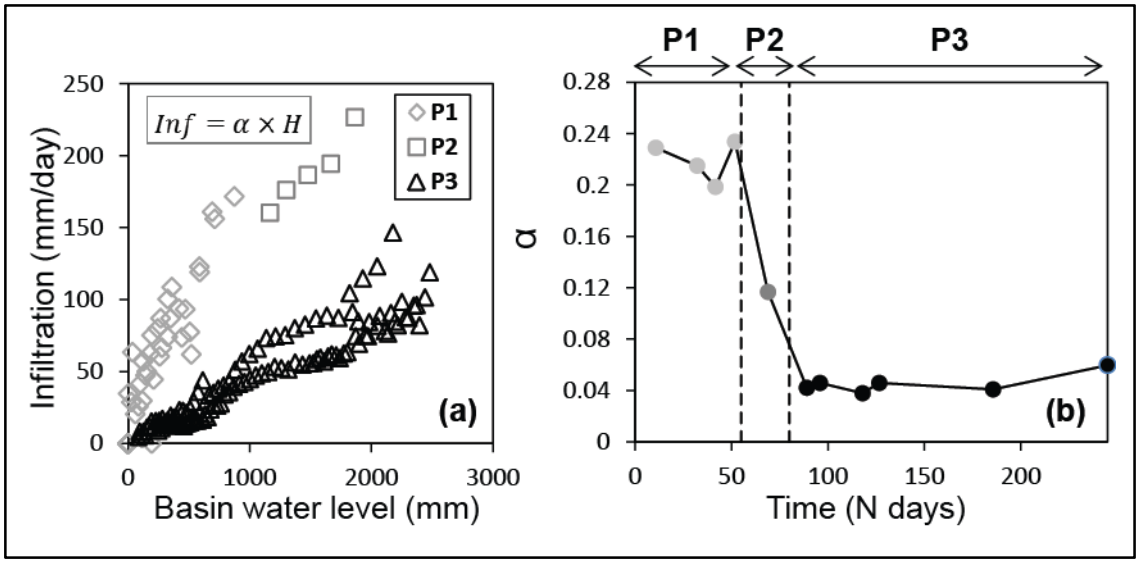

FIGURE 6.7: Infiltration relative to water levels in the basin for each phase of infiltration (a) and proportionality coefficients between infiltration and basin water levels plotted as a function of time. Proportionality coefficients are obtained for each individual recession period following the equation $Inf = \alpha \times H$ (b).

Inputs from the canal are quite high (FIGURE 6.8), and concentrated into short periods of time. Infiltration takes place more homogeneously throughout the observation period, but there are still non-negligible variations that mimic but do not follow perfectly water level variations (FIGURE 6.8). Interestingly, when the recharge mound reaches the base of the aquifer, between 55 and 65 days approximately, infiltration reaches its maximum value around 350 mm/day for a water level in the basin close to 2.6 meters. Regardless of the large amounts of water brought on afterward, and similar basin water levels, recharge remains bounded, reaching at most about 150 mm/day suggesting a de-

crease in the recharge potential. Another way to show this evolution is to investigate the evolution of the relationship between daily infiltration and water levels in the basin (FIGURE 6.7a) for each recession period.

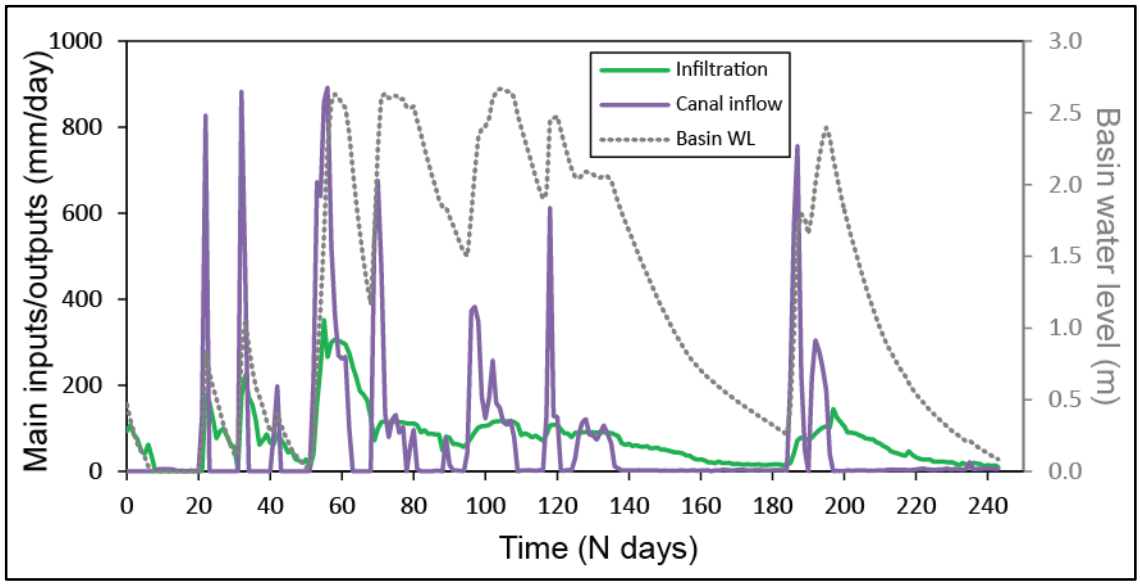

FIGURE 6.8: Infiltration and canal inflow estimated for the observation period. Inflow is episodic and short-lived as it is controlled by the opening and closing of an upstream floodgate managed by a third-party entity.

Infiltration is roughly proportional to water levels in the basin, as expected from Eq. (6.2), but with different relations for the different period of recessions. The coefficient of proportionality, α, decreases strongly with time (FIGURE 6.7) during phase P2. For times greater than 80 days (P3), no significant changes are observed, however the efficiency of the infiltration seems to be reduced by a factor of 6 from the early times until 80 days. This behavior is expected when connecting the basin with the aquifer (Bouwer, 2002; Carleton, 2010) because of the decrease in hydraulic gradient which results from the pore space filling up at the point of hydraulic connection. This further supports the statement that P2 is a transition phase during which the basin becomes hydraulically connected to the aquifer.

	Total contribution (mm)	**Relative contribution (%)**
Rainfall	680	3
Canal inflow	19,230	97
Total estimated input	19,900	100
Pan evaporation	960	5
Infiltration	19,140	95
Total estimated output	20,100	100

TABLE 6.2: Contributions of water budget components

4.2. Vertical hydraulic conductivity

Vertical hydraulic conductivity posterior to hydraulic connection was obtained using Eq. (6.3), from the recession slopes shown in FIGURE 6.9. It was found to vary slightly between each recession slope, ranging from 7.4 × 10^{-6} m.s^{-1} to 9.4 × 10^{-6} m.s^{-1}, averaging 8.1 × 10^{-6} m.s^{-1}. Such values are slightly higher than what is typically expected in the saprolite in this area, but much lower than the most transmissive pathways at the interface between saprolite and the upper fractured granite (FIGURE 6.3) (Boisson, Guihéneuf et al., 2015; Guihéneuf et al., 2014).

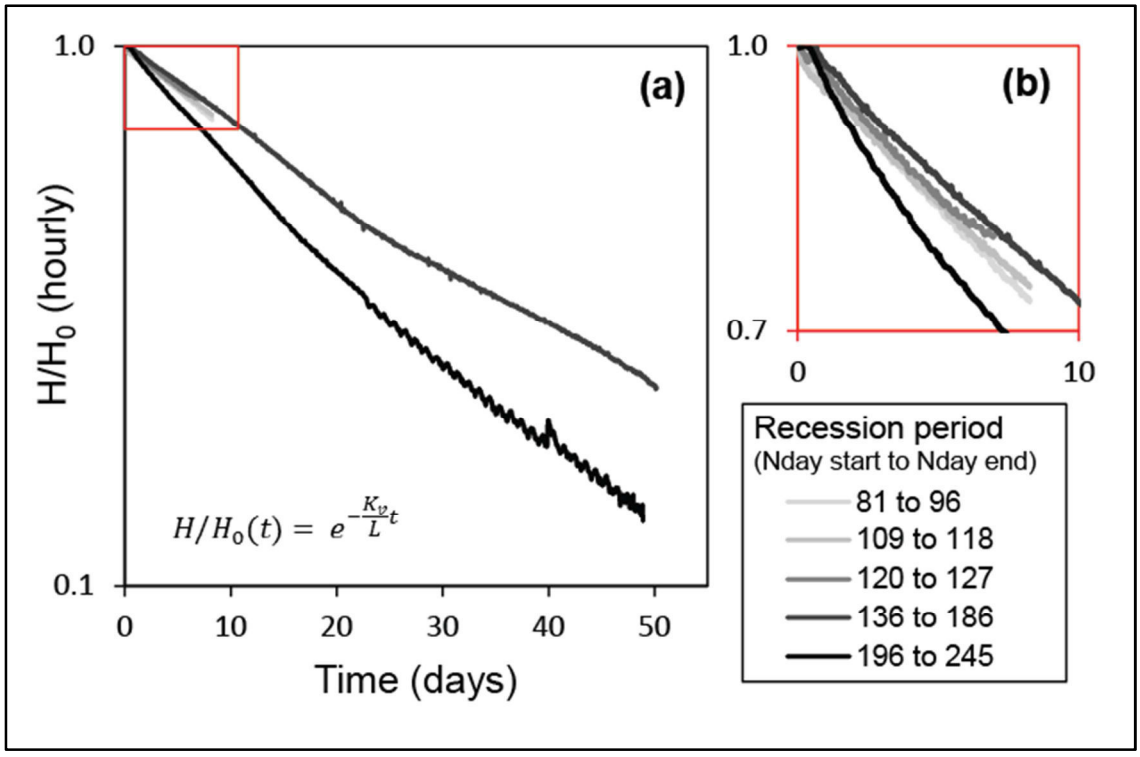

FIGURE 6.9: Recession slopes when the basin is fully connected to the aquifer (P3) at an hourly time-step plotted on a semi-log axis where the slope is equal to $-\frac{K_V}{L}$ (a), and close-up of the shorter recession slopes (b). Each line corresponds to a different recession slope; five different recessions are shown.

4.3. Horizontal hydraulic conductivity and storativity

Calibration of observed groundwater levels to simulated water levels for the disconnected phase (P1) using the Hantush solution resulted in the parameters summed up in TABLE 6.3. The best model fits can be seen in FIGURE 6.10.

RMSE was normalized by the range of variation ($NRMSE = \frac{RMSE}{h_{max} - h_{\min}}$). Model error was satisfactory, $NRMSE$s being weaker than 5%. Averaged to all boreholes hydraulic conductivity was found to be 6.5 × 10^{-5} m.s^{-1} with little variability between both esti-

mates. This estimate is clearly higher than the estimate of the hydraulic conductivity of the saprolite obtained from water level recessions, averaging 8.10^{-6} m.s^{-1}, but very close to what Boisson, Guihéneuf et al., (2015) and Guihéneuf *et al.* (2014) obtained for the weathering interface (FIGURE 6.3, $\bar{T} = 1.3 \times 10^{-4}$ m^2.s^{-1} and thus $\bar{K} \approx 10^{-5}$ m.s^{-1} the interface being a few meters thick). Storativity was found to be around 5×10^{-2}, which is higher than the FIGURE 6.3 weathering interface estimate ($\bar{S} = 9.7 \times 10^{-3}$), denoting a possible influence of the saprolite on the apparent estimated storativity. According to the variations of storativity between CH01 and CH02, it nevertheless seems to weaken as we move away from the basin.

	Distance to basin center (m)	***K*** **(m.s^{-1})**	***S*** **(-)**	***NRMSE*** **(%)**
CH01	100	7.0×10^{-5}	3.0×10^{-2}	1.5
CH02	67	6.0×10^{-5}	7.0×10^{-2}	1.4
	Geometric mean	6.5×10^{-5}	5.0×10^{-2}	

TABLE 6.3: Hydraulic properties obtained from calibration of analytical simulations to observed hydraulic head

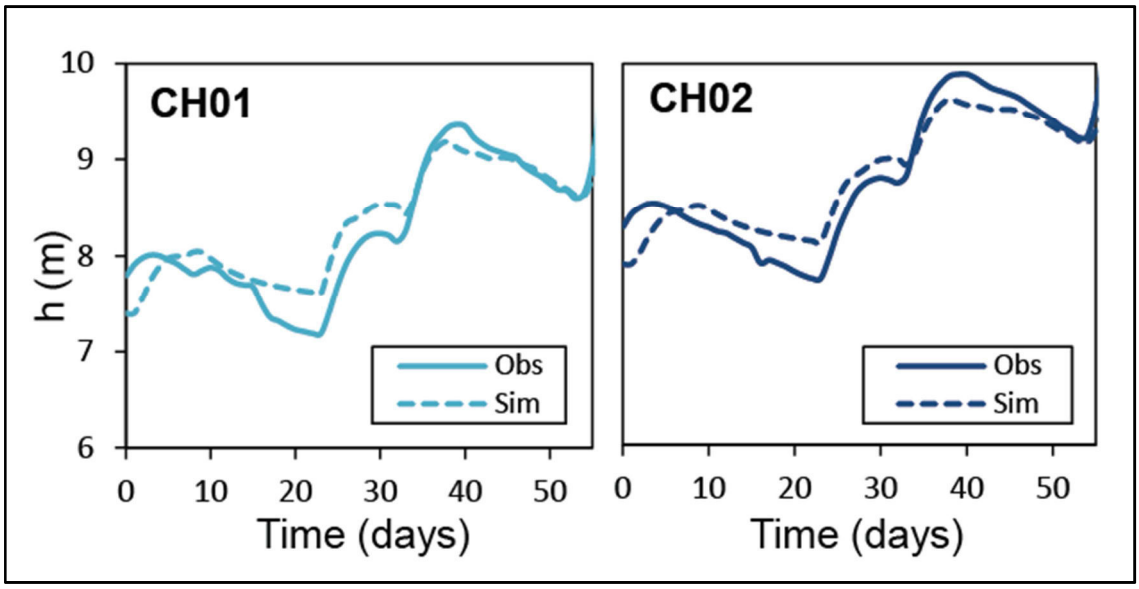

FIGURE 6.10: Observed hydraulic head and simulated hydraulic head using analytical modeling in response to infiltration from the recharge basin when it is disconnected from the water table (P1) for the boreholes closest to the basin (CH01 and CH02)

4.4. Effect of bedrock relief (numerical model)

4.4.1. Synthetic scenarios

Synthetic results obtained from numerical simulations are shown in FIGURE 6.11. The reference model, with parameters in the range of those obtained from analytical

simulations ($K = 10^{-4}$ m.s^{-1} and $S = 10^{-2}$), showed very weak variations and a weak drawup slope (black curve on FIGURE 6.11a and b), which cannot explain observed water level variations from the study site. Recharge dynamics cannot be modeled satisfactorily using these reasonable hydraulic parameters. Sensitivity tests (not shown in FIGURE 6.11) were also performed on K and S. S variations of one order of magnitude led to a difference lower than 2 m. Decreasing K elicited a stronger groundwater response but with a weak drawup slope, again disagreeing with observed data.

The most realistic simulation is obtained when considering a heterogeneous basement, and thus semi-penetrating impermeable boundary conditions. The lateral extension of the depression/compartment at the center of the model controls the slope of the drawup. Smaller lateral extensions of the compartment lead to stronger slopes (FIGURE 6.11a), and as the lateral compartment size is progressively increased, drawup dynamics approach that of the reference scenario (i.e. no boundary effect). The vertical extension of the depression does not have an impact of the slope of the drawup. It does however control the amplitude of variations (FIGURE 6.11b), where a greater difference in altitudes leads to a greater drawup amplitude.

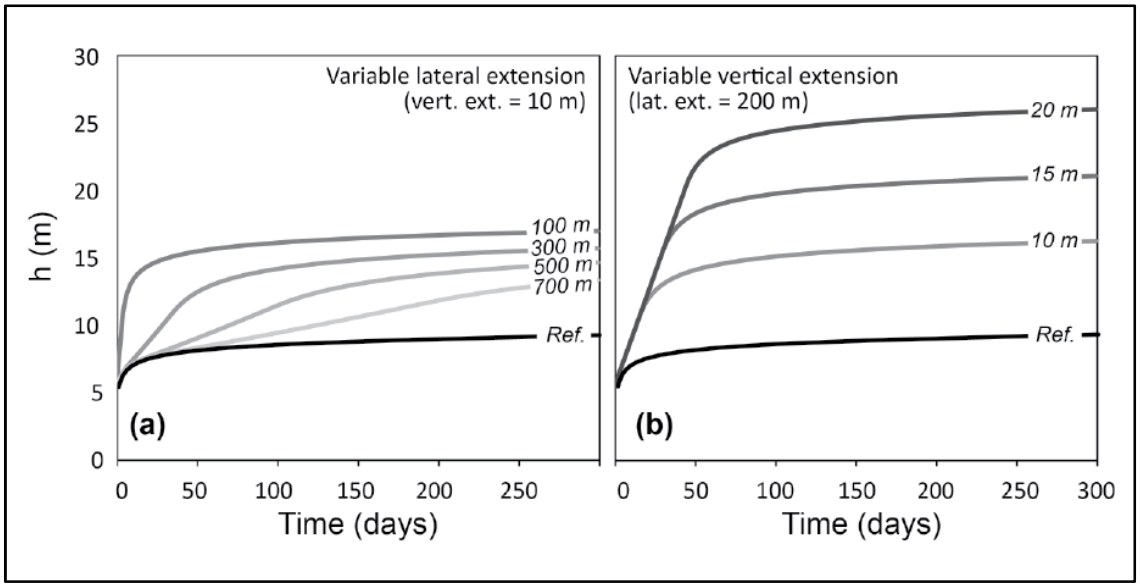

FIGURE 6.11: Simulated hydraulic head for the reference and compartmentalized scenario under constant recharge ($\boldsymbol{R} = 10^{-6}$ m.s^{-1}), where the lateral extension of the compartment is varied (a) and where the vertical extension is varied (b). Set distance to basin is 100 m. $\boldsymbol{K} = 10^{-4}$ m.s^{-1} and $\boldsymbol{S} = 10^{-2}$

4.4.2. Application to the present field case

The application of the compartmentalized scenario to estimated infiltration inputs proved quite successful in recreating the dynamics of the closest boreholes for phase 2 and 3 (FIGURE 6.12) using the hydraulic parameters obtained from analytical modeling

(TABLE 6.3) and varying only the shape of the basement. We obtained a relatively good agreement between the simulated water levels and the observed ones ($NRMSE = 8.7\%$ and 12.1% for CH01 and CH02 respectively). The strong slope of the drawup is successfully reproduced, and the following stabilization of water levels as well. A lateral extension of about 120 m seems to best recreate the recharge dynamics of the study site with the above cited parameters, although storativity was shown to be somewhat overestimated under the influence of the saprolite values owing to the borehole's proximity to the basin. Decreasing storativity to a value closer to that of the weathering interface ($S = 9.7 \times 10^{-3}$) requires increasing the theoretical lateral extension of the compartment to about 200 m to correctly model observations. The calibrated vertical extension was found relatively constant, around 18 m.

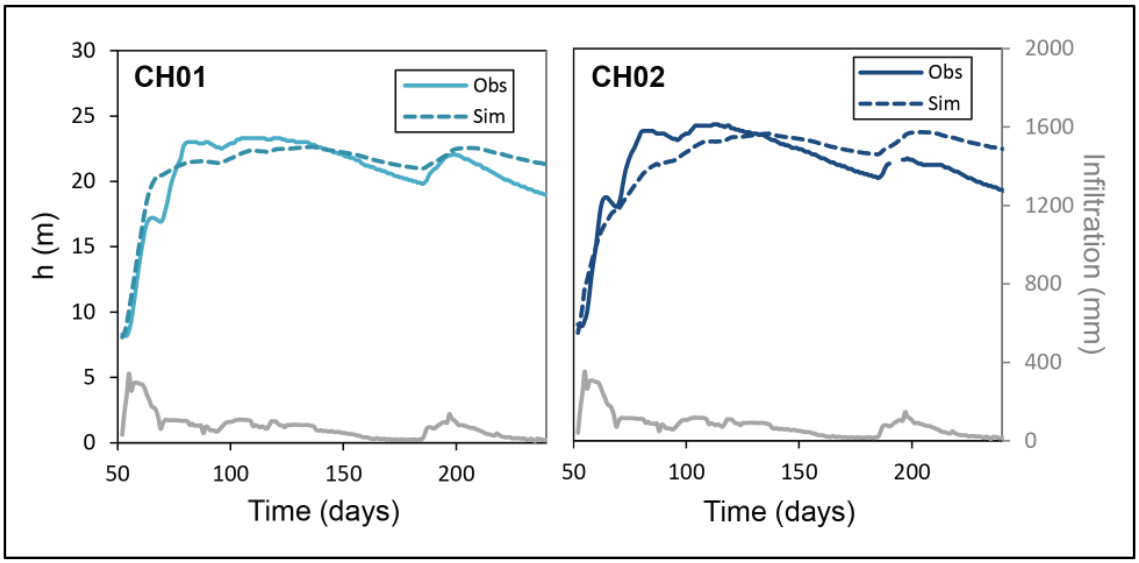

FIGURE 6.12: Observed hydraulic head and simulated hydraulic head using numerical modeling accounting for compartmentalization in response to infiltration from the recharge basin (gray lines) for the boreholes closes to the basin (CH01 and CH02)

There is a slight discrepancy between the model and the simulation, where the simulation under-estimates water levels during the drawup phase and over-estimates them during P3. This is probably because the actual system modeled is in reality much more complex than the model proposed here, as we do not account for flow in fractures, storage effects or matrix effects. The underlying geometry of the interface may also be much more complex than the way it is simulated in the model. We believe this is a testament to the interest this model brings, wherein a very simple numerical model recreated complex dynamics. Note also that it was not possible to simulate remote boreholes using the model as is. Placing the observation point outside of the compartment did recreate the delay in borehole response observed in FIGURE 6.4, but did not allow to simulate the amplitude of the variations correctly. Addressing this issue would imply complexifying

the model to account for a much more complex geometry of the weathering interface, which is currently beyond the scope of this paper.

A schematic summary of recharge dynamics is presented in FIGURE 6.13 in a very simplified way. The hydraulically disconnected phase of groundwater mounding (P1) resembles that of a relatively homogeneous environment. When hydraulic connection begins between the infiltration basin and the aquifer, we observe boundary conditions leading to a rapid increase of water levels because infiltration is focused into a bounded domain. The hydraulic connection also slows the infiltration process. The final stage P3 is much less subject to boundary effects and a pseudo-steady-state is reached, where levels oscillate around a constant value.

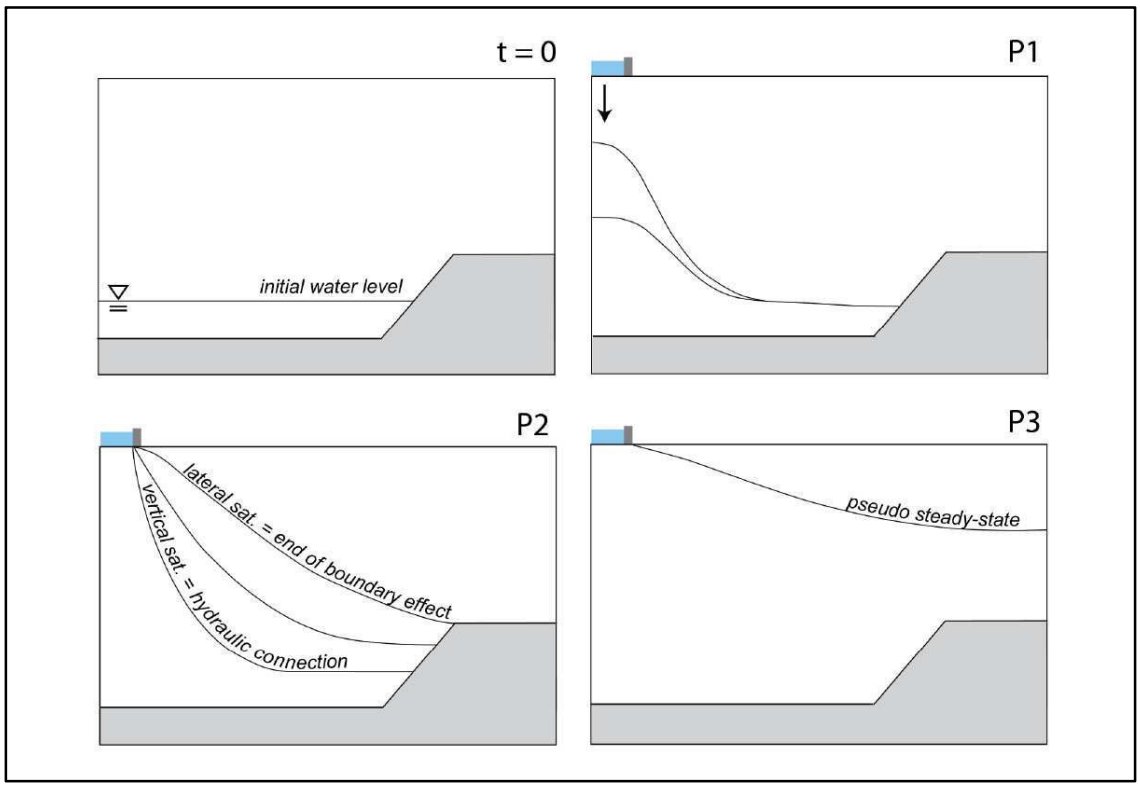

FIGURE 6.13: Schematic representation of hydraulic head variations above the bedrock (gray area) in response to artificial recharge from a recharge basin per phase of infiltration

5. Discussion

5.1. Representativity of hydraulic parameters

Overall infiltration efficiency, i.e. the ratio of infiltration to total inputs, is quite high (96%) in the present case, as opposed to previous studies in similar environments (Boisson, Villesseche et al., 2015: 56% ; Perrin *et al.*, 2009: 54% ; Singh *et al.*, 2004: 67%), but in agreement with efficiencies recorded by the Central Groundwater Board in 2011 of up to 98% in hard rock environments. A possible explanation of this difference is

the age of the infiltration basins. Studies showing low infiltration efficiencies focused on percolation tanks that had not been recently desilted, contrary to the basin studied here (dug in 2015) and those present in the CGWB's case studies. Further, the way in which the basin is supplied, where large amounts of water are brought in short periods of time, leads to an important water depth in the basin (up to almost 3 m). This could contribute to stronger infiltration rates linked to a higher hydraulic head. This is as opposed to typical percolation tanks, which accumulate a few centimeters of runoff over larger extended areas and thus subject to a higher amount of direct evaporation compared to infiltration. Although overall infiltration efficiency is high, infiltration rates decrease significantly with hydraulic connection because of a decrease in hydraulic gradient. Infiltration is then more spread out in time, which allows more evaporation to take place, although the amount evaporated remains much weaker than the overall infiltrated volume. This is not likely to continue to be the case if significant silting occurs.

This study's estimate of vertical permeability ($K_V = 8.1 \times 10^{-6}$ m.s^{-1}), is slightly higher than what Boisson, Guihéneuf et al. (2015) obtained at the same site for the upper saprolite layer (9×10^{-8} to 3×10^{-7} m.s^{-1}), but overall in the same range as other studies performed on saprolite (e.g. George, 1992: 7×10^{-6} m.s^{-1}; Cook *et al.*, 1996: 1×10^{-6} to 1×10^{-5} m.s^{-1}) . Boisson, Guihéneuf et al. (2015) used falling-head borehole permeameter tests, which render point values, whereas the large horizontal extent of the infiltration basin could allow sampling of otherwise undetectable vertical preferential flow paths (i.e. preserved fractures in the saprolite), and thus lead to an increase in hydraulic conductivity (Dewandel et al., 2006).

Horizontal hydraulic properties were found to be in the upper range of values for fractured crystalline rock ($K = 6.5 \times 10^{-5}$ m.s^{-1} and $S = 5.0 \times 10^{-2}$), rather corresponding to the properties of the weathering interface obtained in Boisson, Guihéneuf et al. (2015). The horizontal hydraulic conductivity of the system is thus much higher than the vertical hydraulic conductivity (about 8 times higher). This is consistent with the fact that the vertical hydraulic conductivity is controlled by the less transmissive saprolite, and the lateral hydraulic conductivity by the highly transmissive weathering interface acting as a preferential flow path. Overall, analytical modeling highlighted the strong influence of preferential flow in recharge processes.

5.2. Comparison to inferred interface relief

Previous acquisition of Electrical resistivity tomography (ERT) profiles (Chandra *et al.*, 2009) permitted the mapping of the depth of the weathering interface at the EHP site (FIGURE 6.14). The ERT survey was carried out using a Syscal Jr. Switch with 10m electrode spacing across 9 profiles using a Wenner-Schlumberger configuration (Chandra *et al.*, 2009). Profiles were analyzed using a routine inversion method and a threshold of about 400 Ohm.m (Braun *et al.*, 2009) was set to delineate the limit between fresh and weathered rock (Chandra *et al.*, 2009). Point data was then interpolated using standard kriging techniques.

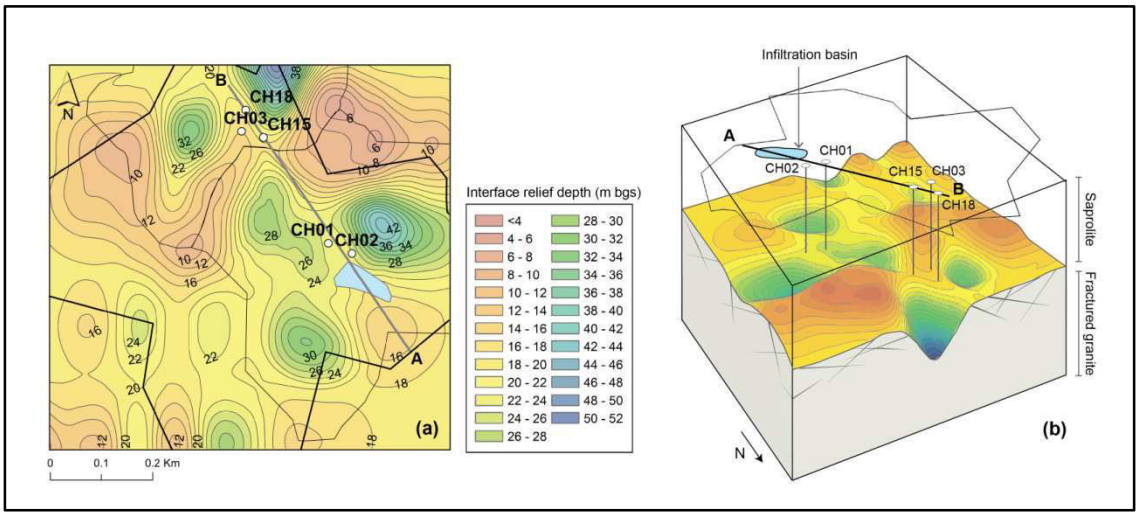

FIGURE 6.14: Depth of the upper fissured layer from ERT surveys (a) and inferred 3D conceptual model of structure (b). Hypothetical compartment delimitation is the thin black lines. For clarity purposes only the wells shown in FIGURE 6.4 are shown here.

The obtained interface is significantly hilly, composed of depressions and crests (the protruding areas), where crests delineate a set of sub-drainage basins (FIGURE 6.14a). The hilliness of the interface relief suggests the system is compartmentalized, which supports the observations made in previous works highlighting the existence of compartmentalization in crystalline environments and its effects on groundwater flow and chemistry (e.g. Guihéneuf et al., 2014; Perrin et al., 2011). Two main compartments were identified: one east of the site and the other north of the site, extending beyond the site limits. The lowest point of the bedrock topography appears to be north of the profile. The compartment over which the infiltration basin is situated is trefoil-like-shaped, with a diameter of about 500 m, a low point at about 42m depth and summits at about 20 m depth (so a height difference of approximately 20 m). This is similar to the dimensions obtained while fitting the numerical simulation to observed water levels (i.e. a radius of 200 m and a height difference of 18 m).

Using the AB profile outlined in FIGURE 6.4, we traced the relief of the bedrock interface obtained from ERT and replaced observed water levels so as to compare observed data to simulations (FIGURE 6.15). The depth of the interface was very similar to the depth estimated from borehole logs. Neighboring boreholes (CH01 and CH02) are situated in a topographic depression, whereas remote boreholes are in a crest area, where the two compartments identified in (FIGURE 6.14a) are separated, CH03 being at the highest point.

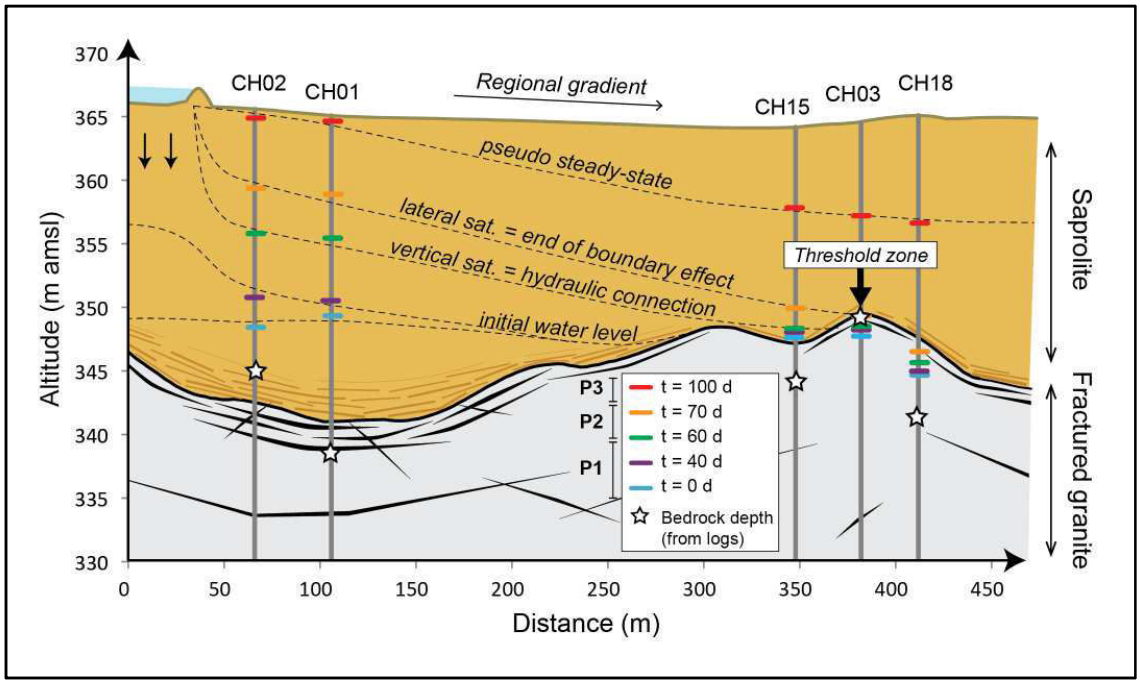

FIGURE 6.15: Comparison of schematic representation of artificial recharge from an infiltration basin with actual hydraulic head measured on-site and aquifer geometry from ERT data

The same phases outlined in FIGURE 6.13 can be transposed to observed data. Prior to the supposed date of hydraulic connection, (in FIGURE 6.15 $t = 0$ and $t = 40$) water level variations are weak and the water table is deep, which corresponds to P1. Then, water levels increase rapidly under the effect of the lateral boundary condition (in FIGURE 6.15 $t = 60$ and $t = 70$), corresponding to P2. This continues until water levels exceed the topographic threshold "downstream" from the basin at about 70 days after the beginning of the observation period. From that point onwards compartments become connected and water levels vary weakly but on a large extent, which corresponds to P3.

This conceptual model supports observations made by Guihéneuf *et al.* in 2014: the hydrogeological system is compartmentalized, and the aquifer connectivity and associated flow regime is a function of water levels relative to the well-connected bedrock interface.

5.3. Artificial recharge modeling

The model most commonly used to explain recharge dynamics was proposed by Bouwer (2002). In this model, two scenarios explain an infiltration basin's dynamics. If the bottom of the basin (the clogging layer) is less conductive than the underlying aquifer then infiltration is controlled by the hydraulic conductivity of the clogging layer. The water within the basin is disconnected from the underlying aquifer, perched over the silting layer. Otherwise, infiltration is controlled by the hydraulic properties of the underlying aquifer. In this case the water table may rise until hydraulic connection takes place, and then the infiltration rate is controlled either solely by gravity and vertical flows (in deep aquifers) or by the slope of the water table mound (in shallow aquifers). This concept was developed assuming homogeneous sedimentary aquifers of infinite lateral extension.

Instances of variable recharge dynamics have been documented in literature, either stemming from progressive and heterogeneous silting (e.g. Racz *et al.*, 2012; Mawer *et al.*, 2016), saturation of the vadose zone (Dillon & Liggett, 1983) or more rarely structural discontinuities (Massuel *et al.*, 2014). In most cases, the influence of heterogeneity on flow is limited to qualitative observations. Very few studies actually model processes with consideration of aquifer geometry (e.g. Ronayne *et al.*, 2008), probably because it is not easy to image the aquifer's geometry and practically impossible to obtain three-dimensional information about hydraulic properties, especially in hard rock context (de Marsily *et al.*, 2005). In this study we successfully quantified the role played by the basement relief (and its associated compartmentalization) on the hydraulic response of the aquifer to recharge, also highlighting the effects of it on recharge propagation and infiltration potentials. This study showed that the relief of the bedrock can produce an effect somehow analogous to the effect of impervious (or semi-impervious) boundaries on drawdown during pumping tests (de Marsily, 1986). In both cases, a change in drawdown slope relative to a situation where no impervious boundary is present is expected. To the best of our knowledge, there are no other instances in literature where this effect was identified during recharge, or as a result of a heterogeneous bedrock relief. Further, because the relief crests are only a semi-penetrating impervious boundary, the increase in drawup slope relative to the reference scenario was shown to provide information on the dimensions of the relief in question, where the larger the depression below the recharge basin the lesser the increase in drawup slope.

The in-depth analysis of the transient aquifer response to recharge in a heterogeneous environment can be used to improve MAR management in crystalline rock. The requirements to perform this type of analysis are (i) an approximation of the aquifer's hydraulic properties, (ii) a map of the contact zone between the saprolite and the granite,

and (iii) knowledge on the (actual or desired) water volumes to be stored in the aquifer. The most challenging aspect of this methodology is obtaining a map of the subsurface, although geophysical methods are becoming increasingly accurate and accessible. One can, for example, cite the development of airborne electromagnetic methods, which allow large-scale high resolution mapping of the subsurface (Sørensen & Auken, 2004). However, if bedrock relief data is unobtainable, we also showed how monitoring groundwater levels in the vicinity of the basin can provide valuable information on bedrock topography and on the storage potentials of the aquifer. As such, not only should the infiltration basin be monitored, but also, if possible, groundwater levels around the basin. Extrapolation of our simple method could improve present-day forward models used for MAR management in such geological environments, and possibly be extended into predictive modeling. From a quantitative standpoint, consideration of the effects of boundary conditions would be useful to regulate inputs in order to limit evaporation losses. If the bedrock topography is known, decision-makers can gain a greater awareness of the extent to which recharge will propagate throughout the aquifer, and choose whether to prioritize a strong localized reaction, which may be easier to retrieve at later times, or a weaker reaction over larger areas depending on the density and extent of the settlements affected by groundwater depletion and which stand to benefit from the augmentation of groundwater resources. Further, implications on water quality are also non-negligible. We highlighted the importance of preferential flow, which implies contaminant attenuation is not likely to take place rapidly enough to mitigate the negative effects of injecting wastewater into the aquifer. The dominance of advective processes over diffusive processes in hard rock (Guihéneuf *et al.*, 2017) will likely aggravate this issue. It is essential this be taken into consideration by decision-makers: the water currently used to feed the network of MAR structures state-wise originates from the Musi River downstream of Hyderabad. However, despite several attempts by various governments, the river Musi is the eighth most polluted river in India, receiving nearly 645 million liters per day of sewage water (Nilesh, 2016). Another element of risk that was identified in this study is that of hydraulic connection between the infiltration basin and the water table, to which fractured crystalline environments are particularly susceptible due to their low transmissivities and variable saprolite thickness. The best way to infer hydraulic connection is through groundwater level observation, but it is still possible to infer that hydraulic connection has taken place when infiltration rates decrease significantly (which may lead the basin to overflow or water levels in the basin to stagnate). Additionally to the loss of infiltration potentials, which may dampen the efficiency of this water stress remediation method and lead to important losses by ET, hydraulic connection may amplify the risk of groundwater contamination. If no unsaturated zone exists below the infiltration basin,

aerobic processes and sorption of contaminants which play an important part in retaining and degrading contaminants, and that depend on residence times, may be impeded.

6. Conclusions

Our study of artificial recharge processes in a fractured crystalline environment highlighted the role the heterogeneity of the horizontal weathering interface depth plays on recharge. During the initial stages of wetting, when the recharge mound is disconnected from the bottom of the basin, infiltration is governed by the vertical properties of the relatively homogeneous and poorly conductive saprolite. The lateral transmission of infiltration inputs reaching the aquifer is ensured mainly by the weathering interface, thus foregrounding the importance of preferential flows. Once hydraulic connection between the infiltration basin and the aquifer takes place, which is relatively rapidly due to the shallowness of the aquifer, two simultaneous phenomena are observed: infiltration potential decreases, and water levels increase strongly and rapidly. It was shown from numerical simulations that this can be interpreted as resulting from the control by the weathering interface relief, where summits act as semi-impervious boundaries, which delimit a set of hydrogeological compartments. The advancement of the infiltration front is thus impeded until the crest separating the east and north hydrogeological compartments is exceeded and the compartment is filled, which focuses infiltration inputs into smaller volumes, explaining the strong and sudden local water level increase. Once the summits are overpassed, the different hydrogeological compartments are connected, and the no-flow boundary effect becomes less critical.

It has yet to be confirmed if the simple analytical and numerical approach used here can be applied more generally in crystalline rock environments, but we believe this is a first step in better understanding the propagation of infiltration fronts in heterogeneous aquifers. This in turn could provide useful information for the aquifer properties and for the management of MAR structures in regards to placement, optimization, and water quality.

Acknowledgments

This study has been carried out at the Indo-French Center for Groundwater Research (BRGM-NGRI). This work has mainly benefited from CARNOT Institute BRGM funding. The Choutuppal Experimental Hydrogeological Park has also benefited from INSU support within the H+ observatory. The authors are very grateful to Marion Crenner and Mohammed Wajiduddin for their fieldwork, Joy Chaudhuri and Vidya Sagar for their geophysical work, and Yata Ramesh, Yata Muthyalu, Pittala Krishna, Nilgonda Kishtaiah and Pittala Anjaiah for their valuable on-site help. The authors are also grateful to ICRISAT for providing evaporation data. The authors are thankful to the editor Peter K. Kitanidis, the associate editor and to the reviewers (John Nimmo and an anonymous reviewer) for their constructive comments, which greatly enhanced the quality of the manuscript.

Chapter 7
Conclusions & perspectives

« The General Assembly (…) recognizes the right to safe and clean drinking water and sanitation as a human right that is essential for the full enjoyment of life and all human rights »

United Nations General Assembly, The human right to water and sanitation, July 28th 2010, A/RES/64/292

1. Conclusions

The general purpose of this thesis was to contribute to the understanding of natural and artificial recharge processes in weathered fractured crystalline rock. The first of its two parts provides the theoretical framework for comprehending the scientific, societal and theoretical challenges discussed in this thesis. The second part presents the numerical and experimental research carried out to address these challenges and further our understanding of groundwater flux dynamics in heterogeneous environments. These investigations may be divided into two main axes of research, each based on observations from a different observatory. The first axis of research focused on natural recharge processes at the catchment scale, based on field research at the Maheshwaram catchment. The second axis was based on research at the Choutuppal Experimental Hydrogeological Park (EHP), a highly monitored and well instrumented observatory aimed at improving our knowledge of flow dynamics in fractured crystalline rock at medium to small scales. The Choutuppal site was equipped with an artificial recharge basin in 2016 as part of a nationwide government initiative to mitigate groundwater depletion through Managed Aquifer Recharge (MAR). Both sites are situated in the state of Telangana (south India), within a few kilometers of its capital, Hyderabad, and both are underlain by Archean granite.

1.1. Catchment-scale natural recharge processes

In this first axis of research, the contributions of *diffuse* and *focused* (indirect + localized) recharge (which together make up *total* recharge) were studied, and found to present significantly different spatial and temporal distributions. Diffuse recharge was quantified using a simple 1D physical infiltration model, while focused recharge was assumed to be the difference between total recharge, estimated previously using the DWTF method, and diffuse recharge. Diffuse recharge is highly dependent on infiltra-

tion, a relatively well known process that is mainly controlled by meteorological conditions (precipitation and evapotranspiration) and the soils' hydraulic properties. Modeling the spatial distribution of annual diffuse recharge showed that the low-lying alluvial valleys resist diffuse recharge under the present conditions, while the soils at the hills and summits of the basin appeared the most receptive to diffuse recharge and the catchment plains presented an intermediate behavior. Also, at the parcel scale, the presence of irrigated agriculture was found to significantly impact recharge dynamics: when an otherwise dry soil is irrigated, this increases its hydraulic conductivity and pressure head, which allow greater quantities of water to percolate down to the aquifer. This observation aligns with other studies that have looked into the effect of irrigation on diffuse recharge (Kurtzman & Scanlon, 2011; Ognianik & Paramonova, 2001). Nevertheless, the actual irrigated surfaces are only a small part of the total catchment area, and when averaged over large scales do not significantly impact total recharge. Additionally, the abstractions necessary to irrigate these parcels far exceeds the increase in recharge resulting from being wetted.

When looking at the temporal distribution of diffuse recharge, and its link to precipitation, this is found to be a highly non-linear process with two significantly different behaviors depending on annual rainfall. For low to moderate rainfall (<1000 mm), diffuse recharge is persistently low and increases only very weakly as precipitation increases. This may be because most of the rainfall on any given year is taken up by evapotranspiration, and the excess stored in the soil without necessarily reaching the aquifer. For high rainfall (>1000 mm), however, soil moisture deficits are met and water may percolate downward in much greater quantities. Many studies which have looked into the relationship between recharge in rainfall under arid and tropical climates (e.g. Acworth et al., 2016; Eilers et al., 2007; Jasechko & Taylor, 2015; Mileham et al., 2009; Taylor et al., 2012) have also suggested a non-linear relationship between rainfall and recharge, in which recharge is biased to heavy rainfall events. Many of these studies, however, are based on qualitative observations, where rainfall is compared to groundwater level variations, or rely on the use of simply soil moisture balance models which do not account for the strong non-linearity of unsaturated flow mechanics.

Focused recharge was inferred from the difference between total recharge estimates—calculated from water level fluctuations—and our estimates of diffuse recharge. This poorly understood phenomenon was found to represent about 55% of total recharge during the analyzed period, though this is highly dependent on annual rainfall. This is in agreement with literature, where focused recharge has often been found or suspected to be a significant contributor to total recharge, especially in (semi-)arid environments (de Vries & Simmers, 2002). For example, Sukhija et al. (2003) found preferential flow recharge to be 75% of total recharge in the case of fractured granites, and 33% in semi-

consolidated sandstones. In the study by D. V. Reddy et al. (2009), matrix flow recharge was shown to represent only 1-5% of rainfall, while preferential flow, in the valley fills, was actually about 16% (but decreased to 5-5.5% in the plains). In Machiwal & Jha (2015) no quantitative estimate is given, but it is noted that recharge was found to be significantly higher in areas where surface-water bodies were present.

Focused recharge was also shown to be relatively independent of evapotranspiration. Greater rainfall led to higher focused recharge, and the relationship between them is highly linear. Nonetheless, in order for focused recharge to occur, runoff must be generated, causing water to flow through the catchment, pond at the surface and infiltrate through *focused* processes. According to our recharge model, runoff was generated when annual rainfall exceeded 500 mm, which is fortunately almost always the case. These particularities highlight the importance of better understanding focused recharge, which appears resilient to temperature and evapotranspiration increases, especially in a context of climate change. Mapping the spatial distribution of focused recharge showed that its patterns are guided mainly by the disposition of the topography and thus of the drainage network, wherein the valley bottoms concentrate runoff in sufficient quantities for indirect recharge to take place. The existence of geological discontinuities was also found to be a possible area of enhanced recharge, in theory providing a preferential flow path in which water may enter the subsurface and recharge the aquifer without being subject to evapotranspiration. Other studies in semi-arid terrain have also noted low-lying alluvial-filled valleys to act as indirect recharge terrains both in hard rock areas (e.g. van Wyk et al., 2012) and sedimentary aquifers (e.g. Acworth et al., 2016; Mahlknecht et al., 2004). The same is true of the importance of geological discontinuities, which have often been associated with localized recharge zones recharge (e.g. Leray et al., 2013; Ruelleu et al., 2010).

1.2. Site-scale artificial recharge processes

In the second axis of research, the dynamics of infiltration from a Managed Aquifer Recharge (MAR) structure and its subsequent distribution and propagation throughout the highly heterogeneous aquifer was monitored. Infiltration efficiencies were found to be quite high, averaging about 97% of the inputs into the basin, which is higher than what previous studies have obtained in similar environments (Boisson, Villesseche et al., 2015: 56% ; Perrin *et al.*, 2009: 54% ; Singh *et al.*, 2004: 67%). Infiltration efficiency decreased significantly, however, when hydraulic connection took place, i.e. when the water table rose to the bottom of the infiltration basin. Lateral propagation of recharge took place mostly in the highly transmissive saprolite/granite interface. This allowed a relatively efficient and rapid lateral transfer of infiltration throughout the aquifer. However, the egg-carton-like disposition of the transmissive interface impeded this lateral propagation beyond the summits of the interface before the compartment was fully flooded. This fo-

cused infiltration inputs into a relatively small volume, causing water levels to rise at a much higher rate than originally predicted, considering the high transmissivity of the interface. The existence and effects of compartmentalization have been highlighted in the past (e.g. Guihéneuf et al., 2014; Perrin et al., 2011), but have never been accounted for in a hydrodynamic model of groundwater mounding for MAR. In fact, current analytical solutions which are widely used to predict the aquifer response to MAR are unfortunately based on a set of assumptions which are not valid in fractured crystalline rock: the media is assumed to be homogeneous and isotropic, and the aquifer of infinite lateral extent. Among the rare studies which have addressed the question of MAR in fractured crystalline rock, many are limited to qualitative observations or water budget approaches (e.g. Alazard et al., 2016; Boisson et al., 2015), which despite their useful contributions, do not consider the effect aquifer heterogeneity may have of MAR propagation within the aquifer. Understanding the topography of this interface, and more generally the geometry of the aquifer, could in the future allow for better modelling of groundwater mounding in areas where MAR is implemented.

2. Perspectives

Several areas of potential improvement were identified throughout this thesis. First and foremost, much of the work presented here is based on the elaboration and validation of models which was only possible because of the exceptional research conditions provided by the instrumentation and monitoring of several sites in granitic terrain for almost 20 years now (data is available at http://hplus.ore.fr/en). But the challenges linked to this type of media, and the need for an improved understanding of their water resources dynamics, are ubiquitous over large areas of the world. Unfortunately, this issue is of the most pressing importance in areas of the world that often lack the infrastructure to gather the necessary data. This is the case, for instance, in much of the African continent, parts of the Middle East, and several Asian countries such as India and China, which also, to compound the problem, face some of the most severe groundwater overexploitation problems.

2.1. Remote sensing and airborne geophysics

There is a need to develop methods that provide data over large areas and in a cost- and time-effective manner, namely remote sensing and geophysical methods. To give a few examples: in the first axis of research, the diffuse recharge model used meteorological data and information on soil type (and their hydrodynamic properties) and land use distribution. In this case, much of the information was collected through time-consuming field campaigns, making only limited use of satellite imagery. Nonetheless, remote sensing methods can and have been used for these purposes in the past: soil type distribution can be inferred from satellite imagery and literature values used to approximate their

properties, or even directly quantified using remote sensing methods (e.g. Anderson & Croft, 2009; Ben-Dor, 2002; Mohanty, 2013). This is also the case when it comes to the determination of land use and land use management practices (e.g. Ambast et al., 2002; Droogers & Bastiaanssen, 2002; Romaguera et al., 2010). With satellite imagery becoming increasingly accurate and easily available, remote sensing methods are increasingly able to provide enough data for recharge models to be developed and used at medium to large scales.

To give another example, our second axis of research relied on knowledge of the saprolite/bedrock interface topography, and its effect on flow propagation. This analysis was only possible because of the extensive electrical resistivity tomography campaigns carried out at the small EHP site. However, the use of airborne geophysics, which allow large-scale high resolution mapping of the subsurface, is becoming more and more commonplace, accessible and accurate (e.g. Sørensen & Auken, 2004; Yihdego & Nzikou, 2018). Large-scale maps of aquifer geometry and compartmentalization would be an immense and necessary contribution to bettering the management of MAR and water resources in general.

2.2. Recharge quantification

2.2.1. Verification of diffuse recharge estimates

Soil moisture balance models and unsaturated/saturated flow equations have been widely used to quantify diffuse recharge. Verifying these estimates with *measured* diffuse recharge would allow verification of many of the hypotheses made here. Diffuse recharge, however, cannot generally be straightforwardly estimated [see **Chapter 3 Section 2.1**]; the absence of baseflow or streamflow (as is the case in many (semi-)arid settings) precludes the measurement of diffuse recharge using streamflow hydrographs, while methods based on tracers in the unsaturated zone often provide estimates of *potential* recharge rather than *actual* recharge (not all water passing through the unsaturated zone becomes recharge). Actual recharge measurements can most accurately be estimated through measured water budgets (for example using lysimeters or soil moisture measurements) which have the disadvantage of providing highly localized measurements. A dense network of point measurements would thus be required to approximate the spatial distribution of recharge. Inverse estimation of recharge through numerical modeling is also an option, but there is a risk of non-uniqueness of the solutions, or of the groundwater head variations used to calibrate the model not being merely the result of diffuse recharge alone.

2.2.2. Quantitative modeling of focused recharge

On another note, focused recharge in this work was approached in a qualitative manner, since it was merely deduced from the discrepancies between total and diffuse re-

charge. Directly accounting for indirect and localized recharge in numerical models poses many issues, such as (i) establishing quantitative relationships between the presence of geological discontinuities and the amount and speed of water traveling in them, (ii) estimating indirect recharge without any knowledge on overall streamflow rates distribution, both in time and space and (iii) obtaining relevant data through field measurements to verify the modelled outputs. Quantification of these processes at large scales is in fact one of the most relevant remaining challenges in recharge estimation, yet very few studies have attempted this (among them Cuthbert et al., 2016 and Maréchal et al., 2009). The task is admittedly difficult, but important, especially in (semi-)arid environments where focused recharge has regularly been shown to be the dominant recharge process. Improving our knowledge of this process is thus essential to a durable and responsible management of groundwater resources in water-scarce environments, particularly in light of the upcoming challenges posed by land use and climate change.

2.2.3. Impact of land use and climate change

Understanding how the land cover and meteorological conditions control the generation and routing of runoff is a first step in identifying areas of potentially enhanced recharge. Understanding how land cover and meteorological conditions affect the partition of water into infiltration, evapotranspiration and runoff is a first step in properly managing groundwater resources in a context of global change. Land use is constantly evolving to meet the increasing need for irrigated agriculture, and climate change is leading to significant changes in temperature and precipitation patterns and intensity. Thus, running recharge models using climate change simulations (for meteorological conditions) and land use change simulations (which rely on political and social factors, influenced by both global drivers, e.g. population growth and an increasing need for climate change mitigation, and local drivers, e.g. market forces and local skills) is necessary to the assess the resilience of groundwater resources to these changes in order to ensure that policy-makers make informed choices regarding land use planning, climate change adaptation and effective water management.

2.3. On the representativity of site-scale analysis

The second research axis of this work was based on a case study in a small experimental site (about 40 ha) and with limited information on the groundwater level evolution and aquifer geometry beyond the site boundaries. The models prepared to better understand the aquifer response to recharge were calibrated only using observations from two nearby borewells. In order to assess whether the observations made at this site are applicable in fractured crystalline environments in general, it would be interesting to replicate this study in a similar environment, possibly with more borewells in the vicinity of the basin and moving away from it, as well as with more information on aquifer ge-

ometry at larger scales. This touches on another point which was not investigated in this thesis, and that is the effect of managed aquifer recharge at the catchment scale. Indeed, there are very few studies investigating the impact of MAR at the catchment scale, and many of these have pointed out the risk of downstream tradeoffs, wherein MAR merely relocates the availability of groundwater, rather than actually adding water to the system. In fractured crystalline environments, specifically, we noted that aquifer compartmentalization impedes the efficient lateral propagation of recharge inputs. This effect, compounded with the risk of downstream tradeoffs at the catchment scale, thus merits thorough investigation.

2.4. Effects of MAR on groundwater quality

Finally, this thesis noted the importance of preferential flow above diffuse flow processes, mechanisms which have a significant effect in terms of groundwater quality, but did not fall under the scope of this research. Completing quantitative MAR models with information of contaminant transport dynamics is essential to addressing the issue of potential groundwater contamination originating from the injection of highly polluted water into the aquifer. In parallel, some studies have noted that MAR may actually contribute to decreasing the concentration of harmful geogenic elements, such as fluoride and arsenic, through dilution. Incorporating contaminant transport dynamics in MAR flow models could also provide insight into this topic.

References

Abdul, A. S., & Gillham, R. W. (1984). Laboratory Studies of the Effects of the Capillary Fringe on Streamflow Generation. *Water Resources Research*, *20*(6), 691–698. https://doi.org/10.1029/WR020i006p00691

Abdul, A. S., & Gillham, R. W. (1989). Field studies of the effects of the capillary fringe on streamflow generation. *Journal of Hydrology*, *112*(1–2), 1–18. https://doi.org/10.1016/0022-1694(89)90177-7

Acworth, R. I. (1987). The development of crystalline basement aquifers in a tropical environment. *Quarterly Journal of Engineering Geology and Hydrogeology*, *20*(4), 265–272. https://doi.org/10.1144/GSL.QJEG.1987.020.04.02

Acworth, R. I., Rau, G. C., Cuthbert, M. O., Jensen, E., & Leggett, K. (2016). Long-term spatio-temporal precipitation variability in arid-zone Australia and implications for groundwater recharge. *Hydrogeology Journal*, *24*(4), 905–921. https://doi.org/10.1007/s10040-015-1358-7

Ahmed, S., Jayakumar, R., & Salih, A. (2008). *Groundwater dynamics in hard rock aquifers. Water Resources*. New Delhi, India: Springer.

Alazard, M., Boisson, A., Maréchal, J. C., Perrin, J., Dewandel, B., Schwarz, T., … Ahmed, S. (2016). Investigation of recharge dynamics and flow paths in a fractured crystalline aquifer in semi-arid India using borehole logs: implications for managed aquifer recharge. *Hydrogeology Journal*, *24*(1), 35–57. https://doi.org/10.1007/s10040-015-1323-5

Alcalá, F. J., Cantón, Y., Contreras, S., Were, A., Serrano-Ortiz, P., Puigdefábregas, J., … Domingo, F. (2011). Diffuse and concentrated recharge evaluation using physical and tracer techniques: results from a semiarid carbonate massif aquifer in southeastern Spain. *Environmental Earth Sciences*, *62*(3), 541–557. https://doi.org/10.1007/s12665-010-0546-y

Alcalá, F. J., & Custodio, E. (2015). Natural uncertainty of spatial average aquifer recharge through atmospheric chloride mass balance in continental Spain. *Journal of Hydrology*, *524*(November 2012), 642–661. https://doi.org/10.1016/j.jhydrol.2015.03.018

Alderwish, A. M. (2010). Induced recharge at new dam sites—Sana'a Basin, Yemen. *Arabian Journal of Geosciences*, *3*(3), 283–293. https://doi.org/10.1007/s12517-009-0075-8

Allen-King, R. M., Halket, R. M., Gaylord, D. R., & Robin, M. J. L. (1998). Characterizing the heterogeneity and correlation of perchloroethene sorption and hydraulic conductivity using a facies-based approach. *Water Resources Research*, *34*(3), 385–396. https://doi.org/10.1029/97WR03496

Allen, R. G., Pereira, L. S., Raes, D., & Smith, M. (1998). Crop evapotranspiration-Guidelines for computing crop water requirements-FAO Irrigation and drainage paper 56. *Fao, Rome*, *300*(9), D05109.

Alley, W. M., La Baugh, J. W., & Reilly, T. E. (2005). Groundwater as an Element in the Hydrological Cycle. In *Encyclopedia of Hydrological Sciences* (pp. 1–14). Chichester, UK: John Wiley & Sons, Ltd. https://doi.org/10.1002/0470848944.hsa153

Alley, W. M., Reilly, T. E., & Franke, O. L. (1999). *Sustainability of Ground-Water Resources. U.S. Geological Survey Circular 1186*. Denver, Colorado.

Allison, G. B., Gee, G. W., & Tyler, S. W. (1994). Vadose-Zone Techniques for Estimating Groundwater Recharge in Arid and Semiarid Regions. *Soil Science Society of America Journal*, *58*(1), 6. https://doi.org/10.2136/sssaj1994.03615995005800010002x

Allison, G. B., & Hughes, M. W. (1978). The use of environmental chloride and tritium to estimate total recharge to an unconfined aquifer. *Soil Research*, *16*(2), 181. https://doi.org/10.1071/SR9780181

Ambast, S. K., Keshari, A. K., & Gosain, A. K. (2002). Satellite remote sensing to support management of irrigation systems: concepts and approaches Télédétection par satellite pour la gestion des systèmes

d'irrigation: concepts et approches. *Irrigation and Drainage*, *51*(1), 25. https://doi.org/10.1002/ird.26.abs

Amini, M., Abbaspour, K. C., Berg, M., Winkel, L., Hug, S. J., Hoehn, E., … Johnson, C. A. (2008). Statistical Modeling of Global Geogenic Arsenic Contamination in Groundwater. *Environmental Science & Technology*, *42*(10), 3669–3675. https://doi.org/10.1021/es702859e

Amini, M., Mueller, K., Abbaspour, K. C., Rosenberg, T., Afyuni, M., Møller, K. N., … Johnson, C. A. (2008). Statistical Modeling of Global Geogenic Fluoride Contamination in Groundwaters. *Environmental Science & Technology*, *42*(10), 3662–3668. https://doi.org/10.1021/es071958y

Amogu, O., Descroix, L., Yéro, K. S., Le Breton, E., Mamadou, I., Ali, A., … Belleudy, P. (2010). Increasing River Flows in the Sahel? *Water*, *2*(2), 170–199. https://doi.org/10.3390/w2020170

Anderson, K., & Croft, H. (2009). Remote sensing of soil surface properties. *Progress in Physical Geography: Earth and Environment*, *33*(4), 457–473. https://doi.org/10.1177/0309133309346644

Anderson, M. P. (2005). Heat as a Ground Water Tracer. *Groundwater*, *43*(6), 951–968. https://doi.org/10.1111/j.1745-6584.2005.00052.x

Anderson, W. P., & Evans, D. G. (2007). On the Interpretation of Recharge Estimates from Steady-State Model Calibrations. *Ground Water*, *45*(4), 499–505. https://doi.org/10.1111/j.1745-6584.2007.00312.x

Anupam, K., & Shinjiro, K. (2013). Climate Change and Groundwater: Vulnerability, Adaptation and Mitigation Opportunities in India. *International Journal of Environmental Science and Development*, (June 2013), 272–276. https://doi.org/10.7763/IJESD.2013.V4.352

Apparasu, S. R. (2018, January 1). Telangana starts free, 24-hour power supply to farmers. *Hindustan Times*. Retrieved from https://www.hindustantimes.com/india-news/telangana-starts-free-24-hour-power-supply-to-farmers/story-jdQCZIRh1oEzkObm9cC3UN.html

Ashby, M. F., & Hallam, S. D. (1986). The failure of brittle solids containing small cracks under compressive stress states. *Acta Metallurgica*, *34*(3), 497–510. https://doi.org/10.1016/0001-6160(86)90086-6

Ayraud, V., Aquilina, L., Labasque, T., Pauwels, H., Molenat, J., Pierson-Wickmann, A.-C., … Davy, P. (2008). Compartmentalization of physical and chemical properties in hard-rock aquifers deduced from chemical and groundwater age analyses. *Applied Geochemistry*, *23*(9), 2686–2707. https://doi.org/10.1016/j.apgeochem.2008.06.001

Bakker, M., Post, V., Langevin, C. D., Hughes, J. D., White, J. T., Starn, J. J., & Fienen, M. N. (2016). Scripting MODFLOW Model Development Using Python and FloPy. *Groundwater*, *54*(5), 733–739. https://doi.org/10.1111/gwat.12413

Bansal, R. K. (2013). Groundwater Flow in Sloping Aquifer under Localized Transient Recharge: Analytical Study. *Journal of Hydraulic Engineering*, *139*(11), 1165–1174. https://doi.org/10.1061/(ASCE)HY.1943-7900.0000784

Barron, O. V., Crosbie, R. S., Dawes, W. R., Charles, S. P., Pickett, T., & Donn, M. J. (2012). Climatic controls on diffuse groundwater recharge across Australia. *Hydrology and Earth System Sciences*, *16*(12), 4557–4570. https://doi.org/10.5194/hess-16-4557-2012

Bauer, S., Liedl, R., & Sauter, M. (2005). Modeling the influence of epikarst evolution on karst aquifer genesis: A time-variant recharge boundary condition for joint karst-epikarst development. *Water Resources Research*, *41*(9), 1–12. https://doi.org/10.1029/2004WR003321

Becker, M. W., & Shapiro, A. M. (2000). Tracer transport in fractured crystalline rock: Evidence of nondiffusive breakthrough tailing. *Water Resources Research*, *36*(7), 1677. https://doi.org/10.1029/2000WR900080

Ben-Dor, E. (2002). Quantitative remote sensing of soil properties (pp. 173–243). https://doi.org/10.1016/S0065-2113(02)75005-0

Berthold, S., Bentley, L. R., & Hayashi, M. (2004). Integrated hydrogeological and geophysical study of depression-focused groundwater recharge in the Canadian prairies. *Water Resources Research*, *40*(6). https://doi.org/10.1029/2003WR002982

Beven, K. (2006). A manifesto for the equifinality thesis. *Journal of Hydrology*, *320*(1–2), 18–36. https://doi.org/10.1016/j.jhydrol.2005.07.007

Beven, K. (2012). *Rainfall-Runoff Modelling. Rainfall-Runoff Modelling: The Primer: Second Edition*. Chichester, UK: John Wiley & Sons, Ltd. https://doi.org/10.1002/9781119951001

Beven, K., & Germann, P. (1982). Macropores and water flow in soils. *Water Resources Research*, *18*(5), 1311–1325. https://doi.org/10.1029/WR018i005p01311

Beven, K., & Germann, P. (2013). Macropores and water flow in soils revisited. *Water Resources Research*, *49*(6), 3071–3092. https://doi.org/10.1002/wrcr.20156

Bhanja, S. N., Mukherjee, A., Ramaswamy, R., Scanlon, B. R., Malakar, P., & Verma, S. (2018). Long-term groundwater recharge rates across India by in situ measurements. *Hydrology and Earth System Sciences Discussions*, 1–19. https://doi.org/10.5194/hess-2018-313

Bhanja, S. N., Mukherjee, A., Rodell, M., Wada, Y., Chattopadhyay, S., Velicogna, I., … Famiglietti, J. S. (2017). Groundwater rejuvenation in parts of India influenced by water-policy change implementation. *Scientific Reports*, *7*(1), 7453. https://doi.org/10.1038/s41598-017-07058-2

Blatt, H., & Jones, R. L. (1975). Proportions of Exposed Igneous, Metamorphic, and Sedimentary Rocks. *Geological Society of America Bulletin*, *86*(8), 1085. https://doi.org/10.1130/0016-7606(1975)86<1085:POEIMA>2.0.CO;2

Bockgard, N., & Niemi, A. (2004). Role of Rock Heterogeneity on Lateral Diversion of Water Flow at the Soil-Rock Interface. *Vadose Zone Journal*, *3*(3), 786–795. https://doi.org/10.2113/3.3.786

Böhlke, J.-K. (2002). Groundwater recharge and agricultural contamination. *Hydrogeology Journal*, *10*(1), 153–179. https://doi.org/10.1007/s10040-001-0183-3

Boisson, A., Baïsset, M., Alazard, M., Perrin, J., Villesseche, D., Dewandel, B., … Maréchal, J. C. (2014). Comparison of surface and groundwater balance approaches in the evaluation of managed aquifer recharge structures: Case of a percolation tank in a crystalline aquifer in India. *Journal of Hydrology*, *519*(2014), 1620–1633. https://doi.org/10.1016/j.jhydrol.2014.09.022

Boisson, A., Guihéneuf, N., Perrin, J., Bour, O., Dewandel, B., Dausse, A., … Maréchal, J. C. (2015). Determining the vertical evolution of hydrodynamic parameters in weathered and fractured south Indian crystalline-rock aquifers: insights from a study on an instrumented site. *Hydrogeology Journal*, *23*(4), 757–773. https://doi.org/10.1007/s10040-014-1226-x

Boisson, A., Villesseche, D., Baisset, M., Perrin, J., Viossanges, M., Kloppmann, W., … Ahmed, S. (2015). Questioning the impact and sustainability of percolation tanks as aquifer recharge structures in semi-arid crystalline context. *Environmental Earth Sciences*, *73*(12), 7711–7721. https://doi.org/10.1007/s12665-014-3229-2

Bonneau, F., Henrion, V., Caumon, G., Renard, P., & Sausse, J. (2013). A methodology for pseudo-genetic stochastic modeling of discrete fracture networks. *Computers & Geosciences*, *56*, 12–22. https://doi.org/10.1016/j.cageo.2013.02.004

Bonnet, E., Bour, O., Odling, N. E., Davy, P., Main, I., Cowie, P., & Berkowitz, B. (2001). Scaling of fracture systems in geological media. *Reviews of Geophysics*, *39*(3), 347–383. https://doi.org/10.1029/1999RG000074

Boucher, M., Favreau, G., Vouillamoz, J. M., Nazoumou, Y., & Legchenko, A. (2009). Estimating specific yield and transmissivity with magnetic resonance sounding in an unconfined sandstone aquifer (Niger). *HYDROGEOLOGY JOURNAL*, *17*(7), 1805–1815. https://doi.org/10.1007/s10040-009-0447-x

Bour, O., Davy, P., Darcel, C., & Odling, N. (2002). A statistical scaling model for fracture network geometry, with validation on a multiscale mapping of a joint network (Hornelen Basin, Norway). *Journal of Geophysical Research*, *107*(B6), 2113. https://doi.org/10.1029/2001JB000176

Boussinesq, M. J. (1868). Mémoire sur l'influence des frottements dans les mouvements réguliers des fluides. *Journal de Mathématiques Pures et Appliquées*, *13*(2), 377–424.

Bouwer, H. (1978). *Groundwater Hydrology*. New York: McGraw-Hill.

Bouwer, H. (2002). Artificial recharge of groundwater: hydrogeology and engineering. *Hydrogeology Journal*, *10*(1), 121–142. https://doi.org/10.1007/s10040-001-0182-4

Bouwer, H., Back, J. T., & Oliver, J. M. (1999). Predicting Infiltration and Ground-Water Mounds for Artificial Recharge. *Journal of Hydrologic Engineering*, *4*(4), 350–357. https://doi.org/10.1061/(ASCE)1084-0699(1999)4:4(350)

Braun, J.-J., Descloitres, M., Riotte, J., Fleury, S., Barbiéro, L., Boeglin, J.-L., … Dupré, B. (2009). Regolith mass balance inferred from combined mineralogical, geochemical and geophysical studies: Mule Hole gneissic watershed, South India. *Geochimica et Cosmochimica Acta*, *73*(4), 935–961. https://doi.org/10.1016/j.gca.2008.11.013

Bredehoeft, J. D. (2002). The Water Budget Myth Revisited: Why Hydrogeologists Model. *Ground Water*, *40*(4), 340–345. https://doi.org/10.1111/j.1745-6584.2002.tb02511.x

Bredehoeft, J. D., Belitz, K., & Sharphansen, S. (1992). The hydrodynamics of the big horn basin - a study of the role of faults. *American Association of Petroleoum Geologists*, *76*(4), 530–546.

Brindha, K., Jagadeshan, G., Kalpana, L., & Elango, L. (2016). Fluoride in weathered rock aquifers of southern India: Managed Aquifer Recharge for mitigation. *Environmental Science and Pollution Research*, *23*(9), 8302–8316. https://doi.org/10.1007/s11356-016-6069-7

Bromley, J., Edmunds, W. M., Fellman, E., Brouwer, J., Gaze, S. R., Sudlow, J., & Taupin, J. D. (1997). Estimation of rainfall inputs and direct recharge to the deep unsaturated zone of southern Niger using the chloride profile method. *Journal of Hydrology*, *188–189*(1–4), 139–154. https://doi.org/10.1016/S0022-1694(96)03157-5

Brooks, R. H., & Corey, A. T. (1964). *Hydraulic properties of porous media.* https://doi.org/citeulike-article-id:711012

Brunner, P., Eugster, M., Bauer, P., & Kinzelbach, W. (2002). Determination of recharge patterns by combining remote sensing and the chloride method. In *IAHS Publ no 277 .2002* (Vol. 277, pp. 17–20). https://doi.org/10.1097/SLE.0b013e31822355ea

Brunner, P., Simmons, C. T., Cook, P. G., & Therrien, R. (2010). Modeling surface water-groundwater interaction with MODFLOW: Some considerations. *Ground Water*, *48*(2), 174–180. https://doi.org/10.1111/j.1745-6584.2009.00644.x

Brutsaert, W. (2008). Long-term groundwater storage trends estimated from streamflow records: Climatic perspective. *Water Resources Research*, *44*(2), 1–7. https://doi.org/10.1029/2007WR006518

Burdine, N. T. (1953). Relative Permeability Calculations From Pore Size Distribution Data. *Journal of Petroleum Technology*, *5*(03), 71–78. https://doi.org/10.2118/225-G

Buss, H. L., Sak, P. B., Webb, S. M., & Brantley, S. L. (2008). Weathering of the Rio Blanco quartz diorite, Luquillo Mountains, Puerto Rico: Coupling oxidation, dissolution, and fracturing. *Geochimica et Cosmochimica Acta*, *72*(18), 4488–4507. https://doi.org/10.1016/j.gca.2008.06.020

Cacas, M. C., Ledoux, E., de Marsily, G., Tillie, B., Barbreau, A., Durand, E., … Peaudecerf, P. (1990). Modeling fracture flow with a stochastic discrete fracture network: calibration and validation: 1. The flow model. *Water Resources Research*, *26*(3), 479–489. https://doi.org/10.1029/WR026i003p00479

Cai, Z., & Ofterdinger, U. (2016). Analysis of groundwater-level response to rainfall and estimation of annual recharge in fractured hard rock aquifers, NW Ireland. *Journal of Hydrology*, *535*, 71–84. https://doi.org/10.1016/j.jhydrol.2016.01.066

Calder, I., Gosain, A., Rao, M. S. R. M., Batchelor, C., Snehalatha, M., & Bishop, E. (2008). Watershed development in India. 1. Biophysical and societal impacts. *Environment, Development and Sustainability*, *10*(4), 537–557. https://doi.org/10.1007/s10668-006-9079-7

Campbell, G. S. (1974). A simple method for determining unsaturated conductivity from moisture retention data. *Soil Science*, *117*(6), 311–314. https://doi.org/10.1097/00010694-197406000-00001

Carleton, G. B. (2010). *Simulation of Groundwater Mounding Beneath Hypothetical Stormwater Infiltration Basins. U.S. Geological Survey Scientific Investigations Report* (Vol. 2010–5102). Retrieved from

https://pubs.usgs.gov/sir/2010/5102/support/sir2010-5102.pdf

Carpenter, T. M., Sperfslage, J. A., Georgakakos, K. P., Sweeney, T., & Fread, D. L. (1999). National threshold runoff estimation utilizing GIS in support of operational flash flood warning systems. *Journal of Hydrology*, *224*(1–2), 21–44. https://doi.org/10.1016/S0022-1694(99)00115-8

Carrera, J., Alcolea, A., Medina, A., Hidalgo, J., & Slooten, L. J. (2005). Inverse problem in hydrogeology. *Hydrogeology Journal*, *13*(1), 206–222. https://doi.org/10.1007/s10040-004-0404-7

Carrera, J., & Martinez-Landa, L. (2000). Mixed discrete-continuum models: A summary of experiences in test interpretation and model prediction. In *Geophysical Monograph Series* (Vol. 122, pp. 251–265). https://doi.org/10.1029/GM122p0251

Castillo, V. M., Martinez-Mena, M., & Albaladejo, J. (1997). Runoff and Soil Loss Response to Vegetation Removal in a Semiarid Environment. *Soil Science Society of America Journal*, *61*(4), 1116. https://doi.org/10.2136/sssaj1997.03615995006100040018x

Castle, S. L., Thomas, B. F., Reager, J. T., Rodell, M., Swenson, S. C., & Famiglietti, J. S. (2014). Groundwater depletion during drought threatens future water security of the Colorado River Basin. *Geophysical Research Letters*, *41*(16), 5904–5911. https://doi.org/10.1002/2014GL061055

Central Ground Water Board. (2011). *Select Case Studies: Rain Water Harvesting and Artificial Recharge*. Ministry of Water Resources, Govt. of India.

Central Ground Water Board. (2013). *Master plan for artificial recharge to ground water in India*. Ministry of Water Resources, Govt. of India.

Chandra, S., Nagaiah, E., Kumar, D., Ahmeduddin, M., Raju, K., Mallesh, D., … Ahmed, S. (2009). *Establishment of International Hydrogeological Park at Chautuppal , Nalgonda District , Andhra Pradesh Delineation of Aquifer Geometry using Electrical Resistivity Tomography : Phase-I. IFCGR Technical Report - Unpublished, 27 pp.*

Chen, M., & Cai, Z. (1995). Groundwater resources and hydro-environmental problems in China. *Episodes*, *18 (1-2)*(1), 66–68.

Cherlet, M., Hutchison, C., Reynolds, J., Hill, J., Sommer, S., & von Maltitz, G. (2018). *World Atlas of Desertification*. Luxembourg. https://doi.org/10.2760/06292

Chiang, W. H., & Kinzelbach, W. (1998). Processing Modflow. *A Simulation Program for Modelling Groundwater Flow and Pollution. User Manual*. Retrieved from http://www.pmwin.net/programs/prevpm/pm4/doc/pmwin41.pdf

Childs, E. C., & Collis-George, N. (1950). The permeability of porous materials. *Proceedings of the Royal Society of London. Series A. Mathematical and Physical Sciences*, *201*(1066), 392–405. https://doi.org/10.1098/rspa.1950.0068

Chilton, P. J., & Foster, S. S. D. (1995). Hydrogeological Characterisation And Water-Supply Potential Of Basement Aquifers In Tropical Africa. *Hydrogeology Journal*, *3*(1), 36–49. https://doi.org/10.1007/s100400050061

Christiansen, L., Binning, P. J., Rosbjerg, D., Andersen, O. B., & Bauer-Gottwein, P. (2011). Using time-lapse gravity for groundwater model calibration: An application to alluvial aquifer storage. *Water Resources Research*, *47*(6), 1–12. https://doi.org/10.1029/2010WR009859

Chuah, C. J., Lye, H. R., Ziegler, A. D., Wood, S. H., Kongpun, C., & Rajchagool, S. (2016). Fluoride: A naturally-occurring health hazard in drinking-water resources of Northern Thailand. *Science of The Total Environment*, *545–546*, 266–279. https://doi.org/10.1016/j.scitotenv.2015.12.069

Clark, I. D., & Douglas, M. (2000). Recharge and Preservation of Laurentide Glacial Melt Water in the Canadian Shield. *Ground Water*, *38*(5), 735–742.

Comte, J.-C., Cassidy, R., Nitsche, J., Ofterdinger, U., Pilatova, K., & Flynn, R. (2012). The typology of Irish hard-rock aquifers based on an integrated hydrogeological and geophysical approach. *Hydrogeology Journal*, 1569–1588. https://doi.org/10.1007/s10040-012-0884-9

Constantz, J., Thomas, C. L., & Zellweger, G. (1994). Influence of diurnal variations in stream temperature

on streamflow loss and groundwater recharge. *Water Resources Research*, *30*(12), 3253–3264. https://doi.org/10.1029/94WR01968

Cook, P. G., Solomon, D. K., Sanford, W. E., Busenberg, E., Plummer, L. N., & Poreda, R. J. (1996a). Inferring shallow groundwater flow in saprolite and fractured rock using environmental tracers. *WATER RESOURCES RESEARCH*, *32*(6), 1501–1509. https://doi.org/10.1029/96WR00354

Cook, P. G., Solomon, D. K., Sanford, W. E., Busenberg, E., Plummer, L. N., & Poreda, R. J. (1996b). Inferring shallow groundwater flow in saprolite and fractured rock using environmental tracers. *Water Resources Research*, *32*(6), 1501–1509. https://doi.org/10.1029/96WR00354

Coudrain-Ribstein, A., Pratx, B., Talbi, A., & Jusserand, C. (1998). L'évaporation des nappes phréatiques sous climat aride est-elle indépendante de la nature du sol? *Comptes Rendus de l'Académie Des Sciences - Series IIA - Earth and Planetary Science*, *326*(3), 159–165. https://doi.org/10.1016/S1251-8050(00)89030-8

Crosbie, R. S., Davies, P., Harrington, N., & Lamontagne, S. (2015). Ground truthing groundwater-recharge estimates derived from remotely sensed evapotranspiration: a case in South Australia. *Hydrogeology Journal*, *23*, 335–350. https://doi.org/10.1007/s10040-014-1200-7

Croteau, A., Nastev, M., & Lefebvre, R. (2010). Groundwater Recharge Assessment in the Chateauguay River Watershed. *Canadian Water Resources Journal*, *35*(4), 451–468. https://doi.org/10.4296/cwrj3504451

Cushman, J. H., & Tartakovsky, D. M. (2016). *The handbook of groundwater engineering: Third edition*. (J. Cushman & D. Tartakovsky, Eds.), *The Handbook of Groundwater Engineering: Third Edition*. Taylor & Francis Group, 6000 Broken Sound Parkway NW, Suite 300, Boca Raton, FL 33487-2742: CRC Press. https://doi.org/10.1201/9781315371801

Cuthbert, M. O. (2010). An improved time series approach for estimating groundwater recharge from groundwater level fluctuations. *WATER RESOURCES RESEARCH*, *46*. https://doi.org/10.1029/2009WR008572

Cuthbert, M. O., Acworth, R. I., Andersen, M. S., Larsen, J., McCallum, A., Rau, G. C., & Tellam, J. H. (2016). Understanding and quantifying focused, indirect groundwater recharge from ephemeral streams using water table fluctuations. *Water Resources Research*, n/a-n/a. https://doi.org/10.1002/2015WR017503

Cuthbert, M. O., & Tindimugaya, C. (2010). The importance of preferential flow in controlling groundwater recharge in tropical Africa and implications for modelling the impact of climate change on groundwater resources. *Journal of Water and Climate Change*, *1*(4), 234–245. https://doi.org/10.2166/wcc.2010.040

Darcel, C., Bour, O., Davy, P., & de Dreuzy, J. R. (2003). Connectivity properties of two-dimensional fracture networks with stochastic fractal correlation. *Water Resources Research*, *39*(10), 1–13. https://doi.org/10.1029/2002WR001628

Darcy, H. (1856). *Les Fontaines Publiques de la Ville de Dijon (The Public Fountains of the City of Dijon)*. Victor Dalmont.

Darling, W. G., & Bath, A. H. (1988). A stable isotope study of recharge processes in the English Chalk. *Journal of Hydrology*, *101*(1–4), 31–46. https://doi.org/10.1016/0022-1694(88)90026-1

Davis, S. N., & Turk, L. J. (1964). Optimum Depth of Wells in Crystalline Rocks. *Groundwater*, *2*(2), 6–11. https://doi.org/10.1111/j.1745-6584.1964.tb01750.x

Davy, P., Le Goc, R., Darcel, C., Bour, O., De Dreuzy, J. R., & Munier, R. (2010). A likely universal model of fracture scaling and its consequence for crustal hydromechanics. *Journal of Geophysical Research: Solid Earth*, *115*(10), 1–13. https://doi.org/10.1029/2009JB007043

Dawes, W., Ali, R., Varma, S., Emelyanova, I., Hodgson, G., & McFarlane, D. (2012). Modelling the effects of climate and land cover change on groundwater recharge in south-west Western Australia. *Hydrology and Earth System Sciences*, *16*(8), 2709–2722. https://doi.org/10.5194/hess-16-2709-2012

de Condappa, D. (2005). *Étude de l'écoulement d'eau à travers la Zone Non-Saturée des aquifères de socle à l'échelle spatiale du bassin versant. Application à l'évaluation de la recharge au sein du bassin versant de Maheshwaram, Andhra Pradesh, Inde.* Université Joseph Fourier.

De Dreuzy, J. R., Méheust, Y., & Pichot, G. (2012). Influence of fracture scale heterogeneity on the flow properties of three-dimensional discrete fracture networks (DFN). *Journal of Geophysical Research B: Solid Earth*, *117*(11), 1–21. https://doi.org/10.1029/2012JB009461

de Golbéry, L., & Chappuis, A. (2012). The Atlas "Water Resources de l'Andhra Pradesh"- Test of visual presentation for informations used by users and managers of water resources from a state of India. *Cartes & Géomatique-Journées d'étude Du Comité Françcais de Cartographie (CFC), Besançon, France*, *213*, 103–106.

de Marsily, G. (1986). *Quantitative hydrogeology*. Paris School of Mines, Fontainebleau.

de Marsily, G., Delay, F., Gonçalvès, J., Renard, P., Teles, V., & Violette, S. (2005). Dealing with spatial heterogeneity. *Hydrogeology Journal*, *13*(1), 161–183. https://doi.org/10.1007/s10040-004-0432-3

de Vries, J. J., & Simmers, I. (2002). Groundwater recharge: An overview of process and challenges. *Hydrogeology Journal*, *10*(1), 5–17. https://doi.org/10.1007/s10040-001-0171-7

Deng, L., Wang, W., Cai, Y., Hu, A., & Sun, D. (2017). A 70-year groundwater recharge record from sandy loess in northwestern China and its climatic implications. *Environmental Earth Sciences*, *76*(24), 1–10. https://doi.org/10.1007/s12665-017-7155-y

Descroix, L., Bouzou, I., Genthon, P., Sighomnou, D., Mahe, G., Mamadou, I., … Olivry, J.-C. (2013). Impact of Drought and Land – Use Changes on Surface – Water Quality and Quantity: The Sahelian Paradox. In *Current Perspectives in Contaminant Hydrology and Water Resources Sustainability* (Vol. 2, p. 64). InTech. https://doi.org/10.5772/54536

Devlin, J. F., & Sophocleous, M. (2005). The persistence of the water budget myth and its relationship to sustainability. *Hydrogeology Journal*, *13*(4), 549–554. https://doi.org/10.1007/s10040-004-0354-0

Dewandel, B., Gandolfi, J.-M., de Condappa, D., & Ahmed, S. (2008). An efficient methodology for estimating irrigation return flow coefficients of irrigated crops at watershed and seasonal scale. *Hydrological Processes*, *22*(11), 1700–1712. https://doi.org/10.1002/hyp.6738

Dewandel, B., Jeanpert, J., Ladouche, B., Join, J. J., & Maréchal, J. C. (2017). Inferring the heterogeneity, transmissivity and hydraulic conductivity of crystalline aquifers from a detailed water-table map. *Journal of Hydrology*, *550*, 118–129. https://doi.org/10.1016/j.jhydrol.2017.03.075

Dewandel, B., Lachassagne, P., & Krishnamurthy, N. S. (2006). A generalized 3-D geological and hydrogeological conceptual model of granite aquifers controlled by single or multiphase weathering. *Journal of Hydrology*, 260–284. https://doi.org/10.1016/j.jhydrol.2006.03.026

Dewandel, B., Maréchal, J. C., Bour, O., Ladouche, B., Ahmed, S., Chandra, S., & Pauwels, H. (2012). Upscaling and regionalizing hydraulic conductivity and effective porosity at watershed scale in deeply weathered crystalline aquifers. *Journal of Hydrology*, *416–417*, 83–97. https://doi.org/10.1016/j.jhydrol.2011.11.038

Dewandel, B., Perrin, J., Ahmed, S., Aulong, S., Hrkal, Z., Lachassagne, P., … Massuel, S. (2010). Development of a tool for managing groundwater resources in semi-arid hard rock regions: Application to a rural watershed in South India. *Hydrological Processes*, *24*(19), 2784–2797. https://doi.org/10.1002/hyp.7696

Dickinson, J. E., Hanson, R. T., Ferré, T. P. A., & Leake, S. A. (2004). Inferring time-varying recharge from inverse analysis of long-term water levels. *Water Resources Research*, *40*(7), 1–15. https://doi.org/10.1029/2003WR002650

Dieter, C. A., Maupin, M. A., Caldwell, R. R., Harris, M. A., Ivahnenko, T. I., Lovelace, J. K., … Linsey, K. S. (2018). *Estimated use of water in the United States in 2015* (Vol. U.S. Geolo). U.S. Geological Survey. https://doi.org/10.3133/cir1441

Dillon, P. J. (2005). Future management of aquifer recharge. *HYDROGEOLOGY JOURNAL*, *13*(1), 313–

316. https://doi.org/10.1007/s10040-004-0413-6

Dillon, P. J., Escalante, E. F., & Tuinhof, A. (2012). *Management of aquifer recharge and discharge processes and aquifer storage equilibrium. IAH contribution to GEF-FAO Groundwater Governance Thematic Paper 4*.

Dillon, P. J., Gale, I., Contreras, S., Pavelic, P., Evans, R., & Ward, J. (2009). Managing aquifer recharge and discharge to sustain irrigation livelihoods under water scarcity and climate change. *IAHS-AISH Publication*, *330*(September), 1–12. Retrieved from http://www.scopus.com/inward/record.url?eid=2-s2.0-78751661981&partnerID=tZOtx3y1

Dillon, P. J., & Jimenez, B. (2008). Water reuse via aquifer recharge: intentional and unintentional practices. *Water Reuse: An International Survey of Current Practice, Issues and Needs*, 260–280. IWA Publishing, London, UK.

Dillon, P. J., & Liggett, J. A. (1983). An ephemeral stream-aquifer interaction model. *Water Resources Research*, *19*(3), 621–626. https://doi.org/10.1029/WR019i003p00621

Dincer, T., Al-Mugrin, A., & Zimmermann, U. (1974). Study of the infiltration and recharge through the sand dunes in arid zones with special reference to the stable isotopes and thermonuclear tritium. *Journal of Hydrology*, *23*(1–2), 79–109. https://doi.org/10.1016/0022-1694(74)90025-0

Dingman, S. L. (2015). *Physical Hydrology Third Edition*. Long Grove, USA: Waveland Press, Inc.

Döll, P., & Fiedler, K. (2008). Global-scale modeling of groundwater recharge. *Hydrology and Earth System Sciences*, *12*(3), 863–885. https://doi.org/10.5194/hess-12-863-2008

Droogers, P., & Bastiaanssen, W. (2002). Irrigation Performance using Hydrological and Remote Sensing Modeling. *Journal of Irrigation and Drainage Engineering*, *128*(1), 11–18. https://doi.org/10.1061/(ASCE)0733-9437(2002)128:1(11)

Duchaufour, P. (1982). *Pedology: Pedogenesis and classification*. (George Allen & Unwin, Ed.). London.

Dunne, T. (1970). Runoff production in a humid area. *United States Department of Agriculture, Agricultural Research Service*, (41–160), 108 pp.

Dunne, T. (1978). Field Studies of Hillslope Flow Processes. In M. J. Kirby (Ed.), *Hillslope Hydrology* (Vol. 227). New York: John Wiley & Sons, Ltd.

Dunne, T., & Black, R. D. (1970). Partial Area Contributions to Storm Runoff in a Small New England Watershed. *Water Resources Research*, *6*(5), 1296–1311. https://doi.org/10.1029/WR006i005p01296

Dunne, T., Zhang, W., & Aubry, B. F. (1991). Effects of Rainfall, Vegetation, and Microtopography on Infiltration and Runoff. *Water Resources Research*, *27*(9), 2271–2285. https://doi.org/10.1029/91WR01585

Ebrahimi, H., Ghazavi, R., & Karimi, H. (2016). Estimation of Groundwater Recharge from the Rainfall and Irrigation in an Arid Environment Using Inverse Modeling Approach and RS. *Water Resources Management*, *30*(6), 1939–1951. https://doi.org/10.1007/s11269-016-1261-6

Edmunds, W. M., Darling, W. G., & Kinniburgh, D. G. (1988). Solute Profile Techniques for Recharge Estimation in Semi-Arid and Arid Terrain. In Intergovernmental Panel on Climate Change (Ed.), *Estimation of Natural Groundwater Recharge* (Vol. 53, pp. 139–157). Dordrecht: Springer Netherlands. https://doi.org/10.1007/978-94-015-7780-9_9

Edmunds, W. M., Fellman, E., Goni, I. B., & Prudhomme, C. (2002). Spatial and temporal distribution of groundwater recharge in northern Nigeria. *Hydrogeology Journal*, *10*(1), 205–215. https://doi.org/10.1007/s10040-001-0179-z

Eilers, V. H. M., Carter, R. C., & Rushton, K. R. (2007). A single layer soil water balance model for estimating deep drainage (potential recharge): An application to cropped land in semi-arid North-east Nigeria. *Geoderma*, *140*(1–2), 119–131. https://doi.org/10.1016/j.geoderma.2007.03.011

Fairhurst, C. (2004). Nuclear waste disposal and rock mechanics: contributions of the Underground Research Laboratory (URL), Pinawa, Manitoba, Canada. *International Journal of Rock Mechanics and Mining Sciences*, *41*(8), 1221–1227. https://doi.org/10.1016/j.ijrmms.2004.09.001

Famiglietti, J. S. (2014). The global groundwater crisis. *Nature Climate Change*, *4*(11), 945–948. https://doi.org/10.1038/nclimate2425

Ferrant, S., Selles, A., Le Page, M., Herrault, P.-A., Pelletier, C., Al-Bitar, A., … Kerr, Y. (2017). Detection of Irrigated Crops from Sentinel-1 and Sentinel-2 Data to Estimate Seasonal Groundwater Use in South India. *Remote Sensing*, *9*(11), 1119. https://doi.org/10.3390/rs9111119

Fetter, C. W. (2000). *Applied hydrogeology*. Prentice hall.

Fletcher, R., Buss, H., & Brantley, S. (2006). A spheroidal weathering model coupling porewater chemistry to soil thicknesses during steady-state denudation. *Earth and Planetary Science Letters*, *244*(1–2), 444–457. https://doi.org/10.1016/j.epsl.2006.01.055

Fogg, G. E., Noyes, C. D., & Carle, S. F. (1998). Geologically based model of heterogeneous hydraulic conductivity in an alluvial setting. *Hydrogeology Journal*, *6*(1), 131–143. https://doi.org/10.1007/s100400050139

Forster, C., & Smith, L. (1988). Groundwater flow systems in mountainous terrain: 2. Controlling factors. *Water Resources Research*, *24*(7), 1011–1023. https://doi.org/10.1029/WR024i007p01011

Fouépé Takounjou, A., Ngoupayou, J. R. N., Riotte, J., Takem, G. E., Mafany, G., Maréchal, J. C., & Ekodeck, G. E. (2011). Estimation of groundwater recharge of shallow aquifer on humid environment in Yaounde, Cameroon using hybrid water-fluctuation and hydrochemistry methods. *Environmental Earth Sciences*, *64*(1), 107–118. https://doi.org/10.1007/s12665-010-0822-x

Fu, G., Chen, S., Liu, C., & Shepard, D. (2004). Hydro-Climatic Trends of the Yellow River Basin for the Last 50 Years. *Climatic Change*, *65*(1/2), 149–178. https://doi.org/10.1023/B:CLIM.0000037491.95395.bb

Gal, L., Grippa, M., Hiernaux, P., Pons, L., & Kergoat, L. (2017). The paradoxical evolution of runoff in the pastoral Sahel: analysis of the hydrological changes over the Agoufou watershed (Mali) using the KINEROS-2 model. *Hydrology and Earth System Sciences*, *21*(9), 4591–4613. https://doi.org/10.5194/hess-21-4591-2017

Gale, I. N., Macdonald, D. M. J., Calow, R. C., Neumann, I., Moench, M., Kulkarni, H., … Palanisami, K. (2006). *Managed Aquifer Recharge : an assessment of its role and effectiveness in watershed management*.

Gale, I. N., Neumann, I., Calow, R. C., & Moench, M. (2002). *The effectiveness of Artificial Recharge of groundwater : a review*.

Gardner, W. R. (1958). Some steady-state solutions of the unsaturated moisture flow equation with application to evaporation from a water table. *Soil Science*, *85*(4), 228–232. https://doi.org/10.1097/00010694-195804000-00006

Gburek, W. J., & Folmar, G. J. (1999). A groundwater recharge field study: site characterization and initial results. *Hydrological Processes*, *13*(17), 2813–2831. https://doi.org/10.1002/(SICI)1099-1085(19991215)13:17<2813::AID-HYP901>3.0.CO;2-6

Gee, G. W., & Hillel, D. (1988). Groundwater recharge in arid regions: Review and critique of estimation methods. *Hydrological Processes*, *2*(3), 255–266. https://doi.org/10.1002/hyp.3360020306

Gehman, C. L., Harry, D. L., Sanford, W. E., Stednick, J. D., & Beckman, N. A. (2010). Estimating specific yield and storage change in an unconfined aquifer using temporal gravity surveys. *Water Resources Research*, *46*(4), 1–16. https://doi.org/10.1029/2007WR006096

George, R. J. (1992). Hydraulic properties of groundwater systems in the saprolite and sediments of the wheatbelt, Western Australia. *Journal of Hydrology*, *130*(1–4), 251–278. https://doi.org/10.1016/0022-1694(92)90113-A

Giacobbo, F., Marseguerra, M., & Zio, E. (2002). Solving the inverse problem of parameter estimation by genetic algorithms: the case of a groundwater contaminant transport model. *Annals of Nuclear Energy*, *29*(8), 967–981. https://doi.org/10.1016/S0306-4549(01)00084-6

Gillespie, P. A., Howard, C. B., Walsh, J. J., & Watterson, J. (1993). Measurement and characterisation of

spatial distributions of fractures. *Tectonophysics*, *226*(1–4), 113–141. https://doi.org/10.1016/0040-1951(93)90114-Y

Gillham, R. W. (1984). The capillary fringe and its effect on water-table response. *Journal of Hydrology*, *67*(1–4), 307–324. https://doi.org/10.1016/0022-1694(84)90248-8

Gilli, E., Mangan, C., & Mudry, J. (2016). *Hydrogéologie-4e éd.: Objets, méthodes, applications*. Dunod.

Gleeson, T., Befus, K. M., Jasechko, S., Luijendijk, E., & Cardenas, M. B. (2016). The global volume and distribution of modern groundwater. *Nature Geoscience*, *9*(2), 161–167. https://doi.org/10.1038/ngeo2590

Gleeson, T., & Manning, A. H. (2008). Regional groundwater flow in mountainous terrain: Three-dimensional simulations of topographic and hydrogeologic controls. *Water Resources Research*, *44*(10). https://doi.org/10.1029/2008WR006848

Gleeson, T., Novakowski, K., & Kyser, K. T. (2009). Extremely rapid and localized recharge to a fractured rock aquifer. *Journal of Hydrology*, *376*(3–4), 496–509. https://doi.org/10.1016/j.jhydrol.2009.07.056

Gleick, P. H. (1993). *Water in crisis: a guide to the worlds fresh water resources*. New York, NY: Oxford University Press.

Glendenning, C. J., van Ogtrop, F. F., Mishra, A. K., & Vervoort, R. W. (2012). Balancing watershed and local scale impacts of rain water harvesting in India—A review. *Agricultural Water Management*, *107*, 1–13. https://doi.org/10.1016/j.agwat.2012.01.011

Golder Associates. (2017). *Hinds Managed Aquifer Recharge Pilot Trial: Phase 1 Report*. Christchurch, NZ.

Government of Andhra Pradesh. (2003). *Andhra Pradesh Water Vision-Methods, Position papers, and District reports* (Vol. II). Water Conservation Mission, Government Insurance Building, Tilak road, Hyderabad, Andhra Pradesh.

Gray, E., & Srinidhi, A. (2013). *Watershed Development in India: Economic valuation and adaptation considerations* (Scaling Up Good Adaptation Practices (SUGAP) Project). Washington, D.C.

Guihéneuf, N. (2014). *Structure des écoulements et propriétés de transport des aquifères cristallins fracturés et altérés : Application au site de Choutuppal (Inde du Sud)*. Université de Rennes 1.

Guihéneuf, N., Boisson, A., Bour, O., Dewandel, B., Perrin, J., Dausse, A., … Maréchal, J. C. (2014). Groundwater flows in weathered crystalline rocks: Impact of piezometric variations and depth-dependent fracture connectivity. *Journal of Hydrology*, *511*, 320–334. https://doi.org/10.1016/j.jhydrol.2014.01.061

Guihéneuf, N., Bour, O., Boisson, A., Le Borgne, T., Becker, M. W., Nigon, B., … Maréchal, J. C. (2017). Insights about transport mechanisms and fracture flow channeling from multi-scale observations of tracer dispersion in shallow fractured crystalline rock. *Journal of Contaminant Hydrology*, *206*(May), 18–33. https://doi.org/10.1016/j.jconhyd.2017.09.003

Gupta, S. K., & Deshpande, R. D. (2004). Water for India in 2050: First-order assessment of available options. *Current Science*, *86*(9), 1216–1224. https://doi.org/10.1080/09537325.2011.621294

Haitjema, H. M., & Mitchell-Bruker, S. (2005). Are Water Tables a Subdued Replica of the Topography? *Ground Water*, *43*(6), 050824075421008. https://doi.org/10.1111/j.1745-6584.2005.00090.x

Halford, K. J. (1999). Effects of Steady-State Assumption on Hydraulic Conductivity and Recharge Estimates in a Surficial Aquifer System. *Ground Water*, *37*(1), 70–79. https://doi.org/10.1111/j.1745-6584.1999.tb00959.x

Hallberg, G. R. (1989). Pesticides pollution of groundwater in the humid United States. *Agriculture, Ecosystems & Environment*, *26*(3–4), 299–367. https://doi.org/10.1016/0167-8809(89)90017-0

Hammond, P. A. (2018). Reliable yields of public water-supply wells in the fractured-rock aquifers of central Maryland, USA. *Hydrogeology Journal*, *26*(1), 333–349. https://doi.org/10.1007/s10040-017-1639-4

Hantush, M. S. (1967). Growth and decay of groundwater-mounds in response to uniform percolation. *Water Resources Research*, *3*(1), 227–234. https://doi.org/10.1029/WR003i001p00227

Harbaugh, A. W. (2005). MODFLOW-2005 , The U . S . Geological Survey Modular Ground-Water Model — the Ground-Water Flow Process. *U.S. Geological Survey Techniques and Methods*, 253.

Harbaugh, A. W., Banta, E. R., Hill, M. C., Mcdonald, M. G., Groat, C. G., Harbaugh, B. A. W., … Mcdonald, M. G. (2000). Modflow-2000 , the U . S . Geological Survey Modular Ground-Water Model User Guide To Modularization Concepts and the Ground-Water Flow Process. *U.S. Geological Survey*, 127. Retrieved from http://www.gama-geo.hu/kb/download/ofr00-92.pdf

Hare, D. K., Briggs, M. A., Rosenberry, D. O., Boutt, D. F., & Lane, J. W. (2015). A comparison of thermal infrared to fiber-optic distributed temperature sensing for evaluation of groundwater discharge to surface water. *Journal of Hydrology*, *530*, 153–166. https://doi.org/10.1016/j.jhydrol.2015.09.059

Harris, J. M., & Roach, B. (2018). *Environmental and Natural Resource Economics: A Contemporary Approach*. New York, USA: Routledge.

Harte, P. T., & Winter, T. C. (1993). Factors affecting recharge to crystalline rock in the Mirror Lake area, Grafton County, New Hampshire. In *US Geological Survey Toxic Substances Hydrology Program, Proceedings of the technical meeting, Colorado Springs, CO.* (pp. 141–150).

Harte, P. T., & Winter, T. C. (1995). Simulations of Flow in Crystalline Rock and Recharge from Overlying Glacial Deposits in a Hypothetical New England Setting. *Ground Water*, *33*(6), 953–964. https://doi.org/10.1111/j.1745-6584.1995.tb00041.x

Hartmann, J., & Moosdorf, N. (2012). Global Lithological Map Database v1.0 (gridded to 0.5° spatial resolution). *PANGEA*. https://doi.org/10.1594/PANGAEA.788537

Hashemi, H., Berndtsson, R., Kompani-Zare, M., & Persson, M. (2013). Natural vs. artificial groundwater recharge, quantification through inverse modeling. *Hydrology and Earth System Sciences*, *17*(2), 637–650. https://doi.org/10.5194/hess-17-637-2013

Haverkamp, R., Desbionne, S., Viallet, P., Angulo-Jaramillo, R., & De Condappa, D. (2016). Soil properties and moisture movement in the unsaturated zone (Chap. 6). *Groundwater Engineering Handbook, Third Edition*, 6–59.

Healy, R. W., & Cook, P. G. (2002). Using groundwater levels to estimate recharge. *Hydrogeology Journal*, *10*(1), 91–109. https://doi.org/10.1007/s10040-001-0178-0

Healy, R. W., & Ronan, A. D. (1996). *Documentation of computer program VS2DH for simulation of energy transport in variably saturated porous media; modification of the US Geological Survey's computer program VS2DT*. Denver, Colorado. https://doi.org/10.3133/wri964230

Healy, R. W., & Scanlon, B. R. (2010). *Estimating Groundwater Recharge* (Vol. 91). Cambridge: Cambridge University Press. https://doi.org/10.1017/CBO9780511780745

Hernández-Mora, N., Martínez, L., Llamas, M. R., & Custodio, E. (2010). Groundwater in the Southern Member States of the European Union: an assessment of current knowledge and future prospects. Country report for Spain, 38. Retrieved from http://www.easac.eu/fileadmin/PDF_s/reports_statements/Spain_Groundwater_country_report.pdf

Hewlett, J. D., & Hibbert, A. R. (1963). Moisture and energy conditions within a sloping soil mass during drainage. *Journal of Geophysical Research*, *68*(4), 1081–1087. https://doi.org/10.1029/JZ068i004p01081

Holzhausen, G. R. (1989). Origin of sheet structure, 1. Morphology and boundary conditions. *Engineering Geology*, *27*(1–4), 225–278. https://doi.org/0013-7952/89

Horton, R. E. (1933). The Role of infiltration in the hydrologic cycle. *Transactions, American Geophysical Union*, *14*(1), 446. https://doi.org/10.1029/TR014i001p00446

Horton, R. E. (1945). EROSIONAL DEVELOPMENT OF STREAMS AND THEIR DRAINAGE BASINS; HYDROPHYSICAL APPROACH TO QUANTITATIVE MORPHOLOGY. *Geological Society of America Bulletin*, *56*(3), 275–370. https://doi.org/10.1130/0016-7606(1945)56[275:EDOSAT]2.0.CO;2

Hsieh, P. (1998). Scale effects in fluid flow through fractured geologic media. Retrieved from https://scholar.google.com/scholar?q=Scale+Effects+in+Fluid+Flow+Through+Fractured+Geologic

al+Media&btnG=&hl=en&num=20&as_sdt=0%2C5

Illman, W. A. (2005). Type curve analyses of pneumatic single-hole tests in unsaturated fractured tuff: Direct evidence for a porosity scale effect. *Water Resources Research*, *41*(4), 1–14. https://doi.org/10.1029/2004WR003703

Illman, W. A. (2006). Strong field evidence of directional permeability scale effect in fractured rock. *Journal of Hydrology*, *319*(1–4), 227–236. https://doi.org/10.1016/j.jhydrol.2005.06.032

Irrigation & CAD Department. (2015). Mission Kakatiya - Mission. Retrieved August 9, 2017, from http://missionkakatiya.cgg.gov.in/homemission

Jackson, C. R. (1992). Hillslope infiltration and lateral downslope unsaturated flow. *Water Resources Research*, *28*(9), 2533–2539. https://doi.org/10.1029/92WR00664

Jakeman, A. J., Barreteau, O., Hunt, R. J., Rinaudo, J.-D., & Ross, A. (2016). *Integrated Groundwater Management*. (A. J. Jakeman, O. Barreteau, R. J. Hunt, J.-D. Rinaudo, & A. Ross, Eds.), *Integrated Groundwater Management*. Cham: Springer International Publishing. https://doi.org/10.1007/978-3-319-23576-9

Jalota, S., & Prihar, S. (1986). Effects of atmospheric evaporativity, soil type and redistribution time on evaporation from bare soil. *Australian Journal of Soil Research*, *24*(3), 357. https://doi.org/10.1071/SR9860357

James, A. J., & Robinson, E. (2001). *Water and Sustainable Rural Livelihoods in Andhra Pradesh: Background paper*.

Jardani, A., Dupont, J. P., Revil, A., Massei, N., Fournier, M., & Laignel, B. (2012). Geostatistical inverse modeling of the transmissivity field of a heterogeneous alluvial aquifer under tidal influence. *Journal of Hydrology*, *472–473*, 287–300. https://doi.org/10.1016/j.jhydrol.2012.09.031

Jasechko, S., & Taylor, R. G. (2015). Intensive rainfall recharges tropical groundwaters. *Environmental Research Letters*, *10*(12), 124015. https://doi.org/10.1088/1748-9326/10/12/124015

Jie, Z., van Heyden, J., Bendel, D., & Barthel, R. (2011). Combination of soil-water balance models and water-table fluctuation methods for evaluation and improvement of groundwater recharge calculations. *Hydrogeology Journal*, *19*(8), 1487–1502. https://doi.org/10.1007/s10040-011-0772-8

Jiménez-Martínez, J., Longuevergne, L., Le Borgne, T., Davy, P., Russian, A., & Bour, O. (2013). Temporal and spatial scaling of hydraulic response to recharge in fractured aquifers: Insights from a frequency domain analysis. *Water Resources Research*, *49*(5), 3007–3023. https://doi.org/10.1002/wrcr.20260

Jing, L. (2003). A review of techniques, advances and outstanding issues in numerical modelling for rock mechanics and rock engineering. *International Journal of Rock Mechanics and Mining Sciences*, *40*(3), 283–353. https://doi.org/10.1016/S1365-1609(03)00013-3

Johnston, C. D. (1987). Preferred water flow and localised recharge in a variable regolith. *Journal of Hydrology*, *94*(1–2), 129–142. https://doi.org/10.1016/0022-1694(87)90036-9

Jones, J. A. A. (2010). Soil piping and catchment response. *Hydrological Processes*, *24*(12), 1548–1566. https://doi.org/10.1002/hyp.7634

Jones, O. R., & Schneider, A. D. (1969). Determining Specific Yield of the Ogallala Aquifer by the Neutron Method. *Water Resources Research*, *5*(6), 1267–1272. https://doi.org/10.1029/WR005i006p01267

Jyrkama, M. I., Sykes, J. F., & Normani, S. D. (2002). Recharge Estimation for Transient Ground Water Modeling. *Ground Water*, *40*(6), 638–648. https://doi.org/10.1111/j.1745-6584.2002.tb02550.x

Kabala, Z. J. (2001). Sensitivity analysis of a pumping test on a well with wellbore storage and skin. *Advances in Water Resources*, *24*(5), 483–504. https://doi.org/10.1016/S0309-1708(00)00051-8

Kacimov, A. R., Zlotnik, V., Al-Maktoumi, A., & Al-Abri, R. (2016). Modeling of transient water table response to managed aquifer recharge: a lagoon in Muscat, Oman. *Environmental Earth Sciences*, *75*(4), 318. https://doi.org/10.1007/s12665-015-5137-5

Keese, K. E., Scanlon, B. R., & Reedy, R. C. (2005). Assessing controls on diffuse groundwater recharge

using unsaturated flow modeling. *Water Resources Research*, *41*(6), 1–12. https://doi.org/10.1029/2004WR003841

Kim, J. H., & Jackson, R. B. (2012). A Global Analysis of Groundwater Recharge for Vegetation, Climate, and Soils. *Vadose Zone Journal*, *11*(1), 0. https://doi.org/10.2136/vzj2011.0021RA

Kinzelbach, W., Aeschbach, W., Alberich, C., Goni, I. B., Beyerle, U., Brunner, P., … Zoellmann, K. (2002). *A Survey of Methods for Analysing Groundwater Recharge in Arid and Semi-arid Regions. Early Warning and Assessment Report Series.*

Kirkby, M. (1988). Hillslope runoff processes and models. *Journal of Hydrology*, *100*(1–3), 315–339. https://doi.org/10.1016/0022-1694(88)90190-4

Knowles, I., Teubner, M., Yan, A., Rasser, P., & Lee, J. W. (2007). Inverse groundwater modelling in the Willunga Basin, South Australia. *Hydrogeology Journal*, *15*(6), 1107–1118. https://doi.org/10.1007/s10040-007-0189-6

Knowling, M. J., & Werner, A. D. (2016). Estimability of recharge through groundwater model calibration: Insights from a field-scale steady-state example. *Journal of Hydrology*, *540*, 973–987. https://doi.org/10.1016/j.jhydrol.2016.07.003

Krásný, J. (2002). Quantitative hardrock hydrogeology in a regional scale. *Norgweg Geol Unders B*, *439*, 7–14.

Krause, S., Blume, T., & Cassidy, N. J. (2012). Investigating patterns and controls of groundwater upwelling in a lowland river by combining Fibre-optic Distributed Temperature Sensing with observations of vertical hydraulic gradients. *Hydrology and Earth System Sciences*, *16*(6), 1775–1792. https://doi.org/10.5194/hess-16-1775-2012

Kumar, M. D., Bassi, N., Kishan, K. S., Chattopadhyay, S., & Ganguly, A. (2016). Rejuvenating Tanks in Telangana. *Economic & Political Weekly*, *lI*(34), 30–34.

Kumar, R., Singh, R. D., & Sharma, K. D. (2005). Water resources of India. *Current Science*, *89*(5), 794–811. https://doi.org/10.1002/047147844X.wr243

Kung, W.-J., Yeh, H.-F., Lin, H.-I., Chen, W.-P., & Lee, C.-H. (2013). An approach to evaluate groundwater recharge from streamflow and groundwater records. *Geosciences Journal*, *17*(3), 353–362. https://doi.org/10.1007/s12303-013-0027-x

Kurtzman, D., & Scanlon, B. R. (2011). Groundwater Recharge through Vertisols: Irrigated Cropland vs. Natural Land, Israel. *Vadose Zone Journal*, *10*(2), 662. https://doi.org/10.2136/vzj2010.0109

Lachassagne, P. (2008). Overview of the hydrogeology of hard rock aquifers: Applications for their survey, management, modelling and protection. In *Groundwater Dynamics in Hard Rock Aquifers: Sustainable Management and Optimal Monitoring Network Design* (pp. 40–63). Springer. https://doi.org/10.1007/978-1-4020-6540-8_3

Lachassagne, P., Wyns, R., & Dewandel, B. (2011). The fracture permeability of Hard Rock Aquifers is due neither to tectonics, nor to unloading, but to weathering processes. *Terra Nova*, *23*(3), 145–161. https://doi.org/10.1111/j.1365-3121.2011.00998.x

Landell Mills Ltd. (2018). *Kabul Managed Aquifer Recharge Project: Environmental Due Diligence Report on Proposed Pilot MAR Sites 3,4, and 6.* Wiltshire, UK.

Lane, J. W., Day-Lewis, F. D., Johnson, C. D., Dawson, C. B., Nelms, D. L., Eddy-Miller, C. A., … Karam, H. (2008). Fiber-Optic Distributed Temperature Sensing: A New Tool for Assessment and Monitoring of Hydrologic Processes. In *Symposium on the Application of Geophysics to Engineering and Environmental Problems 2008* (Vol. Philadelph, pp. 318–326). Environment and Engineering Geophysical Society. https://doi.org/10.4133/1.2963272

Larsson, I. (1984). *Ground water in hard rocks.* Paris, France: United Nations.

Lassabatère, L., Angulo-Jaramillo, R., Soria Ugalde, J. M., Cuenca, R., Braud, I., & Haverkamp, R. (2006). Beerkan Estimation of Soil Transfer Parameters through Infiltration Experiments—BEST. *Soil Science Society of America Journal*, *70*(2), 521. https://doi.org/10.2136/sssaj2005.0026

Le Borgne, T., Bour, O., Paillet, F. L., & Caudal, J. P. (2006). Assessment of preferential flow path connectivity and hydraulic properties at single-borehole and cross-borehole scales in a fractured aquifer. *Journal of Hydrology*, *328*(1–2), 347–359. https://doi.org/10.1016/j.jhydrol.2005.12.029

Leblanc, M. J., Favreau, G., Massuel, S., Tweed, S. O., Loireau, M., & Cappelaere, B. (2008). Land clearance and hydrological change in the Sahel: SW Niger. *Global and Planetary Change*, *61*(3–4), 135–150. https://doi.org/10.1016/j.gloplacha.2007.08.011

Leduc, C., Favreau, G., & Schroeter, P. (2001). Long-term rise in a Sahelian water-table: the Continental Terminal in South-West Niger. *Journal of Hydrology*, *243*(1–2), 43–54. https://doi.org/10.1016/S0022-1694(00)00403-0

Leray, S., de Dreuzy, J.-R., Bour, O., & Bresciani, E. (2013). Numerical modeling of the productivity of vertical to shallowly dipping fractured zones in crystalline rocks. *Journal of Hydrology*, *481*, 64–75. https://doi.org/10.1016/j.jhydrol.2012.12.014

Leray, S., de Dreuzy, J.-R., Bour, O., Labasque, T., & Aquilina, L. (2012). Contribution of age data to the characterization of complex aquifers. *Journal of Hydrology*, *464–465*(August 2014), 54–68. https://doi.org/10.1016/j.jhydrol.2012.06.052

Levison, J. K., & Novakowski, K. S. (2012). Rapid transport from the surface to wells in fractured rock: A unique infiltration tracer experiment. *Journal of Contaminant Hydrology*, *131*(1–4), 29–38. https://doi.org/10.1016/j.jconhyd.2012.01.001

Lezzaik, K., & Milewski, A. (2018). A quantitative assessment of groundwater resources in the Middle East and North Africa region. *Hydrogeology Journal*, *26*(1), 251–266. https://doi.org/10.1007/s10040-017-1646-5

Li, K., Amoozegar, A., Robarge, W. P., & Buol, S. W. (1997). Water Movement and Solute Transport through Saprolite. *Soil Science Society of America Journal*, *61*(6), 1738. https://doi.org/10.2136/sssaj1997.03615995006100060027x

Li, Q., Chen, X., & Bao, A. M. (2011). Evapotranspiration Estimates from Eddy Covariance Tower in Arid and Semi-Arid Areas. *Advanced Materials Research*, *356–360*, 2312–2315. https://doi.org/10.4028/www.scientific.net/AMR.356-360.2312

Limaye, S. D. (2010). Sustainable Ground Water Development in Hard Rock Aquifers in Low-Income Countries and the Role of UNESCO – IUGS - IGCP Project "GROWNET ." *Iranian Journal of Earth Sciences*, *2*, 1–9.

Lin, R., & Wei, K. (2006). Tritium profiles of pore water in the Chinese loess unsaturated zone: Implications for estimation of groundwater recharge. *Journal of Hydrology*, *328*(1–2), 192–199. https://doi.org/10.1016/j.jhydrol.2005.12.010

Liu, C., Zhang, X., & Zhang, Y. (2002). Determination of daily evaporation and evapotranspiration of winter wheat and maize by large-scale weighing lysimeter and micro-lysimeter. *Agricultural and Forest Meteorology*, *111*(2), 109–120. https://doi.org/10.1016/S0168-1923(02)00015-1

Llamas, M. R., & Martínez-Santos, P. (2005a). Intensive Groundwater Use: Silent Revolution and Potential Source of Social Conflicts. *Journal of Water Resources Planning and Management*, (October), 337–342. https://doi.org/10.1177/1354068809342529

Llamas, M. R., & Martínez-Santos, P. (2005b). Intensive Groundwater Use: Silent Revolution and Potential Source of Social Conflicts. American Society of Civil Engineers.

Long, J. C. S., Remer, J. S., Wilson, C. R., & Witherspoon, P. A. (1982). Porous media equivalents for networks of discontinuous fractures. *Water Resources Research*, *18*(3), 645–658. https://doi.org/10.1029/WR018i003p00645

Long, J. C. S., & Witherspoon, P. A. (1985). The relationship of the degree of interconnection to permeability in fracture networks. *Journal of Geophysical Research*, *90*(B4), 3087. https://doi.org/10.1029/JB090iB04p03087

López-Urrea, R., Martín de Santa Olalla, F., Fabeiro, C., & Moratalla, A. (2006). Testing evapotranspiration

equations using lysimeter observations in a semiarid climate. *Agricultural Water Management*, *85*(1–2), 15–26. https://doi.org/10.1016/j.agwat.2006.03.014

Lv, M., Hao, Z., Liu, Z., & Yu, Z. (2013). Conditions for lateral downslope unsaturated flow and effects of slope angle on soil moisture movement. *Journal of Hydrology*, *486*, 321–333. https://doi.org/10.1016/j.jhydrol.2013.02.013

Machiwal, D., & Jha, M. K. (2015). GIS-based water balance modeling for estimating regional specific yield and distributed recharge in data-scarce hard-rock regions. *Journal of Hydro-Environment Research*, *9*(4), 554–568. https://doi.org/10.1016/j.jher.2014.07.004

MacQuarrie, K. T. B., & Mayer, K. U. (2005). Reactive transport modeling in fractured rock: A state-of-the-science review. *Earth-Science Reviews*, *72*(3–4), 189–227. https://doi.org/10.1016/j.earscirev.2005.07.003

Mahlknecht, J., Schneider, J. F., Merkel, B. J., Navarro de Leon, I., & Bernasconi, S. M. (2004). Groundwater recharge in a sedimentary basin in semi-arid Mexico. *Hydrogeology Journal*, *12*(5), 511–530. https://doi.org/10.1007/s10040-004-0332-6

Maliva, R. G. (2015). Managed aquifer recharge: state-of-the-art and opportunities. *Water Science and Technology: Water Supply*, *15*(3), 578–588. https://doi.org/10.2166/ws.2015.009

Malthus, T. (1798). An essay on the principle of population, as it affects the future improvement of society. *Contemporary Sociology*, *2*(3), 340. Retrieved from http://www.esp.org/books/malthus/population/malthus.pdf

Maréchal, J. C., Braun, J. J., Riotte, J., Bedimo, J. P., & Boeglin, J. L. (2011). Hydrological processes of a rainforest headwater swamp from natural chemical tracing in Nsimi watershed, Cameroon. *Hydrological Processes*, *25*(14), 2246–2260. https://doi.org/10.1002/hyp.7989

Maréchal, J. C., Dewandel, B., Ahmed, S., Galeazzi, L., & Zaidi, F. K. (2006). Combined estimation of specific yield and natural recharge in a semi-arid groundwater basin with irrigated agriculture. *Journal of Hydrology*, 281–293. https://doi.org/10.1016/j.jhydrol.2006.02.022

Maréchal, J. C., Dewandel, B., & Subrahmanyam, K. (2004). Use of hydraulic tests at different scales to characterize fracture network properties in the weathered-fractured layer of a hard rock aquifer. *Water Resources Research*, *40*(11), 1–17. https://doi.org/10.1029/2004WR003137

Maréchal, J. C., Ladouche, B., Dörfliger, N., & Lachassagne, P. (2008). Interpretation of pumping tests in a mixed flow karst system. *Water Resources Research*, *44*(5), 1–18. https://doi.org/10.1029/2007WR006288

Maréchal, J. C., Selles, A., Dewandel, B., Boisson, A., & Perrin, J. (2018). An observatory of groundwater in crystalline rock aquifers exposed to a changing environment - Hyderabad (India). *Vadose Zone Journal*, 1–38. https://doi.org/10.2136/vzj2018.04.0076

Maréchal, J. C., Varma, M. R. R., Riotte, J., Vouillamoz, J. M., Kumar, M. S. M., Ruiz, L., … Braun, J. J. (2009). Indirect and direct recharges in a tropical forested watershed: Mule Hole, India. *Journal of Hydrology*, *364*(3–4), 272–284. https://doi.org/10.1016/j.jhydrol.2008.11.006

Maréchal, J. C., Wyns, R., Lachassagne, P., Subrahmanyam, K., & Touchard, F. (2003). Anisotropie verticale de la perméabilité de l'horizon fissuré des aquifères de socle : concordance avec la structure géologique des profils d'altération. *Comptes Rendus Geoscience*, *335*(5), 451–460. https://doi.org/10.1016/S1631-0713(03)00082-8

Martel, S. J. (2006). Effect of topographic curvature on near-surface stresses and application to sheeting joints. *Geophysical Research Letters*, *33*(1). https://doi.org/10.1029/2005GL024710

Martel, S. J. (2017). Progress in understanding sheeting joints over the past two centuries. *Journal of Structural Geology*, *94*, 68–86. https://doi.org/10.1016/j.jsg.2016.11.003

Martinez-Landa, L., & Carrera, J. (2005). An analysis of hydraulic conductivity scale effects in granite (Full-scale Engineered Barrier Experiment (FEBEX), Grimsel, Switzerland). *Water Resources Research*, *41*(3), 1–13. https://doi.org/10.1029/2004WR003458

Martínez-Mena, M., Albaladejo, J., & Castillo, V. M. (1998). Factors influencing surface runoff generation in a Mediterranean semi-arid environment: Chicamo watershed, SE Spain. *Hydrological Processes*, *12*(5), 741–754. https://doi.org/10.1002/(SICI)1099-1085(19980430)12:5<741::AID-HYP622>3.0.CO;2-F

Massuel, S., Perrin, J., Mascre, C., Mohamed, W., Boisson, A., & Ahmed, S. (2014). Managed aquifer recharge in South India: What to expect from small percolation tanks in hard rock? *Journal of Hydrology*, *512*, 157–167. https://doi.org/10.1016/j.jhydrol.2014.02.062

Mawer, C., Parsekian, A., Pidlisecky, A., & Knight, R. (2016). Characterizing Heterogeneity in Infiltration Rates During Managed Aquifer Recharge. *Groundwater*, *54*(6), 818–829. https://doi.org/10.1111/gwat.12423

McCallum, A. M., Andersen, M. S., Rau, G. C., & Acworth, R. I. (2012). A 1-D analytical method for estimating surface water-groundwater interactions and effective thermal diffusivity using temperature time series. *Water Resources Research*, *48*(11), 1–8. https://doi.org/10.1029/2012WR012007

Meinzer, O. E. (1923). *The occurrence of ground water in the United States, with a discussion of principles*. https://doi.org/10.3133/wsp489

Meixner, T., Manning, A. H., Stonestrom, D. A., Allen, D. M., Ajami, H., Blasch, K. W., … Walvoord, M. A. (2016). Implications of projected climate change for groundwater recharge in the western United States. *Journal of Hydrology*, *534*, 124–138. https://doi.org/10.1016/j.jhydrol.2015.12.027

Merritt, M. L., & Konikow, L. F. (2000). Documentation of a computer program to simulate lake-aquifer interation using the MODFLOW Ground-Water Flow Model and the MOC3D Solute-Transport Model. *U.S. Geological Survey Water-Resources Investigations Report 00-4167*, 146.

Michael, H. A., Li, H., Boucher, A., Sun, T., Caers, J., & Gorelick, S. M. (2010). Combining geologic-process models and geostatistics for conditional simulation of 3-D subsurface heterogeneity. *Water Resources Research*, *46*(5), 1–20. https://doi.org/10.1029/2009WR008414

Micklin, P. (2007). The Aral Sea Disaster. *Annual Review of Earth and Planetary Sciences*, *35*(1), 47–72. https://doi.org/10.1146/annurev.earth.35.031306.140120

Migoń, P. (2006). *Geomorphological Landscapes of the World*. (P. Migon, Ed.), *Geomorphological Landscapes of the World*. Dordrecht: Springer Netherlands. https://doi.org/10.1007/978-90-481-3055-9

Mileham, L., Taylor, R. G., Todd, M., Tindimugaya, C., & Thompson, J. (2009). The impact of climate change on groundwater recharge and runoff in a humid, equatorial catchment: Sensitivity of projections to rainfall intensity. *Hydrological Sciences Journal*, *54*(4), 727–738. https://doi.org/10.1623/hysj.54.4.727

Miller, R. W., & Donahue, R. L. (1990). *Soils: an introduction to soils and plant growth*. Prentice-Hall International Inc.

Mizan, A. (2019). *Successive development of decision support tool for groundwater management in over-exploited aquifer of southern India*. National Geophysical Research Institute.

Mohanty, B. P. (2013). Soil Hydraulic Property Estimation Using Remote Sensing: A Review. *Vadose Zone Journal*, *12*(4), 0. https://doi.org/10.2136/vzj2013.06.0100

Molle, F., Shah, T., & Barker, R. (2003). The Groundswell of Pumps : Multilevel Impacts of a Silent Revolution. *Water Management*, (November), 1–18.

Molle, F., Wester, P., & Hirsch, P. (2010). River basin closure: Processes, implications and responses. *Agricultural Water Management*, *97*(4), 569–577. https://doi.org/10.1016/j.agwat.2009.01.004

Molz, F. J. (2004). Stochastic fractal-based models of heterogeneity in subsurface hydrology: Origins, applications, limitations, and future research questions. *Reviews of Geophysics*, *42*(1), RG1002. https://doi.org/10.1029/2003RG000126

Mualem, Y. (1976). Hysteretical models for prediction of the hydraulic conductivity of unsaturated porous media. *Water Resources Research*, *12*(6), 1248–1254. https://doi.org/10.1029/WR012i006p01248

National Research Council. (1996). *Rock Fractures and Fluid Flow*. Washington, D.C.: National Academies Press. https://doi.org/10.17226/2309

Neuman, S. P. (2005). Trends, prospects and challenges in quantifying flow and transport through fractured rocks. *Hydrogeology Journal*, *13*(1), 124–147. https://doi.org/10.1007/s10040-004-0397-2

Neves, M. A., & Morales, N. (2007). Well productivity controlling factors in crystalline terrains of southeastern Brazil. *Hydrogeology Journal*, *15*(3), 471–482. https://doi.org/10.1007/s10040-006-0112-6

Newman, B. D., Campbell, A. R., & Wilcox, B. P. (1998). Lateral subsurface flow pathways in a semiarid Ponderosa pine hillslope. *Water Resources Research*, *34*(12), 3485–3496. https://doi.org/10.1029/98WR02684

Nguyen, T. S., Borgesson, L., Chijimatsu, M., Rutqvist, J., Fujita, T., Hernelind, J., … Jing, L. (2001). Hydro-mechanical response of a fractured granitic rock mass to excavation of a test pit - The Kamaishi mine experiment in Japan. *International Journal of Rock Mechanics and Mining Sciences*, *38*(1), 79–94. https://doi.org/10.1016/S1365-1609(00)00066-6

Nilesh, V. (2016). Hyderabad: Pollutants in Musi rise, river becomes sewage. Retrieved December 6, 2017, from http://www.deccanchronicle.com/lifestyle/pets-and-environment/250716/hyderabad-pollutants-in-musi-rise-river-becomes-sewage.html

Nimmo, J. R. (2005). Unsaturated Zone Flow Processes. In *Encyclopedia of Hydrological Sciences* (pp. 2299–2322). Chichester, UK: John Wiley & Sons, Ltd. https://doi.org/10.1002/0470848944.hsa161

Nimmo, J. R., Creasey, K. M., Perkins, K. S., & Mirus, B. B. (2017). Preferential flow, diffuse flow, and perching in an interbedded fractured-rock unsaturated zone. *Hydrogeology Journal*, *25*(2), 421–444. https://doi.org/10.1007/s10040-016-1496-6

Nimmo, J. R., Healy, R. W., & Stonestrom, D. A. (2005). Aquifer Recharge. In *Encyclopedia of Hydrological Sciences* (pp. 2229–2246). Chichester, UK: John Wiley & Sons, Ltd. https://doi.org/10.1002/0470848944.hsa161a

Nordstrom, D. K., Olsson, T., Carlsson, L., & Fritz, P. (1989). Introduction to the hydrogeochemical investigations within the International Stripa Project. *Geochimica et Cosmochimica Acta*, *53*(8), 1717–1726. https://doi.org/10.1016/0016-7037(89)90293-7

Ognianik, N., & Paramonova, N. (2001). Estimation of real and predicted infiltration recharge for the irrigated area in southern Ukraine. In Gehrels, H and Peters, NE and Hoehn, E and Jensen, K and Leibundgut, C and Griffioen, J and Webb, B and Zaadnoordijk, WJ (Ed.), *IMPACT OF HUMAN ACTIVITY ON GROUNDWATER DYNAMICS* (pp. 95–98).

Oki, T. (2006). Global Hydrological Cycles and World Water Resources. *Science*, *313*(5790), 1068–1072. https://doi.org/10.1126/science.1128845

Ollier, C. D. (1971). Causes of spheroidal weathering. *Earth Science Reviews*, *7*(3), 127–141. https://doi.org/10.1016/0012-8252(71)90005-5

Osterkamp, W. R., Lane, L. J., & Savard, C. S. (1994). Recharge estimates using a geomorphic/distributed-parameter simulation approach, Amargosa River basin. *Water Resources Bulletin*, *30*(3), 493–507. https://doi.org/10.1111/j.1752-1688.1994.tb03308.x

Owor, M., Taylor, R. G., Tindimugaya, C., & Mwesigwa, D. (2009). Rainfall intensity and groundwater recharge: Empirical evidence from the Upper Nile Basin. *Environmental Research Letters*, *4*(3). https://doi.org/10.1088/1748-9326/4/3/035009

Pan, Y., Gong, H., Zhou, D., Li, X., & Nakagoshi, N. (2011). Impact of land use change on groundwater recharge in Guishui River Basin, China. *Chinese Geographical Science*, *21*(6), 734–743. https://doi.org/10.1007/s11769-011-0508-7

Perrin, J., Ahmed, S., & Hunkeler, D. (2011). The effects of geological heterogeneities and piezometric fluctuations on groundwater flow and chemistry in a hard-rock aquifer, southern India. *Hydrogeology Journal*, *19*(6), 1189–1201. https://doi.org/10.1007/s10040-011-0745-y

Perrin, J., Ferrant, S., Massuel, S., Dewandel, B., Maréchal, J. C., Aulong, S., & Ahmed, S. (2012). Assessing water availability in a semi-arid watershed of southern India using a semi-distributed model. *Journal of Hydrology*, *460–461*, 143–155. https://doi.org/10.1016/j.jhydrol.2012.07.002

Perrin, J., Mascre, C., Massuel, S., & Ahmed, S. (2009). Tank management in Andhra Pradesh, India: Percolation versus irrigation. In *IAHS-AISH Publication* (Vol. 330, pp. 28–33). Retrieved from https://www.scopus.com/inward/record.uri?eid=2-s2.0-78751652998&partnerID=40&md5=af84aa4600d3eeee9200c3c29c950020

Pimentel, D., Acquay, H., Biltonen, M., Rice, P., Silva, M., Nelson, J., … D'Amore, M. (1992). Environmental and Economic Costs of Pesticide Use. *BioScience*, *42*(10), 750–760. https://doi.org/10.2307/1311994

Pingali, P. L. (2012). Green Revolution: Impacts, limits, and the path ahead. *Proceedings of the National Academy of Sciences*, *109*(31), 12302–12308. https://doi.org/10.1073/pnas.0912953109

Pinstrup-Andersen, P., & Hazell, P. (1985). The impact of the Green Revolution and prospects for the future. *Food Reviews International*. Retrieved from http://www.tandfonline.com/doi/pdf/10.1080/87559128509540765

Piscopo, V., & Summa, G. (2007). Experiment of pumping at constant-head: An alternative possibility to the sustainable yield of a well. *Hydrogeology Journal*, *15*(4), 679–687. https://doi.org/10.1007/s10040-006-0132-2

Planning Commission (Government of India). (2011). *Mid-Term Appraisal Eleventh Five Year Plan 2007–2012*. New Delhi: Oxford University Press.

Pool, D. R., & Eychaner, J. H. (1995). Measurements of Aquifer-Storage Change and Specific Yield Using Gravity Surveys. *Ground Water*, *33*(3), 425–432. https://doi.org/10.1111/j.1745-6584.1995.tb00299.x

Puigdefábregas, J. (2005). The role of vegetation patterns in structuring runoff and sediment fluxes in drylands. *Earth Surface Processes and Landforms*, *30*(2), 133–147. https://doi.org/10.1002/esp.1181

Racz, A. J., Fisher, A. T., Schmidt, C. M., Lockwood, B. S., & Huertos, M. L. (2012). Spatial and Temporal Infiltration Dynamics During Managed Aquifer Recharge. *Groundwater*, *50*(4), 562–570. https://doi.org/10.1111/j.1745-6584.2011.00875.x

Ramoelo, A., Majozi, N., Mathieu, R., Jovanovic, N., Nickless, A., & Dzikiti, S. (2014). Validation of Global Evapotranspiration Product (MOD16) using Flux Tower Data in the African Savanna, South Africa. *Remote Sensing*, *6*(8), 7406–7423. https://doi.org/10.3390/rs6087406

Rangarajan, R., & Athavale, R. N. (2000). Annual replenishable ground water potential of India—an estimate based on injected tritium studies. *Journal of Hydrology*, *234*(1–2), 38–53. https://doi.org/10.1016/S0022-1694(00)00239-0

Rattan, R. K., Datta, S. P., Chhonkar, P. K., Suribabu, K., & Singh, A. K. (2005). Long-term impact of irrigation with sewage effluents on heavy metal content in soils, crops and groundwater—a case study. *Agriculture, Ecosystems & Environment*, *109*(3–4), 310–322. https://doi.org/10.1016/j.agee.2005.02.025

Reddy, C. S., Jha, C. S., Diwakar, P. G., & Dadhwal, V. K. (2015). Nationwide classification of forest types of India using remote sensing and GIS. *Environmental Monitoring and Assessment*, *187*(12), 1–30. https://doi.org/10.1007/s10661-015-4990-8

Reddy, P. R. (2015). An over view of Irrigation Tanks Rehabilitation in semi arid hard rock terrain. *J. Ind. Geophys. Union*, *19*(4), 481–487. https://doi.org/10.1.1.736.3253

Reddy, D. V., Nagabhushanam, P., Sukhija, B. S., & Reddy, A. G. S. (2009). Understanding hydrological processes in a highly stressed granitic aquifer in southern India. *Hydrological Processes*, *23*(9), 1282–1294. https://doi.org/10.1002/hyp.7236

Reedy, O. C., Jardine, P. M., Wilson, G. V., & Selim, H. M. (1996). Quantifying the Diffusive Mass Transfer of Nonreactive Solutes in Columns of Fractured Saprolite using Flow Interruption. *Soil Science Society of America Journal*, *60*(5), 1376. https://doi.org/10.2136/sssaj1996.03615995006000050012x

Réfloch, A. (2018). *Compréhension expérimentale et numérique des chemins de l'eau sur le champ captant de la Métropole de Lyon*. Université Grenoble Alpes.

Renshaw, C. E., & Pollard, D. D. (1994). Numerical simulation of fracture set formation: A fracture mechanics model consistent with experimental observations. *Journal of Geophysical Research: Solid Earth*, *99*(B5), 9359–9372. https://doi.org/10.1029/94JB00139

Rezaei, A., & Mohammadi, Z. (2017). Annual safe groundwater yield in a semiarid basin using combination of water balance equation and water table fluctuation. *Journal of African Earth Sciences*, *134*, 241–248. https://doi.org/10.1016/j.jafrearsci.2017.06.029

Richards, L. A. (1931). Capillary conduction of liquids through porous mediums. *Physics*, *1*(5), 318–333. https://doi.org/10.1063/1.1745010

Richts, A., Struckmeier, W. F., & Zaepke, M. (2011). WHYMAP and the Groundwater Resources Map of the World 1:25,000,000. In *Sustaining Groundwater Resources* (pp. 159–173). Dordrecht: Springer Netherlands. https://doi.org/10.1007/978-90-481-3426-7_10

Richts, A., & Vrba, J. (2016). Groundwater resources and hydroclimatic extremes: mapping global groundwater vulnerability to floods and droughts. *Environmental Earth Sciences*, *75*(10). https://doi.org/10.1007/s12665-016-5632-3

Ringleb, J., Sallwey, J., & Stefan, C. (2016). Assessment of Managed Aquifer Recharge through Modeling: A Review. *WATER*, *8*(12). https://doi.org/10.3390/w8120579

Rodell, M., Velicogna, I., & Famiglietti, J. S. (2009). Satellite-based estimates of groundwater depletion in India. *Nature*, *460*(7258), 999–1002. https://doi.org/10.1038/nature08238

Rodriguez-Lado, L., Sun, G., Berg, M., Zhang, Q., Xue, H., Zheng, Q., & Johnson, C. A. (2013). Groundwater Arsenic Contamination Throughout China. *Science*, *341*(6148), 866–868. https://doi.org/10.1126/science.1237484

Rohde, M. M., Edmunds, W. M., Freyberg, D., Sharma, O. P., & Sharma, A. (2015). Estimating aquifer recharge in fractured hard rock: analysis of the methodological challenges and application to obtain a water balance (Jaisamand Lake Basin, India). *Hydrogeology Journal*, 1573–1586. https://doi.org/10.1007/s10040-015-1291-9

Romaguera, M., Hoekstra, A. Y., Su, Z., Krol, M. S., & Salama, M. S. (2010). Potential of Using Remote Sensing Techniques for Global Assessment of Water Footprint of Crops. *Remote Sensing*, *2*(4), 1177–1196. https://doi.org/10.3390/rs2041177

Ronayne, M. J., Gorelick, S. M., & Caers, J. (2008). Identifying discrete geologic structures that produce anomalous hydraulic response: An inverse modeling approach. *Water Resources Research*, *44*(8), 1–16. https://doi.org/10.1029/2007WR006635

Roques, C., Bour, O., Aquilina, L., & Dewandel, B. (2016). High-yielding aquifers in crystalline basement: insights about the role of fault zones, exemplified by Armorican Massif, France. *Hydrogeology Journal*, *24*(8), 2157–2170. https://doi.org/10.1007/s10040-016-1451-6

Roques, C., Bour, O., Aquilina, L., Dewandel, B., Leray, S., Schroetter, J. M., … Mougin, B. (2014). Hydrological behavior of a deep sub-vertical fault in crystalline basement and relationships with surrounding reservoirs. *Journal of Hydrology*, *509*, 42–54. https://doi.org/10.1016/j.jhydrol.2013.11.023

Rose, L., Krause, S., & Cassidy, N. J. (2013). Capabilities and limitations of tracing spatial temperature patterns by fiber-optic distributed temperature sensing. *Water Resources Research*, *49*(3), 1741–1745. https://doi.org/10.1002/wrcr.20144

Rovey, C. W., & Cherkauer, D. S. (1995). Scale Dependency of Hydraulic Conductivity Measurements. *Ground Water*, *33*(5), 769–780. https://doi.org/10.1111/j.1745-6584.1995.tb00023.x

Ruelleu, S., Moreau, F., Bour, O., Gapais, D., & Martelet, G. (2010). Impact of gently dipping discontinuities on basement aquifer recharge: An example from Ploemeur (Brittany, France). *Journal of Applied Geophysics*, *70*(2), 161–168. https://doi.org/10.1016/j.jappgeo.2009.12.007

Rushton, K. R., Eilers, V. H. M., & Carter, R. C. (2006). Improved soil moisture balance methodology for recharge estimation. *Journal of Hydrology*, *318*(1–4), 379–399.

https://doi.org/10.1016/j.jhydrol.2005.06.022

Saether, O. M., & Caritat, P. de. (1996). *Geochemical Processes, Weathering and Groundwater Recharge in Catchments*. CRC Press. https://doi.org/10.1007/s00477-015-1181-7

Saha, D., Dwivedi, S. N., Roy, G. K., & Reddy, D. V. (2013). Isotope-based investigation on the groundwater flow and recharge mechanism in a hard-rock aquifer system: the case of Ranchi urban area, India. *Hydrogeology Journal*, *21*(5), 1101–1115. https://doi.org/10.1007/s10040-013-0974-3

Said, A., Nachabe, M., Ross, M., & Vomacka, J. (2005). Methodology for Estimating Specific Yield in Shallow Water Environment Using Continuous Soil Moisture Data. *Journal of Irrigation and Drainage Engineering*, *131*(6), 533–538. https://doi.org/10.1061/(ASCE)0733-9437(2005)131:6(533)

Salameh, E., & El-Naser, H. (2000). Changes in the Dead Sea Level and their Impacts on the Surrounding Groundwater Bodies. *Acta Hydrochimica et Hydrobiologica*, *28*(1), 24–33. https://doi.org/10.1002/(SICI)1521-401X(200001)28:1<24::AID-AHEH24>3.0.CO;2-6

Sami, K. (1992). Recharge mechanisms and geochemical processes in a semi-arid sedimentary basin, Eastern Cape, South Africa. *Journal of Hydrology*, *139*(1–4), 27–48. https://doi.org/10.1016/0022-1694(92)90193-Y

Sanford, W. (2002). Recharge and groundwater models: An overview. *Hydrogeology Journal*, *10*(1), 110–120. https://doi.org/10.1007/s10040-001-0173-5

Sanford, W. (2011). Calibration of models using groundwater age. *Hydrogeology Journal*, *19*(1), 13–16. https://doi.org/10.1007/s10040-010-0637-6

Sarma, D., & Xu, Y. (2014). An approach to sustainable rural water supply in semi-arid Africa with a case study from Namibia. *Hydrogeology Journal*, *22*(7), 1681–1692. https://doi.org/10.1007/s10040-014-1178-1

Sausse, J. (2002). Hydromechanical properties and alteration of natural fracture surfaces in the Soultz granite (Bas-Rhin, France). *Tectonophysics*, *348*(1–3), 169–185. https://doi.org/10.1016/S0040-1951(01)00255-4

Scanlon, B. R., Faunt, C. C., Longuevergne, L., Reedy, R. C., Alley, W. M., McGuire, V. L., & McMahon, P. B. (2012). Groundwater depletion and sustainability of irrigation in the US High Plains and Central Valley. *Proceedings of the National Academy of Sciences*, *109*(24), 9320–9325. https://doi.org/10.1073/pnas.1200311109

Scanlon, B. R., Healy, R. W., & Cook, P. G. (2002). Choosing appropriate techniques for quantifying groundwater recharge. *Hydrogeology Journal*, *10*(1), 18–39. https://doi.org/10.1007/s10040-001-0176-2

Scanlon, B. R., Keese, K. E., Flint, A. L., Flint, L. E., Gaye, C. B., Edmunds, W. M., & Simmers, I. (2006). Global synthesis of groundwater recharge in semiarid and arid regions. *HYDROLOGICAL PROCESSES*, *20*(15), 3335–3370. https://doi.org/10.1002/hyp.6335

Scanlon, B. R., Langford, R. P., & Goldsmith, R. S. (1999). Relationship between geomorphic settings and unsaturated flow in an arid setting. *Water Resources Research*, *35*(4), 983–999. https://doi.org/10.1029/98WR02769

Scanlon, B. R., Reedy, R. C., Stonestrom, D. A., Prudic, D. E., & Dennehy, K. F. (2005). Impact of land use and land cover change on groundwater recharge and quality in the southwestern US. *Global Change Biology*, *11*(10), 1577–1593. https://doi.org/10.1111/j.1365-2486.2005.01026.x

Schaap, M. G., Leij, F. J., & van Genuchten, M. T. (2001). ROSETTA : a computer program for estimating soil hydraulic parameters with hierarchical pedotransfer functions. *Journal of Hydrology*, *251*(3–4), 163–176. https://doi.org/10.1016/S0022-1694(01)00466-8

Seebeck, H., Nicol, A., Walsh, J. J., Childs, C., Beetham, R. D., & Pettinga, J. (2014). Fluid flow in fault zones from an active rift. *Journal of Structural Geology*, *62*, 52–64. https://doi.org/10.1016/j.jsg.2014.01.008

Seiler, K. P., & Gat, J. R. (2007). *Groundwater Recharge From Run-Off, Infiltration and Percolation*. (Springer, Ed.), *Water Science and Technology Library* (Vol. 55). Dordrecht, The Netherlands.

Serrano, S. E. (1995). Analytical Solutions of the Nonlinear Groundwater Flow Equation in Unconfined Aquifers and the Effect of Heterogeneity. *Water Resources Research*, *31*(11), 2733–2742. https://doi.org/10.1029/95WR02038

Shah, E. (2008). Telling Otherwise: A Historical Anthropology of Tank Irrigation Technology in South India. *Technology and Culture*, *49*(3), 652–674. https://doi.org/10.1353/tech.0.0054

Shah, M., Bharti, & Verma, S. (2017). *Reviving Minor Irrigation in Telangana*. Colombo, Sri Lanka. Retrieved from hp://iwmi-tata.blogspot.in

Shah, T. (2005). Groundwater and Human Development: Challenges and Opportunities in Livelihoods and Environment. In *Groundwater Research and Management: Integrating Science into Management Decisions* (Vol. 2000, pp. 14–26).

Shah, T., Giordano, M., & Mukherji, A. (2012). Political economy of the energy-groundwater nexus in India: exploring issues and assessing policy options. *Hydrogeology Journal*, *20*(5), 995–1006. https://doi.org/10.1007/s10040-011-0816-0

Shah, T., Scott, C., Kishore, A., & Sharma, A. (2003). *Energy-Irrigation Nexus in South Asia. Research Report 70*. Colombo, Sri Lanka.

Shapiro, A. M. (2001). Effective matrix diffusion in kilometer-scale transport in fractured crystalline rock. *Water Resources Research*, *37*(3), 507–522. https://doi.org/10.1029/2000WR900301

Sharma, B. R., Villholth, K. G., & Sharma, K. D. (2005). Groundwater Research and Management: Integrating Science into Management Decisions. In B. R. Sharma, K. G. Villholth, & K. D. Sharma (Eds.), *Groundwater Governance in Asia Series - 1*. IWA Publishing.

Shiao, T., Maddocks, A., Carson, C., & Loizeaux, E. (2015). 3 Maps Explain India's Growing Water Risks. World Resource Institute. Retrieved October 24, 2018, from https://www.wri.org/blog/2015/02/3-maps-explain-india-s-growing-water-risks

Siebert, S., Burke, J., Faures, J. M., Frenken, K., Hoogeveen, J., Döll, P., & Portmann, F. T. (2010). Groundwater use for irrigation – a global inventory. *Hydrology and Earth System Sciences*, *14*(10), 1863–1880. https://doi.org/10.5194/hess-14-1863-2010

Simmers, I. (1988). *Estimation of Natural Groundwater Recharge*. (Ian Simmers, Ed.). Dordrecht: Springer Netherlands. https://doi.org/10.1007/978-94-015-7780-9

Simmers, I., Hendrickx, J. M. H., Kruseman, G. P., & Rushton, K. R. (1997). *Recharge of phreatic aquifers in (semi-) arid areas. Journal of Environment Quality* (Vol. 21). https://doi.org/10.2134/jeq1992.00472425002100030036x

Singh, J., Awasthi, M. K., & Sharma, R. K. (2004). Quantification of percolation from percolation Tank. *J. Soil Wat. Conserv. India*, *3 (3&4)*, 128–132.

Singh, R. (2000). Environmental consequences of agricultural development: a case study from the Green Revolution state of Haryana, India. *Agriculture, Ecosystems & Environment*, *82*(1–3), 97–103. https://doi.org/10.1016/S0167-8809(00)00219-X

Singhal, B. B. S., & Gupta, R. P. (2010). *Applied Hydrogeology of Fractured Rocks. Springer*. Dordrecht: Springer Netherlands. https://doi.org/10.1007/978-90-481-8799-7

Slater, L. D., Ntarlagiannis, D., Day-Lewis, F. D., Mwakanyamale, K., Versteeg, R. J., Ward, A., … Lane, J. W. (2010). Use of electrical imaging and distributed temperature sensing methods to characterize surface water-groundwater exchange regulating uranium transport at the Hanford 300 Area, Washington. *Water Resources Research*, *46*(10), 1–13. https://doi.org/10.1029/2010WR009110

Sohrt, J., Ries, F., Sauter, M., & Lange, J. (2014). Significance of preferential flow at the rock soil interface in a semi-arid karst environment. *CATENA*, *123*, 1–10. https://doi.org/10.1016/j.catena.2014.07.003

Sophocleous, M. (2002). Interactions between groundwater and surface water: the state of the science. *Hydrogeology Journal*, *10*(1), 52–67. https://doi.org/10.1007/s10040-001-0170-8

Sophocleous, M., & Devlin, J. F. (2004). "The Water Budget Myth Revisited: Why Hydrogeologists Model," by John D. Bredehoeft, July-August 2002 issue, v. 40, no. 4: 340-345. *Ground Water*, *42*(4), 618–618.

https://doi.org/10.1111/j.1745-6584.2004.tb02630.x

Sørensen, K. I., & Auken, E. (2004). SkyTEM - a new high-resolution helicopter transient electromagnetic system. *Exploration Geophysics*, *35*(3), 194. https://doi.org/10.1071/EG04194

Spalding, R. F., & Exner, M. E. (1993). Occurrence of Nitrate in Groundwater—A Review. *Journal of Environment Quality*, *22*(3), 392. https://doi.org/10.2134/jeq1993.00472425002200030002x

Spanoudaki, K., Paschalinos, Y., Memos, C. D., & Stamou, A. I. (2010). Analytical Solution to the Stream-Aquifer Interaction Problem: A Critical Review. *Global Nest Journal*, *12*(2), 126–139.

Srivastava, R. C., Kannan, K., Mohanty, S., Nanda, P., Sahoo, N., Mohanty, R. K., & Das, M. (2009). Rainwater Management for Smallholder Irrigation and its Impact on Crop Yields in Eastern India. *Water Resources Management*, *23*(7), 1237–1255. https://doi.org/10.1007/s11269-008-9324-y

St. Clair, J., Moon, S., Holbrook, W. S., Perron, J. T., Riebe, C. S., Martel, S. J., … Richter, D. d. (2015). Geophysical imaging reveals topographic stress control of bedrock weathering. *Science*, *350*(6260), 534–538. https://doi.org/10.1126/science.aab2210

Steenhuis, T. S., & Van Der Molen, W. H. (1986). The Thornthwaite-Mather procedure as a simple engineering method to predict recharge. *Journal of Hydrology*, *84*(3–4), 221–229. https://doi.org/10.1016/0022-1694(86)90124-1

Strahler, A. N. (1964). Part II. Quantitative geomorphology of drainage basins and channel networks. *Handbook of Applied Hydrology: McGraw-Hill, New York*, 4–39.

Sukhija, B. S., Reddy, D. V., Nagabhushanam, P., & Hussain, S. (2003). Recharge processes: piston flow vs preferential flow in semi-arid aquifers of India. *Hydrogeology Journal*, *11*(3), 387–395. https://doi.org/10.1007/s10040-002-0243-3

Swedish National Council for Nuclear Waste. (2001). *Nuclear Waste Nuclear Waste State of the Art Report. SOU 2001:35*. Stockholm, Sweden.

Taniguchi, M., & Sharma, M. L. (1990). Solute and heat transport experiments for estimating recharge rate. *Journal of Hydrology*, *119*(1–4), 57–69. https://doi.org/10.1016/0022-1694(90)90034-U

Taylor, R. G., Todd, M. C., Kongola, L., Maurice, L., Nahozya, E., Sanga, H., & MacDonald, A. M. (2012). Evidence of the dependence of groundwater resources on extreme rainfall in East Africa. *Nature Climate Change*, *3*(4), 374–378. https://doi.org/10.1038/nclimate1731

Teatini, P., Comerlati, A., Carvalho, T., Gütz, A.-Z., Affatato, A., Baradello, L., … Paiero, G. (2015). Artificial recharge of the phreatic aquifer in the upper Friuli plain, Italy, by a large infiltration basin. *Environmental Earth Sciences*, *73*(6), 2579–2593. https://doi.org/10.1007/s12665-014-3207-8

Theis, C. V. (1935). The relation between the lowering of the Piezometric surface and the rate and duration of discharge of a well using ground-water storage. *Transactions, American Geophysical Union*, *16*(2), 519. https://doi.org/10.1029/TR016i002p00519

Thornthwaite, C. W. (1948). An Approach toward a Rational Classification of Climate. *Geographical Review*, *38*(1), 55. https://doi.org/10.2307/210739

Thornthwaite, C. W., & Mather, J. R. (1955). The water balance. *Publications in Climatology*, *8*(1), 1–104.

Tsang, Y. W. (1992). Usage of "Equivalent apertures" for rock fractures as derived from hydraulic and tracer tests. *Water Resources Research*, *28*(5), 1451–1455. https://doi.org/10.1029/92WR00361

Twidale, C. R. (1971). *Structural landforms: landforms associated with granitic rocks, faults and folded strata*. Canberra: Australian National University Press.

UNESCO. (1999). *Water resources of hard rock aquifers in arid and semi-arid zones*. (J. W. Lloyd, Ed.). Paris, France: United Nations.

UNESCO. (2004). *Groundwater resources of the world and their use*. (I. S. Zekster & L. G. Everett, Eds.), *IHP-VI, Series on Groundwater No. 6* (Vol. 6). Paris, France: United Nations.

USDA. (1999). *Soil Taxonomy: A Basic System of Soil Classification for Making and Interpreting Soil Surveys (Second Edition). Agriculture Handbook Number 436*.

Van der Gun, J. (2012). *Groundwater and Global Change: Trends, Opportunities and Challenges* (Vol. 1). Paris, France: UNESCO. Retrieved from https://www.un-igrac.org/resource/groundwater-and-global-change-trends-opportunities-and-challenges

Van der Hoven, S. J., Solomon, D. M., & Moline, G. R. (2003). Modeling unsaturated flow and transport in the saprolite of fractured sedimentary rocks: Effects of periodic wetting and drying. *Water Resources Research*, *39*(7), 1–11. https://doi.org/10.1029/2002WR001926

van Genuchten, M. T. (1980). A closed-form equation for predicting the hydraulic conductivity of unsaturated soils. *Soil Science Society of America Journal*, *44*(5), 892. https://doi.org/10.2136/sssaj1980.03615995004400050002x

Van Loon, A. F., Stahl, K., Di Baldassarre, G., Clark, J., Rangecroft, S., Wanders, N., … Van Lanen, H. A. J. (2016). Drought in a human-modified world: reframing drought definitions, understanding, and analysis approaches. *Hydrology and Earth System Sciences*, *20*(9), 3631–3650. https://doi.org/10.5194/hess-20-3631-2016

Van Tonder, G. J., Botha, J. F., Chiang, W. H., Kunstmann, H., & Xu, Y. (2001). Estimation of the sustainable yields of boreholes in fractured rock formations. *Journal of Hydrology*, *241*(1–2), 70–90. https://doi.org/10.1016/S0022-1694(00)00369-3

van Wyk, E., van Tonder, G., & Vermeulen, D. (2012). Characteristics of local groundwater recharge cycles in South African semi-arid hard rock terrains: Rainfall-groundwater interaction. *Water SA*, *38*(5), 747–754. https://doi.org/10.4314/wsa.v38i5.14

Vouillamoz, J. M., Favreau, G., Massuel, S., Boucher, M., Nazoumou, Y., & Legchenko, A. (2008). Contribution of magnetic resonance sounding to aquifer characterization and recharge estimate in semiarid Niger. *JOURNAL OF APPLIED GEOPHYSICS*, *64*(3–4), 99–108. https://doi.org/10.1016/j.jappgeo.2007.12.006

Vouillamoz, J. M., Lawson, F. M. A., Yalo, N., & Descloitres, M. (2014). The use of magnetic resonance sounding for quantifying specific yield and transmissivity in hard rock aquifers: The example of Benin. *Journal of Applied Geophysics*, *107*(February), 16–24. https://doi.org/10.1016/j.jappgeo.2014.05.012

Wada, Y., van Beek, L. P. H., van Kempen, C. M., Reckman, J. W. T. M., Vasak, S., & Bierkens, M. F. P. (2010). Global depletion of groundwater resources. *Geophysical Research Letters*, *37*(20), n/a-n/a. https://doi.org/10.1029/2010GL044571

Warner, J. W., Molden, D., Chehata, M., & Sunada, D. K. (1989). Mathematical analysis of artificial recharge from basins. *Journal of the American Water Resources Association*, *25*(2), 401–411. https://doi.org/10.1111/j.1752-1688.1989.tb03077.x

Warren, J. E., & Root, P. J. (1963). The Behavior of Naturally Fractured Reservoirs. *Society of Petroleum Engineers Journal*, *3*(03), 245–255. https://doi.org/10.2118/426-PA

Werner, A. D., Bakker, M., Post, V. E. A., Vandenbohede, A., Lu, C., Ataie-Ashtiani, B., … Barry, D. A. (2013). Seawater intrusion processes, investigation and management: Recent advances and future challenges. *Advances in Water Resources*, *51*, 3–26. https://doi.org/10.1016/j.advwatres.2012.03.004

White, B. A., & Burbey, T. J. (2007). Evidence for structurally controlled recharge in the Blue Ridge Province, Virginia, USA. *Hydrogeology Journal*, *15*(5), 929–943. https://doi.org/10.1007/s10040-006-0150-0

Winberg, A., Andersson, P., Hermanson, J., Byegård, J., Cvetkovic, V., & Birgersson, L. (2000). *Äspö Hard Rock Laboratory. Final report of the first stage of the Tracer Retention Understanding Experiments. SKB*. Retrieved from http://linkinghub.elsevier.com/retrieve/pii/S0040195101002554

Winter, T. C. (1978). Numerical simulation of steady state three-dimensional groundwater flow near lakes. *Water Resources Research*, *14*(2), 245–254. https://doi.org/10.1029/WR014i002p00245

Winter, T. C. (2001). The concept of hydrologic landscapes. *Journal of the American Water Resources Association*, *37*(2), 335–349. https://doi.org/10.1111/j.1752-1688.2001.tb00973.x

Winter, T. C., Harvey, J. W., Franke, O. L., & Alley, W. M. (1998). *Ground Water and Surface Water A*

Single Resource.

Witherspoon, P. A., Wang, J. S. Y., Iwai, K., & Gale, J. E. (1980). Validity of Cubic Law for fluid flow in a deformable rock fracture. *Water Resources Research*, *16*(6), 1016–1024. https://doi.org/10.1029/WR016i006p01016

Workman, S. R., Serrano, S. E., & Liberty, K. (1997). Development and application of an analytical model of stream/aquifer interaction. *Journal of Hydrology*, *200*(1–4), 149–163. https://doi.org/10.1016/S0022-1694(97)00014-0

Wösten, J. H. M., Pachepsky, Y. A., & Rawls, W. J. (2001). Pedotransfer functions: bridging the gap between available basic soil data and missing soil hydraulic characteristics. *Journal of Hydrology*, *251*(3–4), 123–150. https://doi.org/10.1016/S0022-1694(01)00464-4

Wubda, M., Descloitres, M., Yalo, N., Ribolzi, O., Vouillamoz, J. M., Boukari, M., … Séguis, L. (2017). Time-lapse electrical surveys to locate infiltration zones in weathered hard rock tropical areas. *Journal of Applied Geophysics*, *142*, 23–37. https://doi.org/10.1016/j.jappgeo.2017.01.027

Wyns, R., Baltassat, J.-M., Lachassagne, P., Legchenko, A., Vairon, J., & Mathieu, F. (2004). Application of proton magnetic resonance soundings to groundwater reserve mapping in weathered basement rocks (Brittany, France). *Bulletin de La Societe Geologique de France*, *175*(1), 21–34. https://doi.org/10.1016/S0921-4526(03)00407-1

Yihdego, Y., & Nzikou, M. M. (2017). Application of Airborne Geophysics and Geochemistry to Characterize Groundwater Flow Path. *Geotechnical and Geological Engineering*, *36*(2), 1175–1184. https://doi.org/10.1007/s10706-017-0382-x

Zappa, G., Bersezio, R., Felletti, F., & Giudici, M. (2006). Modeling heterogeneity of gravel-sand, braided stream, alluvial aquifers at the facies scale. *Journal of Hydrology*, *325*(1–4), 134–153. https://doi.org/10.1016/j.jhydrol.2005.10.016

Zhang, Z., Nemcik, J., Qiao, Q., & Geng, X. (2014). A Model for Water Flow Through Rock Fractures Based on Friction Factor. *Rock Mechanics and Rock Engineering*, *48*(2), 559–571. https://doi.org/10.1007/s00603-014-0562-4

Zhou, Y. (2009). A critical review of groundwater budget myth, safe yield and sustainability. *Journal of Hydrology*, *370*(1–4), 207–213. https://doi.org/10.1016/j.jhydrol.2009.03.009

Zlotnik, V. A., Kacimov, A., & Al-Maktoumi, A. (2017). Estimating Groundwater Mounding in Sloping Aquifers for Managed Aquifer Recharge. *Groundwater*, *55*(6), 797–810. https://doi.org/10.1111/gwat.12530

Zomlot, Z., Verbeiren, B., Huysmans, M., & Batelaan, O. (2015). Spatial distribution of groundwater recharge and base flow: Assessment of controlling factors. *Journal of Hydrology: Regional Studies*, *4*, 349–368. https://doi.org/10.1016/j.ejrh.2015.07.005

Annex A
Diffuse recharge

		Scrub				Paddy (perennial)				Fruit				Forest			
	Rainfall	**Alf1.**	**Alf2.**	**Ent.**	**Incept.**	**Alf1.**	**Alf2.**	**Ent.**	**Incept.**	**Alf1.**	**Alf2.**	**Ent.**	**Incept.**	**Alf1.**	**Alf2.**	**Ent.**	**Incept.**
2000	1444	0	0	0	0	717	662	644	749	0	0	0	35	0	0	0	0
2001	657	0	0	0	0	225	168	140	362	0	0	0	0	0	0	0	0
2002	599	0	0	0	0	328	241	165	402	0	0	0	0	0	0	0	0
2003	893	0	0	0	0	597	510	309	682	6	0	0	59	0	0	0	0
2004	758	0	0	0	0	524	433	413	634	0	0	0	0	0	0	0	0
2005	1159	16	0	0	88	877	761	630	1001	124	66	0	133	0	0	0	8
2006	839	0	0	0	0	609	539	524	664	0	0	0	5	0	0	0	0
2007	677	0	0	0	0	476	410	395	609	0	0	0	20	0	0	0	0
2008	1102	0	0	0	31	862	774	716	969	33	6	0	82	1	0	0	20
2009	998	0	0	0	15	644	554	438	838	0	0	0	50	0	0	0	13
2010	1206	131	107	0	233	973	902	882	1132	258	176	13	298	100	0	0	145
2011	535	0	0	0	0	495	404	348	587	0	0	0	0	0	0	0	0
2012	765	0	0	0	0	396	317	247	525	0	0	0	35	0	0	0	0
2013	1074	59	29	0	152	886	793	766	986	333	167	0	250	33	0	0	57
2014	494	0	0	0	0	360	282	271	446	0	0	0	0	0	0	0	0
2015	728	0	0	0	0	563	497	476	630	0	0	0	0	0	0	0	0
Mean	871	13	9	0	32	596	515	460	701	47	26	1	61	8	0	0	15

TABLE A: Mean annual diffuse recharge estimates for the main soil types and land uses for the studied period (01/01/2000-31/12/2015) (in mm/year). Alf1. and Alf2. are Alfisols 1 and Alfisols 2, respectively, Incep. are Inceptisols, and Ent. are Entisols. Tanks are not featured because they occupy a very small portion of land relative to the total.

French summary/Résumé en français

Introduction et sites d'étude

Dans un monde en voie d'industrialisation rapide, les défis en matière de ressources en eau augmentent sans cesse. Une croissance démographique exponentielle, accompagnée d'une forte expansion de l'agriculture irriguée et d'un développement industriel intense accentuent fortement la pressions sur nos systèmes naturels. Les eaux souterraines, qui représentent de loin le plus grand volume d'eau douce liquide sur Terre, comptent parmi les ressources naturelles les plus importantes. Comparées aux eaux de surface, les eaux souterraines sont de meilleure qualité, mieux protégées de la pollution, moins sujettes aux fluctuations saisonnières et pérennes et beaucoup plus uniformément réparties sur de grandes régions. De plus, l'eau souterraine est pour certains pays (par exemple, l'Arabie saoudite, Malte et le Danemark) la seule ou la plus importante source d'eau fraiche, faisant de l'eau souterraine la ressource la plus exploitée au monde (UNESCO, 2004).

L'irrigation est le secteur d'utilisation d'eau le plus important, en particulier dans les pays arides et semi-arides, et représente 70% des prélèvements mondiaux d'eau. L'évolution vers ces conditions d'exploitation a eu lieu au cours d'un phénomène appelé «la révolution silencieuse» (Llamas & Martínez-Santos, 2005b). Cette « révolution », qui a contribué à une augmentation considérable de l'utilisation d'eau souterraine, a commencé au début du XXe siècle pour certains pays (l'Italie, le Mexique, l'Espagne et les États-Unis) et s'est poursuivi au cours des années 70 en Asie du Sud, dans certaines parties de la Chine, au Moyen-Orient et en Afrique du Nord. En Inde, l'utilisation des eaux souterraines est passée de 10 à 20 km^3/an avant 1950 à un record mondial de 250 km^3/an aujourd'hui (Siebert et al., 2010), faisant de l'Inde, de loin, le plus grand exploitant d'eau souterraine au monde. Cet essor s'explique par les nombreuses décisions individuelles de millions d'agriculteurs modestes cherchant à augmenter leur productivité et revenus grâce aux avantages de l'eau souterraine et à une réduction drastique des couts de forage et de pompage. Ces décisions ont par ailleurs été prises sans planification ni coordination centralisées; c'est pourquoi on l'appelle «la révolution silencieuse».

La combinaison de cette augmentation exponentielle du nombre de puits de forage individuels et du manque ou de l'inefficacité de la réglementation sur l'eau a donné lieu à des effets néfastes dans nombreuses régions comme en Asie du Sud, où la situation actuelle a été décrite comme une «anarchie colossale» (T. Shah, 2005). En effet, cette explosion soudaine de la quantité d'eau souterraine exploitée a déclenché une série d'effets secondaires néfastes (Sharma et al., 2005), par exemple : la baisse du niveau des eaux

souterraines, l'assèchement des puits, des coûts d'énergie et de pompage en hausse et une vulnérabilité croissante à la sécheresse et aux fluctuations climatiques.

L'Inde, où environ deux tiers des zones géographiques sont constituées de roches cristallines, est le meilleur exemple des défis propres à la gestion des ressources en eau dans les roches cristallines fracturées. Malheureusement, ce pays est devenu célèbre à cause de ses sévères problèmes de surexploitation des aquifères (Rodell et al., 2009; T. Shah et al., 2012) ; 54% du territoire aujourd'hui fait face à un stress hydrique extrêmement élevé (Shiao et al., 2015). C'est dans ce contexte que le Centre Franco-Indien de recherche sur les eaux souterraines (CEFIRES ou IFCGR en anglais) a été créé en 1999. Il est le fruit d'une coopération entre le Bureau de Recherches Géologiques et Minières (BRGM) et le National Geophysical Research Institute (NGRI). L'un des principaux objectifs de cette collaboration est de mieux comprendre les processus hydrogéologiques dans les roches cristallines fracturées et altérées. À ce jour, une quantité importante de données ont été produites en instrumentant et en surveillant à différentes échelles plusieurs sites situés en terrain granitique archéen, dont deux ont été utilisés pour cette thèse (voir Maréchal et al., 2018) :

- Le premier est le bassin versant de Maheshwaram, situé 40 km au sud-est de Hyderabad. Il a une superficie de 53 km^2 et représente un bassin versant habité typique sur du terrain granitique. Les nombreuses campagnes de terrain et publications basées sur ce site depuis sa création ont permis aux chercheurs de déterminer nombre de ses caractéristiques (telles que les propriétés hydrauliques de l'aquifère et des sols le recouvrant, sa géologie et sa structure, etc.) facilitant grandement l'élaboration et la validation de modèles et d'hypothèses sur les processus hydrogéologiques à moyenne et grande échelle.
- Le second est le site expérimental de Choutuppal, un observatoire hautement instrumenté et monitoré en permanence. Ce site est équipé de 30 puits de forage sur une surface d'environ 40 hectares et permet l'analyse détaillée de processus de moyenne et petite échelle. Comme pour le bassin versant de Maheshwaram, des études antérieures ont fourni une bonne estimation des caractéristiques et des propriétés hydrauliques du site. En 2016, ce dernier a été équipé d'un bassin de recharge artificielle. Ce bassin a été construit dans le cadre d'un projet beaucoup plus vaste lancé par le gouvernement indien, qui vise à réduire la surexploitation des eaux souterraines. Pour ce faire, l'objectif est d'augmenter la recharge globale des eaux souterraines de 9% des précipitations annuelles dans des conditions naturelles à 15% d'ici 2020 (Government of Andhra Pradesh, 2003) grâce à la mise en place massive de bassins de recharge artificielle. Pour cela, la commission centrale des eaux souterraines (en anglais Central Ground Water Board ou CGWB) a proposé la construction de 11 millions de structures de recharge artificielle à l'échelle nationale, ainsi que la réparation, la rénova-

tion et la restauration des structures existantes, les coûts totaux s'élevant à plus de 12 milliards d'USD (Central Ground Water Board, 2013). Le site de Choutuppal constitue donc une opportunité exceptionnelle pour étudier l'efficacité de cette technique de mitigation pour contrer la surexploitation des nappes ainsi que le potentiel des aquifères cristallins à fonctionner en tant que réservoirs pour la recharge artificielle.

Premier axe de recherche

Recharge naturelle dans les aquifères cristallins fracturés

Les facteurs qui régissent l'intensité et la répartition de la recharge à l'échelle du paysage dans les roches cristallines fracturées sont mal connus (Kinzelbach et al., 2002). Ce sont cependant les caractéristiques déterminantes de ce type de roche—les roches cristallines fracturées et altérées sont très hétérogènes—qui rendent difficile l'estimation des flux dans ces milieux ainsi que des propriétés hydrauliques qui les contrôlent. La porosité primaire de ces aquifères étant presque négligeable, leur capacité de stockage dépend de l'existence d'une porosité secondaire, qui résulte de la décomposition chimique et physique de la matrice rocheuse par altération, un processus extrêmement non linéaire dans le temps et dans l'espace (Acworth, 1987; Dewandel et al., 2006; Lachassagne et al., 2011; Wyns et al., 2004). En conséquence, les propriétés hydrauliques de ces aquifères peuvent varier sur plusieurs ordres de grandeur sur de courtes distances, horizontalement et verticalement (Boisson, Guihéneuf et al., 2015; Chilton & Foster, 1995; Dewandel et al., 2012; Maréchal et al., 2004).

On dit de la roche fracturée qu'elle est bimodale (Healy & Cook, 2002), car elle est constituée de réseaux de fractures encastrés dans une matrice à porosité variable. La recharge est donc une combinaison de processus d'écoulement *diffus* (qui ont lieu à travers des dépôts superficiels meubles, c.-à-d. les sols et la saprolite sous-jacente) et de processus d'écoulement préférentiels, qui se déroulent dans des réseaux de fractures (si les fractures affleurent à la surface) et les macropores, lorsque l'eau s'accumule dans les dépressions, les joints et les ruisseaux (recharge *localisée*), et dans les lits des masses d'eau de surface (recharge *indirecte*). Chacun de ces processus est contrôlé par un ensemble de facteurs différents, ce qui les conduit à présenter des dispositions dans l'espace et dans le temps différentes. La recharge *diffuse* dépend principalement de la différence entre précipitations et évapotranspiration et des propriétés hydrauliques du sol, tandis que la recharge *localisée* et *indirecte* dépend beaucoup plus du cadre géologique (pente, densité de drainage, production de ruissellement) et de l'existence d'épisodes pluvieux intenses. Dans un souci de simplification, nous utiliserons ci-après le terme « recharge *focalisée* » pour désigner conjointement la recharge localisée et indirecte (en opposition à la recharge diffuse).

Les proportions relatives de recharge diffuse à localisée sont rarement quantifiées, probablement à cause de la nature intermittente et concentrée (et donc difficile à quantifier) de cette dernière. Néanmoins, parmi les rares études ayant abordé cette question, la plupart ont trouvé que la recharge focalisée constituait une partie significative de la recharge totale (Cuthbert & Tindimugaya, 2010; Machiwal & Jha, 2015; D. V. Reddy et al., 2009; Sukhija et al., 2003; White & Burbey, 2007), en particulier dans les environnements (semi-)arides (de Vries & Simmers, 2002). Par ailleurs, une fois l'eau infiltrée, celle-ci peut être redistribuée dans la zone vadose en s'écoulant latéralement à travers les macropores et les réseaux de fractures (écoulements hypodermiques, en anglais « interflow »), et le rôle de cette déviation des flux latéraux est souvent négligé et généralement mal compris (Bockgard & Niemi, 2004; Harte & Winter, 1995).

1. Méthodologie

Pour mieux comprendre la recharge dans les milieux cristallins, nous avons donc examiné les facteurs qui déterminent la distribution très hétérogène de la recharge ainsi que l'importance des processus de recharge focalisée. La première étape a consisté à estimer la recharge *diffuse* à l'aide d'un modèle hydrodynamique simple associant à la fois une technique de bilan hydrique et des calculs de flux saturés/non-saturés (Dewandel et al., 2008). Le bilan hydrique à est calculé avec une fréquence journalière à l'échelle de la parcelle. Les différentes composantes du bilan hydrique sont la pluie, l'évaporation, le ruissellement, le pompage et l'infiltration. Lorsque le stock d'eau en surface a été estimé, la loi de Darcy pour les milieux non-saturés ou saturés (cela dépend si le sol a atteint la saturation ou non) est utilisée pour estimer l'infiltration. Ces équations dépendent d'un ensemble de paramètres hydrauliques qui régissent le stock d'eau que peux retenir le sol, sa perméabilité et sa pression d'eau à un temps t en fonction de la teneur en eau du sol à ce moment (Nimmo, 2005).

Puisque ce modèle s'applique à l'échelle de la parcelle, le bassin versant de Maheshwaram a été discrétisé en cellules de 100×100 m. Ensuite à chaque cellule a été attribué un type de sol (ce qui détermine ses propriétés hydrauliques) et un usage du sol (qui détermine la quantité d'eau qui y-est irriguée et évaporée). La distribution des types et usages de sol et les paramètres hydrauliques associés, ainsi que les apports quotidiens en eau et l'évapotranspiration de chaque type de culture nécessaires à l'exécution de ce modèle ont été obtenus à partir de données de la littérature, notamment les travaux de thèse de De Condappa (2005) et les travaux de Dewandel et al. (2008). Les estimations spatialisées de recharge diffuse ainsi obtenues ont été analysées pour en déduire l'effet des types de sol, de l'usage du sol, et leur variabilité temporelle en fonction des précipitations.

Malheureusement, les informations sur l'incertitude associée à chacun de ces paramètres mesurés n'étaient pas toujours disponibles. Une quantification complète de

l'incertitude du modèle d'ensemble n'était donc pas possible. Au lieu de cela, une analyse de sensibilité—lors de laquelle l'effet de chaque paramètre sur la dynamique du système est évalué—a été réalisée. La sensibilité est définie comme le taux de variation d'un facteur par rapport à celui d'un autre facteur (Kabala, 2001; Maréchal et al., 2008) : chaque paramètre est modifié par un rapport à une valeur de référence (les paramètres restants demeurent égaux à leur valeur de référence), et en calculant le pourcentage de variation de la recharge ainsi fournie par le modèle. L'ensemble de paramètres de référence a été choisi arbitrairement.

Enfin, une fois que la recharge diffuse a été quantifiée spatialement sur tout le bassin versant, ces estimations de recharge diffuse ont été comparées aux estimations de recharge *totale* précédemment obtenues à partir des fluctuations de la nappe phréatique lors des travaux de thèse de Mizan (2019). La différence entre les deux a été attribuée à l'effet de la recharge focalisée, qui a ensuite été cartographiée et analysée.

2. Résultats et discussion

Tout d'abord, nous avons observé que la recharge diffuse n'est pas très significative. La recharge diffuse moyennée sur l'ensemble du bassin versant pour chaque année varie entre 11 mm (pour 494 mm de pluie, soit 2%) et 92 mm (pour 1074 mm de pluie, soit 9%). La recharge n'est par ailleurs répartie de manière homogène. Les zones irriguées, en particulier les rizières, semblent constituer des zones de recharge préférentielle ($1000 \geq R_{Diff} \geq 250$ mm). L'eau d'irrigation mouille la colonne de sol, ce qui augmente la conductivité hydraulique du milieu non-saturé et permet que plus d'eau s'écoule. Ce phénomène a déjà été observé par le passé (Kurtzman & Scanlon, 2011; Ognianik & Paramonova, 2001), bien que certains aient remarqué que la recharge s'écoulait réellement hors de la zone irriguée par des voies d'écoulement préférentielles sous forme de recharge localisée plutôt que sous forme de recharge diffuse passant à travers la matrice de sol (Kurtzman & Scanlon, 2011). Cependant, même si l'irrigation a pour effet d'augmenter le potentiel d'infiltration de la recharge naturelle, cette hausse reste largement inférieure aux pompages totaux.

Le type de sol influence également la recharge, bien que dans une moindre mesure. Les Inceptisols (sols peu développés avec des horizons pédologiques minces, généralement formés sur les collines et les sommets) apparaissent comme les plus réceptifs à la recharge, alors que les Entisols (sols alluviaux peu développés résultant de l'érosion et du dépôt d'autres matériaux, généralement présents dans les basses terres) semblent résister à la recharge. Cela concorde avec la teneur élevée en argile et la faible perméabilité de ces derniers. Parce que les Entisols sont des sols alluviaux, on les trouve dans les zones de dépressions et leur distribution est généralement guidée par le ruissellement de surface. En tant que tel, le réseau de drainage devient ainsi une zone antagoniste à la recharge diffuse, les zones irriguées étant l'exception.

Le bilan hydrique annuel a montré que la recharge diffuse compte pour seulement 4.6% des précipitations; l'évapotranspiration, suivie du ruissellement (qui peut devenir de la recharge indirecte), sont de loin les principales sorties d'eau, tandis que la moins importante est la recharge diffuse. Mizan (2019) a estimé le ratio de recharge *totale* vis-à-vis des précipitations à environ 10.1% (73 mm), ce qui est assez proche de la moyenne nationale de 9% (Government of Andhra Pradesh, 2003). La recharge *totale* est donc beaucoup plus élevée que la recharge *diffuse*, probablement en raison des contributions de la recharge focalisée. Suivant cette hypothèse, la recharge focalisée représenterait les 40 mm restants de la recharge: cela représente une moyenne de 55% de la recharge totale.

En observant la relation entre la recharge annuelle en les précipitations annuelles, la non-linéarité de cette relation devient très apparente. La recharge diffuse par rapport aux précipitations peut être divisée en deux catégories:

- Pour les précipitations inférieures à 1 000 mm environ (faibles à modérées), la recharge diffuse augmente très peu avec les précipitations et est globalement très faible. Pour expliquer ce phénomène, rappelons-nous que la recharge diffuse dépend fortement de l'humidité du sol et que les années de faible pluviométrie ne suffisent pas pour compenser le déficit en eau du sol présent pendant la plus grande partie de l'année. Dans cette plage de précipitations (faible à modérée), le rapport entre la recharge diffuse et la recharge totale diminue à mesure que les précipitations augmentent. En effet, même si la recharge totale augmente de manière linéaire avec les précipitations (Dewandel et al., 2010; Maréchal et al., 2006; Mizan, 2019), la recharge diffuse reste relativement constante.
- Pour les précipitations supérieures à 1000 mm, la recharge diffuse devient un contributeur important à la recharge totale: les déficits en humidité du sol sont comblés et l'infiltration peut plus facilement atteindre l'aquifère. Cela ne signifie pas que les autres processus de recharge ont diminué, mais que leur contribution relative est moindre.

Afin d'obtenir une estimation approximative de l'endroit où la recharge focalisée a lieu, la carte de recharge *diffuse* moyenne a été soustraite de la carte de recharge *totale* moyenne et la différence supposée égale aux contributions de recharge focalisée. Cartographier la répartition de la recharge focalisée met en évidence les zones les plus sujettes à ces processus ainsi que les zones les plus résistantes. Identifier les causes exactes de cette distribution est cependant une tâche difficile. Contrairement à la recharge diffuse, la recharge focalisée est contrôlée par un grand nombre de facteurs en interaction qui ne sont pas nécessairement facilement identifiables ou pour lesquels il est très difficile d'obtenir des estimations quantitatives de leurs contributions. Ces facteurs incluent, mais ne sont pas limités à: l'existence de chemins d'écoulement préférentiels (par exemple, des

factures qui affleurent, des grandes failles, des zones de contact, des macropores), l'accumulation de ruissellement en surface (contrôlée par la topographie, l'intensité des épisodes de pluie et la couverture végétale) et les pertes d'eau provenant des cours d'eau (également contrôlées par de nombreux facteurs, tels que la perméabilité du lit du cours d'eau, la pente et la densité du réseau de drainage…). Pour cette raison, les observations faites dans ici sont d'ordre qualitatif, et les hypothèses formulées restent sujettes à interprétation.

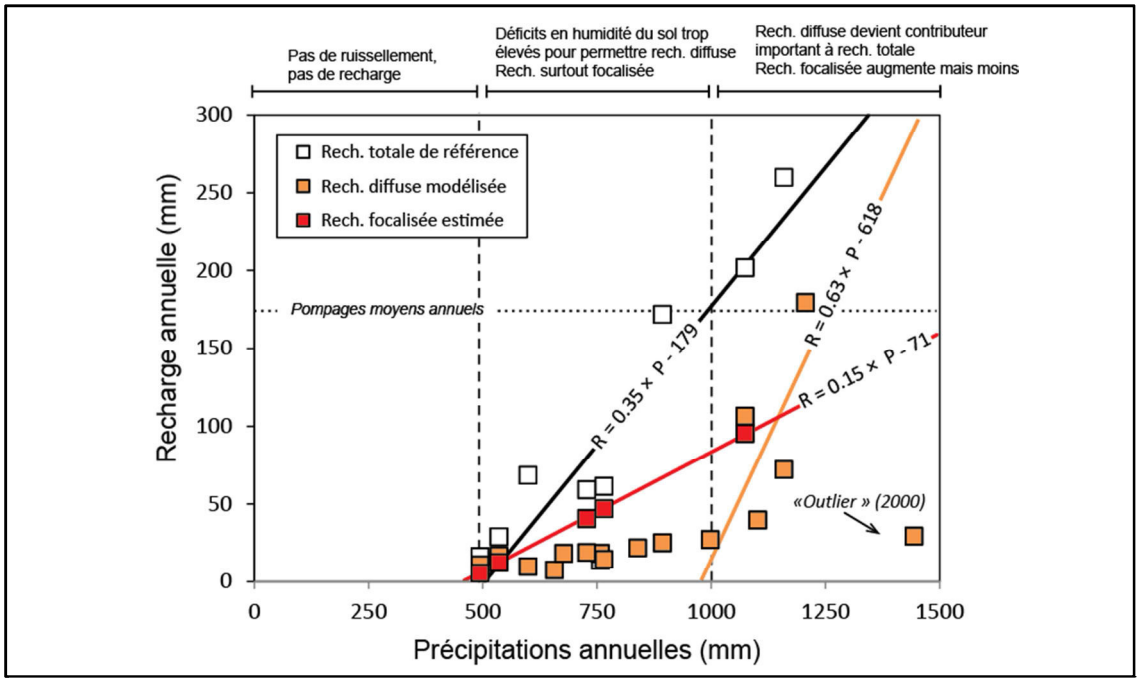

FIGURE F.1 : Schéma récapitulatif illustrant la relation entre les précipitations et la recharge pour la recharge diffuse, la recharge focalisée et la recharge totale.

Premièrement, comme indiqué précédemment, les Entisols, qui se forment préférentiellement dans les réseaux de drainage, sont des zones qui résistent à la recharge diffuse. Néanmoins, les cartes de recharge totale montrent la tendance inverse: ces mêmes zones ont en réalité une recharge *totale* élevée. Cela souligne l'importance des contributions de recharge focalisée. En cas de fortes pluies, la capacité d'infiltration des sols est dépassée, de sorte que l'eau s'écoule et crée des ruisseaux éphémères. Ces épisodes créent des conditions favorables à la recharge *indirecte*. D'autres études sur des terrains en milieu semi-aride ont également révélé que des vallées basses remplies d'alluvions agissaient comme des terrains de recharge indirecte à la fois dans les zones de roches cristallines (par exemple, van Wyk et al., 2012) et les aquifères sédimentaires (par exemple, Acworth et al., 2016; Mahlknecht et al., 2004).

Il est également possible, même en l'absence d'écoulements importants à la surface, que l'écoulement latéral non-saturé déplace l'infiltration vers les parties inférieures du bassin. Cependant, il est connu que l'écoulement latéral à travers la matrice insaturée

déplace une quantité d'eau négligeable à cause des forces capillaires. En fait, la plus grande partie des écoulements latéraux se produit par des discontinuités structurelles subhorizontales telles que des fractures, des macropores ou des transitions lithologiques sous forme d'écoulement préférentiel. Plusieurs études, par exemple, ont montré que les interfaces sol-roche agissaient comme des voies d'écoulement préférentielles et détournaient l'infiltration latéralement (Bockgard & Niemi, 2004; Sohrt et al., 2014), ce qui pourrait entraîner des taux de recharge plus faibles dans les zones drainées et des taux de recharge plus élevés dans les zones d'accumulation.

De plus, il semble qu'il existe un axe N-S de recharge focalisée dans le segment Est du bassin versant. Cela peut être dû en partie à la position du réseau de drainage, mais cela semble également correspondre à la zone de contact entre le granite à biotite et le granite à biotite légèrement plus dur avec dykes pegmatitiques et leucogranitiques. Ceci est cohérent avec la littérature: les zones de contact peuvent être très transmissives et ont peuvent agir en tant que zones de recharge préférentielle. Les discontinuités géologiques peuvent également être associées à des zones de failles fortement fracturées, qui constituent également des drains importants pour la recharge des aquifères (par exemple, Leray et al., 2013; Ruelleu et al., 2010). D'autres discontinuités structurales, tels que les dykes, peuvent agir de la même manière (par exemple, Johnston, 1987), bien que celles-ci puissent également constituer des barrières (Bredehoeft et al., 1992).

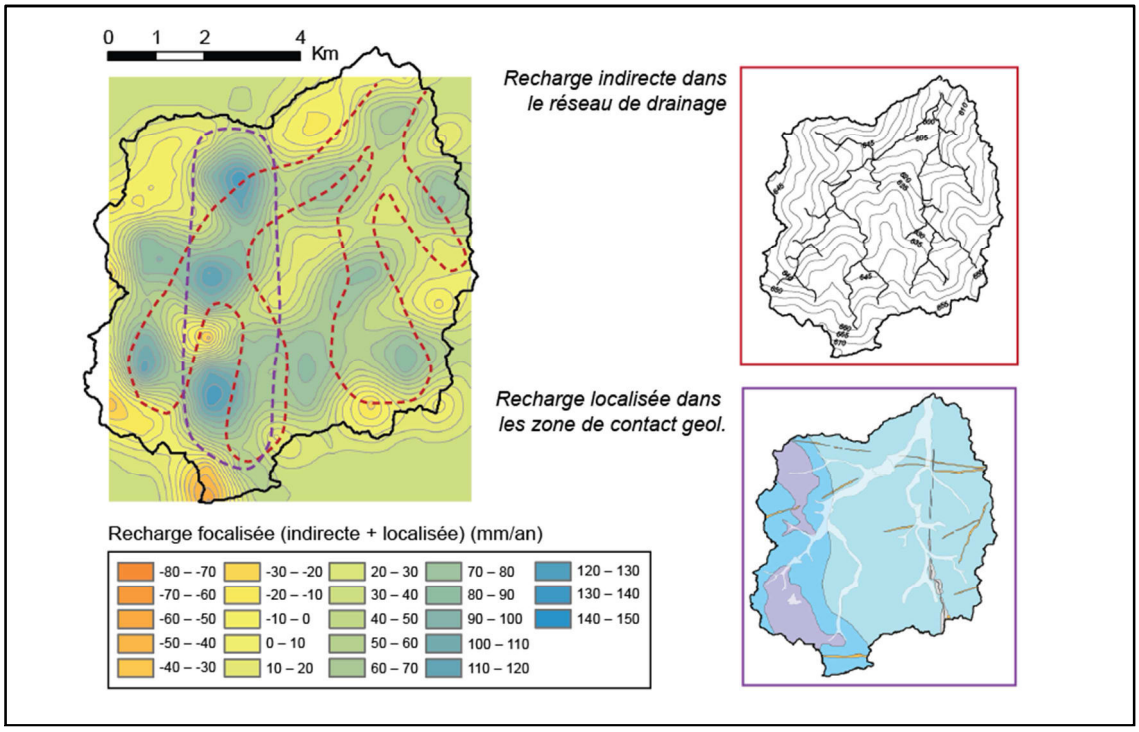

FIGURE F.2 : Carte récapitulative de la distribution estimée de la recharge focalisée à l'échelle du bassin versant et des facteurs potentiellement à l'origine de cette distribution

Second axe de recherche

Recharge artificielle dans les aquifères cristallins fracturés

Pour surmonter les problèmes de pénurie d'eau, des structures de recharge artificielle (ou « contrôlée ») d'aquifères (Managed Aquifer Recharge, MAR en anglais) sont actuellement développées dans de nombreuses régions du monde, y compris sur des terrains peu perméables comme les roches cristallines altérées. Dans un tel contexte géologique, l'efficacité de la recharge artificielle est mal connue. Afin de répondre à cette question et de mieux comprendre les facteurs qui contrôlent la dynamique de la recharge artificielle, un bassin de recharge artificielle a été mis en place dans le parc hydrogéologique expérimental de Telangana (Inde du Sud).

1. Méthodologie

Tout d'abord, les taux d'infiltration ont été estimés à partir des variations de niveau d'eau dans le bassin mesurés en continu à l'aide d'une sonde. Les niveaux d'eaux ont été reliés aux taux d'infiltration via une approche de bilan hydrique combinée avec des simples relations empiriques. En absence d'apports par le canal qui alimente le bassin, tous les termes du bilan hydrique (pluie, évaporation) sont connus, sauf l'infiltration qui est estimée comme le restant du bilan. La relation empirique entre infiltration et niveau d'eau peut alors être établie et utilisée lorsque tous les termes du bilan ne sont pas connus, c'est-à-dire lors du remplissage du bassin (les intrants du canal n'ont pu être mesurés). Les variations du taux d'infiltration dans le temps ont été interprétées et comparées aux autres éléments du bilan afin de faire une estimation de l'efficacité d'infiltration (infiltration/intrants totaux) et de son évolution dans le temps. La loi de Darcy a permis par ailleurs d'estimer la conductivité hydraulique verticale de la saprolite.

En parallèle, les variations des niveaux d'eau souterrains en réponse à l'infiltration de cette structure ont été suivies dans les différents forages présents sur le site. Ces variations ont été interprétées à l'aide d'une solution analytique qui simule la forme et l'évolution du dôme piézométrique qui se crée en réponse à l'infiltration en provenance d'un bassin. Les niveaux d'eau ainsi simulés ont été calibrés en fonction des niveaux d'eau observés pour permettre une estimation de premier ordre de la conductivité hydraulique horizontale et la capacité de stockage du compartiment souterrain.

Enfin, bien que les solutions analytiques s'appliquent simplement, elles ne tiennent pas compte de la géométrie de l'aquifère ni des conditions aux limites. C'est alors qu'un modèle numérique simple a été utilisé pour montrer comment la profondeur de l'interface perméable entre la saprolite et le granite contrôle la dynamique de la recharge et les variations observées des niveaux d'eau. Les simulations numériques ont été basées sur des modèles conceptuels très simples. Tout d'abord, un scénario synthétique avec une recharge constante a été testé afin d'analyser la relation de cause à effet entre les condi-

tions aux limites imposées par le relief du substratum rocheux et la réponse de la nappe phréatique à la recharge. Ensuite, dans une deuxième étape visant à mieux reproduire la dynamique de la recharge, les taux d'infiltration réels estimés ont été utilisés comme entrées dans le modèle. Deux scénarios ont été testés en utilisant deux configurations de modèle: un scénario de référence, dans lequel il n'y a pas de compartimentation, et un scénario compartimenté. Le scénario de référence a été utilisé pour simuler la réponse de la nappe phréatique dans des conditions homogènes avec un substrat rocheux subhorizontal. L'autre scénario tient compte des conditions aux limites plus complexes imposées par le relief du substrat rocheux, il comporte une dépression au centre. La dépression visait à représenter une dépression topographique de l'interface granite/saprolite, comme il ressort des sondages de résistivité (ERT) précédents que le bassin de recharge est situé au-dessus d'une dépression du substrat rocheux.

2. Résultats et discussion

L'efficacité globale d'infiltration, c'est-à-dire le ratio d'infiltration par rapport au total des intrants, est assez élevée (96%) dans le cas présent, par rapport aux études précédentes dans des environnements similaires (Boisson, Villesseche et al., 2015 : 56%; Perrin et al., 2009 : 54%; Singh et al., 2004 : 67%), mais en accord avec les valeurs enregistrées par la CGWB en 2011, pouvant atteindre 98% dans les environnements de roches cristallines. Cependant, bien que l'efficacité globale d'infiltration soit élevée, les taux d'infiltration ont diminué de manière significative lorsque la nappe souterraine a atteint la base du bassin d'infiltration (on parle de *connexion hydraulique*) en raison d'une diminution du gradient hydraulique. L'infiltration est alors plus étendue dans le temps, ce mène à des taux d'évaporation plus élevés, bien que la quantité évaporée reste beaucoup plus faible que le volume infiltré global. Il est peu probable que cela continue d'être le cas si le bassin devient significativement envasé par la précipitation de composés organiques et inorganiques au fond qui entravent le processus d'infiltration.

L'estimation de la perméabilité *verticale* de cette étude ($K_V = 8.1 \times 10^{-6}$ m.s^{-1}) est légèrement supérieure à celle de Boisson, Guihéneuf et al., (2015) obtenus au même site pour la couche supérieure de saprolite (9×10^{-8} à 3×10^{-7} m.s^{-1}), mais globalement du même ordre de grandeur que d'autres études réalisées sur la saprolite (par exemple, George, 1992 : 7×10^{-6} m.s^{-1}; Cook et al., 1996: 1×10^{-6} à 1×10^{-5} m.s^{-1}). Les propriétés hydrauliques *horizontales* se situent dans la plage supérieure des valeurs pour la roche cristalline fracturée ($K = 6.5 \times 10^{-5}$ m.s^{-1} et $S = 5.0 \times 10^{-2}$), et correspondent plutôt aux propriétés de l'interface entre la couche altérée supérieure et le substrat rocheux fracturé sous-jacent obtenue pour notre site expérimental dans Boisson, Guihéneuf et al., 2015.

Quant au modèle numérique, la simulation la plus réaliste est obtenue en considérant un sous-sol hétérogène (compartimenté), et donc des conditions aux limites imperméables

semi-pénétrantes. L'extension latérale de la dépression / du compartiment au centre du modèle contrôle la pente de la remontée du niveau d'eau. De plus petites extensions latérales du compartiment conduisent à des pentes plus fortes (une augmentation plus rapide) et, à mesure que la taille du compartiment latéral augmente, la dynamique de la remontée se rapproche de celle du scénario de référence (c.-à-d. aucun effet de limite). L'extension verticale de la dépression n'a pas d'impact sur la pente de la remontée, mais contrôle toutefois l'amplitude des variations, où une différence d'altitude plus importante entraîne une plus grande amplitude de la remontée du niveau. L'application du scénario compartimenté avec en entrée l'infiltration estimée a permis de recréer la dynamique des forages les plus proches du bassin en utilisant les paramètres hydrauliques obtenus à partir de la modélisation analytique et en modifiant uniquement les dimensions (hauteur et extension latérale) de la dépression. De plus, les dimensions ainsi obtenues correspondent assez bien à la forme du substrat rocheux obtenu par tomographie de résistivité électrique.

En somme, les variations de niveau d'eau peuvent être divisées en trois phases. Avant la date supposée de la connexion hydraulique, (entre t = 0 et t = 40 j), les variations du niveau de l'eau sont faibles et la nappe phréatique est profonde, ce qui correspond à *P1*. Ensuite, les niveaux d'eau augmentent rapidement sous l'effet de la condition aux limites latérale (entre t = 60 et t = 70 j), ce qui correspond à *P2*. Cela se poursuit jusqu'à ce que les niveaux d'eau dépassent le seuil topographique «en aval» du bassin qui délimite la dépression environ 70 jours après le début de la période d'observation. À partir de ce moment, les « compartiments » se connectent et les niveaux d'eau varient légèrement mais ce à grande échelle : cela correspond à *P3*.

Très peu d'études modélisent réellement les processus hydrogéologiques en tenant compte de la géométrie de l'aquifère (par exemple Ronayne et al., 2008), probablement parce qu'il n'est pas facile d'imager la géométrie de l'aquifère et qu'il est pratiquement impossible d'obtenir des informations en trois dimensions sur les propriétés hydrauliques, en particulier dans le contexte des roches cristallines (de Marsily et al., 2005). Dans cette étude, nous avons quantifié avec succès le rôle joué par le relief du socle (et sa compartimentation associée) sur la réponse hydraulique de l'aquifère à la recharge, en soulignant également ses effets sur les potentiels de propagation de la recharge et d'infiltration. Cette étude a montré que le relief du substrat rocheux peut produire un effet analogue à celui des limites imperméables (ou semi-imperméables) sur le rabattement au cours des essais de pompage (de Marsily, 1986). Dans les deux cas, une variation de la pente de variation de niveau d'eau par rapport à une situation dans laquelle aucune limite imperméable n'est présente est attendue. À notre connaissance, il n'y a pas d'autres cas dans la littérature où cet effet a été identifié pendant un épisode de recharge. En plus, les crêtes de relief n'étant qu'une limite imperméable semi-pénétrante, il a été montré que

l'augmentation de la pente de la remontée par rapport au scénario de référence donnait des informations sur les dimensions du relief en question, où plus la dépression est grande moindre est la pente de la remontée.

L'extrapolation de notre méthode simple pourrait améliorer les modèles actuels utilisés pour la gestion de la recharge artificielle dans de tels environnements géologiques. D'un point de vue quantitatif, il serait utile de prendre en compte les effets des conditions aux limites pour réguler les entrées afin de limiter les pertes par évaporation. Si la topographie du substrat rocheux est connue, les décideurs peuvent être plus conscients du degré de propagation de la recharge dans l'aquifère et choisir de donner la priorité à une réaction localisée forte, plus facile à récupérer ultérieurement, ou plus faible mais sur des zones plus vastes en fonction de la densité et de l'étendue des agglomérations affectées par l'épuisement des eaux souterraines. De plus, les implications sur la qualité de l'eau sont également non négligeables. Nous avons souligné l'importance des flux préférentiels, ce qui implique que l'atténuation des contaminants n'aura probablement pas lieu assez rapidement pour atténuer les effets négatifs de l'injection d'eaux usées dans l'aquifère (l'eau actuellement utilisée pour alimenter le réseau de structures de recharge provient de la rivière Musi en aval d'Hyderabad, malheureusement le huitième fleuve le plus pollué de l'Inde).

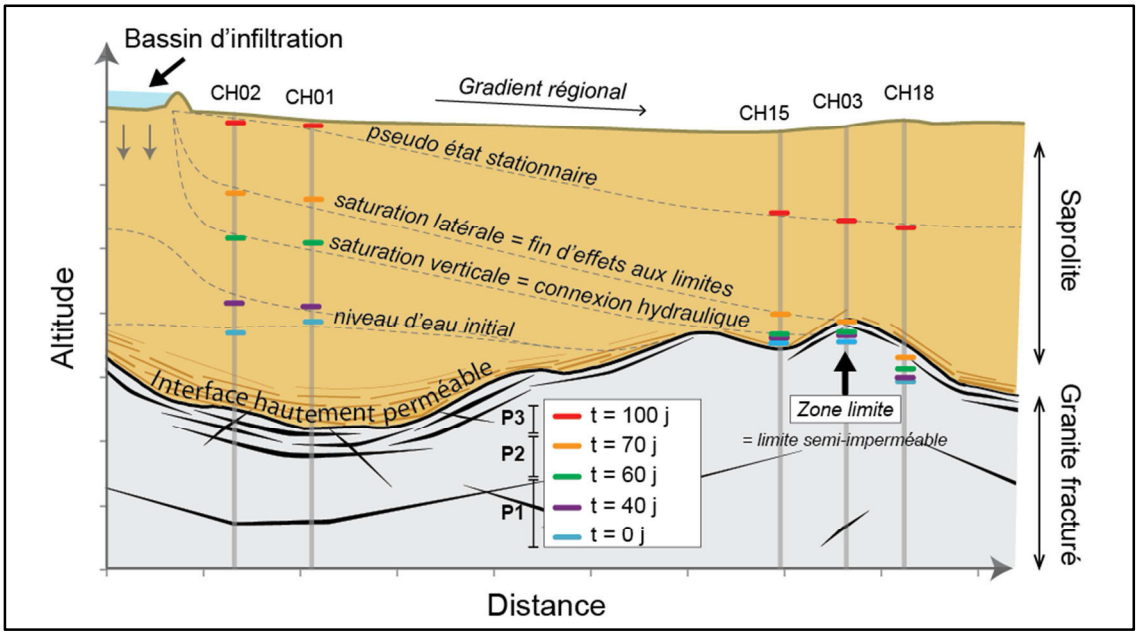

FIGURE F.3 : Représentation schématique des variations de niveau d'eau au-dessus du substrat rocheux (zone grise) en réponse à une recharge artificielle à partir d'un bassin d'infiltration.

UNIVERSITE ECOLOGIE
BRETAGNE GEOSCIENCES
LOIRE AGRONOMIE ALIMENTATION

UNIVERSITÉ DE RENNES 1

Titre : Impact de l'hétérogénéité sur la recharge naturelle et artificielle des aquifères cristallins altérés et fracturés

Mots clés : Recharge des eaux souterraines, Recharge artificielle, Roche cristalline altérée et fracturée, Hétérogénéité

Résumé : Les facteurs qui régissent l'intensité et la répartition de la recharge naturelle et artificielle dans les aquifères cristallins altérés et fracturés sont mal connus. Ce sont cependant les caractéristiques déterminantes de ce type de roche—ces roches sont très hétérogènes—qui rendent difficile l'estimation des flux dans ces milieux ainsi que des propriétés hydrauliques qui les contrôlent. La première partie de ce manuscrit fournit un état des connaissances sur la recharge des eaux souterraines et ses méthodes d'estimation, permettant de comprendre les défis scientifiques et sociétaux abordés dans cette thèse. La deuxième partie présente les travaux numériques et expérimentaux menés pour approfondir notre compréhension de la dynamique des flux d'eaux souterraines dans ces milieux hétérogènes à plusieurs échelles. Le premier axe de recherche porte sur les processus de recharge naturelle à l'échelle du bassin versant. La recharge *diffuse* a été modélisée avec un modèle physique simple d'infiltration et comparée à des estimations préalables de recharge *totale*. Nos résultats illustrent la forte dépendance de la recharge aux précipitations et à l'irrigation, et l'importance de la recharge *focalisée*. Les facteurs responsables de la distribution spatiale de la recharge sont aussi étudiés.
Le deuxième axe est basé sur le suivi de la mise en eau d'un bassin de recharge artificielle dans un site hautement monitoré et bien équipé. Ces observations ont été interprétées avec des modèles analytiques et numériques. Ces modèles ont mis en évidence l'existence de flux préférentiels horizontaux, mais aussi d'une compartimentation latérale qui entrave la propagation des intrants de recharge.

Title : Impact of heterogeneity on natural and managed aquifer recharge in weathered fractured crystalline rock aquifers

Keywords : Groundwater recharge, Managed Aquifer Recharge, Weathered fractured crystalline rock, Heterogeneity

Abstract: The factors governing the intensity and distribution of natural and artificial recharge in weathered and fractured crystalline aquifers are poorly understood. However, it is the defining characteristics of this type of rock—these rocks are very heterogeneous—that make the estimation of fluxes and the hydraulic properties controlling them difficult. The first of its two parts provides the theoretical framework on groundwater recharge processes and its estimation methods for comprehending the scientific and societal challenges discussed in this thesis. The second part presents the numerical and experimental work carried out to deepen our understanding of the dynamics of groundwater flows in these heterogeneous underground environments at several scales. The first line of research focuses on natural recharge processes at the watershed scale. *Diffuse* recharge was modeled with a simple physical infiltration model and compared to previous estimates of *total* recharge. Our results highlight the strong dependence of recharge on rainfall and irrigation, and the importance of focused recharge. The factors responsible for the spatial distribution of recharge are also studied.
The second axis is based on the monitoring of the filling of an artificial recharge basin at a highly monitored and well-equipped site. These observations were interpreted with analytical and numerical models to improve our knowledge of flow dynamics in fractured crystalline rocks at the medium scale. These models illustrated the existence of preferential horizontal flows, but also of a lateral compartmentalization that hinders the propagation of recharge inputs.